Conodonts, microfacies and palaeoenvironment during the mid-Tournaisian Event - comparison of platform and basin (lower Mississsippian, Germany and Belgium)

Inaugural – Dissertation

zur

Erlangung des Doktorgrades

der Mathematisch-Naturwissenschaftlichen Fakultät

der Universität zu Köln

vorgelegt von

Sarah Esteban Lopez

aus Langenfeld

Berichterstatter: Prof. Dr. Hans-Georg Herbig
(Gutachter)

                        Prof. Dr. Martin Melles

Tag der mündlichen Prüfung: 30. April 2020

Abstract

The globally traceable mid-Tournaisian Event (lower Carboniferous, Mississippian) was the result of glacio-eustatic sea-level fluctuations and its formation a matter of ongoing discussions. Two opposing sides postulate either a formation during a transgression or during an episode of a waxing ice sheet. Here, an attempt is made to clarify the formation mechanisms, employing conodont biostratigraphy, conodont biofacies zonation, microfacies analysis and sequence stratigraphy. A review of the existing conodont biozonation models for the lower Carboniferous visualizes the differences that are the result of varying accumulation realms, and allows the correlation between the models. Sequence stratigraphy is used to support the correlation. The review also questions the usefulness of "standard" biozonation models as they cannot be applied to conodont faunas originating from shallow-water environments.

Three studies from the Rhenish Mountains (Riescheid, Gladenbach, Wettmarsen) and one from the eastern Belgian Namur-Dinant Basin (Dolhain) represent different settings along a platform-basin transect and were used to reconstruct the conditions during the mid-Tournaisian Event.

The section Riescheid, that is situated within the Herzkamp Syncline in the western Rhenish Mountains exposes middle Famennian to Upper Viséan strata of the Kulm facies (basin facies). The middle Tournaisian Kahlenberg Fm consists of dark shales and a package of intercalated calciturbidites and was accumulated during the Transgressive Systems Tract (TST) and Highstand Systems Tract (HST) of Sequence 2. The retrieved very poor conodont fauna indicates the affiliation to the *isosticha*-Upper *crenulata* Zone and the Siphonodellid Biofacies that represents lower slope to basin environments. The microfacies analysis allows the reconstruction of the sedimentational conditions. They reveal the accumulation of hemipelagic calciturbidites in distal, lower slope environments.

The Gladenbach section, situated in the eastern Rhenish Mountains, exposes middle Tournaisian strata. They differ from the "normal" facies due to their origin from the allochthonous Hörre Nappe. The Gladenbach Fm, equivalent to the Kahlenberg Fm and the lower part of the Hardt Fm, consists of dark, bituminous limestones and intercalated dark shales, representing many turbiditic fining upward cycles. These can be assigned to the Transgressive Systems Tract (TST) and HST of Sequence 2 and the lower part of Sequence 3. The rich conodont fauna allows the recognition of the Lower *crenulata*, *isosticha*-Upper *crenulata* and Lower *typicus* zones and the assignment to the Siphonodellid-Polygnathid Biofacies (lower slope and basin) of the Gladenbach Fm. The microfacies analysis reveals an accumulation realm in a deep basin close to the lower slope.

The section Wettmarsen is situated in the Remscheid-Altena Anticline in the Rhenish Mountains and exposes middle Famennian to middle Tournaisian strata of the Kulm type facies. It contains a depositional gap between Upper Devonian and lower Carboniferous. Sequence 2 as well as the Lowstand Systems Tract (LST) and undifferentiated TST/HST of Sequence 3 can be recognized. The calciturbidite bed of the Kahlenberg Fm originated from a high rising intrabasinal swell on top of the former Devonian Balve reef complex southwest of the section. A rich conodont fauna could be retrieved from this calciturbidite bed, allowing the assignment to the *isosticha*-Upper *crenulata* Zone. An allocation to middle to upper shelf slope areas was possible, based on the gnathodid-dominated conodont fauna and the microfacies analysis.

The recently cut (2010), hardly studied eastern Belgian Dolhain section is situated in the Verviers Syncline within the Vesdre-Aachen sedimentation area and exposes uppermost

Famennian to Ivorian strata. The Pont d'Arcole Fm is composed of a variety of shales and limestones, representing Sequence 2 together with the pure limestone succession of the overlying Landelies Fm. Dark shales in the middle part of the Pont d'Arcole Fm represent the maximum flooding interval (mfi). Strongly increasing percentages of limestone beds above indicate the beginning of the HST. A single rich conodont fauna directly above the mfi indicates the Lower *crenulata* Zone. The polygnathid-pseudopolygnathid dominated fauna, as well as microfacies and sequence stratigraphy indicate deep (outer) shelf below wave base.

In the studied sections from the Rhenish Mountains the middle Tournaisian Kahlenberg Fm and the Gladenbach Fm represent accumulations of deep basins or deep distal slope areas that in part were fed by calciturbidites deriving from deeper water and lower, middle and upper slope deposits. The studied section of the Pont d'Arcole Fm is a deep open-shelf succession.

In summary, the results of this study support an exaggerated transgression resulting in the mid-Tournaisian Event.

Kurzfassung

Der weltweit nachweisbare mid-Tournaisian Event (unteres Karbon, Mississippium) war das Resultat von glazio-eustatischen Meeresspiegelschwankungen und seine Entstehungsmechanismen werden immer noch diskutiert. Zwei konkurrierende Lager postulieren entweder eine Entstehung während einer Transgression oder während eines Zeitintervalls wachsender Eisschilde. In dieser Arbeit wird versucht die Entstehungsmechanismen durch die Anwendung von Conodonten-Biostratigraphie, Conodonten-Biofazieszonierung, Mikrofaziesanalyse und Sequenzstratigraphie zu rekonstruieren. Ein Review der bestehenden Conodonten-Biozonierungen des unteren Karbons visualisiert die Unterschiede, die aufgrund von unterschiedlichen Ablagerungsräumen entstehen und ermöglicht die Korrelation der verschiedenen Modelle. Sequenzstratigraphie wird angewand um die Korrelationsergebnisse zu untermauern. Es wird ausserdem hinterfragt, inwieweit „Standard" Modelle sinvoll sind, wenn sie nicht auf Flachwasserbereiche angewandt werden können.

Drei Studien aus dem Rheinischen Schiefergebirge (Riescheid, Gladenbach, Wettmarsen) und eine Studie aus dem ost-belgischen Namur-Dinant Becken (Dolhain) repräsentieren verschiedene Ablagerungsbereiche entlang eines Plattform-Becken-Profils und wurden genutzt um die Bedingungen während des mid-Tournaisian Events zu rekonstruieren.

Das Profil Riescheid, welches sich innerhalb der Herzkamp-Mulde im westlichen Rheinischen Schiefergebirge befindet, schließt Schichten der Kulmfazies (Beckenfazies) des mittleren Famennium bis zum Oberen Viséum auf. Die Kahlenberg-Fm des mittleren Tournaisium besteht aus dunklen Tonsteinen und einem eingeschalteten turbiditischen Kalkstein-Paket und wurde während des Transgressive Systems Tract (TST) und Hightstand Systems Tract (HST) der Sequenz 2 abgelagert. Die sehr Individuen-arme Conodontenfauna weist auf eine Zugehörigkeit zur *isosticha*-Oberen *crenulata*-Zone und zur Siphonodellid Biofazies hin, welche Bereiche des unteren Hangs und Beckens repräsentiert. Die Mikrofaziesanalyse erlaubt die Rekonstruktion der sedimentären Bedingungen und weist auf die Ablagerung von hemipelagischen turbiditischen Kalksteinen in distalen, unteren Hangbereichen hin.

Das Profil Gladenbach, welches sich im östlichen Rheinischen Schiefergebirge befindet, schließt Schichten des mittleren Tournaisum auf. Die Abfolge dort unterscheidet sich von der „normalen" Fazies aufgrund ihres Ursprungs innerhalb der allochthonen Hörre-Decke. Die Gladenbach-Fm (Äquivalent der Kahlenberg-Fm und dem unteren Teil der Hardt-Fm) besteht aus dunklen, bituminösen Kalksteinen und eingeschalteten dunklen Tonsteinen und setzt sich

aus mehreren turbiditischen fining-upward-Zyklen zusammen. Diese können dem TST und HST der Sequenz 2 und dem unteren Teil der Sequenz 3 zugeordnet werden. Die reichhaltige Conodontenfauna erlaubt die Zuteilung der Gladenbach-Fm zur *isosticha*-Obere *crenulata*- und Untere *typicus*-Zone sowie zur Siphonodellid-Polygnathid-Biofazies (unterer Hang und Becken). Die Mikrofaziesanalyse erlaubt die Rekonstruktion eines Ablagerungsraums, der sich im tiefen Becken nahe zum unteren Hang befand.

Das Profil Wettmarsen befindet sich im Remscheid-Altena-Sattel im Rheinischen Schiefergebirge und schließt Schichten der Kulmfazies des mittleren Famennium bis zum mittleren Tournaisium auf. Eine Aufschlusslücke umfasst Schichten des Oberen Devons bis ins untere Karbon. Im Profil können die Sequenz 2 sowie der Lowstand Systems Tract (LST) und der undifferenzierte TST/HST von Sequenz 3 nachvollzogen werden. Die turbiditische Kalksteinbank der Kahlenberg-Fm stammt von einer hochaufragenden Schwelle innerhalb des Beckens, welche sich auf dem ehemaligen devonischen Balver Riffkomplex südwestlich des Profils befindet. Eine reichhaltige Conodontenfauna konnte aus dieser turbiditischen Kalksteinbank gewonnen werden und ermöglichte die Zuordnung zur *isosticha*-Oberen *crenulata*-Zone. Basierend auf der Conodontenfauna, die von Gnathodiden dominiert wird sowie der Mikrofaziesanalyse konnte der Ablagerungsraum dem mittleren bis oberen Hang zugeordnet werden.

Das kürzlich (2010) entstandene, kaum bearbeitete ost-belgische Profil Dolhain befindet sich in der Verviers Mulde, innerhalb des Vesdre-Aachen-Sedimentationsraums und schließt Schichten des obersten Famennium bis Ivorium auf. Die Pont d'Arcole-Fm setzt sich aus variierenden Tonsteinen und Kalksteinen zusammen und kann, zusammen mit den reinen Kalksteinen der darüber liegenden Landelies-Fm, der Sequenz 2 zugeordnet werden. Dunkle Tonsteine im mittleren Bereich der Pont d'Arcole-Fm repräsentieren das maximum flooding Intervall (mfi). Darüber weisen stark zunehmende Anteile von Kalksteinbänken auf den beginnenden HST hin. Eine reiche Conodontenfauna direkt über dem mfi zeigt die Untere *crenulata*-Zone an. Die Polygnathid-Pseudopolygnathid dominierte Fauna sowie Mikrofazies und Sequenzstratigraphie weisen auf tiefen (äußeren) Schelf unterhalb der Wellenbasis hin.

In den untersuchten Profilen des Rheinischen Schiefergebirges repräsentieren die mittel-tournaisische Kahlenberg-Fm und die Gladenbach-Fm Ablagerungen des tiefen Beckens oder distalen unteren Hangbereichs, die teilweise von Kalziturbiditen aus Tieferwasser-Bereichen des unteren, mittleren oder oberen Hangs gespeist werden. Das untersuchte Profil der Pont d'Arcole-Fm ist eine Abfolge des tiefen offenen Schelfs.

Zusammenfassend ist zu sagen, dass die Ergebnisse dieser Studie die Existenz einer starken Transgression, die im mid-Tournaisien Event resultierte, unterstützen.

Acknowledgements

Contents

1. Introduction

The sedimentary accumulations of the mid-Tournaisian Event, also known as Lower Alum Shale Event, are of Mississippian (lower Carboniferous) age (353-357 Ma BP, STD 2016) and are globally recognizable.

Palaeontology, stratigraphy and sedimentology of the lower Carboniferous accumulations of the Aachen and Velbert area in the Rhenish Mountains have been extensively studied for almost 200 years due to the former economic importance of the Pb-Zn ore deposits of the Aachen area and the rich fossil-deposits of the Velbert Anticline (AMLER & HERBIG 2006). Difficulties to stratigraphically correlate the "Kohlenkalk" (carbonate platform) of Belgium and the Aachen area with the "Kulm" (deep-water accumulations) facies of the Rhenish Mountains were already obvious back then and inspired to further investigate these two facies developments. Following the basic works of the 19th and early 20th century, the main inventory in both areas was achieved and ceased in the 1930s (AMLER & HERBIG 2006). At this time, also the first correlations with neighbouring areas were concluded. For detailed descriptions of the history of the geologic investigations of the lower Carboniferous in the Velbert area see THOMAS (1993) and AMLER et al. (1994).

After the publications of VERHOOOGEN (1934), VARLAMOFF (1936), and PAUL (1937a, b, c) of the Dinantian of Aachen and the correlation with the adjoining Belgian and German Carboniferous exposures the number of scientific publications declined. Later studies provided a better comparison with eastern Belgium (BOONEN & KASIG 1979, SWENNEN & VIAENE 1985, SWENNEN et al. 1982, PEETERS et al. 1992, 1993). LALOUX et al. (1996a, b, 2000) mapped eastern Belgian areas and introduced new lithological units. Subsequently a general new lithostratigraphical classification of the Belgian Dinantian was introduced by POTY et al. (2001). Essential sequence stratigraphical interpretations of the Devonian-Carboniferous boundary and the lower Tournaisian of the Dinant Syncline and southern Belgium, as well as a comparison with the Kulm facies of the northern Rhenish Mountains, were published by VAN STEENWINKEL (1990, 1993a, b). A first classification of the sequence stratigraphy of the Belgian Dinantian followed (HANCE et al. 2001). The biostratigraphical foundation of the "Kohlenkalk" facies in the Franco-Belgian and Campine basins was especially achieved by many studies of CONIL and co-authors (e.g., CONIL et al. 1986, 1990).

The lower Carboniferous and therefore also the middle Tournaisian of the Lower Rhine Embayment remained mostly unknown until several new boreholes were drilled in the 1980s (AMLER & HERBIG 2006, cum lit.). With the results from the borehole data the structural reconstruction of the underground of the Lower Rhine Embayment could be considerably improved (WREDE & HILDEN 1988, WREDE 1998, DROZDZEWSKI et al. 1998). The "Krefelder Achsenaufwölbung" (Krefeld Axial Culmination), a sigmoidal structure that connects the Carboniferous of the westernmost Rhenish Mountains with the Aachen-Ardenne area, proves that, as already mentioned by BLESS et al. (1976), the Carboniferous in the underground of the Lower Rhine Embayment palaeogeographically belongs to the eastern part of the "Kohlenkalk" shelf of the Brabant Massif (AMLER & HERBIG 2006).

In the Velbert area, east of the River Rhine, SCHMIDT (1923) was the first to recognize the time-equivalence of the Kulm and Kohlenkalk facies and attempted to correlate them. A detailed description of the lithology and fossil content of the lower Carboniferous of the Velbert Anticline was accomplished by the end of the 1930s within the series "Die Fauna des deutschen Unterkarbons" (AMLER & HERBIG 2006). New approaches in the 1960s to 1980s elucidated the stratigraphy using spores, conodonts and foraminifera (AMLER & HERBIG 2006 and references therein). FRANKE et al. (1975) also examined the sedimentology,

facies development, and palaeogeography of the Velbert area. More recent publications focused on palaeontological topics (HAUDE & THOMAS 1989, RICHTER & AMLER 1994, WEBER 1997) including the lower Carboniferous of Aprath (Herzkamp Syncline) that already belongs to the Kulm facies (THOMAS 1992, RATHMANN & AMLER 1992). AMLER & HERBIG (2006) introduced a formal lithostratigraphic subdivision for the Velbert Anticline.

The difficulties in the correlation of "Kohlenkalk" and "Kulm" facies also become obvious in the conodont zonation erected for those areas. Fig. 1 compares German, Belgian and European condont zonations of the lower part of the Mississipppian. Goniatite stages (cd I,

System	Subsystem	Stages	Time (Ma)	Belgian Stages	North American Stages	Goniatites	German conodont zonation	Belgian conodont zonation	European conodont zonation
CARBONIFEROUS	Mississippian/ lower Carboniferous	Viséan		Moliniacian p.p.			*homopunctatus*	*homopunctatus*	*Gn. homopunctatus*
		"upper"	346	Osagean		cd II (=*Pericyclus*-Stage)	*anchoralis*	*anchoralis*	*Sc. anchoralis - Dol. latus*
		Tournaisian		Ivorian			*typicus* Upper / Lower	*carina*	upper *Gnathodus typicus*
		"middle"	353				*isosticha*-Upper *crenulata*	*Gnathodus*	*isosticha*-Upper *crenulata*
				Hastarian	Kinderhookian		Lower *crenulata*	*Siphonodella*	*crenulata*
		"lower"				cd I (=*Gattendorfia*-Stage)	*sandbergi* U/L		*quadruplicata* / *sandbergi*
							duplicata U/L		*hassi* / *duplicata* / *bransoni*
			361				*sulcata*		*sulcata*

Fig. 1 Chronostratigraphy and conodont biostratigraphy of the lower part of the Mississippian (Tournaisian - lower Viséan). German conodont zonation from HERBIG & STOPPEL (2006), Belgian conodont zonation from POTY et al. (2014), revised European conodont zonation from KAISER (2009) and ARETZ et al. (2020). Note well: lower, middle and upper Tournaisian substages are not formally recognized, but widespreadly used in the European Kulm basins.

cd II) were traditionally used to classify the Dianantian (Tournaisian and Viséan) and are listed in Fig. 1 to enable comparison with older literature. The mid-Tournaisian Event can be correlated with the upper part of the Hastarian or Kinderhookian and covers the interval of the Lower *crenulata* and *isosticha*-Upper *crenulata* conodont zones, respectively the upper *Siphonodella* zone, including the *Gnathodus* (Sub-)zone. In the European conodont zonation it equates the *crenulata* and *isosticha*-Upper *crenulata* zones.

Fig. 1 lists the system, subsystem, stages and conodont zonations as they are used within this work. The lower part of the Mississippian (lower Carboniferous) resembles the Tournaisian that is informally separated in a "lower", "middle" and "upper" Tournaisian. The Belgian Hastarian can be correlated with the informal "lower" and "middle" Tournaisian, whereas the Belgian Ivorian coincides with the "upper" Tournaisian. The Viséan constitutes the middle part of the Mississippian. The Moliniacian is the lowermost

of three substages of the Viséan. The Kinderhookian and Osagean North American Stages represent the Tournaisian and the lower part of the Viséan.

In the Carboniferous, regressive and transgressive phases originated from glacio-eustatic sea-level changes and therefore their deposits are global in distribution (e. g. DAVYDOV et al. 2012).

The predominantly dark to blackish coloured deposits of the mid-Tournaisian Event developed during deep- as well as shallower-water (above 200 m) conditions (KREBS 1968). For the Rhenish Mountains KREBS (1968) suggested a scenario of a shallow sea with an inflowing undercurrent and outflowing surface waters. The outflow supplies the undercurrent with plankton and causes, despite very low sedimentation rates, anaerobic conditions at the sea floor (KREBS 1968). According to KREBS (1968) the transgression was the most relevant sea level rise in the Rhenohercynian Zone during the lower Carboniferous. It was the result of ongoing subsidence (KREBS 1968) at the base of the Lower *crenulata* Conodont-Zone.

Other authors (e.g., HERBERT & SARMIENTO 1991, LLOYD 1982) suggested that warm (up to 30°C) relatively heavy surface waters with increased salinity experienced downwelling and therefore caused stagnant anoxic conditions at the bottom (GURSKY 1997, GURSKY 2006). GURSKY (1997) explained the anoxic conditions as a result of a transgression. Nutrient-rich soils were reworked, and highly productive shelf areas increased the input of C_{org}-rich material in the Kulm basin. At the same time, the O_2-ratio decreased because of increasing oxidation. Both factors lead to the sedimentation of phosphorite-rich black pelites.

SIEGMUND et al. (2002) explained the phosphatic, condensed shales of the mid-Tournaisian Event as indication for low current energy and anoxic conditions, in the water column and sediment as well (based on C/S ratios). They ascribed these conditions to eutrophication and high organic productivity caused by upwelling, improvement of the oceanic ventilation due to warm climate conditions, and volcanic nutrient input.

However, based on the ubiquitous evidence of bottom-currents, LAZAR et al. (2012) in general doubted whether there were ever extended time periods of a stratified water-column and anoxic bottom water conditions. They identified burrows and disturbed laminae in different shales that indicate benthic life, suggesting at least periodical oxygenation of the bottom water. Bioturbation happens soon after the deposition of the still very soupy sediment (80-90 % water content). Afterwards, structures experienced the same compaction as the sediment, leading to an unfamiliar appearance and making the identifiation difficult. This might be one of the reasons for the long-lasting misconception that black shales are anoxic and biota-free deposits.

According to ROSS & ROSS (1985, 1987, 1988) a transgression commenced at the end of the Upper Devonian and reached its peak during the Tn2a (middle Tournaisian). Subsequently, the sea level remained relatively high during the lower Carboniferous, intermitted by several phases of a slightly falling sea level (GURSKY 2006).

Strata that formed during the middle Tournaisian transgression are known from the European Variscides (Holy Cross Mountains/Poland, Moravia, Thuringia, The Rhenish Mountains, Belgium, France, the Cantabrian Mountains/NW Spain). They also occur in Morocco and as far as in the Urals, NE Siberia, China and North America (Canada, United States) (BECKER et al. 2006, HERBIG & BENDER 1992, SIEGMUND et al. 2002). They are also known from Belgium, the Rhenish Mountains and Marocco (BECKER et al. 1993, BECKER et al. 2006, POTY 2016). The accumulations can be divided into basin and platform facies. The platform

facies is dominated by mostly dark limestones and the basin facies by mostly blackish mudstones, a transition zone is marked by intercalations of these two facies.

According to Buggisch (2006), carbonate $\delta^{13}C$ and $\delta^{18}O$ values from conodont apatite suggest climatic cooling during the late Tournaisian, resulting from low atmospheric CO_2 concentrations. Because a waxing ice-cap and cooling of low-latitude surface waters do not match rising sea levels, Buggisch (2006) questioned the assumption that the mid-Tournaisian Event corresponded to a transgression. Similar results, based on $\delta^{13}C$ and $\delta^{18}O$ values from brachiopod shells, were presented by Mii et al. (1999). They assume a cooling and glaciation in the Tournaisian, beginning in the middle Kinderhookian. Wallace & Elrick (2014) support this assumption, based on their investigations on middle Tournaisian carbonates in central and western Montana. The isotopic shifts in $\delta^{18}O$ values of conodont apatite show several glacial-to-interglacial sea surface temperature (SST) changes of up to 4°C. The measurements imply that, in addition to an overall cooling and glaciation in the early Mississippian, the middle Tournaisian was characterized by superimposed orbital-scale climate changes which controlled pronounced changes in glacial ice volumes, eustatic changes, coastal-upwelling intensities, and tropical SSTs. Another finding of the study of the Tournaisian carbonates is, that tropical cooling is launched before polar cooling sets in, accompanied by initial sea-level fall due to glacier expansion.

It exists an ongoing discussion whether a transgression (Ross & Ross 1985, 1987, 1988; Krebs 1968, Gursky 1997, 2006) or a waxing ice cap (Mii et al. 1999, Buggisch 2006, Wallace & Elrick 2014) controlled the conditions under which the mid-Tournaisian sediments accumulated.

For the southeastern part of Laurussia, i. e. the area of this study, a moderately humid climate was assessed for the Tournaisian (Gursky 2006).

The study of conodont elements began in the late 19th century. Pander (1856) was the first to describe conodonts and assigned them to an unknown group of fishes, also introducing the term "conodont". In contrast to Pander (1856), Hinde (1879) supposed that differently shaped specimens were components of a single conodont species. Until the new suprageneric classification by Ulrich & Bassler (1926), many different opinions as to the zoologic affinities and the appropriate taxonomic base existed. Ulrich & Bassler (1926) supported Pander's assumption that only one morphotype would consitute a single species. The publications by Branson & Mehl (1933, 1934a, 1934b) initiated intensive conodont studies in Missouri for two decades, strongly increasing taxonomic diversity. From the 1940s onwards, acetic acid was used to extract conodont faunas from limestones, which allowed to assemble larger collections of well-preserved specimens in contrast to the common assemblage from shales or other disaggregated rocks before (Sweet 1988). The following expansion of large and stratigraphically well-controlled conodont collections evoked growing concerns about the taxonomy, culminating in the mid 1960s in an "era of multielement taxonomy" (Sweet 1988). While the study of conodonts was mainly carried out in North America between 1926 and 1950, the interest spread into nearly every part of the world after this period and the close coordination and cooperation among conodont researchers enabled a rapid growth of knowledge about conodonts (Sweet 1988). A significant achievement was the discovery of the relationship between the colour of the conodont element and the enclosing rocks by Epstein et al. (1977) and the development of the Colour Alteration Index (CAI).

Lower Carboniferous, mainly North American faunas were described by Hinde (1879), Roundy et al. (1926), Gunnell (1931), Branson (1934), Branson & Mehl (1933, 1934a, b,

1938a, b, 1941a, b), COOPER (1939) and HASS (1953, 1959) and provided an elaborate basis for conodont systematics and biofacies. Conodont faunas in Germany were described and discussed by e. g. BISCHOFF & ZIEGLER (1956), BISCHOFF (1957), VOGES (1959), CLAUSEN et al. (1989), BENDER et al. (1991), HERBIG & STOPPEL (2006), KAISER et al. (2017) and ESTEBAN LOPEZ et al. (2019). As exemplary studies on Belgian conodont research GROESSENS (1971, 1974), BELKA & GROESSENS (1986), and CONIL et al. (1990) are listed.

Essential works on the zonation of lower Carboniferous conodonts were published by SANDBERG et al. (1978) and LANE et al. (1980), who introduced the standard *Siphonodella* and post-*Siphonodella* zonations.

KAISER & CORRADINI (2011), PLOTITSYN & ZHURAVLEV (2016), KAISER et al. (2017), ZHURAVLEV (2017a, 2017b, 2019) and ZHURAVLEV & PLOTITSYN (2017, 2018) focused on the genus *Siphonodella* that is widely distributed in the lower Carboniferous and common in the samples described within this work.

The studied sections are situated in the Rhenish Mountains (sections Riescheid, Gladenbach and Wettmarsen) and in eastern Belgium in the Namur-Dinant Basin (section Dolhain). The sampling was focused on the strata of the middle Tournaisian Kahlenberg Fm, the equivalent Gladenbach Fm of the Hörre Nappe and the Pont d'Acrole Fm, cropping out in the Velbert Anticline and throughout the Aachen area and Belgium. The sections from the Rhenish Mountains represent deep-water accumulations influenced by turbidity currents originating from upper to middle slope areas. The Belgian section represents platform accumulations below the wave base.

The objectives of this work are:
- First or newly carried out sampling of conodont faunas in different facies of the middle Tournaisian
- Review and comparison of existing conodont biostratigraphic zonation models of the lower Carboniferous
- Establishment of microfacies types of all sections and reconstruction of sedimentary processes and the palaeoenvironment
- Application of conodont stratigraphy and biofacies zonation in order to confirm the age of the strata and to reconstruct the palaeoenvironment
- Application of sequence stratigraphy to correlate the studied sections and to support the reconstruction of sedimentary processes and the palaeoenvironment
- Identification of similarities and differences in the studied sections
- Testing the two very different assumptions of the origin of the mid-Tournaisian Event, which either accumulated during a transgression or during a phase of a waxing ice cap

1.1 Lower Alum Shale Event in the German Rhenish Mountains and in Belgium

The Lower Alum Shale Event (BECKER 1993) constitutes a widespread facies that was deposited during a transgressive phase, caused by glacio-eustatic sea-level changes (DAVYDOV et al. 2012). In Germany, it is mainly represented by the Kahlenberg Fm (ex: Liegende Alaunschiefer, KORN in AMLER & GEREKE 2003, STD 2016). It can be correlated to the Belgian Pont d'Arcole Fm (Hastarian, Diantian) and the Gladenbach Fm of the Hörre Zone, an allochthonous nappe within the eastern Rhenish Mountains.

This globally traceable event, also known as *crenulata*-transgression or *crenulata* Event (BECKER et al. 2006, KALVODA et al. 1999) caused, by the deposition of dark mudstones, black shales and dark limestones on the Anglo-Brabant platform (Fig. 2: green areas around the London-Brabant Massif), to a widespread facies alignment during the lower part of the middle Tournaisian (AMLER & HERBIG 2006).

Fluvial-lacustrine deposits
- Low to moderate sand content

Basin-fill deposits
- Deltaic (medium to coarse-grained sands)
- Shallow-marine (siliciclastic)
- Flysch (fine-grained)
- Deep-marine (bituminous, fine-grained)

Carbonate deposits
- Open-marine shelf (carbonates)
- Shallow-marine (coarse-grained, carbonates)

Sediment source and transport direction
- Caledonian uplands
- Variscan Orogen

- Erosional area
- Variscan Deformation Front (final position)
- Variscan Deformation Front
- Normal fault

Fig. 2 Dinantian palaeogeography of the area around Germany and Belgium, modified after KOMBRINK et al. in DOORNENBAL & STEVENSON (2010).

In the German Kulm basins (e.g., Rhenish Mountains, Thuringia), the transgression caused the disappearance of goniatite faunas at the end of the *Gattendorfia*-Stufe (cu I) as the formation of cephalopod limestones on drowned swell areas above Givetian to Frasnian reef structures ceased (BECKER 1993). It is marked by the extinction of all nectic and benthic macro-invertebrates as well as a radiolarian bloom (HERBIG 2011). Worldwide records (e.g., North America, SANDBERG et al. 1983 and China, BAI & NING 1988) report a discontinuity of pelagic macro-biota across the lower/middle Tournaisian boundary (BECKER 1993).

In Germany, a revision of the lithostratigraphic subdivisions proposed by KORN (2003, 2006, 2010) resulted in a more dynamic scheme for the Mississippian strata of the Rhenohercynian Kulm basin. Later adjustments of hierarchical ranks within units and reduction of the multitude of names resulted in the renaming of the "Liegende Alaunschiefer" to Kahlenberg-Formation.

In the Rhenohercynian Basin (within the Rhenohercynian Zone in Fig. 2), the lower Carboniferous is characterized by a pelagic starved basin stadium dominated by nectic and planktonic/pseudoplanctonic organisms such as radiolaria, conodonts and ammonoids (BENDER et al. 1993). Conodont faunas indicate pelagic, basinal conditions during the sedimentation of the Lower Alum Shale (BENDER et al. 1993).

In phosphorite nodules of the Lower Alum Shale, original sedimentary structures, such as laminae, composed of radiolarians, are preserved. Shales are compacted at a ratio of at least 1:6, and therefore nodules provide an excellent possibility to investigate the original sedimentary structures. The numerous radiolarians in the phosphorite nodules proof the presence of very great numbers of these organisms opposed to the surrounding shales, where they have been lost during the diagenetic removal of SiO_2 (BENDER et al. 1993).

In most of the Rhenish Kulm Basin, the Kahlenberg Fm is composed of typical black shales. They are thin-layered, fine-grained, contain organic matter (C_{org}) up to 7 %, and are free of carbonate. They also show the same lithology over vast extensions, lack fossils, except for rare phosphatized forms, contain phosphorite nodules, have varying pyrite content, and hardly contain any clastic material (KREBS 1968). GURSKY (1997) also mentions sparsely occurring layers hardened by siliceous material.

The Velbert Anticline in the westernmost Rhenish Mountains marks the transition into shallower facies, as seen by lateral substitution of the Kahlenberg Fm by the Pont d'Arcole Fm. In the area between the Velbert Anticline and Aachen, the "Pont d'Arcole Fm" always has a sharp contact to the underlying sediments of the Hastière Fm (AMLER & HERBIG 2006). This sharp contact is often marked by a sudden colour change from light coloured accumulations to dark shales (BENDER et al. 1993) and can be interpreted as a major sequence boundary (KORN 2010).

Referring to ARETZ et al. (2006), the "Pont d'Arcole Fm" (open-marine shelf on Fig. 2) and its deep-water equivalent, the "Kahlenberg Fm" (deep-marine on Fig. 2), form the best lithostratigraphic marker horizon into and in the Kulm basin.

In Belgium, the Pont d'Arcole Fm is one of the most argillaceous units of the Tournaisian (BERTOLA et al. 2013). However, relatively high carbonate contents of the shales imply that the carbonate production slowed down but did not fully cease (POTY et al. 2011).

In accordance with BERTOLA et al. (2013), the accumulations of the Pont d'Arcole Fm are barren of bioturbation and contain only rare open marine fossils. Such conditions suggest a quiet, probably locally dysoxic environment below the storm wave base. Distal storm deposits transported bioclast-rich beds into the accumulation area of the shales (BERTOLA et al. 2013).

In Belgium, the mid-Tournaisian Event corresponds to the RC1γ Subzone (CONIL et al. 1990, POTY et al. 2011) of the Tournaisian coral zones described by POTY (1985). The base of the RC1γ Subzone marks the base of the Pont d'Arcole Fm and is characterized by the appearance and dispersal of *Uralinia* (HANCE et al. 2006). The Pont d'Arcole Fm can also be correlated to the Cf1α" foraminifer subzone sensu CONIL et al. 1990 (HANCE & POTY 2002), which now is in the middle part of foraminifer zone MFZ 2 (POTY et al. 2006).

The coral zones, as well as the foraminiferal zones, can be applied in several European countries, in Asia and North Africa (Conil et al. 1990, Poty et al. 2014).

Conodont zonation is more difficult within the Belgian lower to middle Tournaisian due to the platform facies development. Therefore, there are fewer Belgian conodont zones within this interval than in basinal realms (for correlation of cononodont zones see chapter 2). Groessens (1974) defined three conodont zones (*Siphonodella, Polygnathus communis carina, Scaliognathus anchoralis*) for the Tournaisian. The *Siphonodella* Zone covers the time interval from "Tn1b" to "Tn2c" (Groessens 1974), in which the Pont d'Arcole Fm ("Tn2a" = middle Hastarian) is included.

In the Tournaisian (Hastarian and Ivorian) of Belgium, four third order sequences are recognized, a fifth cycle straddles the Tournaisian-Viséan boundary. The Pont d'Arcole Fm lies within the TST of Sequence 2 and consists of dark shales, crinoidal packstones and locally crinoidal cherty dolostones, alternating with each other. It correlates with the Lower Limestone shale of SW England and lies within the Mesothemic cycle D1b of Ramsbottom (1973) (Hance & Poty 2002).

In the area of the Velbert Anticline the *crenulata*-transgression caused the vast collapse of the carbonate production. Dark grey, slightly calcareous shales prevail in the Pont d'Arcole Fm. In the Herzkamp Syncline adjoining to the southeast, already typical black shales of the Kahlenberg Fm occur. In the Riescheid section, at its southern flank, the Lower Alum Shale facies is overlain by a dark, finely laminated, fine-grained limestone, that can be assigned to the *isosticha*-Upper *crenulata* conodont Zone (Lane & Ziegler 1978, Hartenfels et al. 2016). This limestone is interpreted to be the calciturbiditic highstand-shedding of Sequence 2, very similar to the time-equivalent Gladenbach Fm in the eastern Rhenish Mountains (Herbig & Bender 1992) (Amler & Herbig 2006, Herbig 2016). A thin package of overlying black shales, grading rapidly into siliceous shales and cherts, is not part of the Kahlenberg Fm anymore, but forms the TST of Sequence 3, respectively the base of the overlying Hardt Fm.

In the Belgian Namur-Dinant Basin the Pont d'Arcole Fm shows a similar development. It is encased by the limestones of the underlying Hastière Fm (lower Tournaisian) and the overlying Landelies Fm (middle to upper Tournaisian).

In the Dolhain section, the Pont d'Arcole Fm is composed of shaly limestones, and partly calcareous and siliceous shales of dark colour, showing a gradual transition to the limestones of the Landelies Fm as indicated by an increasing frequency and thickness of limestone beds that occur in the upper part of the Pont d'Arcole Fm. Bioclastic levels and numerous limestone nodules often contain fossils (Poty et al. 2011). First an increase of the water depth can be observed (culminating in dark grey shales), followed by a decrease that becomes obvious by the increasing presence of limestone beds.

1.2 Material and methods

Depending on the outcrop conditions the localities could directly be measured, described, and sampled or had to be cleaned from rock debris before. Limestone and shale samples were taken, making sure to sample all the occuring rock types and to have an appropriate sample interval for conodont stratigraphy.

In the laboratory, rock fragments were selected for the preparation of thin sections (for further proceeding see chapter 1.2.2). Samples for conodont extraction were subsequently selected and weighed before dissolving them in a 10% acetic acid or formic acid solution (for further description see chapter 1.2.1).

Based on the identified conodont elements, microfacies, and microfossils in thin-sections an attempt was made to reconstruct the original accumulation realm. Single-element conodont taxonomy was applied because multielement reconstructions for Tournaisian conodonts is still doubtful and not very common. All samples have been stored at the University of Cologne in the Institute of Geology and Mineralogy for future analyses.

In Riescheid, in the interval of the Kahlenberg Fm, ranging from bed 91b to bed 107TOP (HARTENFELS et al., 2016), 42 limestone and shale samples were taken. 16 limestone samples were selected to extract conodonts, whereas material of 41 shale and limestone samples was used for the preparation of thin-sections. Most of the conodont samples were barren, only sample Ri104c-e yielded five conodont elements.

The samples of the Gladenbach section were collected in 1990 by H.-G. Herbig & P. Bender. Sixteen samples were taken, most of them originating from fine-grained calciturbidites, only sample 7 originated from a siliceous limestone bed. First results including microfacies, cyclicity, and an overview of occurring microbiota from acid residues and thin-sections of carbonate rocks were published by HERBIG & BENDER (1992). Ostracoda described from the Gladenbach Fm (BLUMENSTENGEL et al. 1997) have been derived in part from these samples. Picked and partly sorted conodonts are the courtesy of P. Bender, thin-sections are the courtesy of H.-G. Herbig. The conodonts were restudied and new SEM photographs were generated within the scope of this study. A total of 4522 conodont elements were counted and identified. The existing thin sections (5.0 x 5.0 cm) were also restudied, and new photographs were taken, focusing on calcareous microbiota.

In Wettmarsen a single sample of the calciturbidite bed of the Kahlenberg Fm (middle Tournaisian) was taken to study the microfacies and the conodont fauna. The sample was very rich in conodonts and yielded 191 elements. Two thin-sections were produced before dissolving the remaining sample material for the conodont extraction.

In Dolhain, 34 rock samples originating from limestones, shaly limestones, calcareous shales, dark grey shales and siliceous shales were collected and eight samples were chosen for conodont extraction, yielding 102 conodont elements. Thirty-two thin-sections were prepared, including the thin-section of a not further studied coral found in bed 16.

1.2.1 Conodont extraction

Approximately 1 kg of limestone was collected for each sample. The limestone was cracked into smaller fragments. After determination of the exact sample weight, the limestone fragments were put into 10 l-buckets. The buckets were filled with a 10% acetic acid or formic acid solution in order to dissolve the carbonate fraction of the rock. After the end of the reaction the liquid was carefully decanted and refilled with fresh water for several times. The residue was then sieved and separated in five grain size fractions (> 4mm, 2.0-4.0mm, 1.0-2.0mm, 0.1-1.0mm, <0.1mm). After drying in the drying-oven, a heavy liquid

separation (LST Fastfloat, density: 2.80 ± 0.02g/mL) of the grain size fraction 0.1-1.0 mm was performed, separating conodonts and other heavier particles from the main portion of the residue. The heavy fraction was then studied using a Leica GZ6 binocular, and the conodonts were separated from the remaining residue using a picking dish. Conodonts from the Wuppertal Rniescheid section were directly picked without previous heavy liquid separation. Afterwards, the conodonts were identified, and SEM pictures were produced with a Zeiss Sigma 300VP.

1.2.2 Production of thin-sections

Before being able to cut the shales, they had to be molded in resin. Afterwards, the limestones and the hardened shales were cut in slices, and one surface was polished. The polished surface was then glued to a glass slide (7.5 x 10 cm), and the remaining rock was then first cut off and secondly grinded down, to a thickness of approximately 30-50 μm. The thin-sections were then studied under a Leica GZ6 binocular to examine microfacies and microfossils.

1.2.3 Abbreviations

ac. – *aculeatus*, *An*. – *Anchignathodus*, *Ba*. – *Bactrognathus*, *Bi*. – *Bispathodus*, *Br*. – *Branmehla, Cl*. – *Cloghergnathus*, *Clyd*. – *Clydagnathus*, *c*. – *communis*, *ca*. – *carina*, *D*. – *Dinodus*, *Do*. – *Dollymae*, *Dol*. – *Doliognathus*, *E*. – *Elictognathus*, *Eo*. – *Eotaphrus*, *Fa*. – *Falcodus*, Fm - Formation, FSST – Falling Stage Systems Tract, *Gn*. – *Gnathodus*, *H*. – *Hibbardella*, *Hi*. – *Hindeodella*, HST – Highstand Systems Tract, *I*. – *Icriodus*, LST – Lowstand Systems Tract, M – Morphotype, *M*. – *Mehlina*, *Me*. – *Mestognathus*, mfi – maximum flooding interval, *N*. – *Neopolygnathus*, NDB – Namur-Dinant Basin, *Neop*r. – *Neoprionidus*, *O*. – *Ozarkodina*, *Pa*. – *Palmatolepis*, *Pan*. – *Pandorinellina*, *Pa*r. –*Paragnathodus*, *Pat*. – *Patrognathus*, *Po*. – *Polygnathus*, *Pr*. – *Protognathodus*, *pr*. – *primus*, *Ps*. – *Pseudopolygnathus*, RKB – Rhenish Kulm Basin, *Sc*. – *Scaliognathus*, *Si*. – *Siphonodella*, *Sp*. – *Spathognathodus*, *St*. – *Staurognathus*, *Ta*. – *Taphrognathus*, *tr*. -*tiangulus*, TST – Transgressive Systems Tract, *Vo. – Vogelgnathus*.

2. Review of conodont zonation

The end of the "standard" biozonation? – Review and correlation of Tournaisian and lower Viséan (Mississippian) conodont biozonations

Abstract

The review of biozonation based on conodonts from the Tournaisian and Viséan shows that a world-wide applicable standard conodont zonation is very problematic. The presented biozonations for deep-water environments coincide in most parts with the standard zonation of SANDBERG et al. (1978) and LANE et al. (1980), whereas the biozonations for shallower-water environments only show minor conformities. Especially for conodont faunas originating from shallow-water environments the comparison with the "standard" zonation is not very successful. Therefore, we correlated numerous existing regional conodont biozonations for the Tournaisian and Viséan to allow a comparison despite differing conodont species that define the individual conodont zones. Sequence stratigraphy from the Belgian shallow-water environment (Namur-Dinant Basin, latest in POTY 2016, cum lit.) and the German deep-water Rhenish Kulm Basin (HERBIG 2016) were used to support the correlation. The 3rd order sequences of the Rhenish Kulm Basin correlate well with the conodont biozones, as their boundaries coincide with formation boundaries that are defined by conodont zones.

2.1. Introduction

In the past, numerous conodont biozonations were established. Many of them are only applicable regionally (e.g., VOGES 1959, GROESSENS 1974, PERRET 1989, HANCE et al. 2006, MALEC 2014), whereas others are considered to allow a world-wide correlation (SANDBERG et al. 1978, LANE et al. 1980, ZIEGLER & LANE 1987). The fact, that certain conodont species only occurred in certain ecological niches complicates the biostratigraphic correlation of differing depositional environments. It also reflects the main problem of the standard conodont biozonation. Some of the Tournaisian and Viséan conodont species that are used within these "standard" zonations are absent in the sedimentary record of many regions around the world. Many workers made the experience that a species, used to define a certain conodont zone, was absent in the rock successions studied by them and therefore erected own adjusted regional biozonations (e.g., KAISER et al. 2009, PERRET 1989, PERRET 1993). The correlation of the various regional conodont biozonations allows the comparison of different Tournaisian and Viséan sedimentary realms, where the "standard" zonations cannot be applied, and raises the question about the general applicability and suitability of the latter.

2.2. Conodont biozonations

The existing conodont biozonations for the Tournaisian and Viséan can be subdivided in three groups. The global "standard" biozonation, and regional deep-water biozonations are presented in Fig. 3, whereas regional intermediate and shallow-water biozonations are presented in Fig. 5.
The following chapters provide information on the geographic setting, information on the characteristics of the respective biozonations (correlation with conodont biozonations) as well as the properties of the investigated rock successions.

2.2.1 The global standard conodont biozonation

Sandberg et al. (1978) proposed a zonation for open-marine rock sequences of Europe and North America as a tool to correlate biostratigraphic units with standard stratigraphic units, as well as important rock units, much more precisely than before. Their biozones are based on conodont studies from Central Europe (Germany) and North America (Rocky Mountains and Upper Mississippi Valley). The life-span of *Siphonodella* from the late Devonian Middle *costatus*-Zone (note revision by Spaletta et al. 2017 of Middle and Upper *costatus* zones to *Bispathodus ultimus* Zone) to the top of the Kinderhookian (Tn3a) was used to erect seven biozones.

The proposed standard zonation by Ziegler & Lane (1987) is based on the occurence of worldwide identifiable evolutionary cycles in pectiniform conodont elements. From the upper Devonian to lower Pennsylvanian they recognized seven evolutionary cycles. Two of those cycles, the 5th in the Tournaisian and the 6th in the Viséan to lower Namurian, are considered in this review. The first appearance of the genus *Siphonodella* at the end of the Devonian and its rise in the Tournaisian form the base for this standard zonation, followed by the Mississipian genus *Gnathodus* which arose while the siphonodellids vanished. The next evolutionary step towards the top of the lower *typicus*-Zone was, beside the blossoming of the gnathodids and pseudopolygnathids, the worldwide emergence of the family Bactrognathodontidae, which experienced the extinction of most species near the top of the *anchoralis* Zone. No more significant evolutionary bursts of conodonts could be recognized thereafter.

The preliminary post-*Siphonodella* global standard zonation by Lane et al. (1980) is based on conodont faunas from western Europe and central and western North America and considers the interval from the Upper Tournaisian (*isosticha*-Upper *crenulata* Zone) to the Lower Viséan (above *texanus* Zone). The zonation is based on evolutionary first appearances of zone-defining taxa. The erected zones are also used in the proposed standard zonation by Ziegler & Lane (1987) as given in Fig. 3.

2.2.2 Regional conodont biozonation

The following biozonations, although of very different actualism, focus on a more or less regional application. First, biozonations for deep-water facies are presented (Fig. 3), followed by zonations for intermediate and shallower-water (Fig. 5). Fig. 4 and Fig. 6 show overview maps of the investigated areas in Europe and North America, respectively.

In Germany, deep-water accumulations settled in the Kulm basins. The biozonation presented herein is from the Rhenish Mountains.

Voges (1959) focused his studies on the Kulm facies of the Sauerland (northeastern part of the Rhenish Mountains). He examined the lower Carboniferous units of the Hangenbergkalk, Liegende Alaunschiefer (= Kahlenberg Fm), and Lydit- and Kieselkalkhorizonte (= Hardt Fm, Hillershausen Fm). Conodonts, obtained from limestones and imprints of conodont faunas in lydite horizons and alum shales, were used to erect a biozonation that - due to the very early state of knowledge - differs explicitly from the two zonations mentioned above.

Herbig & Stoppel (2006) reviewed the knowledge of lower Carboniferous conodonts for Germany (Rhenish Mountains). Their conodont zonation follows Gereke (2002) who used the *Siphonodella* standard zonation by Sandberg et al. (1978) for the lower and middle Tournaisian and the post-*Siphonodella* standard zonation of Lane et al. (1980) for the upper Tournaisian.

Fig. 3 Deep-water biozonation models, dashed lines mark uncertain boundaries, thick lines mark the Famennian-Tournaisian (Devonian-Carboniferous) and Tournaisian-Viséan boundary, striped signature represents periods without a conodont zone. Gaps, white areas represent stratigraphic intervals that were not studied by the particular author, dark grey areas mark Belgian sequences, light grey areas follow German sequences. – Note different chronostratigraphic scales used by authors.   * for discussion of the name see chapters 2.2.2 and 9

Correlation chart of deep-water conodont biozonation models (younger at top → older at bottom):

Author / Region	Biozones
Herbig (2016) 3rd order sequences	6, 5, 4, 3, 2, 1
Poty (2016) 3rd order sequences	6, 5, 4, 3, 2, 1
Malec (2014) after Wendt et al. (2009) — Holy Cross Mts (Poland)	praebilineatus, texanus, anchoralis, cuneiformis, delicatus, crenulata, sandbergi, duplicata, sulcata
Kalvoda et al. (1999) — Moravian-Silesian Zone (Middle Europe) deep-water	typicus, isosticha-Upper crenulata, Lower crenulata, sandbergi, duplicata, sulcata
Raven (1983)[1] Cantabrian Mnts; García-López & Sans-López (2002)[2] Cantabrian Mts	Gn. texanus Zone, Sc. anchoralis Zone[2], anchoralis-latus Zone[1], pseudosemiglaber Zone[1], cooperi-communis Zone[1], S. sulcata[2] Zone, Protognathodus fauna[1]
Perret (1993) — Pyrenees	Pseudognathodus homopunctatus, Sc. anchoralis, Gn. punctatus Siphonodella, Si. cooperi, Si. duplicata, Si. sulcata Pr. kockeli
Kaiser et al. (2009)[1] Carnic Alps, Graz Paleozoic, Montagne Noire, Pyrenees; Perri & Spalletta (1998)[2] Carnic Alps	texanus-homopunctatus, anchoralis-latus[2], U. typicus[2], L. typicus[2], isosticha-Upper crenulata[2], crenulata[1], quadruplicata[1], sandbergi[1], hassi[1]*, duplicata[1], bransoni[1], sulcata[1]; (U/L sandbergi[1], U/L duplicata[1], sul-cata[1])
Herbig & Stoppel (2006) — Germany, Kulm	homopunctatus, anchoralis, Upper/Lower typicus, isosticha-Upper crenulata, Lower crenulata, sandbergi, Upper/Lower duplicata, sulcata (cuII / cuI)
Korn & Weyer (2003) nach Ji (1985) — Rhenish Mts	crenulata Zone, quadripartita Zone, sandbergi Zone, hassi Zone*, duplicata Zone, bransoni Zone, sulcata Zone
Voges (1959) — Germany, Kulm	anchoralis-bilineatus-Interregnum, anchoralis-Zone, upper/lower Siphonodella crenulata Zone, Siphonodella-triangula-triangula-Zone, Siphonodella-triangula-inaequalis-Zone, kockeli-dentilineata-Zone (cuIIγ, cuIIβ, cuIIα, cuI)
Ziegler & Lane (1987) proposed standard zonation	texanus, anchoralis-latus, Upper typicus, Lower typicus, isosticha-U. crenulata, Lower crenulata, sandbergi, Upper duplicata, Lower duplicata, sulcata
Sandberg et al. (1978) — Europe, N-America	isosticha-Upper crenulata, Lower crenulata, sandbergi, Upper duplicata, Lower duplicata, sulcata
Substages	Chadian (late, early), Courceyan (late, early)
Stages	Viséan; Moliniacian, Ivorian, Hastarian; Tournaisian ("upper", "middle", "lower")

Voges (1959) subdivision markers: V2, V1b, V1a, Tn 3b-c, Tn3a, Tn 2b.

A more recent work on the stratigraphy of the Rhenish Mountains was published by Korn & Weyer (2003). They restudied five (Hasselbachtal, Oese, Apricke, Ober-Rödinghausen railway cut, Ober-Rödinghausen, road cut) Devonian-Carboniferous boundary sections at the northern margin of the Rhenish Mountains in order to investigate the lithology and attempted a correlation based on the carbonate content. Ammonoids and conodonts were used to confirm the correlation. The biozonation of Ji (1985) that covers the Upper Devonian to the lower middle Tournaisian was used and correlated with several conodont zonations of previous authors. Following Plotitsyn & Zhuravlev (2016), Zhuravlev & Plotitsyn (2017) and Zhuravlev & Plotitsyn (2018) we use the name "*Siphonodella hassi* Ji" provisionally (for further explanation see chapter 9) and therefore herein keep the name "*hassi* Zone" by Ji (1985).

A high-resolution correlation of condensed pelagic successions of the Carnic Alps, Montagne Noire (southern France) and the French Pyrenees was established by Kaiser et al. (2009). In the conodont biozonation their *quadruplicata* Zone is consistent with the Upper *sandbergi* Zone, and due to episodic rarity or the absence of siphonodellids close to the D/C boundary, the base of the Carboniferous is alternatively drawn with the entry of *Pr. kuehni* Ziegler & Leuteritz (1970). Again, the name "*hassi* Zone" was used.

Perri & Spaletta (1998) studied 19 lower Carboniferous pelagic limestone sequences of the Carnic Alps (northern Italy). For these deep-water deposits they applied the zonation by Lane et al. (1980) and Ziegler & Lane (1987). Based on the fact, that *Gn. typicus* and *Gn. texanus* are less frequent in European Carboniferous sequences than in North America, more frequent coeval species (*Gn. cuneiformis, Gn. punctatus, Ps. homopunctatus, Lo. cracoviensis, Gn. praebilineatus*) were used for biozonal subdivisons. In spite of that, they kept the *typicus* Zone for the late Tournaisian but named the lower Viséan *texanus-homopunctatus* Zone.

The following three zonations were applied in Spain and the French Pyrenees.

- Numerous outcrops that are characteristic for the carbonates of the Carboniferous in the Pyrenees (regions Bigorre, Béarn and Basque) were surveyed and analyzed by Perret (1989, 1993). As result, a general lithostratigraphic and biostratigraphic zonation was established. The lithology is dominated by pelagic basinal sediments (black shales with phosphatic nodules and lydites) and deeper marine platform carbonates (micritic nodular carbonates, finely laminated dark carbonates). Perret (1989, 1993) compared her own conodont zonation with several other zonations of the Pyrenees.
- Raven (1983) focused his studies on three large palaeogeographical units (Asturian geanticline, Palencian Basin, Asturo-Leonesian Basin) of the Cantabrian Mountains (northern Spain) and their diagenesis. However, due to limitations of the sequences and conodont faunas (*Pa.* occurs almost only in the Palencian Basin, *Si.* is very rare and specimens are broken, many hiatuses interrupt the condensed sequences) a detailed biozonation subdivision was not possible. Therefore, Raven (1983) proposed a conodont zonation model, modified after Higgins (1971), based on samples from the Asturo-Leonesian basin and the Asturian geanticlines.
- Garcia-Lopez & Sans-Lopez (2002) revised the biostratigraphy of the Devonian to lower Carboniferous of the Bernesga Valley (southern slope of the Cantabrian Zone) using conodont data, and discussed a correlation with other fossil groups. The rich cosmopolitan conodont faunas of the lower Carboniferous allow a correlation with the standard biozonation.

Deep-water accumulations in the Czech Republic and Poland can be found in the Moravian-Silesian Zone and the Holy Cross Mountains and are covered by the following two zonations.

- KALVODA et al. (1999) examined three deep-water carbonate successions in the Moravian-Silesian Zone (Czech Republic) at the D/C boundary in order to test the influence of eustatic, climatic and tectonic controls on sedimentation as well as conodont palaeoecology and taphonomy. They distinguished several eustatic sea-level changes and established a biofacies model for the studied interval. Their conodont zonation follows the standard biozonation, but is less differentiated.

Fig. 4 Overview map of Europe with the localities of the here presented conodont biozonations marked by asterisks.

- Deep-water carbonates from the D/C boundary in the region of the Holy Cross Mountains (Poland) and adjacent areas were investigated by MALEC (2014). For biostratigraphical purposes he used conodonts, microspores and deep-water ostracodes. The used conodont zonation follows WENDT et al. (2009), used for lower Tournaisian to Moscovian deposits (open marine, deltaic, shallow-subtidal, fluvial and continental) in the Algerian Sahara and is a compilation from SANDBERG et al. (1978), LANE et al. (1980), BELKA (1985), HIGGINS (1985), ZIEGLER & SANDBERG (1990), SKOMPSKI et al. (1995) and NEMYROVSKA (1999).

The two following publications concentrated on intermediate accumulation depths (carbonate platform, transition to basinal realm, basin slope) situated in Poland and the Czech Republic (Fig. 4, Fig. 5).

- BELKA (1985) investigated the conodont fauna of eight cores originating from lower Carboniferous carbonate rocks of the Moravia-Silesia Basin (southern

Fig. 5 Shallow-water biozonations, dashed lines mark uncertain boundaries, thick lines mark the Famennian-Tournaisian (Devonian-Carboniferous) and Tournaisian-Visean boundary, vertically ruled signature represents periods without conodont record, due to sedimentary gaps, or intervals out of the scope of the study. white areas represent stratigraphic intervals that were not studied by the particular author. Dark grey areas mark Belgian sequences, light grey areas follow German sequences.

Poland). Facies analysis permitted to distinguish the carbonate platform, the platform margin, the foreslope and the basin. For the conodont zonation the preliminary zonation (Sandberg et al. 1978, Lane et al. 1980) was adopted and some modifications were proposed to facilitate the usage. One modification was the replacement of the *typicus* Zone by the *cuneiformis* Zone, due to the rarity of *Gn. typicus* in European deposits. In contrary *Gn. cuneiformis* is frequent in Europe and North America.

- Foraminifera and conodont faunas in different facies of the basin slope at the D/C boundary in the southern part of the Moravian Karst (Czech Republic) were studied by Kalvoda et al. (2015). The four investigated sections revealed strong correlations in stratigraphy and biofacies to other European areas. An Eastern European conodont zonation was correlated with modified zonations by Ji (1985) and Kaiser et al. (2009).

The following publications focus on zonation models for shallow-water accumulations. For the shallow-water accumulations of Belgium four examples are given.

- Groessens (1971) was the first to erect a zonation based on conodonts for the upper Tournaisian of Belgium. He studied several localities in Belgium and divided the Tournaisian into two big conodont intervals. The *Siphonodella* beds range from the Calcaire d'Hastiere (Tn1b) to the Calcschistes de Maredsous (Tn2c) and the Gnathodid beds characterize the complete upper Tournaisian and can be further subdivided. The fine partition is based on the continuous evolution of worldwide known index fossils. Groessens (1971) used foraminifers to correlate his biozones with the traditional Belgian lithostratigraphic units but gave no graphic representation of his zonation. Webster & Groessens (1990) pictured the conodont zonation in their review. Later, Groessens (1974) established a biozonation based on conodonts for the Belgian shallow carbonate shelf accumulations of the Dinantian (Tournaisian and Viséan). Strikingly, he did not partition the *Siphonodella* Zone as it is done in previous zonations elsewhere. This is due to the fact that the Dinant Synclinorum is characterized by an extremly monotonous conodont fauna (high abundance, low diversity). Especially the siphonodellids do not allow a further subdivision and only the appearance of *Gn.* enables to differentiate the upper part of the *Siphonodella* Zone.

- The Dinantian and Namurian of the Franco-Belgian and Campine Basin were correlated by Conil et al. (1990). The distributioin of most characteristic and common fossil groups (conodonts, foraminifers, corals) was illustrated in three range charts. The conodont biozonation is very finely partitioned, especially in the upper Tournaisian and therefore not represented in Fig. 5. As observed by other authors neither *Si. praesulcata* nor *Si. sulcata* could be recognized in the basin and therefore, the exact conodont-based base of the D/C-boundary remains unknwon. Conil et al. (1990) noticed that abrupt fossil changes mark the bases of the Hastarian (base of Tournaisian), Ivorian, Moliniacian and Warnantian stages.

- During the lower Tournaisian, sediments in southern Belgium were accumulated on a ramp, whereas in the upper Tournaisian the environment shifted to shelf settings. Hance et al. (2006) identified four third-order sequences for that timespan and, based on the studies and reviews of Groessens (1974), Belka & Groessens (1986), Conil et al. (1990) and Webster & Groessens (1990) figured the presently valid conodont biozonation (Fig. 5).

Studies on Chinese and Russian shallow-water conodonts are depicted by the following two examples.

- Transgression-regression cycles of upper Famennian and lower Tournaisian age were examined by Ji & Ziegler (1992) to study the phylogeny, speciation and zonation of *Si.* in shallow-water facies accumulations of China. They recognized eight *Si.* species, three of them also reported from Russia. They subdivided the lower Carboniferous into six nearshore biofacies zones and illustrated the Russian species and their ranges within the Chinese *Si.* zonation.

Fig. 6 Map of Ozark Plateau, triangles mark conodont bearing localities used by Boardman et al. (2013), grey box within the small map of the USA marks the area of the Ozark Plateau.

- The Dinantian biozones in Ireland (Jones & Somerville 1996) can be correlated with zonations in Belgium (after Conil et al. 1990) and Russia (after Vdovenko et al. 1990, Makhlina 1996) (Fig. 5). The Irish zonation is based on data from exploration boreholes and mining companies that have been released in the 1980s, from the Dublin Basin, Shannon Trough and the platform areas of the Irish Midlands.

The final example in Fig. 5 concerns outer-shelf deeper-water environments along the southwestern edge of the Ozark Plateau (Kansas, Oklahoma, Missouri and Arkansas, United States) (Fig. 6).

- Boardman et al. (2013) investigated the Kinderhookian and Osagean formations of this area. They established an updated high-resolution zonation based on data from Thompson (1967) and Thompson & Fellows (1970), as well as on additional

data from 54 newly measured and sampled sections in southwestern Missouri, northwestern Arkansas and northwestern Oklahoma. It shows that the biozonation strongly deviates from the standard zonation and further zonations used in Europe.

2.3. Zonation structure and defining conodont species

Except for SANDBERG et al. (1978), many of the authors, assembled in the biozonation tables (Fig. 3, 5), did not give detailed descriptions of the conodonts used for their zonation models. In this chapter, defining conodonts of different zonations are discussed, based on reference to the standard biozonation. The present discussion on redefinition of the D/C-boundary (KAISER 2009, KAISER et al. 2009, BECKER et al. 2016) is not considered herein.

2.3.1 *sulcata* Zone (SANDBERG et al. 1978)

Lower limit: defined by the first appearance of *Si. sulcata* (HUDDLE 1934)
Upper limit: defined by the first appearance of *Si. bransoni* JI (1985) (= *Si. duplicata* (BRANSON & MEHL 1934), M1 (Morphotype 1))

Associated fauna: *Si. praesulcata, Pr. kuehni, Pr. meischneri, Pr. collinsoni, Pr. kockeli, Bi. stabilis* (here and in the following, *Bi. stabilis* is not differentiated further, because there were no additional specifications in the original text)*, Bi. ac. aculeatus, Bi. ac. anteposicornis, N. c. communis, Po. c. carina, Po. purus purus, Po. purus subplanus, Po. inornatus, Po. longiposticus, Po. spicatus, Ps. dentilineatus* and several further species of *Ps.* According to SANDBERG et al. (1978) *Pa. gracilis gracilis* may range into the lower part of the *sulcata*-Zone, but newer studies confirm that *Pa. gracilis gracilis* is reworked and does not occur in the *sulcata* Zone. *Pat. variabilis* occurs in this zone in the Western United States but not in Germany.

HERBIG & STOPPEL (2006) reported *Si. praesulcata, Si. sulcata, Bi. aculeatus, Bi. stabilis, N. c. communis, Po. symmetricus, Po. inornatus, Po. purus, Po. spicatus, Pr. meischneri, Pr. collinsoni, Pr. kockeli, Pr. kuehni, Ps. pr. primus* and *Ps. multistriatus* to be present in the **sulcata Zone** in Germany.

PERRET (1989, 1993) named this zone ***Siphonodella sulcata - Protognathodus kockeli* Zone**, upper and lower limit are in accordance with SANDBERG et al. (1978). As accompanying fauna in the Pyrenees she listed *Si. sulcata, Si. duplicata*, various *Pat., Ps. multistriatus, Ps. triangulus, Ps. c. carina, Po. spicatus* and *Pr. praedelicatus*.

The informal ***Protognathodus* fauna Zone** by HIGGINS & WAGNER-GENTIS (1982) was used by RAVEN (1983) for the lowest Tournaisian in the Cantabrian Mountains. In samples containing many specimens of *N. communis* several species of the genus *Pr.*, such as *Pr. kockeli, Pr. meischneri, Pr. kuehni* or *Pr.* spec. A VAN ADRICHEM BOOGAERT (1967) were present.

GARCIA-LOPEZ & SANS-LOPEZ (2002) reported findings of *Ps. dentilineatus, N. c. communis, P. inornatus, Ps. pr. primus, Bi. stabilis, Pr. kockeli, Pr. kuehni, Pr. meischneri and Si.* sp*.* in the *sulcata*-Zone in the Cantabrian Mountains.

KALVODA et al. (2015) defined the **sulcata Zone** in the Moravian Karst by the first occurrence of *Si. sulcata* and *Pr. kuehni*. The associated fauna consists of *Pr. meischneri, Pr. collinsoni* and *Pr. kockeli*. *Po. purus purus* and *Po. purus subplanus* have their FADs (first appearance date) in the zone.

The **homosimplex Zone** and the **levis Zone** by JI & ZIEGLER (1992), erected for South China, correlate with the *sulcata*-Zone by SANDBERG et al. (1978).

homosimplex Zone

Lower limit: defined by first appearance of *Si. simplex* Ji & Ziegler (1992)

Upper limit: defined by first appearance of *Si. levis* (Ni 1984)

Associated fauna: *Si. simplex* occurs with *N. c. communis, N. c. communis* with transverse ridges, *Po. inornatus, Po. longiposticus, Po. streeli, Po. parapetus, Bi. stabilis, Bi. ac. aculeatus, Pat.variabilis, Clyd. cavusformis, Clyd. gilwernensis* and *Pr. meischneri*.

levis Zone

Lower limit: defined by first appearance of *Si. levis* (Ni 1984)

Upper limit: defined by first appearance of *Si. sinensis* Ji (1985)

Associated fauna: *Si. levis* occurs with *Si. homosimplex, N. c. communis, N. c. communis* with transverse ridges, *Po. inornatus, Po. lobatus, Po. longiposticus, Po. streeli, Po. inparapetus, Pat. variabilis, Clyd. cavusformis, Clyd. gilwernensis, Pr. meischneri, Bi. ac. aculeatus* and *Bi. stabilis.*

2.3.2 Lower *duplicata* Zone (Sandberg et al. 1978)

Lower limit: defined by the first appearance of *Si. bransoni* Ji (1985) (= *Si. duplicata* (Branson & Mehl 1934), M1)

Upper limit: defined by the first appearance of *Si. cooperi* Hass (1959), M1

Associated fauna: *Si. duplicata* appears shortly after *Si. bransoni*, other important species in this zone are *Si. sulcata, Ps. dentilineatus, Ps. pr. primus* (including *Ps. triangulus inaequalis* as apossible junior synonym), *N. c. communis, Po. inornatus, Po. longiposticus, Po. purus purus, Po. purus subplanus, Bi. stabilis, Bi. ac. aculeatus, Pr. kockeli, Pr. kuehni, Pr. collinsoni, Pr. meischneri,* and rare *Pat. variabilis.*

Following Herbig & Stoppel (2006) *Si. praesulcata, Si. sulcata, Si. duplicata, Bi. ac. aculeatus, Bi. stabilis, N. c. communis, Po. symmetricus, Po. inornatus, Po. spicatus, N. c. carina, Po. purus, Ps. primus primus, Ps. multistriatus, Ps. triangulus, Pr. meischneri, Pr. collinsoni, Pr. kockeli, Pr. kuehni* and *Pr. praedelicatus* occur in the **lower *duplicata* Zone** in German deposits.

In the Moravian Karst, Kalvoda et al. (2015) subdivided their ***duplicata* Zone**, that correlates with the Lower *duplicata* Zone by Sandberg et al. (1978), in *bransoni* and *duplicata* Zone (following Ji, 1985, not depicted in Fig. 4). The *bransoni* Zone is based on *Si. bransoni* (= *Si. duplicata* M1) which is accompanied by *Ps. pr. primus* (first occurrence in the zone), *Ps. marginatus, Si. sulcata, Po. purus,* and *Po. purus subplanus*. The younger *duplicata* Zone (Kalvoda et al. 2015) is characterized by its index fossil *Si. duplicata*.

In the Carnic Alps, Kaiser et al. (2009) subdivided the Lower *duplicata* Zone into the *bransoni* Zone below and *duplicata* Zone above, now widely used in Europe and beyond (Fig. 1).

The shallow-water ***sinensis* Zone** by Ji & Ziegler (1992) coincides with the Lower *duplicata* Zone by Sandberg et al. (1978) that is applicable in deeper-water environments.

Lower limit: defined by first appearance of *Si. sinensis* Ji (1985)

Upper limit: defined by firs appearance of *Si. dasaibaensis* Ji, Qin & Zhao (1990)

associated fauna: Besides *Si. sinensis, Si. homosimplex, Si. levis, Po. inornatus, Po. lobatus, Po. rostratus, N. c. communis, Bi. stabilis* and *Bi. ac. aculeatus* are very common, *Po. Streeli* is rare.

The ***Siphonodella crenulata-Siphonodella lobata* Zone** by Boardman et al. (2013), erected for the Ozark Uplift (Kansas, Arkansas, Oklahoma & Missouri, United States), covers the lower part of the Tournaisian. In this work it was not possible to correlate the zone boundaries with the other zonation models.

Lower limit: defined by first appearance of *Si. lobata* (Branson & Mehl 1934) and

Si. crenulata (COOPER 1939) (seems to appear earlier than elsewhere)
associated fauna: common species are *Po. symmetricus, Ps. fusiformis* and *Ps. crenulatus*

2.3.3 Upper *duplicata* Zone (SANDBERG et al. 1978)

Lower limit: defined by the first appearance of *Si. cooperi* HASS (1959), M1
Upper limit: defined by the first appearance of *Si. sandbergi* KLAPPER (1966)
Associated fauna: *Si. sulcata, Si. duplicata* and *Si. bransoni*; *Si. cooperi* M1, appears almost simultaneously with *Si. duplicata* sensu HASS. The higher part of the Upper *duplicata*-Zone is marked by the almost simultaneous appearance of *Si. obsoleta* and *Si. cooperi* M2 in Europe and North America and of *Si. carinthiaca* in Europe. Additional important forms are *Ps. pr. primus, N. c. communis, Po. inornatus, Po. longiposticus, Po. purus purus, Po. purus subplanus, Bi. stabilis, Bi. aculeatus aculeatus, E. laceratus, Pr. kockeli, Pr. kuehni, Pr. collinsoni, Pr. meischneri* and uncommon *Pat. variabilis* and *Pan.* sp.
HERBIG & STOPPEL (2006) report the following species to be present in the upper **duplicata Zone** of Germany: *Bi. ac. aculeatus* and *Pr. kuehni* terminate within this zone. *Bi. stabilis, Si. sulcata, Si. duplicata, N. c. communis, Po. symmetricus, Po. inornatus, Po. purus, Po. spicatus, N. c. carina, Ps. pr. primus, Ps. multistriatus, Ps. triangulus, Pr. meischneri* and *Pr. praedelicatus* range throughout the zone and *Po. mehli* appears at the beginning of the *duplicata*-Zone. Although SANDBERG et al. (1978) define the upper *duplicata*-Zone with the first appearance of *Si. cooperi*, the species first occurs at the beginning of the younger *sandbergi*-Zone in the table of HERBIG & STOPPEL (2006).
PERRET (1989, 1993) did not subdivide the **duplicata Zone**. She defines the *duplicata* Zone with the appearance of *Si. duplicata* (=lower limit of lower *duplicata*-Zone of SANDBERG et al. 1978) at the base and *Po. mehli* in the upper part of the zone. During the whole range of the zone *N. c. communis, N. c. carina, Po. symmetricus Po. inornatus, Po. purus, Po. spicatus* and *Ps. triangulus* are numerous in the Pyreneean deposits.
The biozonation of JI (1985) covers the Upper Devonian to the lower middle Tournaisian. He substituted the Upper *duplicata* Zone for the "*hassi* Zone" (e. g. also used in KORN & WEYER 2003 and in KAISER et al. 2009). Following PLOTITSYN & ZHURAVLEV (2016), ZHURAVLEV & PLOTITSYN (2017) and ZHURAVLEV & PLOTITSYN (2018) we use the name "*Siphonodella hassi* JI" provisionally and therefore keep the "*hassi* Zone" by JI (1985).
The **belkai Zone** of KALVODA et al. (2015), ranges from within the upper part of the Lower *duplicata* Zone into the *sandbergi* Zone of the standard zonation of SANDBERG et al. (1978). It is characterized by "*Si. hassi*" (for discussion see chapter 9) and marked by the first appearance of *Si.* cf. *lobata*. In the Moravian Karst it is associated with *Si.* cf. *belkai, Ps. multistriatus, Ps. nodomarginatus, Ps. fusiformis, Po. fornicatus* and *Po. longiposticus*.

2.3.4 *sandbergi* Zone (SANDBERG et al. 1978)

Lower limit: defined by the first appearance of *Si. sandbergi* KLAPPER (1966)
Upper limit: defined by the first appearance of *Si. crenulata* (COOPER 1939)
Associated fauna: *Si.* species that range through the zone are *Si. sulcata, Si. obsoleta, Si. cooperi* M2, *Si. hassi* (for discussion see chapter 9) and *Si. duplicata. Si. bransoni* and *Si. cooperi* M1 are present in the *sandbergi* Zone but do not range as high as the first occurrence of *Si. lobata* close to the top of the zone. *Si. carinthiaca* is present in most of the zone and overlaps the lowest occurrence of *Si. lobata*. The following *Si.* species have their first occurrences in the *sandbergi* Zone and range higher: *Si.* cf. *Si. isosticha, Si. quadruplicata* and *Si. lobata.* Other important species are *Ps. dentilineatus, Ps. pr. primus,*

N. c. communis, Po. purus purus, Po. inornatus, Po. longiposticus, Bi. crassidentatus, Bi. stabilis, Bi. ac. aculeatus, E. laceratus, with uncommon *Pat. variabilis, Pan.* sp. and *N. c. carina* in North America and with *Ps.* cf. *Ps. fusiformis* sensu VOGES (1959) in Germany. *Si. lobata* and *Po. radinus* sensu VOGES (1959) have their first occurrences near the top of the zone.

In German deposits *Si. duplicata, Bi. stabilis, N. c. communis, Po. symmetricus, Po. inornatus, N. c.s carina, Po. purus Po. mehli, Ps. pr. primus, Ps. multistriatus, Ps. triangulus* and *Pr. praedelicatus* occur throughout the **sandbergi** Zone. *Si. cooperi, Si. sandbergi, Si. obsoleta, Si. lobata* and *Si. quadruplicata* have their first appearance within the zone (other authors, however report *Si. quadruplicata* already in the *duplicata* or *"hassi* Zone", e. g. KORN et al. 1994, ZHURAVLEV & PLOTITSYN 2018). *Si. sulcata, Pr. meischneri* and *Po. spicatus* die out in the lower part of the zone (HERBIG & STOPPEL 2006).

KAISER et al. (2009) and KORN & WEYER (2003) after JI (1985) subdivided the *sandbergi* Zone into a *sandbergi* Zone below and a *quadruplicata* Zone above, now widely used in Europe and beyond (Fig. 1).

JI & ZIEGLER (1992) erected the **dasaibaensis** Zone for South China, which equals the time range of Upper *duplicata* and *sandbergi* zones.

Lower limit: defined by first appearance of *Si. dasaibaensis* JI, QIN & ZHAO (1990)

Upper limit: defined by first appearance of *Si. eurylobata* JI (1985)

Associated fauna: *Si. homosimplex, Si. levis, Si. sinensis, Si. dasaibaensis, Si.* sp. A nov. (by JI & ZIEGLER 1992), *Si. obsoleta, D. leptus, D. fragosus, N. c. communis, Po. inornatus, Po. lobatus, Po. rostratus, Po. lancinatus, Po. monohumerus, Po. longiposticus, Bi. ac. aculeatus* and *Bi. stabilis* are very common. *Si.* cf. *isosticha* occurs only rarely.

2.3.5 Lower *crenulata* Zone (SANDBERG et al. 1978)

Lower limit: defined by the first appearance of *Si. crenulata* (COOPER 1939)

Upper limit: defined by the first appearance of *Gn. delicatus* BRANSON & MEHL (1938)

Associated fauna: next to *Si. crenulata* the *Si.* species that range throughout this zone are *Si.* cf. *Si. isosticha, Si. obsoleta, Si. cooperi* M2, *Si. quadruplicata* and *Si. lobata.* Species that die out within this zone are *Si. sulcata, Si. sandbergi, Si. hassi,* and *Si. duplicata. Si. obsoleta ---> isosticha* and *Si. isosticha* have their first occurrences within the Lower *crenulata* Zone. Other important species include *Ps. marginatus, Ps. tr. triangulus, Ps. pr. primus, Ps. dentilineatus, Ps. fusiformis, Ps. lobatus, N. c. communis, Po. inornatus, Po. longiposticus, Bi. stabilis, Bi. aculeatus, "Sp." crassidentatus, "Sp." abnormis, E. bialatus, E. laceratus, Fa. angulus, D. fragosus, D. leptus* and *D. yougquisti.* In North America *Pat. andersoni, Pan.* sp., *N. c. carina, Pr. kockeli, An. penescitulus* and *Ps. radinus* occur scarce, which indicates that they may be "stragglers" (SANDBERG 1976) from a more shoreward or shallower biofacies.

HERBIG & STOPPEL (2006) listed the following conodonts in their table of German Mississippian conodonts for the Lower *crenulata* Zone: *Bi. stabilis, N. c. communis, Po. symmetricus, Po. inornatus, N. c. carina, Po. mehli, Ps. pr. primus, Ps. multistriatus, Ps. triangulus, Pr. praedelicatus, Si. cooperi, Si. obsoleta, Si. lobata* and *Si. quadruplicata* range throughout the zone. *Po. purus, Si. duplicata* and *Si. sandbergi* terminate within the zone and *Si. crenulata* appears in this zone.

The **cooperi** Zone used by PERRET (1989, 1993) in the Pyrenees is equivalent to the *sandbergi* and Lower *crenulata* Zone by SANDBERG et al. (1978). It contains *Si. duplicata, Si. cooperi, Si. obsoleta, Si. quadruplicata, Si. isosticha, Si. lobata, Si. explicata, Si. crenulata, Po. mehli, Po.*

inornatus, Po. symmetricus, Po. purus, N. c. communis, N. c. carina, Ps. triangulus and *Ps. multistriatus.*

The ***cooperi-communis* Zone** by Raven (1983) is based on the *Siphonodella cooperi-Polygnathus communis* Zone by Higgins (1974). It begins in the upper Upper *duplicata*-Zone and ranges to the end of the Lower *crenulata*-Zone of Sandberg et al. (1978). Raven (1983) redefined the upper boundary of the zone at the first occurrence of *Gn. pseudosemiglaber*. The zone is dominated by *N. c. communis* and *Po. inornatus* but characterized by few specimens of *Gn. delicatus, Gn. cuneiformis, Gn. typicus, Si. obsoleta* and *Si. cooperi*. Referring to Raven (1983), the proposed name of the zone by Higgins (1974) was unfortunate, as *Si. cooperi* is very rare and *N. c. communis* is very common in all faunas of Famennian and Tournaisian age in the Cantabrian Mountains and therefore the name-giving species are either often not traceable or present in other conodont zones as well (*N. c. communis* occurs in the *sulcata* to *anchoralis* zones).

The ***crenulata partial-range* Zone** of Belka (1985) corresponds to the Lower *crenulata* Zone by Sandberg et al. (1978).

Lower limit: defined by first appearance of *Si. crenulata* (Cooper 1939)

Upper limit: defined by first appearance of *Gn. delicatus* Branson & Mehl (1938)

Associated fauna: *Si. crenulata* (both morphotypes), *Si. duplicata, Si. cooperi* M2, *Si. lobata, Si. quadruplicata, Si. obsoleta, Bi. ac aculeatus, Bi. stabilis, N. c. communis, Po. inornatus, Po. purus purus, Po. purus subplanus, Po. symmetricus, Po. triangulus,* non-platform elements: *E. peculiaris, D. fragosus, D. leptus* and *D. wilsoni*

From the Moravian Karst Kalvoda et al. (2015) reported the ***quadruplicata* Zone**, which equals the upper part of the *sandbergi*- and the Lower *crenulata*-Zone of Ziegler & Lane (1987). The zone is recognized by the presence of the index fossil *Si. quadruplicata*, associated by *Si.* cf. *sandbergi, Si. lobata*, "*Si. hassi*" (for discussion see chapter 9)*, Si. obsoleta, Ps. tr. triangulus, Po. inornatus inornatus* and *Po. inornatus rostratus*. This fauna is accompanied by the following species that correspond to the *crenulata*-Zone: *Si. crenulata, Si.* cf. *crenulata* (elements bearing transitional features from *Si. hassi*)*, Si. cooperi, Po. parapetus, N. c. communis* (assumption of the author, no image in the original publication)*, Po. purus purus* (assumption of the author, no image in the original publication) and *M.* sp. Note well that the zone corresponds to the *Si. quadruplicata* Zone of the Russion platform (Jones & Sommerville 1996, after Vdovenko et al. 1990), but differs from the *quadruplicata* Zone of Kaiser et al. (2009) from the Carnic Alps that only equivalents the Upper *sandbergi* Zone.

In Belgium, the ***Siphonodella* Zone** by Groessens (1974) covers the time span from the beginning of the *sulcata* Zone to the end of the Lower *crenulata*-Zone by Sandberg et al. (1978); the uppermost part of the *Siphonodella* Zone by Groessens (1974) is characterized by *Gnathodus* and coincides with the *isosticha*-Upper *crenulata* Zone by Sandberg et al. (1987). Due to unfavorable facies conditions siphonodellids are very rare in Belgian deposits. The species described by Groessens (1974) in this zone are *Si. cooperi, Si. obsoleta, Po. inornatus, Ps. dentilineatus* and *Ps. pr. primus*. Hance et al. (2006) indicate the consecutive entry of siphonodellid species in the zone, without indicating (sub-) zonal boundaries.

The **Early *eurylobata* Zone** of Ji & Ziegler (1992) coincides with the Lower *crenulata* Zone of Sandberg et al. (1978).

Lower limit: defined by first appearance of *Si. eurylobata* Ji (1985)

Upper limit: defined by last appearance of *Si. sinensis* Ji (1985)

Associated fauna: *Si. homosimplex, Si. levis, Si. sinensis, Si. dasaibaensis, Si. eurylobata, Si. obsoleta, Si. crenulata* M2, *Si.* cf. *isosticha, Si. isosticha, D. leptus, D. fragosus, D.* ? *wilsoni, N. c. communis, Po. inornatus, Po. rostratus, Po. bischoffi, Po. lancinatus, Po. monohumerus, Po. longiposticus, Bi. ac. aculeatus* and *Bi. stabilis* are very common in this zone.

The **Siphonodella cooperi-Gnathodus delicatus Zone** of BOARDMAN et al. (2013) covers the middle part of the Kinderhookian (lower to middle part of the Tournaisian) in the Mid-west of the United States. The exact boundaries of the zone are difficult to evaluate. The zone is defined by the presence of *Si. cooperi, Si. quadruplicata, Pr. praedelicatus, Pr.* n sp. 1 BOARDMAN et al., 2013 and the likely ancestor to *Gn. puntatus* (*Gn*. n. sp. 1, BOARDMAN et al. 2013) as well as the appearances of *Gn. delicatus* and *Gn. typicus.* The occurrence of earliest gnathodids, however indicates that the zone, at least partially coincides with the *isositcha*-Upper *crenulata* Zone (LANE et al. 1980).

2.3.6 *isosticha*-Upper *crenulata* Zone (SANDBERG et al. 1978)

Lower limit: defined by the first appearance of *Gn. delicatus* BRANSON & MEHL (1938)
Upper limit: defined by the last appearance of *Si. isosticha* (COOPER 1939), last appearance of the genus *Siphonodella* and appearance of *Gn. typicus* M2

Associated fauna: The ranges of *Si. crenulata, Si. lobata, Si. quadruplicata, Si. cooperi* M2, *Si. obsoleta ---> isosticha* and *Si.* cf. *Si. isosticha* terminate within this zone. *Gn. delicatus* and *Gn. punctatus* range throughout and above this zone. Other important species that occur throughout this zone are *N. c. communis, Po. inornatus, Po. longiposticus, Bi. stabilis, D. fragosus, D. leptus, D. youngquisti, E. bialatus, E. laceratus, Fa. angulus* and *Ps. tr. triangulus. Ps. tr. pinnatus* first appears in this zone and ranges higher whereas *Ps. marginatus* apparently terminates within the *isosticha-* Upper *crenulata*-Zone. *Pat. andersoni, An. penescitulus, Ps. radinus* and *N. c. carina* occur only erratically and in small numbers throughout this zone. Transitional forms between *Gn. punctatus* and *Gn. semiglaber* first appear near the top of the zone.

In contrast to SANDBERG et al. (1978) HERBIG & STOPPEL (2006) erroneously indicated in their table, without further discussion, *Si. isosticha* as well as some other siphonodellid species to range up to the end of the Lower *typicus* Zone or even higher. This was mostly based on VOGES (1959) who did not yet recognize the *typicus* Zone between his Upper *crenulata* and *anchoralis* zones. Referring to HERBIG & STOPPEL (2006) *Bi. stabilis, N. c. communis, Po. symmetricus, Po. inornatus, N. c. carina, Po. mehli, Ps. pr. primus, Ps. multistriatus, Ps. triangulus, Ps. pinnatus, Pr. praedelicatus, Si. cooperi, Si. obsoleta, Si. lobata, Si. quadruplicata* and *Si. crenulata* range throughout the **isosticha-Upper *crenulata* Zone** in German deposits. *Gn. punctatus, Gn. delicatus* and *Si. isosticha* appear at the beginning of the zone and *Gn. semiglaber* occurs in the upper part of the zone.

From the Carnic Alps, PERRI & SPALETTA (1998) also report *Ps. multistriatus, Si. isosticha* and *Do. sagittula* as associated fauna in the **isosticha-Upper *crenulata* Zone**.

BELKA (1985) erected the **delicatus consecutive-range Zone** that corresponds to the *isosticha*-Upper *crenulata*-Zone by SANDBERG et al. (1978)

Lower limit: defined by first appearance of *Gn. delicatus* BRANSON & MEHL (1938)
Upper limit: defined by first appearance of *Gn. cuneiformis* MEHL & THOMAS (1947)
Associated fauna: *Gn. delicatus, Gn. punctatus, Gn. typicus* M1, *N. c. communis, N. c. carina, Po. flabellus, Po. inornatus, Bi. stabilis, Clyd. unicornis, Pr. praedelicatus. Si. obsoleta, Si.*

obsoleta ---> *isosticha* and *Si. isosticha* extinct within this zone; *Me. groessensi, Eo. bultyncki* and *Ps. multistriatus* M1 have their first appearance in the zone.

The **Late *erylobata* Zone** by Jɪ & Zɪᴇɢʟᴇʀ (1992), established for South China, correlates with the *isosticha*-Upper *crenulata* Zone by Sᴀɴᴅʙᴇʀɢ et al. (1978).

Lower limit: defined by the last appearance of *Si. sinensis* Jɪ (1985)

Upper limit: defined by the last appearance of *Si. levis* (Nɪ 1984)

Associated fauna: *Si. homosimplex* and *Si. levis* dominate the zone, whereas Si*. eurylobata* is relatively rare. Other occurring species are *Si. crenulata* M2, *Si. obsoleta, Si. isosticha, Po. inornatus, Po. bischoffi, Po. rostratus, N. c. communis, D. fragosus, Bi. ac. aculeatus* and Bi*. stabilis.*

Bᴏᴀʀᴅᴍᴀɴ et al. (2013) erected the ***Siphonodella cooperi hassi*-Lower *Gnathodus punctatus* Zone** that coincides with the *isosticha*-Upper *crenulata* Zone by Sᴀɴᴅʙᴇʀɢ et al. (1978). The zone is defined by the appearance of *Gn. punctatus* in addition with the high abundance of *Si. cooperi hassi* (Tʜᴏᴍᴘsᴏɴ & Fᴇʟʟᴏᴡs 1970) and the first appearance of *Gn. semiglaber* within this zone.

2.3.7 Lower *typicus* Zone (Lᴀɴᴇ et al. 1980)

Lower limit: defined by first appearance of *Gn. typicus* Cᴏᴏᴘᴇʀ (1939) M2

After Hᴇʀʙɪɢ & Sᴛᴏᴘᴘᴇʟ (2006) the following species occur throughout the zone: *Bi. stabilis, N. c. communis, Po. symmetricus, Po. inornatus, N. c. carina, Po. mehli, Ps. multistriatus, Ps. triangulus, Ps. pinnatus, Pr. praedelicatus, Si. cooperi* (exact range is unknown within this zone), *Si. obsoleta, Si. lobata, Si. quadruplicata* (exact range is unknown within this zone)*, Gn. punctatus, Gn. delicatus* and *Gn. semiglaber. Ps. pr. primus, Si. crenulata and Si. isosticha* die out at the end of the zone whereas *Gn. cuneiformis* and *Gn. typicus* first appear at the beginning of the Lower *typicus* Zone. For the erroneous attribution of siphonodellids to the zone see chapter 2.3.6.

Bᴇʟᴋᴀ (1985) proposed to substitute the *typicus* Zone by the ***cuneiformis* Zone** because *Gn. typicus* is relatively rare in European sediments and *Gn. cuneiformis* can be found in European and North American deposits and the stratigraphic distribution of both species nearly overlaps. In the Carnic Alps *Gn. typicus* is very rare and therefore Pᴇʀʀɪ & Sᴘᴀʟʟᴇᴛᴛᴀ (1998), following Bᴇʟᴋᴀ (1985), used *Gn. cuneiformis* to define the base of the Lower *typicus* Zone.

The ***Polygnathus communis carina*-Upper *Gnathodus puntatus* Zone** and the **Lower *Pseudopolygnathus multistriatus* Zone** by Bᴏᴀʀᴅᴍᴀɴ et al. (2013) are in accordance with the Lower *typicus* Zone by Lᴀɴᴇ et al. (1980).

The ***Polygnathus communis carina*- Upper *Gnathodus puntatus* Zone** coincides with the base of the Osagean.

Lower limit: defined by first appearance of *N. c. carina* Hᴀss (1959)

Upper limit: defined by first appearance of *Ps. multistriatus* Mᴇʜʟ & Tʜᴏᴍᴀs (1947)

Associated fauna: The defining species *N. c. carina* is accompanied by *N. c. communis, Gn. punctatus, Gn. semiglaber* and *Gn*. n. sp. 2 Bᴏᴀʀᴅᴍᴀɴ et al, 2013.

Lower *Pseudopolygnathus multistriatus* Zone

Lower limit: defined by first appearance of *Ps. multistriatus* Mᴇʜʟ & Tʜᴏᴍᴀs (1947)

Upper limit: defined by first appearance of *Gn. cuneiformis* Mᴇʜʟ & Tʜᴏᴍᴀs (1947)

Associated fauana: The zone is also characterized by the first appearance of the genus *Ba.* and the appearances of several new, not named species of the genus *Gnathodus* (Bᴏᴀʀᴅᴍᴀɴ et al. 2013).

2.3.8 Upper *typicus* Zone (LANE et al. 1980)

Lower limit: defined by first occurrence of *Ps. nudus* PIERCE & LANGENHEIM (1974) and
      Ps. oxypageus LANE, SANDBERG & ZIEGLER (1980)

Upper limit: defined by first appearance of either *Dol. latus* or *Sc. anchoralis*

Associated fauna: *Ps. oxypageus, Do. bouckaerti, Ps. pinnatus, Gn. semiglaber* and *Gn. cuneiformis*.

In Germany the species *Bi. stabilis, N. c. communis, N. c. carina, Po. symmetricus, Po. inornatus, Po. mehli, Ps. multistriatus, Ps. triangulus, Ps. pinnatus, Pr. praedelicatus, Si. obsoleta, Gn. punctatus, Gn. delicatus, Gn. semiglaber, Gn. cuneiformis* and *Gn. typicus* occur throughout the Upper *typicus*-Zone. *Ps. nudus* and *Ps. oxypagaeus* first appear at the beginning of the zone and *Pr. cordiformis* appears within the Upper *typicus* Zone (HERBIG & STOPPEL 2006). For the presumed occurrence of siphonodellids see chapter 2.3.6.

Because PERRI & SPALLETTA (1998) could not detect any specimens of the defining species for the base of this zone in the Carnic Alps, they used associated taxa.

The ***Gnathodus punctatus-Siphonodella* Zone** established in the Pyrenees by PERRET (1989, 1993) includes the *isosticha*-Upper *crenulata*, Lower *typicus* and Upper *typicus* zones of SANDBERG et al. (1978) and LANE et al. (1980). The base of the zone is marked by the appearance of the gnathodids and the replacement of the siphonodellids. It is also characterized by the presence of *Ps. pinnatus. Gn. punctatus, Gn. delicatus, Gn. cuneiformis, Gn. semiglaber, Gn. typicus, Gn. pseudosemiglaber, Sc. anchoralis, Po. inornatus, Po. symmetricus, N. c. communis, N. c. carina, Po. mehli, Po. purus, Pr. praedelicatus, Pr. cordiformis, Ps. triangulus, Ps. multistriatus, Ps. pr. primus, Bi. stabilis, Pr. cordiformis, Do. hassi, Do. bouckaerti* and *Eo. bultyncki*.

The ***pseudosemiglaber* Zone** of RAVEN (1983) includes the *isosticha*-Upper *crenulata* Zone, the Lower *typicus* and the Upper *typicus* zones, i. e. has the same range as the *Gn. punctatus-Siphonodella* Zone in the Pyrenees. He reported associations of *Gn. pseudosemiglaber, Si., Ps. marginatus, Ps. pr. primus* and *Po. purus* from the zone. The lower limit is defined by the first occurrence of *Gn. pseudosemiglaber* and the upper limit by the first occurrence of *Sc. anchoralis* or *D. latus.* The associated fauna is dominated by various species of the genus *Gn.* and accompanied by species of *Po., Si., Ps.* and *Bi.* According to RAVEN (1983) *Ps. marginatus, Si. isosticha and Si.* spec. A VAN ADRICHEM BOOGAERT (1967) only occur within this zone.

The ***cuneiformis* consecutive-range Zone** by BELKA (1985) correlates with the Lower and Upper *typicus* zones of LANE et al. (1980).

Lower limit: defined by first appearance of *Gn. cuneiformis* MEHL & THOMAS (1947)

Upper limit: defined by first appearance of *Sc. anchoralis europensis* LANE & ZIEGLER (1983)
      and/or *Dol. latus* BRANSON & MEHL (1941b)

Associated fauna: *Ps. multistriatus* M1, *N. c. communis, Po. flabellus, Po. inornatus, Po. longiposticus, Me. groessensi, Bi. stabilis;* within this zone *Pr. cordiformis, Ps. osypageus, Ps. pinnatus, Do. bouckaerti* and *Sc. praeanchoralis* enter; *Gn. punctatus* and *Gn. delicatus* die out before the end of the zone

The ***Polygnathus communis carina* Zone** erected by GROESSENS (1974), and still in use (e. g. CONIL et al. 1990, HANCE et al. 2006) for the Belgian deposits coincides with the Lower *typicus* and Upper *typicus* zones of LANE et al. (1980). Its base marks the base of the Ivorian substage. The zone is characterized by the species *N. c. carina* and begins after the extinction of the genus *Si.* in Belgium. It is accompanied by *Ps. multistriatus, Ps. triangulus pinnatus, Ps. triangulus triangulus* and *Gn. semiglaber.* GROESSENS (1974) also erected four sub-zones the ***Dollymae hassi* and *Dollymae* sp. A. VOGES Subzone**, the ***Spathognathodus***

(=Eotaphrus) **cf.** *bultyncki* **Subzone**, the ***Spathognathodus (=Eotaphrus) bultyncki* Subzone** and the ***Dollymae bouckaerti* Subzone**. Later, a fifth subzone, the *P. c. carina* Subzone was inserted between the *D. hassi* and *E.* cf. *bultyncki* subzones (see Conil et al. 1990).

The ***Dollymae hassi* and *Dollymae* sp. A. Voges Subzone** forms the base of the *Po. communis carina* Zone. *Do. bouckaerti, D.* sp. A and *D. hassi* are present within the sub-zone. The beginning of the ***Spathognathodus (Eotaphrus)* cf. *bultyncki* Subzone** was chosen by Groessens (1974) to lie within the Tn3b/Tn3c boundary and is characterized by the name giving species/its eponym. The ***Spathognathodus (Eotaphrus) bultyncki* Subzone** is defined by the presence of *Sp. bultyncki* and ends with the appearance of *Do. bouckaerti*. The ***Dollymae bouckaerti* Sub-zone** is defined by the presence of *D. bouckaerti*.

The **Upper *Pseudopolygnathus multistriatus-Gnathodus cuneiformis* Zone** erected by Boardman et al. (2013) in the U. S. Midwest correlates with the Upper *typicus* Zone by Ziegler & Lane (1987).

Lower limit: defined by appearance of *Gn. cuneiformis* Mehl & Thomas (1947) within the range of *Ps. multistriatus* Mehl & Thomas (1947)

Upper limit: defined by first appearance of *Dol. latus* Branson & Mehl (1941b) or *Sc. anchoralis* Branson & Mehl (1941b)

Associated fauna: *St. cruciformis* and *Gn.* n. sp. 9 (*aff. antetexanus*) first appear within this zone, and great abundances of *Ba. excavata* are present.

2.3.9 *anchoralis* Zone (Bischoff 1957)

The *anchoralis* Zone (including differing naming such as *Scaliognathus anchoralis* Zone, *anchoralis-latus* Zone, etc.) is one of the most wide-spread, almost globally recognized conodont zones of the Mississippian. Established by Bischoff (1957) and subsequently used by Voges (1959) in Germany, its faunal content and ranges remained virtually unchanged (Lane et al. 1980). Specific differentiation of subspecies of *Scaliognathus* were done by Lane & Ziegler (1983).

Lower limit: defined by first appearance of *Sc. anchoralis europensis* Lane & Ziegler (1983) and/or *Dol. latus* Branson & Mehl (1941)

Upper limit: defined by first appearance of *Gn. texanus* Roundy (1926)

Associated fauna: the life-span of *Sc. anchoralis europensis* and *Hi. segaformis* is almost identical with the range of the zone; other species that terminate within the zone are *Dol. latus, Eo. burlingtonensis, Bi. stabilis, Po. bischoffi, Po. flabellus, Po. inornatus, Ps. multistriatus* M1, *Ps. oxypageus, Ps. pinnatus, Pr. cordiformis, Gn. cuneiformis, Gn. delicatus, Gn. typicus* M2 and *Me. groessensi., Gn. pseudosemiglaber* and *Gn. semiglaber* have their first appearance within the zone but range higher. Reports of *Gn. homopunctatus* and *Gn. symmutatus* probably rely on reworked *Sc. anchoralis* at the base of the overlying *Gn. homopunctatus* Zone.

Referring to Herbig & Stoppel (2006) *Bi. stabilis, N. c. communis, Po. inornatus, Po. mehli, Ps. multistriatus, Ps. triangulus, Ps. pinnatus, Gn. delicatus* and *Pr. cordiformis* die out at the end of the *anchoralis* Zone in Germany. The occurrence of *Si. obsoleta* is erroneous (see chapter 2.3.6). *Po. symmetricus, N. c. carina, Pr. praedelicatus, Gn. punctatus, Gn. typicus, Ps. nudus* and *Ps. oxypageus* terminate already within the zone. *Gn. semiglaber* and *Gn. cuneiformis* range throughout the *anchoralis*-Zone and *Po. bischoffi* and *Gn. pseudosemiglaber* first appear at the beginning of this zone. *Gn. texanus, Gn. austini* and *Me. beckmanni* occur within the uppermost part of the zone. The following species appear at the beginning of the zone and terminate within it: *Do. bouckaerti, Dol. latus* and *Sc.*

anchoralis fairchildi. Sc. anchoralis europensis, Sc. a. anchoralis and *Hi. segaformis* occur only throughout this zone and *Do. hassi* is only present in the last third of the *anchoralis-*Zone.

Perri & Spalletta (1998) followed Lane et al. (1980) and used the term ***anchoralis-latus* Zone** in the Carnic Alps. They defined the zone by the presence of *Sc. anchoralis* (*Sc. anchoralis anchoralis* and *Sc. anchoralis europensis*) and *Dol. latus.* Along with them *Hi. segaformis, Ps. pinnatus* M2, *Gn. pseudosemiglaber, Gn. cuneiformis* and *Gn. semiglaber* are present.

According to Perret (1989, 1993) the ***Scaliognathus anchoralis* Zone** is characterized by the presence of the genus *Scaliognathus*. It begins with the appearance of *Sc. praeanchoralis, Sc. dockali, Sc. anchoralis fairchildi* and *Dol. latus* and ends with the disappearance of *Scaliognathus. Pr. praedelicatus, Ps. triangulus, N. c. carina, Po. mehli, Do. bouckaerti* and *Pr. cordiformis* only occur in the lower half of the zone. *Bi. stabilis, Po. inornatus, Po. symmetricus, Gn. delicatus, Gn. cuneiformis* and *Ps. pinnatus* appear until the top of the zone. *Gn. semiglaber, Gn. pseudosemiglaber* and *Gn. typicus* continue into the next zone after this zone. Other species that are present in the upper part of the *Sc. anchoralis* Zone in the Pyrenees are *Hi. segaformis* and different *Sc. anchoralis* subspecies.

Also, Raven (1983) used the term "***anchoralis-latus* Zone**". Using the species *Ps. pinnatus* and *Po. bischoffi* he saw the possibility to subdivide the zone in three parts in the Cantabrian Mountains. The lower part is abundant in *Ps. pinnatus*, the middle part contains *Ps. pinnatus* and *Po. bischoffi* and in the upper part only *Po. bischoffi* is present.

Belka (1985) established the ***anchoralis* interval-range Zone** that coincides with the *anchoralis-latus* Zone of Lane et al. (1980).

In Belgium, the ***Scaliognathus anchoralis* Zone** first defined by Groessens (1974) coincides with the general faunal aspect of the zone. Next to the index fossil *Sc. anchoralis, Gn. simplicatus, Gn. texanus pseudosemiglaber, Ps. longiposticus, Po. bischoffi, N. c. communis, Po.* cf. *inornatus* and *Po. inornatus* are present in the zone. The genus *Ps.* disappears within the zone. Furthermore Groessens (1974) subdivided this zone in three subzones. Later, zonal names were adjusted (see Conil et al. 1990). From below: *Scaliognathus fairchild* subzone (ex: ***Dol. latus* Subzone**, characterized by the presence of *Dol. latus* and rare specimens of *Eo. Burlingtonensis*), *anchoralis latus* subzone (ex: ***Eotaphrus burlingtonensis* Subzone**), *Polygnathus bischoffi* Subzone (ex: ***Scaliognathus anchoralis* Subzone**, which covers the realm between the last *Eo.* and the first *Mestognathus*). Moreover, due to improved stratigraphic data by foraminifers, the *Mestognathus praebeckmanni* Zone, defined by the entry of the eponymic species just at the end of the range of *Sc. anchoralis europensis* (Belka & Groessens 1986) was included in the uppermost Tournaisian. As *Sc. anchoralis* overlaps with the range of *M. praebeckmanni* (and *M. beckmanni*), the zone was included as a subzone to the *anchoralis* Zone. This also necessitated the emendation of the Molinacian substage, which led to the correlation of its base with the base of the Viséan (Poty et al. 2006). However, the zone has only local value, as the index taxon is already reported from the Upper *typicus* Zone in Moravia (Kalvoda 2002). *Gn. homopunctatus* enters shortly above and defines the base of the *homopunctatus* Zone.

The ***Scaliognathus anchoralis-Doliognathus latus* Zone**, the ***Bactrognathus distortus lanei* Zone** and the ***Polygnathus mehli-Gnathodus sublineatus* Zone** of Boardman et al. (2013) coincide with the *anchoralis* Zone.

Scaliognathus anchoralis-Doliognathus latus Zone

Lower limit: defined by first appearance *of Sc. anchoralis* Branson & Mehl (1941b) and/or
         Dol. latus Branson & Mehl (1941b)

Upper limit: defined by first appearance of *Ba. distortus lanei* Chauff (1981)

Associated fauna: *Ps. pinnatus, Ba. distortus,* and two new, not formally named species of the genus *Gnathodus*, resembling *Gn. antetexanus* and *Gn. bilineatus* appear in this zone.

***Bactrognathus distortus lanei* Zone**
Lower limit: defined by first appearance of *Ba. distortus lanei* CHAUFF (1981)
Upper limit: defined by first appearance of *Gn. sublineatus* LANE & ZIEGLER (1983)
Associated fauna: *Gn.* n. sp. 12 (*aff. pseudosemiglaber* of numerous authors) appears within the zone.
The ***Polygnathus mehli-Gnathodus sublineatus* Zone** is defined by the first appearance of *Gn. sublineatus* and the high abundance of *Po. mehli*. The zone also contains *Gn.* n. sp. 13 BOARDMAN et al. (2013) (possible morphologically primitive species of a *Gn. texanus* clade) and *Gn. sublineatus*.

2.3.10 *homopunctatus* Zone (PERRET, 1977)

Gnathodus homopunctatus (now *Pseudognathodus homopunctatus*, see discussion IN SANZ-LOPEZ et al. 2018) can be used as an index to approximate the base of the Viséan if the defining foraminifer taxon *Eoparastaffella simplex* is missing (DEVUYST et al. 2003). Therefore, the usage of the name *homopunctatus* Zone is strongly recommended to substitute the name *texanus* Zone used in the standard zonation of LANE et al. (1980).
In the Pyrenees PERRET (1989, 1993) recognized the beginning of the ***Pseudognathodus homopunctatus* Zone** by the disappearance of *Sc. anchoralis, Hi. segaformis, Ps. pinnatus* and *Gn. delicatus* as well as by the abundant and diversified appearance of the genus *Ps.* with *Ps. homopunctatus* and *Ps. symmutatus* from the base of the zone. The genus *Gn.* is well represented in this zone by *Gn. texanus, Gn. austini, Gn. pseudosemiglaber, Gn. semiglaber* and *Gn. praebilineatus*. A little bit later in the zone *Par. commutatus* and *Vo. campbelli* appear. The mid-point of the zone is marked by the disappearance of *Po. bischoffi, Gn. semiglaber, Gn. pseudosemiglaber* and the appearance of *Gn. bilineatus*.
According to HERBIG & STOPPEL (2006), the following species range in Germany throughout this zone: *Gn. semiglaber, Gn. texanus, Gn. austini, Me. beckmanni. Gn. cuneiformis* and *Po. bischoffi* die out within, and *Gn. pseudosemiglaber* at the end of the zone. *Ps. homopunctatus* and *Lo. commutata* first appear at the beginning of the *homopunctatus* Zone and *Gn. praebilineatus* and *Gn.* ex. gr. *girtyi* first appear in the last third of the zone.
In the Carnic Alps, PERRI & SPALLETTA (1998) interpreted an abrupt change in the conodont fauna association as boundary between the *anchoralis* Zone and their ***texanus-homopunctatus* Zone**. The boundary coincides with the first appearance of *Gn. texanus, Ps. homopunctatus, Lo. cracoviensis, Gn. praebilineatus* and *Ps. symmutatus*. The associated fauna mainly consists of *Gn. semiglaber, Gn. pseudosemiglaber* and *Gn. cuneiforis. Gn. texanus* seems to be very rare. As *Ps. homopunctatus* is numerically best represented, they named the zone *texanus-homopunctatus*-Zone.
The ***texanus* consecutive-range Zone** and the ***austini* consecutive-range Zone** by BELKA (1985) correlate with the *texanus* Zone of LANE et al. (1980) and the *homopunctatus* Zone by PERRET (1989, 1993).

***texanus* consecutive-range Zone**
Lower limit: defined by first appearance of *Gn. texanus* ROUNDY (1926)
Upper limit: defined by first appearance of *Gn. austini* BELKA (1985)
Associated fauna: *Gn. homopunctatus, Gn. mermaidus, Gn. pseudosemiglaber, Gn. semiglaber, Gn. symmutatus, Par. cracoviensis, P. commutatus.* In the shelf-areas in

shallow-water environments *Me. beckmanni, Cavusgnathus convexus and Cl. globenskii* are present. *N. c. communis* terminates within this zone.

austini consecutive-range Zone

Lower limit: defined by first appearance of *Gn. austini* Belka (1985)

Upper limit: defined by first appearance of *Gn. bilineatus bilineatus* (Roundy 1926)

Associated fauna: the fauna is very similar to that of the *texanus* consecutive-range Zone. *Gn. praebilineatus* first appears at the base of the zone and *Me. beckmanni* occurs throughout. Other associated species are *Par. commutatus, Par. cracoviensis, Gn. texanus, Gn. mermaidus, Gn. homopunctatus* and *Gn. symmutatus*.

Also, in Belgium, the entry of *Pseudogn. homopunctatus* indicates the base of the Viséan and gives name to the corresponding zone (see previous chapter).

The **Gnathodus bulbosus Zone**, the **Lower Gnathodus "texanus" Zone**, the **Middle Gnathodus "texanus" Zone** and the **Upper Gnathodus "texanus"-Gnathodus s. sp. 15 aff. punctatus Zone** of Boardman et al. (2013) correspond to the *texanus* Zone of Lane et al. (1980), respectively to the *homopunctatus* Zone.

2.4. Conclusions

This review of conodont biostratigraphy showed that a world-wide conodont-zonation for the reviewed Tournaisian-lower Viséan interval is not applicable. Due to different water depths, sedimentary environments, and palaeobiogeographic provinces different species occur in different parts of the world.

The zonations for Germany, the Carnic Alps, the Pyrenees, the Holy Cross Mountains and the Moravian-Silesian Zone can be correlated with the proposed standard zonation by Ziegler & Lane (1978), partially with slight variations. They all have in common that their sediment accumulations were formed in deeper-water environments. In many cases, the biozonations erected for intermediate to shallow-water environments use completely different species and are therefore not comparable to the standard zonations. Thus, the "standard" conodont biozonation is only useful if the applied conodont faunas originate from the environment typifying these zonal markers and the associated taxa.

Hence, it is most important to correlate the numerous existing conodont biozonations, and, thus, to correlate stratigraphic successions around the world.

Sequence-stratigraphy is a powerful tool to support conodont biostratigraphy. The sequence-stratigraphy of Poty (2016) for the Belgian Namur-Dinant Basin (see Fig. 3, Fig. 5) is also applicable in sedimentary successions from southwestern England, southern Poland and southern China. The sequence-stratigraphic approach of Herbig (2016) for the Rhenish Kulm Basin (see Fig. 3, Fig. 5) can be transferred to other European and North African Kulm basins.

The sequence-stratigraphy of Poty (2016) for the Belgian Namur-Dinant Basin is biostratigraphically correlated with foraminifers and rugose corals found in predominantly shallow water carbonate deposits, because conodonts are often very rare in the sedimentary record of Belgium, especially in the lower and middle Tournaisian and in the Viséan. They were not considered by Poty (2016), but correlations can be found in Poty et al. (2006). Five of the ten third-order cycles of the Dinantian are represented in our review of Tournaisian to early Viséan (Moliniacien) conodont zones. Their boundaries of cycles/system tracts usually correspond to members and formations. During the Tournaisian and Viséan high variations of the sea-level and periods of emersion between

FSST and LST are recorded by the third-order sequences. Most probably they are of glacio-eustatic origin (Gɪʟᴇꜱ 2009, Pᴏᴛʏ et al. 2015, Pᴏᴛʏ 2016).

The Tournaisian sequences 1-4 of Hᴇʀʙɪɢ (2016) for the Rhenish Kulm Basin are biostratigraphically mostly correlated with conodonts. At the western basin margin (Velbert Anticline), the base of Sequence 5 is very well defined by foraminifers. The lower and middle Viséan sequences 6-8 are difficult to assess by lithostratigraphic and biostratigraphic means. However, in general the sequences of the German Kulm Basin have less biostratigraphic control than the Belgian platform sequences. In cases, the LSTs are not recognized, e. g. at the base of the mid-Tournaisian Sequence 2. Probably, this is due to sediment starvation caused by minimized sediment influx from widespread emergent platforms and low sea-levels (Hᴇʀʙɪɢ 2016). In these cases, the TST was taken as base of the sequence. Summing up, different biostratigraphic zonations, between platform and basin, insufficient, biostratigraphic control and unrecognized LSTs in the Kulm basin still might cause slightly differing sequence boundaries. Thus, refinement of sequence stratigraphy would help to support the correlation of conodont zonations.

3. Review of biofacies models

The distribution of conodont species throughout a section is an efficient tool to assign different parts of the succession to potential changing depositional realms between platform and basin.

Seddon (1970) was the first to recognize patterns in the Frasnian conodont distribution in Western Australia. Seddon & Sweeet (1971) stressed the facies dependency of conodonts and proposed a depth stratification model for their distribution assuming a pelagic life mode (Klapper & Barrick 1978, Hartenfels 2020). Druce (1973) introduced a lateral segregation model (dependent on factors such as variation in food supply) as well as a pelagic model, whereas Barnes & Fahraeus (1975) proposed a nektobenthic model for Ordovician conodonts (Klapper & Barrick 1978).

The basic concept of lateral conodont biofacies, related to linear belts parallel to the palaeo-coastline, has been introduced by Sandberg (1976) for the Upper Devonian (Fammenian) in the western U.S.

In general, except for the highly specialized niches with dominance of a single genus, two genera constitute 75 to 80 % of the total platform conodont population. Based on this concept Sandberg (1976) erected the **Palmatolepid-Bispathodid Biofacies** (I, continental rise and slope**), Palmatolepid-Polygnathid Biofacies** (II, shallow to moderately deep water on the continental shelf), **Polygnathid-Icriodid Biofacies** (III, moderately shallow water on the outer cratonic platform), **Polygnathid-Pelekysgnathid Biofacies** (IV, shallow water of normal salinity on the inner craton platform) and the **Clydagnathid Biofacies** (V, very shallow, brackish to normally saline water on offshore banks and in associated lagoons). Further shallow-water biofacies, that do not tackle the scope of the present study were added by Sandberg & Ziegler (1979), Sandberg & Poole (1977) and Sandberg & Dreesen (1984) who introduced an extended biofacies model for the western U.S. and southern Belgium. Sandberg et al. (1988) also defined that the name giving genera have to reach at least 70 % of the conodont fauna. Ziegler & Weddige (1999) stressed the importance of the diffuse boundaries of the existing biofacies zones (I-IX) and, therefore, the importance of conodont elements that are transitional between biofacies zones.

These Famennian biofacies zonations are only marginally useful for our work, when considering the reworked Upper Devonian conodont faunas of the Gladenbach Fm (see chapter 6.5) and the Kahlenberg Fm of Wettmarsen (see chapter 7.5).

Clausen et al. (1989) used uppermost Famennian (Lower to Upper *praesulcata* Zone) and Tournaisian (*sulcata* Zone to *sandbergi* Zone) platform conodonts from sections at the northern rim of the Rhenish Mountains to illustrate the development of the depositional realm by changing conodont biofacies in time. They distinguished four biofacies occurring from the *praesulcata* to *sandbergi* conodont zones. They distinguished a basinal **Palmatolepid-Bispathodid Biofacies** (1, *praesulcata* Zone), followed in time by a shallower, swell related **Protognathodid Biofacies** (2, *sulcata* Zone), a **Polygnathid-Siphonodellid Biofacies** (3, *sulcata* Zone/latest Lower *duplicata* Zone) on deep swells and slopes, and finally a basinal **Siphonodellid Biofacies** (4, *sandbergi* Zone). Clausen et al. (1989) examined younger accumulations only in few outcrops, and therefore did not include them in their model.

Kalvoda (1991) interpreted the habitats of platform conodonts from the middle and upper Tournaisian. In the *isosticha*-Upper *crenulata* Zone he differentiated the most basinal **Bispathodid Biofacies** (I), the **Siphonodellid Biofacies** (II) ranging from the basin on the lower slope, and the **Gnathodid-Pseudopolygnathid Biofacies** (III) ranging from upper parts of the lower slope across middle and upper slope to the platform margin. Due

to the extinction of the siphonodellids, only biofacies (I) and (III) remained in the Lower *typicus* Zone (Fig. 7). *N. c. communis* occurred in all depositional realms and, therefore, was interpreted as an epipelagic taxon.

	CONODONT BIOFACIES	BISPAT-HODID I	NO CONODONTS II	GNATHODID - PSEUDOPOLYGNAT. III	?
Lower typicus Zone	environ-mental reconstu-ction		Euphotic Bi	N.c.c.	
			Dysphotic	Ps	
			Aphotic		
			Aerobic	G	
			Dysaerobic		

	CONODONT BIOFACIES	BISPAT-HODID I	SIPHONODEL. II	GNATHODID - PSEUDOPOLYGNAT. III	?
isosticha - Upper crenulata Zone			Euphotic Bi	N.c.c.	
			Dysphotic Si	Ps	
			Aphotic		
			Aerobic	G	
			Dysaerobic		

Fig. 7 Conodont biofacies model showing interpreted palaeoecology of platform elements of the *isosticha*-Upper *crenulata* and Lower *typicus* zones in open marine facies. Bi, *Bispathodus*; N.c.c., *Neopolygnathus communis communis*; Ps, *Pseudopolygnathus*; G, *Gnathodus*; Si, *Siphonodella* (by Kalvoda 1991).

For the *anchoralis* Zone Kalvoda (1991, 1994) adopted the model of Sandberg & Gutschick (1984) described below. A synoptic diagram of the late Famennian and Tournaisian conodont biofacies was presented by Kalvoda et al. (1999) (Fig. 8). They used the term "mesopelagic zone" for the taxa *Palmatolepis* and *Siphonodella* to refer to the greater depth, in which these two taxa can be found, compared to the taxa present in the "epipelagic zone". However, the terms do not refer to certain water depths. Also, Kalvoda et al. (1999) were faced with certain problems due to the fact that the beds they sampled resulted from turbidity currents (calciturbidites). For example, conodont assemblages often did not cross the 70% threshold necessary to define a conodont biofacies as a result of mixed sources; or reworked older faunas were present in the conodont assemblages, indicating erosion of underlying deposits. Therefore, they combined the study of conodont faunas, sedimentological and stratigraphical interpretation of calciturbidites and related deep-water accumulations to test the reliability of condont faunas as a tool to detect changes in the carbonate depositional system.The biofacies model by Sandberg & Gutschick (1984; based on Sandberg & Gutschick 1979 and Gutschick & Sandberg 1983) described seven uppermost Tournaisian conodont biofacies from the *anchoralis* Zone ranging from the basin to the shoreline (Fig. 9).

The **Bispathodid Biofacies** (I) represents starved basin areas, the **Scaliognathid-Doliognathid Biofacies** (II) occurs in starved basins and at the toe of the lower foreslope; the three name-giving genera are interpreted as epipelagic nekton or plankton. The **Gnathodid-Pseudopolygnathid Biofacies** (III) is present in the lower to upper slope; the
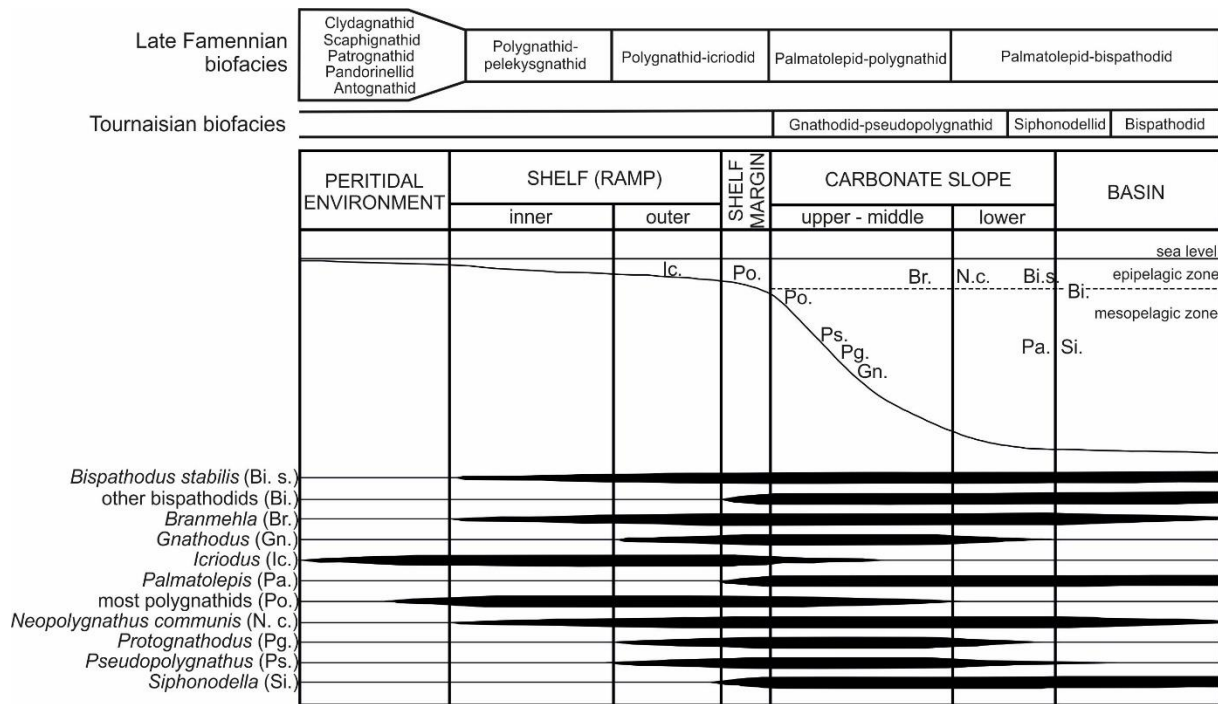
Fig. 8 Palaeoecologic distribution of conodont taxa during the upper Famennian to middle Tournaisian by KALVODA et al. (1999) (based on SANDBERG 1976, LANE et al. 1980, GUTSCHICK & SANDBERG 1983, DREESEN et al. 1986, DREESEN 1992 and KALVODA 1991, 1994).

corresponding two genera are believed to thrive in the water column relatively close to the sediment surface. The **Eotaphrid Biofacies** (IV) appears at the shelfedge of the carbonate platform, the **Hindeodid Biofacies** (V) can be found on the outer carbonate platform, the **Pandorinellinid (?) Biofacies** (VI) on the inner carbonate platform and in tidal lagoon and sabkha environments. Finally, the **Mestognathid (?) Biofacies** (VII) is only represented in tidal lagoon and sabkha environments. *N. c. communis*, presumably an
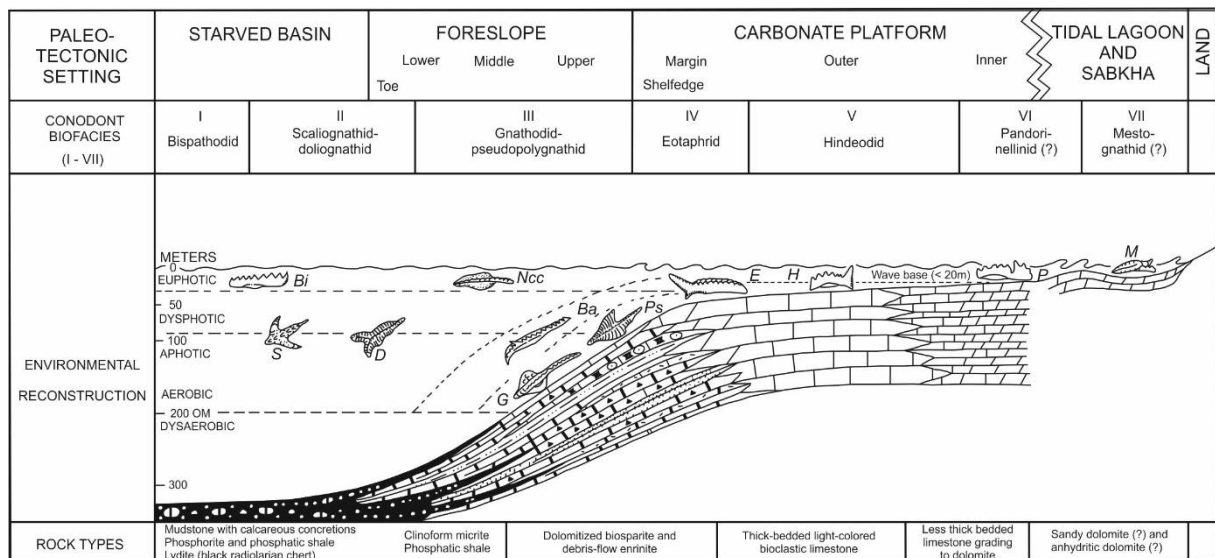
Fig. 9 Conodont biofacies zonation of platform conodonts of the uppermost Tournaisian *anchoralis* Zone and interpreted palaeoecology, Ba: *Bactrognathus*, Bi: *Bispathodus*, D: *Doliognathus*, E: *Eotaphrus*, G: *Gnathodus*, H: *Hindeodus*, M: *Mestognathus*, Ncc: *Neopolygnathus communis communis*, P: *Pandorinellina*, Ps: *Pseudopolygnathus*, S: *Scaliognathus*, modified after SANDBERG & GUTSCHICK (1984).

epipelagic drifter or swimmer is ubiquitous and common in most biofacies, except for the most offshore and the two most nearshore biofacies zones (I, VI VII). Therefore, the species has to be excluded from any biofacies analysis. The models of KALVODA (1991), as well as its extension by KALVODA et al. (1999) that also include results from SANDBERG & GUTSCHICK (1984) is most important for the biofacies reconstruction of the studied sections in the Rhenish Mountains (Gladenbach, Wettmarsen).

4. Geology of the Rhenish Mountains and southern Belgium

The Rhenish Mountains and the Southern Belgian Ardennes are parts of the Rhenohercynian zone of the Central European Variscan Mountains and were situated within the intratropical belt during the Early Carboniferous (Fig. 10). The Central European Variscides experienced the continent-continent collision between Laurussia and Gondwana that finally resulted in the formation of the supercontinent Pangaea. The Central-European Variscides were traditionally (KOSSMAT 1927) divided in three NE-SW striking zones (Rhenohercynian, Saxothuringian and Moldanubian zones), that were later supplemented by the Mid-German Crystalline zone (BRINKMANN, 1948) which initially was interpreted as a "structural high" between the Rhenohercynian and Saxothuringian zones. During the Variscan Orogeny the accretion of various peri-Gondwana terranes or microplates of the Armorican Terrane Assemblage (FRANKE 1995) resulted in the closure of several oceans, amongst them the Rheic Ocean (ECKELMANN et al. 2014).
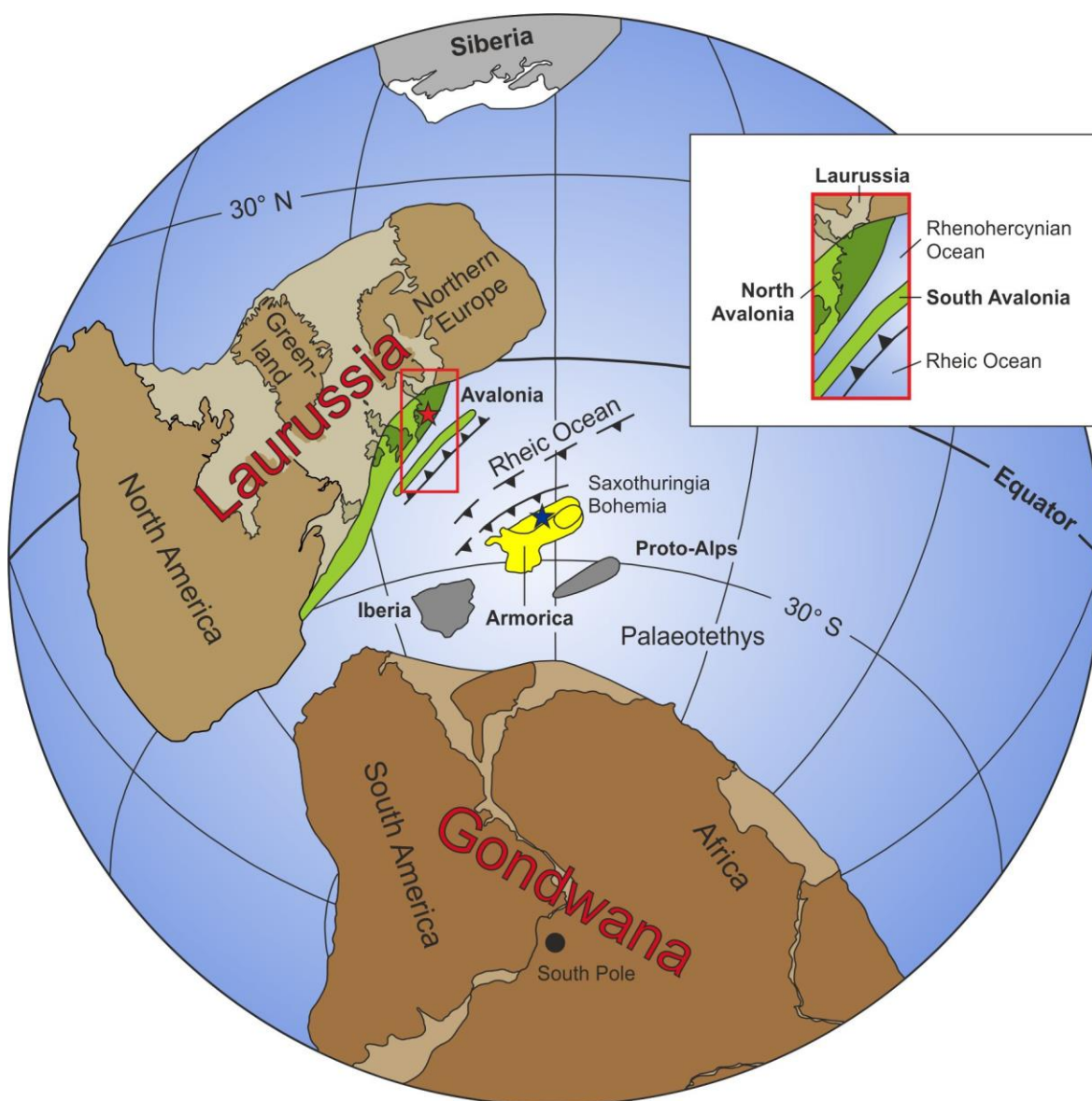
Fig. 10 Reconstruction of the plate tectonics from the Late Devonian to early Carboniferous, red asterisk: position of the autochthonous Rhenish Mountains, blue aterisk: source area of the nappe units in the southeastern Rhenish Mountains, from ECKELMANN et al. (2014).

The Rhenohercynian Zone, respectively the Rhenish Mountains as part of it, depicts a classical fold-and-thrust belt (e.g., Matte 1986, Franke & Oncken 1990, Franke et al. 1990, Franke & Oncken 1995, Franke 2000). The Devonian and Carboniferous successions of the Rhenish Mountains were deposited on Avalonian crust at the southeastern margin of the Laurussian continent that formed during the Caledonian orogeny in the latest Silurian.

The eastern part of the Rhenish Mountains is formed by several autochthonous, par-autochthonous and allochthonous units (Eckelmann et al. 2014). The latter are subsumed as Gießen-Harz nappe complex (Fig. 11).

The tectonic setting of southern Belgium is relatively complicated as a result of the Variscan deformation and varies in the Rhenohercynian Zone. The Midi-Eifel Thrust Fault separates from west to east (par-)autochthonous tectonic units in the north (contained in the Hainaut and Namur sedimentation areas) from allochthonous tectonic units in the south (contained in the Avesnois, Dinant, Condroz, and Vesdre-Aachen sedimentation areas) (Fig. 11) (Poty et al. 2011, after Poty 1997). Prior to the Variscan deformation all tectonic units were situated in a single basin, i. e. the Namur-Dinant Basin (Aretz et al. 2006). During the Variscan deformation the Brabant Massif, north of the Rhenohercynian Zone, formed a solid tectonic block, strongly influencing the distribution of platforms and basins, respectively the boundaries of the mentioned sedimentation areas. Sedimentation in the Namur-Dinant Basin (NDB) extended eastwards into the Vesdre Massif and the Aachen region and westwards into the Avesnois and Boulonnais in northern France (Poty et al. 2011, after Poty 1997). Due to important vertical movements of tectonic blocks, the NDB was connected to the Visé area during the Late Devonian and the Tournaisian (Poty 1982, 1991, Poty & Delculée 2011) and also to the Campine Basin north of the Brabant Massif, along the eastern margin of the Brabant Massif in the Visé area. Later, during the late Tournaisian and Viséan, the Basin was separated from the Campine Basin by the rising Booze-Le-Val-Dieu ridge (Poty & Delculée, 2011). An eastward connection of the NDB to the German Kulm Basin existed through the Aachen area during the Tournaisian. A lack of middle and upper Viséan deposits document the end of this connection due to an uplift of the area. The first stage of the Variscan emersion of the Ardenne Massif prevented a southward connection of the NDB to the Rhenohercynian Basin during the Dinantian. The overall poor connections to the adjacent basins explain the depleted and restricted inner platform facies in the Viséan accumulations of the NDB (Poty 2016).

During the late Devonian and early Carboniferous proximal facies prevailed in the northern part of the NDB, whereas the southern part acted as a shallow basin and was characterized by a deeper-water facies. Nonetheless, only platform sediments were deposited. Deeper water sediments of the Kulm facies are not known in Belgium, but suggested further in the south, as westward facies prolongation into the Kulm-type Cornubian or Munster Basin (lower Carboniferous) of the British Isles. In contrast to this assumption, the presence of proximal carbonate facies in the southern Avesnois sedimentation area (northern France) proves at least the local or regional presence of platform areas (rather than a basin) in the south (Poty et al. 2011, Denayer et al. 2015).

Overall, the sedimentation south of the Brabant Massif during the Early Carboniferous was related to an extensional regime and thickness variations of the deposits were caused by synsedimentary faulting (Poty, 1997). This synsedimentary faulting was also the reason for differing accommodation rates and lateral differentiation of the sedimentation areas, mentioned above.
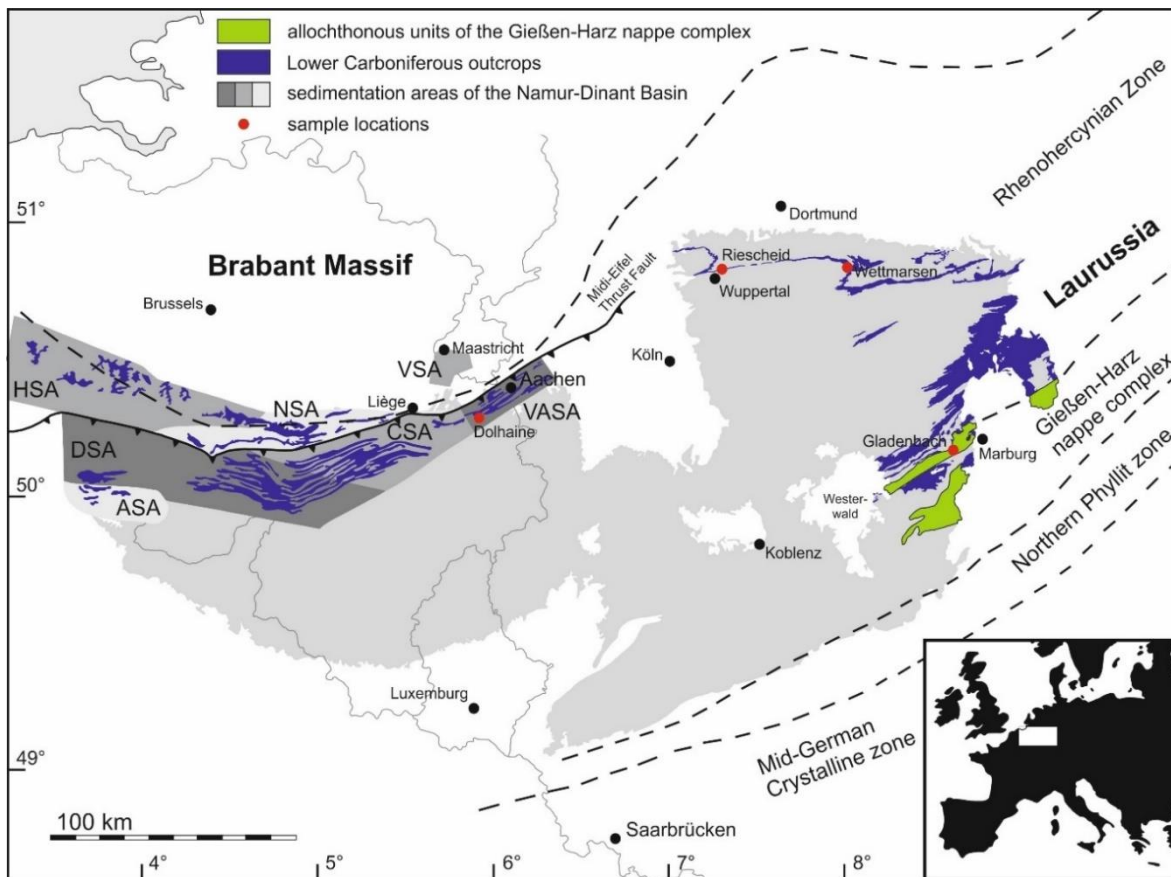
Fig. 11 Overview map of the Rheno + Ardenne Massive, showing outcrop areas of the Lower Carboniferous, sedimentation areas of the Belgian Namur-Dinant Basin and allochthonous units of the Gießen-Harz nappe complex (including the Hörre Zone); NSA: Namur sedimentation area, CSA: Condroz sedimentation area, DSA: Dinant sedimentation area, HSA: Hainaut sedimentation area, ASA: southern Avesnois sedimentation area, VSA: Visé sedimentation area, VASA: Vesdre-Aachen sedimentation area; index map: position within Europe (modified after Aretz et al. 2006, Eckelmann et al. 2013).

The **Vesdre-Aachen sedimentation area** (VASA) (Aretz et al. 2006), which is located within the allochthonous tectonic units southeast of the Brabant Massif includes the Dolhain section that is studied within the framework of this work. It is the eastern continuation of the CSA and NSA but displays an incomplete stratigraphic succession characterized by more proximal facies. A gradual transition to the CSA can be observed in the west, and the northern parts display similarities to the NSA. The succession in the eastern part of the VASA is less complete and already ends in the Moliniacian (early Viséan), whereas the more complete transition to the CSA also contains late Viséan rocks. A dolomitization of the Tournaisian strata as well as the accompanying evaporitic palaeokarst horizons are characteristic in most parts of the VASA. The VASA continues north-eastwards under the thick Tertiary cover of the Lower Rhine Embayment (Aretz et al. 2006, Denayer et al. 2015), but sedimentary facies changes with increasing distance from the Brabant Massive. However, the major structural elements can be traced into the subsurface across the Lower Rhine embayment into the westernmost Rhenish Mountains (see chapter 1) but the tectonic style changes from tight upthrusts and overthrusts to wide-spanned anticlines and upthrusted synclines in the Rhenish Mountains.

In spite of the structural coherence, different facies between the platform facies around the Brabant Massive and the Kulm facies of the Rhenish Mountains are obvious and known

since long time (e.g., Sᴇᴅɢᴡɪᴄᴋ & Mᴜʀᴄʜɪsᴏɴ 1842, Pᴀᴜʟ 1937a, b, c Vᴀɴ Sᴛᴇᴇɴᴡɪɴᴋᴇʟ 1990). During most of the Tournaisian, the Velbert Anticline still was part of the platform (Hᴇʀʙɪɢ et al. 2014, Hᴇʀʙɪɢ 2016) but a rapid transition into deep-water Kulm facies is recorded along its southern flank, respectively in the tight Herzkamp Syncline adjoining towards the southeast. Due to the facies changes, lithostratigraphy and biostratigraphic zonations differ (Fig. 12). In cases, also sequence stratigraphic correlations are problematic (Fig. 12).

Very obvious are the differences of the conodont zonation in the lower and middle Tournaisian (see also chapter 2). In the German Kulm Basin, five zones can be recognized, whereas in Belgium the *Siphonodella* Zone spans the complete time interval, though a local *Gnathodus* (Sub-)zone was delineated in its top (Cᴏɴɪʟ et al. 1990, Pᴏᴛʏ et al. 2006). In the shallow carbonate platform facies of the NDB, siphonodellids are rare (Hᴀɴᴄᴇ & Pᴏᴛʏ 2006, Hᴀɴᴄᴇ et al. 2006) and the evolutionary lineage from *Si. praesulcata* to *Si. sulcata* that marks the Devonian/Carboniferous Boundary (base of the Hastarian) cannot be found. In the Anseremme section (proposed neostratotype for the Hastarian by Hᴀɴᴄᴇ & Pᴏᴛʏ 2006) the first *Si. sulcata* is found 7 m above the base of the Hastarian (Hᴀɴᴄᴇ & Pᴏᴛʏ 2006, Pᴏᴛʏ et al. 2014) and, therefore, the boundary is based on the disappearance of Devonian macrofauna of the *praesulcata* Zone (Cᴏɴɪʟ et al. 1986). The first occurence of *Si. sulcata* supposedly marks the increasing water depth, reaching a depth required by the deeper-water-dwelling siphonodellids (Wᴇʙsᴛᴇʀ & Gʀᴏᴇssᴇɴs 1990).

The boundary between the Hastarian and Ivorian corresponds to the appearance of *N. c. carina*. It enters in more offshore facies during deepening i. e. at the base of TST of Sequence 3, just after the disappearance of the siphonodellids (Hᴀɴᴄᴇ et al. 2006, Hᴀɴᴄᴇ & Pᴏᴛʏ 2006, Pᴏᴛʏ et al. 2014). In the German Kulm successions, *N. c. carina* is already known from the *duplicata* Zone (Hᴇʀʙɪɢ & Sᴛᴏᴘᴘᴇʟ 2006) and in the herein described Riescheid

System	Series	Stages	Belgian Stages	German conodont zonation		Sequences Herbig et al. (2016)		Regional Stratigraphy Rhenish Kulm Basin	Belgian conodont zonation	Sequences Poty et al. (2014)		Regional Stratigraphy eastern NDB (Condroz sedimentation area)
CARBONIFEROUS	Mississippian/ lower Carboniferous	Viséan	Moliniacian p.p.	*homopunctatus*		5	HST / TST / LST	Hillershausen Fm	*homopunctatus*	5	TST / LST	
		Tournaisian „upper"	Ivorian	*anchoralis*		4	HST / TST / LST	Kohleiche Fm (only in the Herzkamp Syncline)	*anchoralis*	4	FSST / HST / TST / LST	Avins Fm / Flémalle Fm / Martinrive Fm
				typicus	Upper / Lower	3	TST/ HST / LST	Hardt Fm	*carina*	3	FSST / HST / TST	Ourthe Fm / Yvoir Fm
		„middle"	Hastarian	*isosticha-* Upper *crenulata*		2	HST	Kahlenberg Fm	*Gnathodus* – – – – – *Siphonodella*	2	FSST / HST / TST / LST	Landelies Fm / Pont d'Arcole Fm
				Lower *crenulata*			TST					
		„lower"		*sandbergi*	U / L	1	FSST / TST/ HST / LST	Hangenberg beds		1	FSST / HST / TST	Hastière Fm
				duplicata	U / L							
				sulcata								

Fig. 12 Belgian and German conodont zonation and sequences, regional stratigraphy of the Rhenish Kulm Basin and the eastern Namur-Dinant Basin (NDB), note that the subdivision in lower, middle and upper Tournaisian is informal; LST: Lowstand Systems Tract, HST: Highstand Systems Tract, TST: Transgressive Systems Tract, FSST: Falling Stage Systems Tract; German conodont zonation: Hᴇʀʙɪɢ & Sᴛᴏᴘᴘᴇʟ (2006); German sequences: Hᴇʀʙɪɢ (2016); regional stratigraphy of the Rhenish Kulm Basin: Aᴍʟᴇʀ & Hᴇʀʙɪɢ (2006), Hᴇʀʙɪɢ (2016) modified from Aᴍʟᴇʀ & Hᴇʀʙɪɢ (2006); all Belgian subdivisions from Pᴏᴛʏ et al. (2014).

section (chapter 5), and in the Gladenbach Fm (chapter 6) the species occurs in the Lower *crenulata* and *isosticha*-Upper *crenulata* zones. Therefore, it is obvious that *N. c. carina* can only be used as defining species of a local zone in the Belgian successions. The local *Gnothodus* (Sub-)zone in the top of the *Siphonodella* Zone apparently coincides with the *isosticha*-Upper *crenulata* Zone, as gnathodids first appear at the base of the latter.

Another obvious source of differences is the sequence stratigraphy and the system tracts recognized therein. In Belgium, Sequence 1 ends at the base of the upper member of the Hastière Fm, whereas in Germany the top of Sequence 1 is considered to correspond to the boundary between Hangenberg beds and Kahlenberg Fm, respectively Hastière Fm and Pont d'Arcole Fm. However, the LST of Sequence 2 was not recognized in Germany, and the TSTs of Sequence 2 are time equivalent in both countries. In Germany, TST and HST are in cases not separated, as the HST is mainly masked by continuous black shale deposition. Exceptions are environments that are characterized by calciturbidites originating from highstand shedding. They are further elucidated in chapters 5, 6, 7. Opposed to Belgium, a FSST is exceedingly rarely observed (HERBIG 2016) and nor recorded from the herein considered Tournaisian-lower Viséan interval.

In Belgium Sequence 3 is recognized within the DSA and CSA (HANCE et al. 2001, POTY et al. 2014) starting above a minor hiatus at the base of the Yvoir Fm, respectively Maurenne Fm and ending at the top of the Ourthe Fm. In the RKB Sequence 3 coincides with the Hardt Fm, respectively the Lower and Upper *typicus* Zone.

Generally, Sequence 3 is not recognizable in the RKB because condensed sedimentation during the preceding Sequence 2 and concomitant subsidence of the RKB resulted in further deepening of the basin and, thus, overrode the effects of sea-level changes. Only in few cases, the sequence is recorded, e. g. at the western basin margin (e. g. Riescheid section, chapter 5), and on some intrabasinal swells, e. g. in the Wettmarsen section that was shortly mentioned by HERBIG (2016) to contain the LST and an undifferentiated TST/HST (or the HST only) of Sequence 3 wich is further elucidated herein (chapter 7). Also, in the Hörre Zone, the lower part of Sequence 3 is now proved (chapter 6). In the Riescheid section, the sequence starts with black shales that form the base of the Hardt Fm. They belong to the upper part of the *isosticha*-Upper *crenulata* Zone (p. 44). Thus, the base of the sequence is time-equivalent to Belgium, where it is placed within the uppermost *Siphonodella* Zone. However, due to generally missing fossils, the base of the Hardt Fm is traditionally considered to be above the *isosticha*-Upper *crenulata* Zone, thus pretending a slightly diachronous base of the sequence. It also has to be stressed, that in parts of the Belgian CSA LST deposits are missing due to a hiatus. There, oldest deposits of the sequence belong to the TST, commencing like generally depicted in the RKB after the extinction of siphonodellids at the base of the *carina* Zone.

In the Belgian CSA the LST and TST of Sequence 4 are represented by the Martinrive Fm, the Flémalle and Avin Fm form the HST and FSST; in the northern DSA, the Leffe Fm constitutes the complete sequence, but in the southern DSA the upper part of the formation contains the LST of Sequence 5. Based on rugose corals, Sequence 4 starts slightly below the base of the *anchoralis* Zone in Belgium. In Germany its base is correlated with the base of the *anchoralis* conodont Zone and, thus, almost time equivalent.

At the western basin margin of the RKB (Velbert Anticline) Sequence 4 remained without differentiation into system tracts. Probably only an undifferentiated TST/HST is developed. In the Herzkamp Syncline, adjoining towards the southwest, a thin veneer of fine-grained sandstone and sandy shales forms the LST, black alum shales and flasered to nodular limestones form the TST and HST of Sequence 4 (HERBIG 2016) that coincides with the

Kohleiche Fm. On high rising intrabasinal swells (Erdbach-Langenaubach reef, SW RKB) all system tracts of Sequence 4 were recognized, but on low rising intrabasinal swells, exemplified by the Drewer section, the sequence remained undifferentiated, consisting only of deeper water limestones of the Kattensiepen Fm.

In Belgium Sequence 5 is only present in the DSA (outer shelf area) and in the tectonic graben settings of the VSA. LST, TST, HST and FSST are formed by the Sovet Fm in the northern DSA. In the southern DSA the upper part of the Leffe Fm corresponds to the LST, and the Molignée Fm to the remaining systems tracts of Sequence 5 (POTY et al. 2014). Sequence 5 straddles the Tournaisian-Viséan boundary (latest Ivorian-earliest Moliniacian). Its base is isochronous between the Dublin Basin, southern Belgium and the westernmost RKB, as demonstrated by BABEK et al. (2010, see also HERBIG 2016). In the RKB outside of the Velbert Syncline the base of the sequence is well marked by sediments of the basal Hillershausen Fm, locally from the upper Hardt Fm wich seems to range higher up in the Herzkamp Syncline (Riescheid section) than elsewhere in the RKB. Only on the high-rising intrabasinal swell on top of the Erdbach-Langenaubach reef, also LST breccias are observed. Strata from the TST (in Erdbach-Langenaubach from HST) yielded conodonts of the *homopunctatus* Zone. Therefore, HERBIG (2016) generally correlated the base of the sequence with the base of the Viséan. This, however only seems to pretend a diachronous base of the sequence. Both, the Belgian and the German Sequence 5 correlate with the lower part of the *homopunctatus* Zone (POTY et al. 2014, HERBIG 2016).

5. Wuppertal-Riescheid

5.1 Introduction

In a former railway-cut in Wuppertal-Wichlinghausen middle Famennian to Upper Viséan strata of the Kulm facies are well exposed. The section is known for its Famennian admixture of outer shelf faunas with relatively rich miospore records (Higgs & Streel 1984, 1994) and for its extraordinary lower Carboniferous (Mississippian) units that differ from the deeper-water successions of the Northern Sauerland and the neritic limestones (Kohlenkalk facies) of the Ardennes Shelf, that extend to the Velbert Anticline in the NW. Therefore, the succession has been repeatedly studied in the past. Currently, the Riescheid section is one of the best opportunities to study the rocks of the Kulm facies in the Herzkamp Syncline (see also Hartenfels 2011).

The section has been described by Paeckelmann (1922), Fuchs & Paeckelmann (1928), Franke et al. (1975), Zimmerle et al. (1980), Aretz et al. (2006), Hartenfels & Becker (2009), Hartenfels (2011) and Hartenfels et al. (2016).

The north dipping section is the only continuous profile of Upper Devonian to lower Carboniferous accumulations in the Wuppertal area (Paeckelmann 1928). Based on lithological studies of thin sections and x-ray diffractometer analyses of the mineral composition the section was divided into 11 lithological units (Zimmerle et al. 1980) that mark the section as a "typical Kulm succession" (Aretz et al. 2006).

There were also several studies on the fossil content of this section, among them examinations of conodonts (Lane & Ziegler 1978), trilobites (Brauckmann 1982, 1992), spores (Higgs & Streel 1984), radiolarians (Seo & Won 2009, Won & Seo 2010) and acritarchs (Weldon, 1996). 1-D models, and a simulated burial and temperature history of the black shales were reconstructed with rock analyses by Uffmann et al. (2012).

A revision of the lithostratigraphical subdivisions proposed by Korn (2003, 2006, 2010) resulted in a simpler, more dynamic scheme for the Mississippian strata of the Rhenohercynian Kulm basin (pers. comm. H.-G. Herbig for the German Subcommission on Carboniferous Stratigraphy). Adjustments of hierarchical ranks of some units and a reduction of the multitude of names also affected the hitherto used lithostratigraphy of the Riescheid section (Korn 2003, Aretz et al. 2006). The section can be subdivided as follows. The lithological units 2 to 4 of Zimmerle et al. (1980) form the Kahlenberg Fm (former "Liegender Alaunschiefer") and are followed by unit 5, now belonging to the lower part (=lower tongue) of the Hardt Fm (traditionally "Schwarze Kieselschiefer"). Unit 6-7 compose the Kohleiche Fm. The only 0.2 m thick unit 6 resembles the Richrath beds that are correlated with the thicker Richrath Member in the Velbert Anticline adjoining towards the NW. Unit 7 is composed of a specific nodular limestone facies of the Herzkamp Syncline. Unit 8 is the upper part (= upper tongue) of the Hardt Fm. Unit 9 belongs to the Hillershausen Fm, unit 10 forms the Bromberg Fm, and unit 11 represents the Dieken Fm.

Here we concentrate on the Kahlenberg Fm, which is represented by the units 2 to 4 by Zimmerle et al. (1980) and lies within the middle Tournaisian (Tn2a). As discussed before, the Kahlenberg Fm represents the TST and HST of Sequence 2. The TST started at the base of the middle Tournaisian (Lower *crenulata* Zone).

At Riescheid, the Kahlenberg Fm is composed of dark shales (TST) overlain by a carbonate unit (HST). Zimmerle et al. (1980), who had already identified the carbonates of the Kahlenberg Fm (unit 3) as being deposited by turbidites, classified the unit as "allodapic limestone".

5.2 Geological setting and description of the section

The Riescheid section is situated at the southern flank of the Herzkamp Syncline and the northwestern flank of the Remscheid-Altena Anticline (Fig. 13) in the western Rhenish Mountains (51°17'15,2''N, 07°11'32,4''E, 4709 Wuppertal-Barmen) and exhibits a steep northward dip.
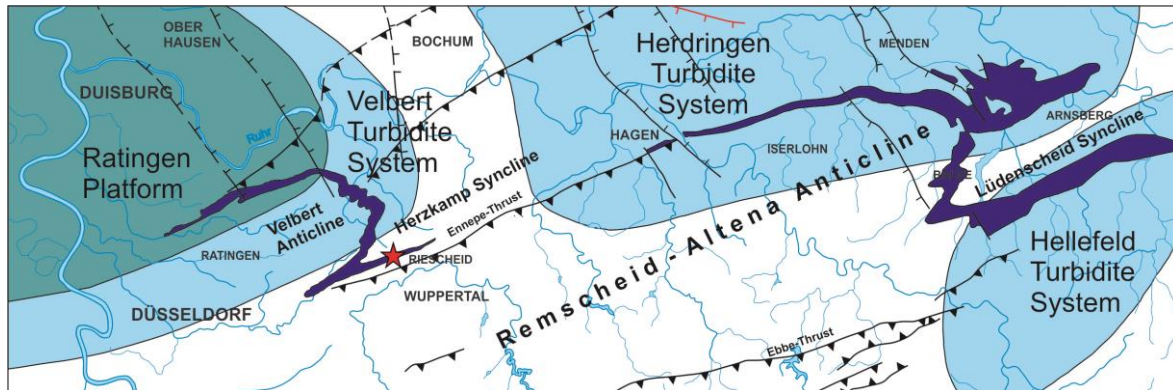
Fig. 13 Lower Carboniferous outcrop areas (dark blue) in the northern Rhenish Mountains, red asterisk marks the position of the Riescheid section on the southern flank of the Herzkamp Syncline; platform (greenish) and Viséan turbidite systems (light blue) based on Korn (2010).

The Velbert Anticline in the NW of the section was part of a rapidly subsiding trough in the upper Fammennian (Upper Devonian) and accumulated the fine-grained, shallow-water siliciclastics (nearshore "Condroz Sandstone" facies) of the Velbert Fm (Hartenfels et al. 2016). Without evident transition, the deeper basinal facies in the E/SE is exposed in the Wuppertal area. Paproth et al. (1986, based on Schmidt 1935) assumed that the facies boundary mostly illustrates differences in relative depositional energy, not in water depth. In contrast, the shallow-water faunal assemblages of the Velbert Fm that are dominated by brachiopods, and the pelagic fauna of the Herzkamp Syncline evidence a palaeoslope. The constant transport of silt and fine sand by turbidites into the basinal areas underline the presence of a palaeoslope (Hartenfels et al. 2016). The siliciclastic detritus mainly originated from the Old Red Continent (London-Brabant Massif and/or Mid Netherlands High) but was also provided by topographic highs within the basin. Material from these highs was transported by turbidity currents towards the N and NW (Hartenfels et al. 2016). In the uppermost Famennian and lower Carboniferous the palaeogeographic contrast between the Velbert Anticline and the Wuppertal area continued, resulting in a deeper water succession in the Wuppertal area during the lower Carboniferous. The, globally recognizable transgression during the middle Tournasian, caused a major facies levelling (Hartenfels et al. 2016). In the Velbert area the upper Tournaisian is not recorded, whereas the Viséan succession is composed of calciturbidites (Velbert turbidite system, Korn 2010) originating from a northwestern shallow-water platform, called Ratingen platform (see Fig. 13), proving a significant slope (Hartenfels et al. 2016, also see Amler & Herbig 2006, Franke et al. 1975). The Riescheid section is not situated within the Velbert Turbidte System (Korn 2010). However, it was first affected by turbidites during the middle Tournaisian Kahlenberg Fm deriving from a forebulge (Herbig 2016). The Viséan calciturbidites have been derived either from the Herdringen Turbidite System (Fig. 13) or another, unknown source within the Kulm Basin.

The Lower Alum Shale at the base of the Kahlenberg Fm (Fig. 14, Fig. 16) represents the TST of Sequence 2 (Herbig 2016). The limestones of the Kahlenberg Fm are calciturbidites, and represent the HST of Sequence 2 (Herbig 2016). The lowermost part of the overlying lower Hardt Fm consists of organic-rich black shales (containing siphonodellids), confirming an affiliation to the upper part of the *isosticha*-Upper *crenulata* Zone (Fig. 14, Fig. 16). They represent the TST of Sequence 3. Radiolarians of Assemblage 1 Won & Seo (2010) (Groos-Uffenorde in Becker et al. 1993) confirm the middle Tournaisian age. The following laminated, siliceous black shales with bedded cherts contain phosphorite nodules near the base and in the middle part (Hartenfels et al. 2016) and form the HST during continuous deeper-water conditions and reduced terrestrial influence (Herbig 2016). The LST of Sequence 3 cannot be observed in Riescheid, similar to most Mississippian sequences in the Rhenish Kulm Basin. The base of the overlying Kohleiche Fm (Fig.) consists of about 0,2 m thick fine-grained sandy black shales (containing pyrite and phosphate nodules) and laminated, fine-grained sandy green shales (containing densely packed broken phosphate nodules) that are known as "transitional beds" (Zimmerle et al. 1980) or "Richrath Beds" (Franke et al. 1975, Amler & Herbig 2006, Aretz et al. 2006, Hartenfels et al. 2016). They are followed by 2,7 m of flasered, rarely nodular limestones, that can be correlated with the Erdbach II Limestone (based on conodonts, Kürschner et al. 1993, Lane & Ziegler 1978, Lane et al. 1980, Park 1983, Becker et al. 1993; rare ammonoids, Paeckelmann 1922, Fuchs & Paeckelmann 1928, Kullmann in Paproth & Streel 1982 and in Brauckmann & Meyer 1982; and a single trilobite, Brauckmann & Meyer 1982). The fine-grained black and green shales constitute the LST/TST of Sequence 4. The HST of Sequence 4 is represented by the overlying limestones of the Kohleiche Fm. The boundary between sequences 4 and 5 lies within the uppermost Tournaisian, but is not recognized within the limestones (Herbig 2016). Above, more than 5 m thick black bedded cherts with phosphorite nodules in certain horizons and a thin black shale horizon at the base constitute the uppert part of the Hardt Fm. They are sharply separated from the underlying limestones of the Kohleiche Fm and constitute the undifferentiated TST/HST of Sequence 5 (Herbig 2016).

The rocks of the Kahlenberg Fm and lower Hardt Fm (units 2 to 4 by Zimmerle et al. 1980) described herein can be lithologically subdivided as follows (Hartenfels et al. 2016):

Black Shale (Unit 2 of Zimmerle et al. 1980)
The black shales are composed of an approximately 120 cm thick package of mainly dark-grey shales (beds 91a-d, Fig. 15a, b) missing macrofauna, except for very rare *Guerichia* (Becker et al. 1993). Higgs & Streel (1984, 1994) dated it as HD Zone (based on one sample), which lies within the middle Tournaisian. Therefore, this hypoxic shale unit can be correlated with the Lower Alum Shale beds of the Sauerland and with the Pont d´Arcole Formation (*peracuta* Shale, Tn 2a) of the Ardennes and Aachen region (see Herbig et al. 2001, Amler & Herbig 2006, Aretz et al. 2006). In contrast to the typical Lower Alum Shale, Zimmerle et al. (1980) found no pyrite and noted only slightly enhanced C_{org} levels. The origin of the dark colour thus remains enigmatic. Evidence of volcanogenic clay particles might be a possible explanation.

Calciturbidites (Unit 3 of Zimmerle et al. 1980)
The calciturbidites (beds 92-107, Fig. 15) are 573 cm thick and are medium- to thick-bedded (Fig. 15b), very fine-grained, partly laminated and slightly dolomitized with low C_{org} values (Zimmerle et al. 1980). Single carbonate beds reach thicknesses of up to 50 cm (Fig. 15d).
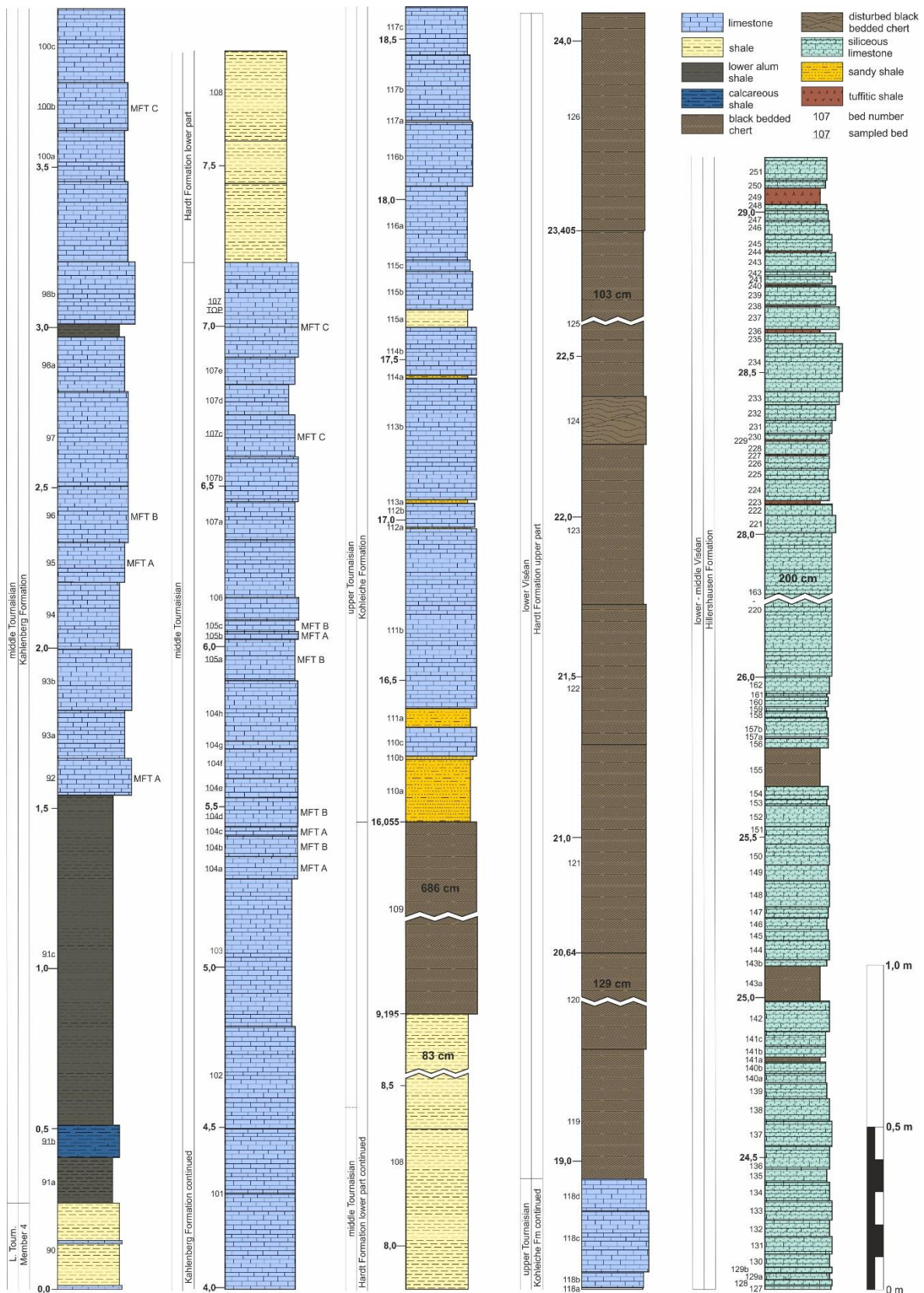
Fig. 14 Complete section-log of lower Tournaisian to middle Viséan succession exposed in Riescheid; modified from HARTENFELS et al. (2016).

Due to weathering they split into thinner layers of only several cm or mm (Fig. 15c). In the outcrop dolomitization is mainly observed along bedding planes, but microscopic analyses reveal abundant subhedral dolomite crystals throughout the rock.

In spite of apparent uniformity, three different microfacies types (MFT) are discerned. All are very fine-grained packstones, but accumulated under varying flow regimes and reveal a changing intensity of bioturbation (see below).

A small conodont fauna of the *isosticha*-Upper *crenulata* Zone was reported by LANE & ZIEGLER (1978), notably containing of *Gn. punctatus* and *Si.* cf. *isosticha*, and was also listed in PARK (1983) (*Si. obsoleta*, *Si. isosticha*, *Gn. punctatus*) and by BECKER et al. (1993; note: Bed 60 must read Bed 50). Therefore, the calciturbidite unit and the underlying black shale unit form the biostratigraphic equivalent of the Pont d´Arcole Formation.

Hydrodynamic sorting within the very fine-grained calciturbidites (HERBIG & MAMET 1993) seems responsible for missing agglutinating foraminifers and mainly absent conodonts (only few tiny, mostly broken conodonts were found in new samples). t

Regardless, a few *Si. isosticha* (Pl. 13, Figs. 12, 13), *Si.* cf. *crenulata* (Pl. 13, Fig. 2) and *Gnathodus* sp. (Pl. 9, Figs. 9-10) could be retrieved from beds 104c-e (upper part of unit 3). They are the first middle Tournaisian conodonts figured from Riescheid. They confirm the conodont fauna by LANE & ZIEGLER (1978). Missing ornamentation (except for a reticulate pattern, see Pl. 13, Figs. 2, 12, 13) and the small size of the elements (juvenile specimens) underline the influence of hydrodynamic sorting.

Black shale (Unit 4 of ZIMMERLE et al. 1980)
An about 1.7 m thick package of black shale (Bed 108, Fig. 15a, f) was deposited after the waning of calciturbidite shedding in the upper part of the underlying Kahlenberg Fm which is predominated by MFT C (bioturbated packstone). These finely laminated shales form mm to cm thick beds and faint bioturbation can be observed. Unit 4 is darker than the black shales of Unit 2, due to much higher C_{org} values (almost up to 4 %, ZIMMERLE et al. 1980). A partially volcanogenic origin of clay particles has been postulated. Siphonodellids (*Si. cooperi* and *Si. obsoleta*, GROOS-UFFENORDE in BECKER et al. 1993) in the lowermost 10 cm prove an age high in the middle Tournaisian *isosticha*-Upper *crenulata* Zone.

5.3 Microfacies

The middle Tournaisian calciturbidites (unit 3 of ZIMMERLE et al., 1980) of the Kahlenberg Fm in the section Riescheid can be divided into three microfacies types.

5.3.1 MFT A: Finely laminated, fine-grained packstone (Pl. 1, Figs. 1, 4-5, 7, 14)

The most abundant MFT consists of tiny calcite grains (micropeloids, microbioclasts, and undifferentiated crystalline calcite; 10-50μm) and lenses or layers of slightly coarser grains (in part detrital quartz). Parallel lamination predominates (Pl. 1, Fig. 1), but isolated ripple bedding (Pl. 1, Fig. 5) is observed. In places, faint erosional surfaces occur between laminae. Bioturbation is rare (Pl. 1, Fig. 4). Tiny, rare bioclasts (< 1 mm) consist of echinoderms (Pl. 1, Fig. 7), thin-shelled ostracodes, thin-shelled bivalves (Pl. 1, Fig. 14) and conodonts. Other components are plant fragments, mica, pyrite, quartz, and plagioclase.

This MFT represents accumulations of turbidity currents close to the western margin of the Kulm Basin that during the middle Tournaisian, in general, is characterized by deposition of black shales.

Fig. 15 Outcrop conditions of the Kahlenberg Fm in the Riescheid section **a**: calciturbidites in the center surrounded by dark shales of the Kahlenberg Fm (right side) and the Hard Fm (left side), diameter of picture: approx.: 10,5 m; **b**: calciturbidite beds 92-97, dark shales of Kahlenberg Fm on right side (bed 91), bottle: 23 cm; **c**: limestone beds 98b-101, bed 100b: 15 cm; **d**: limestone beds 103-107, bed 104a-g: 53 cm; **e**: limestone beds 104a-107, bed 104a-g: 53cm, slightly different angle than in Fig 14d; **f**: calciturbidite beds 107, 107TOP and adjoining dark shales (bed 108) of the Hardt Fm, bed 107TOP: 20cm.

The small grain size is related either to a fine-grained source or very distal deposition. The different grain sizes and different lamination patterns show variations in the flow regime. Coarser grains and ripple marks were deposited by stronger currents.

5.3.2 MFT B: Widely spaced, ripple-laminated packstone (Pl. 1, Figs. 2, 8-13)

In general, the same components occur as in MFT A, however lamination is more irregular wider spaced, displaying ripple bedding, and seemingly unlaminated intervals (Pl. 1, Fig. 2). Bioclasts are dominated by scattered radiolaria (Pl. 1, Fig. 8) but also consist of ostracodes (Pl. 1, Fig. 9), echinoderm and crinoid fragments, brachiopod fragments, conodonts and foraminifera. Of special interest is the occurrence of *Magnella reitlingerae* NEUMANN et al., 1975 (Pl. 1, Figs. 10-13), a poorly known *incertae sedis* described from Pragian to Moscovian shallow water carbonates. In Germany, it was hitherto only known from "Strunian" inner ramp deposits of the NW Velbert Anticline and from upper Famennian fine-grained calciturbidites of the Hörre belt in the southeastern Rhenish Massif (HERBIG & TRAGELEHN 1997).

MFT B was also accumulated on a flank in a distal setting, but under quieter conditions than MFT A; the laminated areas display episodes of down-streaming sediment, the unlaminated pelmicritic areas in between represent quiet episodes with only scattered influx of pelagic background material taking place. This MFT contains less clay than MFT A.

5.3.3 MFT C: Bioturbated packstone (Pl. 1, Figs. 3, 6)

The composition is similar to MFTs A and B, but lamination is obscured by bioturbation (Pl. 1, Fig. 3). MFT C is missing in the lower part of the unit and seems to become more common up-section. This points to waning sediment shedding. According to the microfacies, all calciturbidites are of hemipelagic origin; shallow water components are completely missing except for tiny *Magnella* and rare echinoderm debris. According to size and skeletal texture, both are easily transported across wide distances. The very fine-grained (20-50 µm) components – mostly reworked mud and diminutive fossil debris – are also responsible for the mostly missing gradation. Therefore, the source has to be a deeper water intrabasinal swell. In fact, FRANKE et al. (1975) postulated a lower Carboniferous swell ("forebulge") for the Herzkamp Syncline to account for the peculiar regional facies.

This third MFT probably accumulated in a similar way as MFT A, but was completely disturbed by bioturbation afterwards, which led to the cloudy-wavy appearance. Some samples also show a second phase of bioturbation represented by bioturbation spurs surrounded by stylolithes/stylocumulate in the already bioturbated "matrix" (e. g. sample 107.1, 107.2). Dolomitization (Pl. 1, Fig. 6) occurs along the bedding planes.

5.4 Biostratigraphy and sequence stratigraphy

The conodont fauna is very sparse with only six retrieved conodont elements (Pl. 9, Figs. 9a, b, 10; Pl. 13, Figs. 2, 12, 13; Pl. 14, Fig. 7) that were found in sample Ri 104c-e. The sample (**Fehler! Verweisquelle konnte nicht gefunden werden.**) contains two specimens of *Si. isosticha,* one specimen of *Siphonodella* sp., one specimen of *Si*. cf. *crenulata* and two specimens of *Gnathodus* sp. The sparsity of the conodont elements does not allow any conclusions regarding biofacies, but in comparison with the lithology and the previously made findings by other authors (LANE & ZIEGLER 1978, PARK 1983 in BECKER et al. 1993) this conodont fauna can be used to confirm the middle Tournaisian age and the affiliation to

the *isosticha*-Upper *crenulata* Zone. Especially the presence of the gnathodids allows the assignment, as gnathodids do not yet occur in the
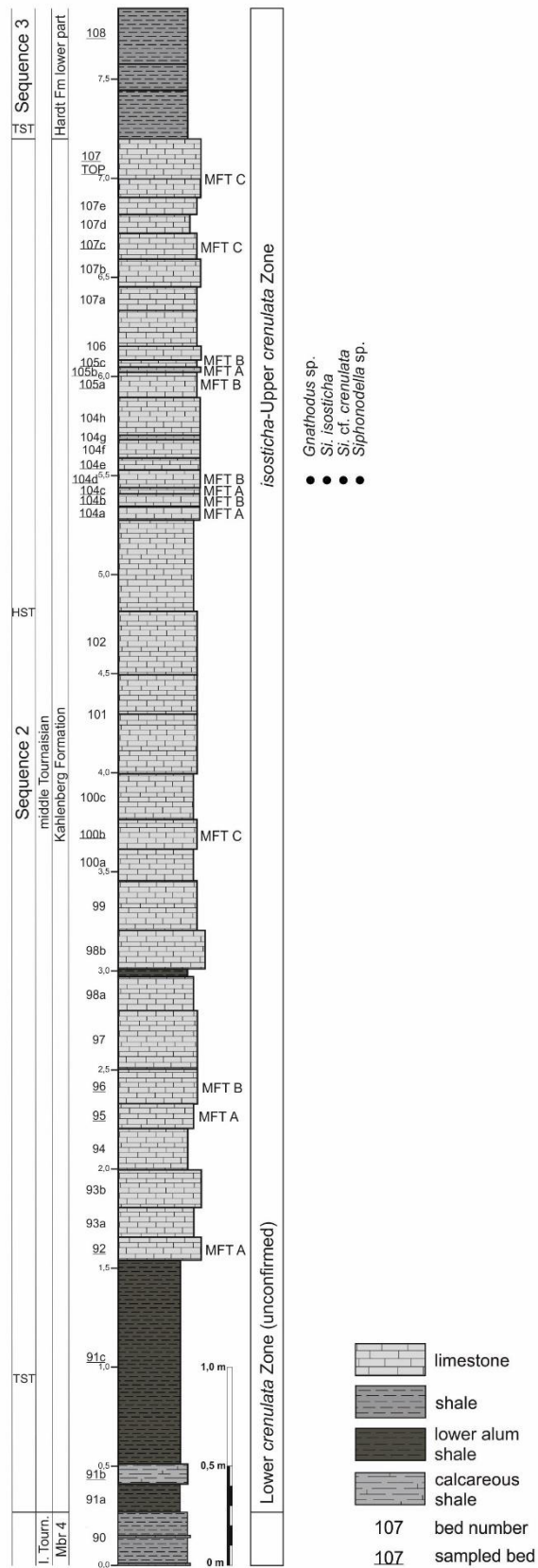
Fig. 16 Section log of the lower and middle Tournaisian of the Riescheid section, including sequences, microfacies types and conodont zonation and retrieved conodont species; unconfirmed

49

Lower *crenulata* Zone is pictured due to its concurrent occurrence with the TST of Sequence 2; modified after HARTENFELS et al. (2016). Note that *isosticha*-Upper *crenulata* Zone reaches into the lowermost part (TST) of Sequence 3.

Lower *crenulata* Zone, whereas *Si. isosticha* and *Si. crenulata* can be found in both zones. Because all other samples were barren, we were not able to define the lower base of the *isosticha*-Upper *crenulata* Zone that is assumed to lie somewhere within the calciturbidite succession. Therefore, no boundary towards the underlying *crenulata* Zone was marked in Fig. 16.
Siphonodellids (*Si. cooperi*, *Si. obsoleta*) from the lower part of the lower Hardt Fm were reported by GROOS-UFFENORDE (in BECKER et al. 1993) and confirm an affiliation to the upper part of the *isosticha*-Upper *crenulata* Zone (Fig. 16).

The blackish shale at the base of the Kahlenberg Fm (Fig. 14, Fig. 16; unit 2 of ZIMMERLE et al. 1980) represents the TST of Sequence 2 (HERBIG 2016). In biostratigraphic terms, the base of Sequence 2, normally coincides with the base of the Lower *crenulata* Zone. This could not be confirmed in Riescheid, but the onset of the "Lower Alum Shale" facies is a reliable lithological marker. The following limestones of the Kahlenberg Fm are calciturbidites related to highstand shedding, originating from an intrabasinal swell, and representing the HST of Sequence 2 (HERBIG 2016) still commencing in the *isosticha*-Upper *crenulata* Zone.
The shales of the lower part of the lower Hardt Fm form the TST of Sequence 3 (HARTENFELS et al. 2016, HERBIG 2016).

5.5 Biofacies of Wuppertal Riescheid
In the section Riescheid only six conodonts were found in sample Ri104c-e, originating from a hemipelagic calciturbidite. All other samples were barren. Therefore, a proper conodont biofacies reconstruction is not possible. However, it is conspicuous that four of the six conodont elements are siphonodellids. According to the schemes and models by CLAUSEN et al. (1989), KALVODA (1991) and KALVODA et al. (1999) that were erected for the lower and middle Tournaisian, this might indicate a Siphonodellid Biofacies of lower slope to basin environments. This is in accordance with carbonate microfacies and sequence stratigraphic interpretation that suggest a hemipelagic source of the caciturbidites.

5.6 Conclusions
The middle Tournaisian Kahlenberg Fm in the Riescheid section begins with blackish shales that contain a thin package of calcareous shale. They represent deeper-water accumulations with little to no input of calcareous material that developed under shallower-water conditions. These deeper-water accumulations represent the typical
Kulm facies in the Herzkamp Syncline and were deposited during the TST of Sequence 2. According to lithostratigraphic correlation, they are assumed to coincide with the Lower *crenulata* Zone, although this could not be confirmed by conodont findings.
The following unit of medium- to thick-bedded limestones is composed of distal turbidites that accumulated under changing flow regimes. They represent the HST of the middle Tournaisian transgression (Sequence 2). All turbidites are of hemipelagic origin as documented by the biogenic content that is mainly missing shallow-water components. Only *Magnella reitlingerae* NEUMANN et al., 1975 and the echinoderm fragments are shallow-water components, but due to hydrodynamic sorting their presence can be

explained. A deeper-water intrabasinal swell probably northwest of Riescheid in the Herzkamp Syncline (forebulge) was the source of the calciturbidites.

Episodes that mark the down-stream movement of turbiditic material along the slope can be recognized by parallel lamination and ripple marks (stronger currents). Quiet episodes are characterized by unlaminated areas in the packstones that experienced only influence of scattered background components. Towards the top of the limestone unit, a shift in the appearance of the packstones can be observed. The lamination, induced by the turbiditic currents, is strongly disturbed by bioturbation leading to a cloudy appearance. Therefore, quiet episodes without turbidite inflow that allowed soft-bodied organisms to dwell in the sediment must have occurred repeatedly. In general, this points to varying turbidite influx in the top of the limestones.

Rare conodont findings have been reported by other authors (LANE & ZIEGLER 1978, PARK 1983 in BECKER et al. 1993: Kahlenberg Fm; GROOS-UFFENORDE in BECKER et al. 1993: lower Hardt Fm). Own specimens could only be retrieved from one sample in the upper part of the limestone unit, in an interval where lamination caused by turbidites could still be observed. The retrieved specimens were unornamented, except for reticulate patterns, and of slightly smaller size than conodonts from other examined sections. This leads to the assumption that we retrieved juvenile specimens, resulting from hydrodynamic sorting in the turbidites.

6. Gladenbach

6.1 Introduction

The Gladenbach Fm, is mostly composed of middle Tournaisian (lower Mississippian) calciturbidites that are equivalent to the Kahlenberg Fm and the lower part of the Hardt Fm recognized in the Kulm succession along the northeastern and northern margin of the Rhenish Mountains (e.g., HERBIG et al. 2017). The formation depicts an "anomalous" facies development in comparison to the "normal" facies in the adjacent Dill-Eder and Lahn synclines due to its position within an allochthonous nappe. The Hörre Nappe constitutes one of the differentiated allochthonous units in the eastern and southeastern part of the Rhenish Mountains (ECKELMANN et al. 2014, FRANKE et al. 2017) (Fig. 17). The study of the differing facies development and faunal content of the Upper Devonian to lower Carboniferous (Mississippian) succession of the Hörre Nappe is of major importance, in order to understand its formation and origin in relation to the autochthonous succession further to the NW. Herein, the taxonomy and biofacies of the conodont fauna and the calcareous microbiota from the type section of the Gladenbach Fm are presented. This is a major contribution to the microfauna of the middle Tournaisian, which is scarcely known from the German Kulm basins. Conodont biofacies enables to reconstruct the approximate depositional realm in a slope-basin setting and its development through time.

The first note of the "anomalous" facies of the Hörre Zone that separates the Lahn Syncline from the Dill-Eder Syncline was given by KAYSER (1893), who believed the rocks to be of Devonian age. Therefore, he interpreted the Hörre to be an anticline. Later, KAYSER (1899) compared the rocks of the Hörre to those of the Kellerwald. Based on lithologic comparisons AHLBURG (1918) again concluded that most of the Hörre is of Devonian age. Finally, BISCHOFF & ZIEGLER (1956) were able to estimate a more accurate age (toIIβ, toIIα, toV, cuII; corresponding to lower, middle, upper Famennian and Tournaisian) based on conodonts and precise field work.

Based on the different facies developments in the adjacent synclines, and the early Upper Devonian greywacke sedimentation, a nappe concept for the Hörre Zone was established early and it was interpreted as a southeast-derived, allochthonous tectonic unit (ENGEL et al. 1983). Other studies (BENDER & BRINCKMANN 1969, BENDER 1978, 1989) that recognized a facies transition between the Hörre and the adjacent, marginal areas of the Lahn and Dill-Eder synclines as well as microstructural investigations (ENTENMANN 1990) assumed a parautochthonous origin of the zone. Deep seismic reflection data (FRANKE et al. 1990) did not give any new insights into its structural relations. BENDER & KÖNIGSHOF (1994) studied metamorphic patterns based on the conodont colour alteration index (CAI) and described the Hörre Zone as an autochthonous unit. Finally, ECKELMANN et al. (2014) studied age clusters of zircons that have been derived from greywackes and sandstones from various localities of the Rhenish Mountains. The age clusters from the Hörre yielded a typical Gondwana signature. Thus, the allochthonous nature of a "Hörre Nappe", deriving from the Armorican Terrane Assemblage south of the Rhenish Mountains, could be unequivocally proved. This assumption is corroborated by specific fossil assemblages from the Steinhorn Nappe, which is situated South of the Hörre (Fig. 17).

BENDER (1978) and BENDER & HOMRIGHAUSEN (1979) described the lithology and biostratigraphy of the Hörre Nappe in greater detail. The siliciclastic sediments of the Upper Devonian and lower Carboniferous in particular were studied by HOMRIGHAUSEN (1979) and ENTENMANN (1991). Both authors interpreted the depositional realms as well as the

palaeogeographic development of the Hörre Zone (Homrighausen 1979) and the palaeoflow regime (Entenmann 1991). Herbig & Bender (1992) described the lithology, carbonate microfacies, and cyclic development of the Gladenbach Fm. They recognized a 3rd order shallowing-upward cycle subdivided into 4th and 5th order minor cycles, and correlated the succession with a transgressive and highstand systems tract. It was correlated with the global "mid-Tournaisian transgression" of the Lower *crenulata* and *isosticha*-Upper *crenulata* conodont zones, which in the autochthonous starved basin facies of the Rhenish Mountains is expressed by the Kahlenberg Fm (former "Liegende Alaunschiefer"). Herbig (2016) assigned the Gladenbach Fm to the 3rd order Sequence 2 and the lower part of 3rd order Sequence 3 of the European Mississippian sequence stratigraphic scheme (Fig. 18).

Bischoff (1957) was the first who worked on the conodont biostratigraphy of the Rhenohercynian lower Carboniferous. He included two conodont faunas from Gladenbach, which he assigned to the *Siphonodella*-Subzone ("cuIIα-β, middle and upper Tournaisian"). The conodont faunas were recovered from two dark bituminous limestones and yielded approximately 50% siphonodellids. Blumenstengel et al. (1997) described the ostracod fauna of the Gladenbach Fm. A preliminary account on the conodont biostratigraphy of the Gladenbach Fm in its type locality was given by Esteban Lopez et al. (2019).

6.2 Geological Setting and description of the section

Within the Rhenoherynian Zone of the European Variscan orogenic belt, the Rhenish Mountains are a typical asymmetric foreland basin with overthrusted, complex nappe structures in its southeastern, proximal part. The Hörre Nappe is the northernmost nappe, separated by the parautochthonous Kamm-Quarzit, the Bicken-Ense Nappe and Wildestein Nappe (Schindler et al. 2017) from the autochthonous rocks of the Dill-Eder Syncline further northwest (Fig. 17). The youngest rocks of the Hörre have been uplifted at the northwestern margin of the nappe. The southeastern margin is formed by a thrust fold named "Weidbacher Überschiebung" by Kegel (1934) (Kockel, 1958).

The Hörre itself is a long, narrow outcrop belt, two to eight kilometers wide, more than 50 km long (Bender, 1978), consisting of Upper Devonian and lower Carboniferous (Mississippian) rocks. It is confined by Neogene vulcanites of the Westerwald in the Southwest and disappears below Permotriassic redbeds of the Frankenberg Bucht northwest of Marburg in the Northeast. The southwest-northeast striking Dill-Eder Syncline and Lahn Syncline confine the Hörre to the Northwest, respectively to the Southeast (Bender 1989) (Fig. 17).

The tectonic deformation of these three structural units shows distinctive differences. The Hörre Nappe experienced more intense folding and thrusting than the Dill-Eder and Lahn synclines (Eckelmann et al. 2014). Also, the lithofacies of the Hörre Zone differs from the other units. Especially noteworthy is the early shedding of greywackes, that are present since the lower Famennian, as well as upper Famennian (Weitershausen Fm) and middle Tournaisian (Gladenbach Fm) detrital carbonates. Upper Devonian and lower Carboniferous volcanic rocks are almost completely absent, in spite of ash layers that are intercalated in some formations (Eckelmann et al. 2014) e.g., also in the type locality of the Gladenbach Fm, immediately above bed 16 (own observation) of the Hörre. Rock successions in the immediate neighbourhood of the Hörre also show facies developments differing from the "normal" facies (e. g. Wildestein Nappe) and interfinger with the Hörre facies (Bender 1989).
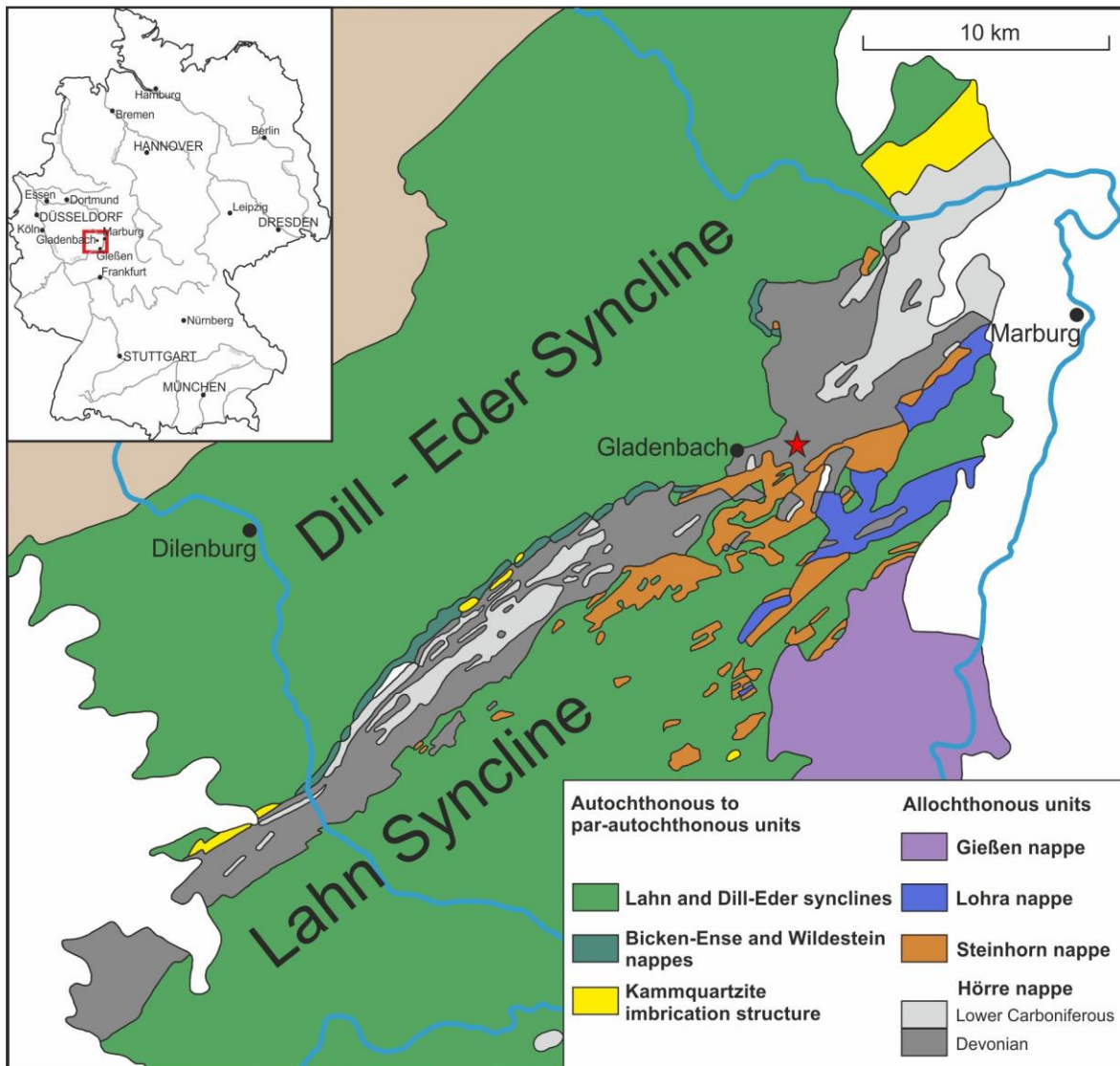
Fig. 17 Structural map of the Lahn-Dill area, with the Hörre Nappe in grey colours, red asterisk marks location of the Gladenbach section, red box in small map indicates location of the main map within Germany, modified after Eckelmann et al. (2014).

The Hörre Nappe comprises a lower Famennian to supposedly middle Viséan succession (Schindler et al. 2017, Herbig et al. 2017). The succession starts with the Petersburg Fm, consisting of varicoloured, in part silty and siliceous shales (Lower to Uppermost *crepida* conodont zones). It is overlain by shales, sandstones and greywackes of the Ulmbach Fm (*rhomboidea* through upper *trachytera* conodont zones). Shales and detrital, thin-bedded carbonates of the Weitershausen Fm follow (Lower *postera* to Middle *praesulcata* conodont zones). The overlying earliest Carboniferous Endbach Fm (Upper *praesulcata* through *sandbergi* conodont zones) consists of shales, quartzitic sandstones and thin-bedded greywackes. Siliceous shales, black alum shales, cherts and turbiditic limestones of the Gladenbach Fm (Lower *crenulata* into *typicus* conodont zones) follow. They are succeeded by shales with intercalations of greywackes of the Bischoffen Fm. Its lower part still yielded conodonts of the *typicus* Zone; younger conodonts are not known from the Hörre Nappe. The top of the succession is composed of the unfossiliferous Elnhausen Fm that consists of shales and thick-bedded greywackes (Bender & Stoppel 2006, Bender 2008).

An overview of the biostratigraphic, lithostratigraphic and sequence stratigraphic subdivision of the upper Famennian and Tournaisian formations in the autochthonous northwestern parts of the Rhenish Mountains and the Hörre Nappe is given in Fig. 18.

In the type locality of the Gladenbach Fm, east of Gladenbach (Sheet Gladenbach 5217, r 3472440, h 5626270), 15 km SW of Marburg, the formation is approximately 14 m thick and consists of black bituminous limestones and intercalated dark shales (Fig. 20). The type profile is intersected by few eastward dipping faults (BENDER in BENDER et al. 1971, ZIEGLER 1971, HERBIG & BENDER 1992). Base and top of the formation are not exposed (HERBIG & BENDER 1992).

Chrono-strat.		Conodont zonation		3rd order seq.	Traditional lithostratigraphy Rhenish Kulm Basin	approved formal lithostratigraphy Rhenish Kulm Basin		Hörre Zone
		Sandberg et al. 1978, Herbig 2016	Hartenfels 2011, Becker et al. 2016					Bender & Stoppel 2006, Bender 2008
MISSISSIPPIAN	TOURNAISIAN	*Sc. anchoralis*		4	Erdbach Limestone II and equivalents	Böhmig-hausen Mb	Kohleiche Fm / Kattensiepen Fm / Erdbach Lmst. II	Bischoffen Fm
		typicus U. / L.		3	Schwarze Kieselschiefer and Lydite	Hardt Fm		
		isosticha- U. *crenulata*		2	Liegende Alaunschiefer	Kahlenberg Fm		Gladenbach Fm
		L. *crenulata*	*Si. crenulata*					
		sandbergi	*Si. quadruplicata*	1	Hangenberg Limestone	Hangenberg Shale		Endbach Fm
			Si. sandbergi					
		duplicata U.	„*Si. hassi*"					
		L.	*Si. duplicata*					
			Si. bransoni					
		sulcata	*Si. sulcata* / *Pr. kuehni*					
DEV.	FAM.	Upper *praesulcata*	*Pr. kockeli*		Hangenberg Sandstone			
		Middle *praesulcata*	*costatus-kockeli interregnum* / *Si. praesulcata*					

Fig. 18 Stratigraphy, conodont zonation and 3rd order sequences of the Upper Devonian and Mississippian Rhenish Kulm Basin and the Hörre Zone (lithostratigraphy Hörre Zone: BENDER 2008, BENDER & STOPPEL 2006, Conodont zonation: BECKER et al. 2016, HARTENFELS 2011, HERBIG 2016, SANDBERG et al. 1978, 3rd order sequences and lithostratigraphy of the Rhenish Kulm Basin: HERBIG 2016). Note that only in the Riescheid section the base of the Hardt Fm and the corresponding base of Sequence 3 is proved to be in the upper part of *isosticha*-Upper *crenulata* Zone.

In spite of these shortcomings, the locality is the only sufficiently exposed succession of the formation. Throughout the section many turbiditic fining upward cycles, beginning with a more or less prominent limestone bed, can be recognized. HERBIG & BENDER (1992) counted 24 of those turbiditic 5th order cycles, which can be grouped in five 4th order cycles. The cycles start with calciturbidites, siliceous limestones or thin-bedded limestones, followed by one or various of the following lithologies: silty to fine-grained sandy shales, siliceous shales, dark grey shales, calcareous-siliceous shales and calcareous shales. Fissile shales, siliceous shales, and, in ideal cases, bedded cherts form the top of the cycles. The upper part of the cycles is regarded to represent the hemipelagic to autochthonous basinal background sedimentation.

Calciturbidites

The calciturbidites of the section can be differentiated into (1) massive, dark grey to black limestones (wackestones, packstones and grainstones) and (2) thin-bedded, dense limestones (wackestones and packstones) (HERBIG & BENDER 1992).

(1) The massive limestones usually form 10-30 cm (rarely 60 cm) thick beds (Fig. 19c, d), that are platy or erosively cut into the underlying sediments (Fig. 19c, d). In some cases, channel-like interfingering beds form up to 75 cm thick limestone units and small channel structures are probably overprinted and deformed by the overlying load. The limestone beds show low-angle cross bedding in the lower part and horizontal lamination in the upper part. In other cases, the base is horizontally laminated and the top is structureless. Completely structureless, dense beds occur as siliceous limestones, especially in the lower part of the section. Many beds or bed complexes throughout the section have a silicified base.

Macroscopically, the limestones are very fine-grained to dense, only one bed with a basal intraclastic pebble layer, was observed.

On polished sections HERBIG & BENDER (1992) observed general grading in most cases. An idealized bed starts with a very fine-grained structureless arenitic layer, that grades into indistinct horizontal bedding, rarely into low-angel cross bedding. Further up the beds are distinctly densely laminated, partly due to interbedding of radiolarian-rich laminae (microfacies B1, strongly affected by pressure solution) and intraclastic-bioclastic laminae (microfacies A1). The uppermost layer of the ideal bed consists of homogenous mud. Echinoderm debris can occur within the basal arenitic layer or form separate layers. Most beds only show an indistinctly graded, massive or laminated lower part and a homogenous top. Only sample 9, a 60 cm thick bed, displays an ideally developed, 15 cm thick sequence in its top.

(2) The thin-bedded, dense limestones show black and brown weathering and consist of impure lime-mudstones. They are frequently argillaceous and rarely slightly siliceous. Lamination, as well as clay partings and *Planolites* (more frequent towards the top of the beds) occur. The mudstones usually split into 2-5 cm thin beds (Fig. 19a, b, c), occurring in up to 35 cm thick packages (Fig. 19a). In the uppermost part of the section HERBIG & BENDER (1992) observed strongly weathered mudstones with faint cross-bedding in up to 20 cm thick beds, always overlying an 1-4 cm thick, dense or laminated siliceous limestone layer, showing a distinct erosive base.

The study of polished sections (HERBIG & BENDER 1992) revealed homogenous, structureless mudstones.

Shales

Several varieties of shales and transitions between them occur in the section and were shortly described by HERBIG & BENDER (1992). They represent hemipelagites with extremely fine-grained detrital influx.

Dark grey to black shale is an important lithology and shows strong lithological similarities with the general "Lower Alum Shale" facies.

The calcareous, siliceous and silty to fine-grained sandy shales appear in 0,5-3 cm thick, platy beds (Fig. 19c), sometimes displaying lamination or sandy partings. Plant debris and

Fig. 19 The Gladenbach Fm in its type locality **a**: uppermost part of section, red arrows indicate fining upward 5th order cycles according to HERBIG & BENDER (1992). Bipartite calciturbidite bed (sample 31-1, 31-2) is the lowermost bed yielding conodonts of the Lower *typicus* Zone; **b**: topmost, thin calciturbidite beds of section (sample 32, 33) within platy lime mudstone package; **c**: sharp contact at base of calciturbidite bed (sample 27), slightly incising into underlying calcareous shales, that, in turn, are underlain by shales (calcareous shales are laminated and fissile, whereas non-calcareous shales appear in thicker bedded lithology), scale 0.4 m; **d**: thickest calciturbidite package of the section (sample 13 to 19) with evident channelized basal contact and internal erosional contact, above sample 16 bentonitic tuffitic layer and recessing lime mudstone bed, followed by second calciturbidite set with channelizing and thickness variations of single beds. Vertical scale bar 0.6 m.

Planolites are scarce. The sandy shales are in rare cases associated with centimeter thick layers of fine-grained sandstones.

Rare pure shales are characterized by their fissility, but at first sight in the outcrop appear as thin homogenous beds (Fig. 19a).

Bedded Chert

Bedded chert is restricted to an isolated very thin bed (between bed 4 and bed 5) in the lower part of the section. It represents the autochthonous basinal sedimentation (HERBIG & BENDER 1992).

6.3 Microfacies

For the turbiditic limestones of the Gladenbach section, HERBIG & BENDER (1992) erected two main facies groups that can be further subdivided in facies types. The thin-sections were restudied within the scope of this work. The facies groups and facies types are distinguished from each other based on structure and component contents.

The two main facies groups are:

A: Grainstones and packstones with reworked platform material, mostly from deeper-water

B: Wackestones and packstones with predominating hemipelagic biota and absence of shallow-water components

6.3.1 MFT A1: Fine-grained intraclastic-bioclastic grainstone/packstone (Pl. 2, Figs. 1, 5-6, 8-9, 12, 17)

The micritic or microsparitic (Pl. 2, Fig. 1) matrix contains small intraclasts (pseudopeloids), microbioclasts and small bioclasts that have, in general, diameters of 0,1-0,25 mm (exceptionally 0,4 mm; echinoderm detritus might reach bigger sizes, because of special hydrodynamic behavior). Among the dominating echinoderm fragments (Pl. 2, Fig. 6) and spines and brachiopod shells and spines (Pl. 2, Fig. 8), the bioclasts consist of ostracodes (Pl. 2, Fig. 9), radiolarians and bivalve shells. Conodonts (Pl. 2, Fig. 5), calcareous algae, calcareous foraminifera, sponge spicules (Pl. 2, Fig. 17) and calcisphaera only occur rarely. Brachiopods, echinoderms and the rare calcareous foraminifera become more frequent towards the upper part of the section.

Non-biogenic components are lithoclasts (in some cases with sparry calcite rim, Pl. 2, Fig. 12), cortoids, peloids, pyrite, dolomite, plagioclase and quartz, all of which are not very frequent.

Bioclasts and flat lithoclast-lenses are observed in current-induced horizontal lamination as well as in scarce cross bedding. In some cases, bioclasts and lithoclasts are parallel arranged to pressure solution laminae (often microstylolite swarms). In the uppermost part of the section, beginning with bed 26, lamination disappears.

Lamination can also be observed in transitional areas of two facies types, consisting of interbedded laminae of both facies types. Those transitional areas are characterized by increasing numbers of radiolarians, sponge spicules and ostracodes. They indicate a development towards facies type B1 that occurs in the upper part of the section, beginning with bed 19. Graded areas with coarsening-upward also indicate this phenomenon.

This facies type only occurs in the calciturbidites.

6.3.2 MFT A2: Ooid-bearing intraclastic-bioclastic packstone (Pl. 2, Figs. 2, 15-16)

This facies type is least abundant with only two assigned samples (31-1, 31-2). It occurs only in the upper part of the section in the calciturbidites. It is the coarser grained (component size 0,3 -0,4 mm Ø) version (Pl. 2, Fig. 2) of the previously described facies type A1.

The mainly sparitic and micritic matrix contains echinoderm fragments, radiolarians, bivalve shells and brachiopods. Furthermore, sponge spicules, calcareous algae, calcareous foraminifera and conodonts occur rarely. Besides the conspicuous ooids (Pl. 2, Figs. 15, 16), peloids, lithoclasts, dolomite, plagioclase and angular detrital quartz grains are present (Pl. 2, Fig. 15).

Pressure solution is obvious due to stylolites and diagenetically overprinted areas can be observed by partial dolomitization. Lamination can not be observed in this facies type.

The flow-regime of this facies type must have been stronger than that of the previously described facies type A1, being able to transport bigger-sized bioclasts. The unlaminated calciturbidites of this facies type were probably produced by turbidity currents exceeding the velocity that is necessary to produce horizontal lamination or cross bedding.

6.3.3 MFT B1: Radiolarian-rich wackestone/packstone (Pl. 3, Figs. 3, 13-14, 18)

This microfacies type is most abundant with 21 samples assigned to it. The micritic matrix is often partly or completely recrystallized. Radiolarians (Pl. 2, Fig. 18) are most common, accompanied by less frequent echinoderm fragments and spines, brachiopod shells and spines, bivalve fragments, ostracodes, sponge spicules (Pl. 2, Fig. 18), rare conodonts, rare calcisphaera, rare trilobites and rare calcareous algae. Rare compacted *Planolites* burrows occur. Non-biogenic components can be pyrite, quartz, dolomite, plagioclase and rare lithoclasts, which are sometimes surrounded by a sparry calcite rim.

Horizontal layering is well recognizable by laminar arranged bioclasts. It is caused by current orientation but becomes less common in the upper part of the section (beginning at bed 18). Grain size, packing and identifiable biota often decrease upwards within beds, indicating a transition towards facies type B2.

Pressure solution is common and recognizable by stylocumulate (Pl. 2, Figs. 3, 14), stylonodular and stylolaminar structures (Pl. 2, Fig. 13), and by recrystallisation (styloreactate) that in cases results in completely recrystallized matrix (neomorphic calcite). The common radiolarians all are recrystallized calcite ghost structures.

The facies type occurs in calciturbidites and siliceous limestones. The turbiditic material of this facies type derived from deeper environments than the ones forming facies types A1 and A2.

6.3.4 MFT B2: Microlithoclastic-microbioclastic wackestone/packstone (Pl. 2, Figs. 4, 7, 10-11, 19-21)

The micritic matrix (Pl. 2, Fig. 4) contains, besides indeterminable microbioclasts, a bioclast assemblage similar to that of facies type B1, consisting of ostracodes, bivalve shells, echinoderm fragments and spines (Pl. 2, Fig. 10), brachiopod shells and spines. Calcareous algae, radiolarians (Pl. 2, Fig. 20), calcareous foraminifera, conodonts, compacted *Planolites* sections (Pl. 2, Fig. 21), sponge spicules and calcisphaera (Pl. 2, Fig. 11) only occur sporadically. In bed 32 the microproblematica *Magnella reitlingerae* NEUMANN et al., 1975

(Pl. 2, Fig. 7) could be recognized. Microlithoclasts (e.g., pseudopeloids) are common. Intraclasts, lithoclasts (in some cases with a sparry calcite rim), pyrite, dolomite, quartz and plagioclase occur.

Horizontal layering is recognizable by the laminar arranged bioclasts and lithoclasts that are often assembled along or parallel to stylolaminar structures, hinting to secondary, diagenetically enhanced lamination. Towards the upper portion of the section (beginning with bed 20) the lamination disappears. Calcitized radiolarians are often strongly deformed and overprinted by partial solution (Pl. 2, Fig. 19). Stylonodular structures, as well as the differentiation of matrix into calcitic styloreactate (dirty white, Pl. 2, Fig. 19) and non-calcareous stylocumulate (black, Pl. 2, Fig. 19) show the effects of pressure solution.

The facies type occurs in limestones, siliceous limestones and calciturbidites.

6.4 Biostratigraphy and sequence stratigraphy

The conodont succession throughout the section (Fig. 20) is subdivided according to the "standard conodont zonation" introduced by SANDBERG et al. (1978) and LANE et al. (1980), that is generally applied in the German Kulm Basin (GEREKE 2002, HERBIG & STOPPEL 2006). The lower limit of the Lower *crenulata* Zone is defined by the first appearance of *Si. crenulata* and ends below the first appearance of *Gn. delicatus,* which defines the base of the following *isosticha*-Upper *crenulata* Zone. *Si. crenulata* M2 occurs from the beginning of the section up to bed 28. Unfortunately, *Gn. delicatus* is not present in the section, but *Gn. typicus*, that often accompanies *Gn. delicatus*, occurs at bed 24, sample 24-2. Therefore, the lower part of the section, up to the base of bed 24 is attributed to the Lower *crenulata* Zone. Associated species as described by SANDBERG et al. (1978) that range through the zone are *Si. obsoleta, Si. cooperi, Si. quadruplicata* and *Si. lobata*. Within the zone *Si. sulcata* and *Si. duplicata* die out but both species are present up into the *isosticha*-Upper *crenulata* Zone, possibly due to reworking. *Si. isosticha* has its first appearance in the zone. Other important species according to SANDBERG et al. (1978) that also occur in the section are *Ps. tr. triangulus, Ps. fusiformis, Ps. pr. primus, N. c. communis, Po. inornatus, Bi. st. stabilis* and *Bi. ac. aculeatus* (here it first occurs in the *isosticha*-Upper *crenulata* Zone).

From bed 24 onwards, the *isosticha*-Upper *crenulata* Zone is recognized (Fig. 20). SANDBERG et al. (1978) defined the top of the *isosticha*-Upper *crenulata* Zone by the last appearance of the genus *Siphonodella*. Referring to them, *Si. isosticha* is the highest ranging species. The erroneous occurrence of some siphonodellid species in German successions above, in part up to the top of the uppermost *anchoralis* Zone (VOGES 1959, HERBIG & STOPPEL 2006) obviously relies on the very early conodont zonation of VOGES (1960), who did not yet recognize the Lower and Upper *typicus* zones above a still undivided "crenulata Zone", or on reworked conodonts. The last appearance of *Si. isosticha* accompanied by *Si. crenulata* M2 and undetermined siphonodellids in the Gladenbach section is at bed 28, which records a major faunal break concerning decreasing conodont diversity and abundance, and increasing rarity of conodont-bearing beds above (ESTEBAN et al. 2019). Thus, all gnathodids are extremely rare. However, the last siphonodellid in the section, *Si. hassi* JI occurs at bed 30, which is tentatively regarded as the uppermost bed of the zone (Fig. 20). Referring to SANDBERG et al. (1978) *Si. crenulata* (here only the M2 continues to the top of the *isosticha*-Upper *crenulata* Zone), *Si. lobata* (in Gladenbach terminating in the upper part of the Lower *crenulata* Zone), *Si. quadruplicata* and *Si. cooperi* terminate within the zone. The following accompanying species range throughout the zone: *Gn. punctatus* (here it first occurs in the
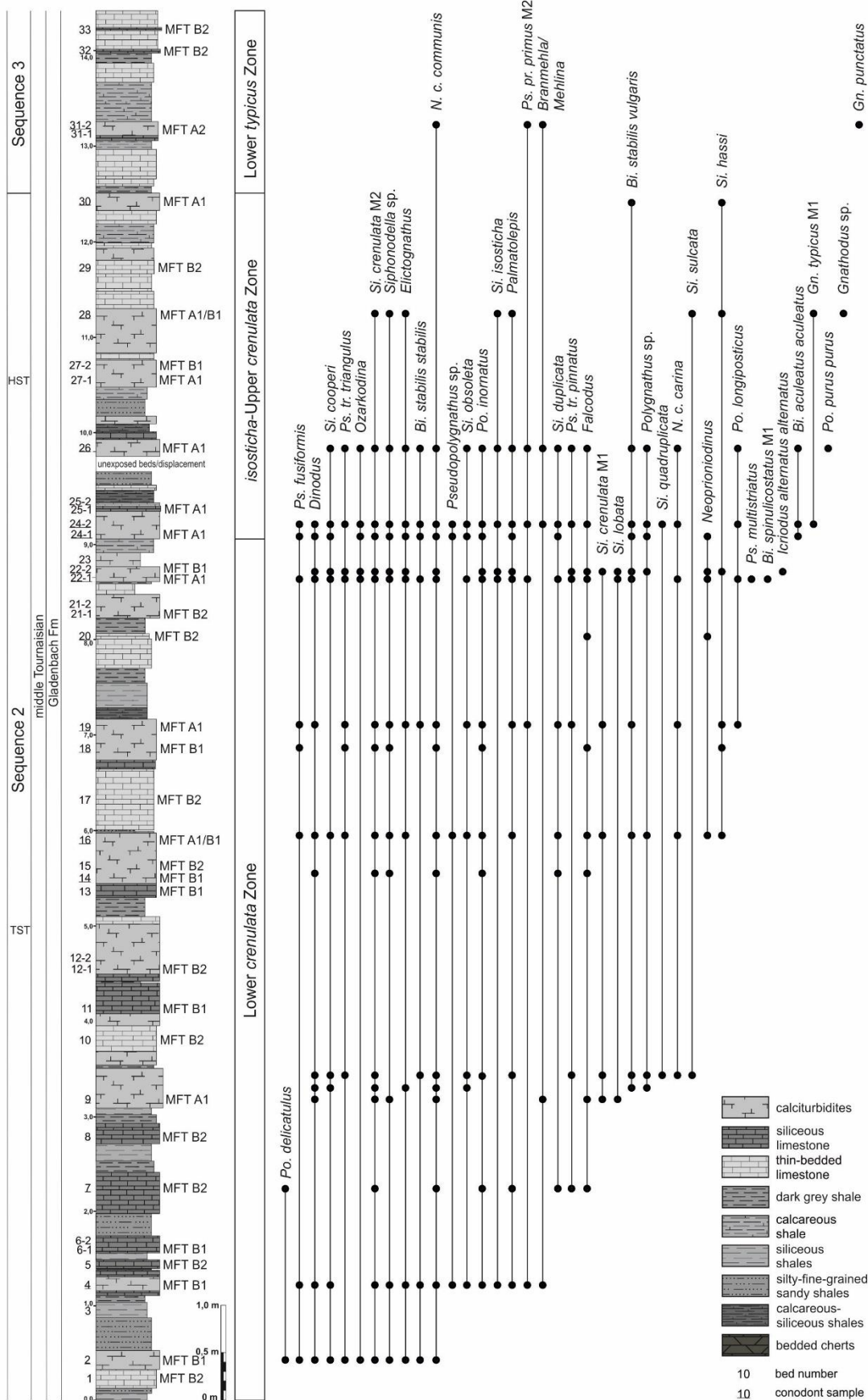
Fig. 20 Section log of the Gladenbach section and distribution of selected conodont genera, conodont zonation, microfacies and sequence stratigraphy; "unexposed beds" refers to minor upthrust that apparently suppressed only few beds; section log after HERBIG & BENDER (1992).

Lower *typicus* Zone), *N. c. communis, Po. inornatus, Bi. st. stabilis, Ps. tr. triangulus* and *Ps. tr. pinnatus*. The lower limit of the following Lower *typicus* Zone is defined by the first appearance of *Gn. typicus* M2 and the extinction of the siphonodellids below (Lane et al. 1980). *Gn. typicus* M2 is very rare in European conodont faunas. Therefore, Belka (1985) proposed to use the more common *Gn. cuneiformis* as zonal marker. Its first appearance is estimated to be slightly above that of *Gn. typicus* M2, and it is well represented in North American and European deposits. As neither *Gn. typicus* M2, nor *Gn. cuneiformis* are present in our samples, only the extinction of the siphonodellids could be used to approach the lower limit of the Lower *typicus* Zone. In conclusion, beds above bed 30 are assigned to the Lower *typicus* Zone. The following species, also listed by Lane et al. (1980) are normally present in the zone: *Gn. typicus* M1 and M2 (in Gladenbach, M1 only occurs in the underlying *isosticha*-Upper *crenulata* Zone, M2 does not occur), *Gn. punctatus, N. c. communis, N. c. carina* (only present in the preceding zone) and *Ps. multistriatus* (here only present in the Lower *crenulata* Zone).

Throughout the section 15 conodont genera and 29 species could be recognized, accompanied by not further studied ramiform conodont elements. Specimens of the genus *Palmatolepis*, occurring in the interval between bed 4 and 28, *Icriodus alternatus alternatus*, occurring in bed 22-2, *Po. delicatulus* occurring in bed 2 and 7 and *Ozarkodina*, occurring in the interval between bed 2 and 26 are reworked Upper Devonian taxa. They prove the reworking of the corresponding beds in the source area and/or the thalweg of the calciturbidites. They should have been derived from the conodont-bearing Famennian formations (Petersburg Fm, Ulmbach Fm and Weitershausen Fm) of the Hörre succession. Already Bischoff & Ziegler (1956) noticed Upper Devonian reworked conodonts in the rocks of the Hörre Zone.

The Lower *crenulata* Zone and *isosticha*-Upper *crenulata* Zone coincide with Sequence 2 of the sequence stratigraphy that can be correlated from Belgium to the Rhenish Kulm Basin. The Lower *typicus* Zone coincides with the lower part of Sequence 3 (Herbig 2016). Sequence 2 in the Rhenish Kulm Basin begins at the base of the Lower *crenulata* Zone with a TST, caused by a globally recognizable transgression known as the "Lower Alum Shale Event" (Becker 1993) or "mid-Tournaisian Event" which depicts the most important sea-level rise within the Rhenish Kulm Basin during the Mississippian. A LST, as it is recognized in Belgium, is not present in the Rhenish Kulm Basin (Herbig 2016). Due to its position near a slope, in Gladenbach the TST can be recognized by the dominance of calciturbidites that interrupt the typical dark shale sedimentation. The waning of the transgression, i. e. decreasing accommodation space, is demonstrated by the decreasing frequency of the different shales and siliceous limestones and increasing frequency and thickness of calciturbidite beds. It marks the transition into the HST (Fig. 20). The sequence boundary at the base of Sequence 2 (not exposed in the Gladenbach section) normally is recognized by a sharp colour change from grey to black shales (e. g. at Drewer, Dexbach; Korn 2010, Herbig et al. 2006) or a gradual transition (e.g., Kohleiche, Siegmund et al. 2002) at the base of the Kahlenberg Fm (equivalent of the Gladenbach Fm). In the Rhenish Kulm Basin, the boundary between Sequence 2 and Sequence 3 is thought to coincide with the base of the Lower *typicus* Zone (Herbig 2016; Fig. 20). In Gladenbach, the Sequence 3 can be recognized by the increased appearance of the different shales. However, regarding biostratigraphic data from the Riescheid section (chapter 5.4) and Belgium, the base of the Sequence 3 is in the uppermost part of the *isosticha*-Upper *crenulata* Zone. In Gladenbach, the sequence boundary therefore already might coincide with the sharp faunal break above bed 28 that,

first, is the last thick calciturbidite bed of the section and, second, the last bed with abundant deep-water indicating siphonodellids (chapter 6.5).

6.5 Biofacies of Gladenbach

In the study of the calciturbidites of the Gladenbach Fm a compilation of the biofacies models presented in chapter 3 were used.

In detail, the model of SANDBERG (1976) is considered concerning the reworked Devonian conodonts. The scheme of CLAUSEN et al. (1989) and KALVODA (1991, 1994, 1999) were used for the interpretation of the middle Tournaisian Lower *crenulata* and *isosticha*-Upper *crenulata* zones. We counted not only platform elements, but also involved some genera of ramiform elements (e. g. *Dinodus, Elictognathus, Ozarkodina*) (Tab. 1, Fig. 21a), though, for biofacies reconstruction only platform (Pa) elements were considered (Fig. 21b, c).

The interpretation of the conodont biofacies has to consider the origin of the conodonts from calciturbidites, which represent a mixed fauna from the source and thalweg of the turbidites. The admixture from pelagic rain is minor due to the rapid sedimentation process of turbidites.

For the biofacies reconstruction, all samples with less than 10 conodont elements were excluded. Unfortunately, above bed 28, the number of conodont elements in the samples was so low, that it could not be used for biofacies reconstruction. Sample 20 is excluded for the same reason.

Conodont Zone	Lower *crenulata* Zone														*isosticha*-Upper *crenulata* Zone					Lower *typicus* Zone
Samples	2	4	7	9-1	9-2	9-3	14	16	18	19	20	22-1	22-2	22-3	24-1	24-2	26	28	30	31-2
Bispathodus aculeatus aculeatus														3	1	4	1			
Bispathodus spinulicostatus M1												1								
Bispathodus stabilis stabilis	1	1			2					3		8		2	7	11	9			
Bispathodus stabilis vulgaris					1			3		4		5	1	7	15	12	14		1	
Branmehla/Mehlina sp.		1	3	1						3		6		4	4	23	8			1
Dinodus sp.	1	1		1	4	1	1	4		2		4	4	4	3	23				
Elictognathus sp.	3	1			1			8		2		7	1	6	5	37	3	1		
Falcodus sp.			1	1			1	2	2		1	1	4			15	1			
Gnathodus punctatus																				1
Gnathodus typicus																1		1		
Ganthodus sp.																	1			
Icriodus alternatus alternatus													1							
Neopolygnathus communis carina						1		1		1		1		1		1	1			
Neopolygnathus communis communis	2	2	4	1	4	9	2	28	2	26		35	55	24	17	85	35			1
Neoprioniodus sp.								1			1	7	4	6	6					
Ozarkodina sp.	2											19	10		18	95	49			
Palmatolepis sp.		1	2			3		2		8		25	34	10	9	89	19	2		
Polygnathus delicatulus	1		1																	
Polygnathus inornatus		1	1			15	2	16	3	39		57	16	16	12	82	61			
Polygnathus longiposticus										1		1				5	2			
Polygnathus purus purus																	1			
Polygnathus sp.				1	1			3					2		3	5	1			
Pseudopolygnathus fusiformis	1	1						2	2	2		2		3	1	2				
Pseudopolygnathus multistriatus												3					1			
Pseudopolygnathus primus primus M2		1							1			1		1	1	2	5			1
Pseudopolygnathus triangulus pinnatus			1			3				4		2	11	1		11	4			
Pseudopolygnathus triangulus triangulus	1					3		1	1	9		5	1	1		34	3			
Pseudopolygnathus sp.		1						6							1	1				
Siphonodella cooperi	1				1	1		8				14	50	7	4	41	12			
Siphonodella crenulata M1				1		22		3		17			46	4				1		
Siphonodella crenulata M2	4	16	3	2	5	9	5	56	5	26		43	111		39	194	24	4		
Siphonodella duplicata			1				1	12		3		10		29	2	5	9			
Siphonodella isosticha		5											31	37		22	24	2		
Siphonodella hassi Ji								4	2	4			1	1				1	1	
Siphonodella lobata				1								2	1							
Siphonodella obsoleta		1			2	1		25		7		47			40	79	21			
Siphonodella quadruplicata						1								2		1				
Siphonodella sulcata						2													1	
Siphonodella sp.	8	21		1	10		1	75	3	17		62	5	32	13	164	35	5		
ramiform elements	11	25	11	5	10	66	14	87	8	39	4	129	46	135	124	365	162	10		3
Total number of conodont elements	36	79	25	16	30	141	27	347	28	218	6	528	413	345	326	1413	505	30	2	7

Tab. 1 Distribution and numbers of conodont species of the Gladenbach section

The gap in the conodont distribution at bed 20 is very evident (Tab. 1). Only six conodont specimens are present in this sample, all of which are ramiform elements (Tab. 1) and, therefore, do not allow a biofacies analysis. The extreme reduction in conodont quantity, compared to the previous and the following sample, apparently is an effect of the different

lithology and their sedimentation processes, as bed 20 consists of thin-bedded limestone with predominantly hemipelagic biota (microfacies B, see chapter 6.3.3, 6.3.4), and most other conodont samples originated from thicker calciturbidite beds (fine-grained intraclastic-bioclastic grainstones and packstones, microfacies A1, see chapter 6.3.1). The calciturbidites of facies type A contain material that was transported downslope and, in many cases, reworked older material. In most cases, the primary conodont fauna might be affected by hydrodynamic sorting. In contrast, the thin-bedded hemipelagic limestones (microfacies type B2) generally contain very few conodonts or are barren. A faunal and environmental shift probably caused the low conodont element numbers in bed 30 and 31-2. First, the decline of the siphonodellids in the upper part of the *isosticha*-Upper *crenulata* Zone coincides with the appearance of the gnathodids at the base of the zone. Second, the base of a Sequence 3 of HERBIG (2016) at the base of the Lower *typicus* Zone (or already in the uppermost part of the *isosticha*-Upper *crenulata* Zone, as discussed above) marks the decline of the water depth and a major change in the composition of the calciturbidites (microfacies A2, see chapter 6.3.2).

Throughout the section (Fig. 21c), the conodont fauna (without the reworked Devonian conodont elements) is mainly dominated by siphonodellids (36-87,5 % of Pa elements) and polygnathids (0-54,5 % of Pa elements). Together they constitute 84-100 % of the fauna in the main part of the section up to bed 28. Therefore, the section is mainly composed of a mixture of a Siphonodellid Biofacies and a Siphonodellid-Polygnathid Biofacies. Accordingly, those biofacies represent environments of deep swell and slope (CLAUSEN et al. 1989), respectively lower slope to basin (KALVODA et al. 1999) (see chapter 3, Fig. 8). In summary, this implicates a deep-water source for the turbidites, confirming the results of the carbonate microfacies analysis.

N. c. communis (5-30 % of Pa elements, Fig. 21b, c), an epipelagic drifter or swimmer, is relatively frequent and can be observed in the Gladenbach section between bed 2 and bed 26 (Fig. 21b, c). Ramiform elements are ubiquitous throughout the section (11-52% of the total conodont fauna, Fig. 21a) and do not show a particular trend in their distribution.

When inspecting the siphonodellids in detail (Tab. 1, Fig. 21b) it is evident that *Si. crenulata* M2 is the most common species occurring in all but two samples (bed 20 and 22-3).

The Upper Devonian conodont genera and species *Palmatolepis, Ozarkodina, Po. delicatulus and I. alternatus alternatus* occur throughout the section up into bed 28, except for beds 9-1, 9-2, 14, 18 and the almost barren bed 20. They compose 0,5-13,5% of the total fauna, reaching the highest values in the interval between bed 22-1 (8,5 %) and bed 26 (13,5 %). These taxa prove continued reworking of Upper Devonian strata during the Lower *crenulata* and *isosticha*-Upper *crenulata* zones. No reworked conodonts are recorded from the Lower *typicus* Zone (beds 30, 31). This might be related to the scarce recovery of conodonts, but more probably to a major change in the carbonate source. In contrast to all underlying calciturbidites, the coarse-grained, ooid-bearing calciturbidite of sample 31 was shed from the platform margin and apparently passed the slope without significant erosion.

Palmatolepis is the most common reworked Upper Devonian genus and constitutes up to 15 % of the reworked Pa elements (Fig. 21b). *Ozarkodina* is the next common genus, appearing in beds 2, 22-1, 22-2, 24-1, 24-2 and 26, and, when present, is often equally numerous as *Palmatolepis* (see Tab. 1). *Po. delicatulus* and *I. alternatus alternatus* are very rare appearing only twice (bed 2, 7) respectively once (bed 22-2). When only considering
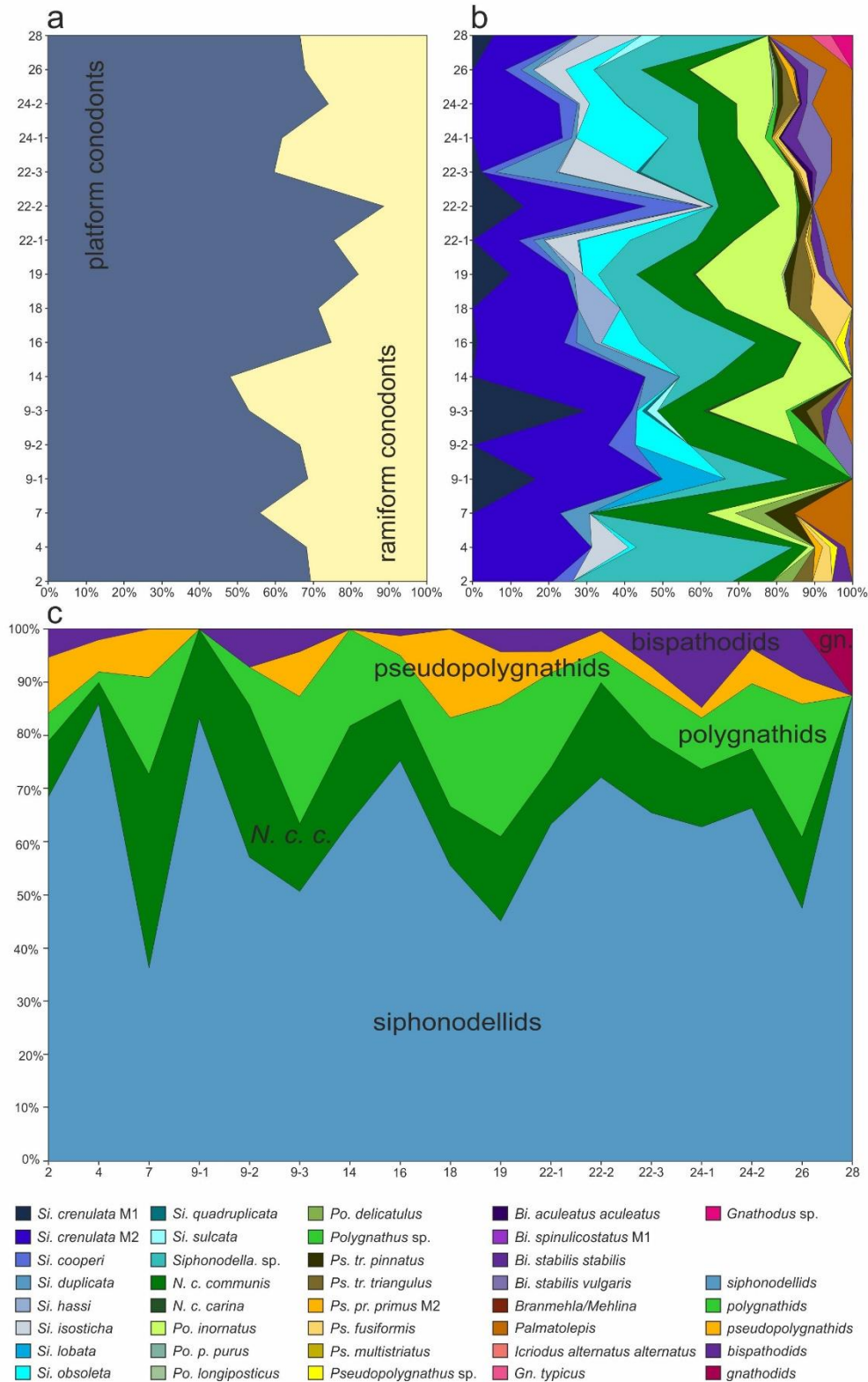
Fig. 21 Distribution of conodont species and genera, samples 20, 30 and 31-2 are excluded due to conodont element numbers >10 **a**: distribution of platform conodonts vs. ramiform conodonts **b**: distribution of platform species **c**: distribution of genera, reworked Devonian faunas are excluded, *N. c. c.* is pictured separately because in the biofacies models it is separated from the other polygnathids; **a** and **b** bed/sample numbers on y-axis, **c** bed/sample numbers on x-axis; blue colours: siphonodellids, green colours: polygnathids and neopolygnathids, dark brown and yellow colours: pseudopolygnathids, purple colours: bispathodids, pink colours: gnathodids

the reworked Devonian conodonts the distribution is as follows: *Palmatolepis* 28-100%, *Ozarkodina* 22-72%, *Po. delicatulus* 33%, *I. alternatus alternatus* 2%. A pure palmatolepid biofacies is not present, but when involving the Upper Devonian to lower Carboniferous genus *Bispathodus* a Palmatolepid-Bispathodid Biofacies (lower slope to basin) as introduced by Sandberg (1976) and applied by Clausen et al. (1989) and Kalvoda et al. (1999) can be assumed for the reworked Upper Devonian fauna (see chapter 3).

In the overall conodont distribution there are no differences between the Lower *crenulata* and the *isosticha*-Upper *crenulata* zones and, therefore, no change in the biofacies. However, there are conspicuous siphonodellid-peaks (72-85 % siphonodellids of Pa elements), depicting a Siphonodellid Biofacies (Clausen et al. 1989, Kalvoda et al. 1999, lower slope and basin environments) occurring at beds 4, 16, 22-2 and 28 (Fig. 21b, c). They apparently mark periods of deepest water conditions, but are not recognized in microfacies or cyclicity.

At the top of the section, in the uppermost *isosticha*-Upper *crenulata* Zone and the Lower *typicus* Zone (Fig. 20), a shift in genera and a sudden decrease in the total number of conodont elements (Tab. 1) is observed. the Lower *typicus* Zone is dominated by gnathodids, bispathodids, pseudopolygnathids and polygnathids, but total numbers are too low for biofacies reconstruction.

6.6 Conclusions

The middle Tournaisian Gladenbach Fm (equivalent of Kahlenberg Fm and lower part of Hardt Fm) represents a special facies development within the allochthonous Hörre Nappe that derived from the Armorican Terrane Assemblage. It contains a rich conodont fauna and, therefore, represents an important contribution to the knowledge of microfossils of this time-interval. The Gladenbach Fm in its type locality is composed of various calciturbiditic limestones, different shales and rare cherts. Depending on the varying sea-level the admixture of these different lithologies changes.

The calciturbidites are either composed of massive limestones that in part erosively cut into the underlying sediments and reveal low-angle cross bedding at the base and horizontal lamination in the upper part of the beds, or lamination in the lower part and structureless areas in the upper part. Alternatively, the calciturbidites are composed of thin-bedded, dense limestones that are frequently argillaceous and rarely slightly siliceous, structured by lamination, *Planolites* burrows and faint cross-bedding. Sedimentary structures such as cross-bedding, horizontal lamination and erosive bases depict the higher energetic flow-regime of the calciturbidites. In contrast, structureless bed intervals and *Planolites* burrrows represent episodes of almost quiet conditions. They either represent the tail of turbidites, or predominant hemipelagic sources.

The different shales are composed of extremely fine-grained detritus of hemipelagic origin and developed within the basin during quiet episodes undisturbed by calciturbidites.

Bedded chert occurs only once in the lower part of the section and represents the autochthonous basinal sedimentation.

The lowermost part of the section is dominated by silty to fine-grained sandy shales and siliceous limestones originating from the lower slope of a deep basin (hemipelagic biota dominate, shallow-water components are missing). They are already attributed to the TST of Sequence 2, which coincides with the Lower *crenulata* Zone. Upsection, clearly

recognizable calciturbidites become frequent. They originate mainly from the lower slope, but reworked biota from shallower water occur already.

Further upsection, decrease in the frequency of the different shales marks the transition towards the HST of Sequence 2 that is dominated by thicker calciturbidite beds and packages. The HST coincides mostly with the *isosticha*-Upper *crenulata* Zone and shows a shift towards increasing input from shallower water.

Reworked Upper Devonian conodont elements in the Lower *crenulata* and *isosticha*-Upper *crenulata* zones prove the intense reworking of strata in the source area and on the thalweg of the calciturbidites.

A dominance of upper slope and platform edge components is observed in the uppermost part of the section at the base of the Lower *typicus* Zone. Immediately above, an increased appearance of the different shales can be recognized. Also, a major shift in the conodont fauna can be observed. The siphonodellids disappear completely and the overall diversity, that was already reduced in the upper part of the *isosticha*-Upper *crenulata* Zone, decreases even more. The faunal shift in the uppermost part of the *isosticha*-Upper *crenulata* Zone is considered to indicate the base of Sequence 3. The rapid and strong reduction in the conodont abundance and diversity is coupled with an increasing rarity of conodont-bearing beds.

7. Wettmarsen

7. 1 Introduction

Middle Famennian (*velifer* Zone) to middle Tournaisian rocks crop out in the small, mostly overgrown former quarry south of Wettmarsen (51°22'55,36''N, 7°54'45,2''E, 4613 Balve). Similar to many other outcrops in the area of the Balve reef complex it contains a depositional gap between Upper Devonian and lower Carboniferous rocks. In this study of the lower Carboniferous (middle Tournaisian) calciturbidites of Wettmarsen (Kahlenberg Fm) a rich conodont fauna could be retrieved. The finding of the extraordinary rich conodont fauna is especially exceptional as carbonate beds are rare in the "Liegende Alaunschiefer" of the autochthonous successions of the Rhenish Kulm Basin, and other outcrops such as Wuppertal-Riescheid (see chapter 5, Hartenfels et al. 2016) only yielded very few conodonts.

The first mentioning of conodonts of the former undifferentiated *Si. crenulata* Zone (now Lower *crenulata* + *isosticha*-Upper *crenulata* zones and Lower + Upper *typicus* zones) originating from a limestone bed within sandstones in the Wettmarsen section was given by Schäfer (1975; based on Voges, 1959, 1960). The section itself was shortly described and figured in an unpublished field guide (Stoppel, with contributions of Heuser, Krebs, Schäfer & Uffenorde 1977) and in more detail by Schäfer (1978). Due to a conodont fauna, the underlying Devonian limestones could be assigned to the *velifer* Zone (middle Famennian). A single limestone bed, within sandstones that could be attributed to the former Liegende Alaunschiefer (Kahlenberg Fm), contained conodonts of the formerly undifferentiated *Si. crenulata* Zone with reworked Upper Devonian elements of the *velifer* Zone. Schäfer (1978) assigned the cephalopod limestones at the base of the section more precisely to the Middle to Upper *velifer* Zone.

Herbig (2016) assigned the lower sandstone beds and calciturbidite bed to the undifferentiated Sequence 2 of the German Kulm Basin. Here we were able to differentiate the LST (shale above the Devonian limestones above a SB 1), the TST (lower sandstone beds) and the HST (calciturbidite bed) of Sequence 2. The following sandstone bed and overlying black bedded cherts (Hardt Fm) represent the LST, respectively the TST/HST of Sequence 3.

7.2 Geological Setting and description of the section

The former small quarry south of Wettmarsen is situated in the central part of the Remscheid-Altena Anticline in the Rhenish Mountains (Fig. 22) within the vicinity of the Givetian to Frasnian Balve reef complex (SW of the section). Referring to Stichling et al. (2015) the Hagen-Balve reef belt probably formed a fringing reef in the center of the Remscheid-Altena Anticline around a synsedimentary high, that before, up to the lower Givetian, was an actively inversed structure (Schudack 1993).

The Remscheid-Altena Anticline is a more than 100 km long and 10-15 km wide structure within the northeastern Rhenish Mountains. In the north it adjoins the Herzkamp Syncline and in the south the Lüdenscheid Syncline (Clausen in Luppold et al. 1994). It depicts a typical Kulm facies and its early Carboniferous succession begins with the nodular limestones of the Hangenberg beds followed by the black alum shales of the Kahlenberg Fm that developed during the deepening of the basin (Korn 2010). The alum shales grade into the black siliceous shales of the Hardt Fm, marking the boundary between sequences 2 and 3 (Herbig 2016). At the base of the Viséan, increasing carbonate sedimentation sets in, dominated by coarsely grained calciturbidites intercalated with greenish siliceous shales

and cherts (KORN 2010: Hillershausen Fm). The calciturbidites originate from the Herdringen Turbidite System (KORN 2010) and prove the presence of a source and slope towards northern/northwestern directions.
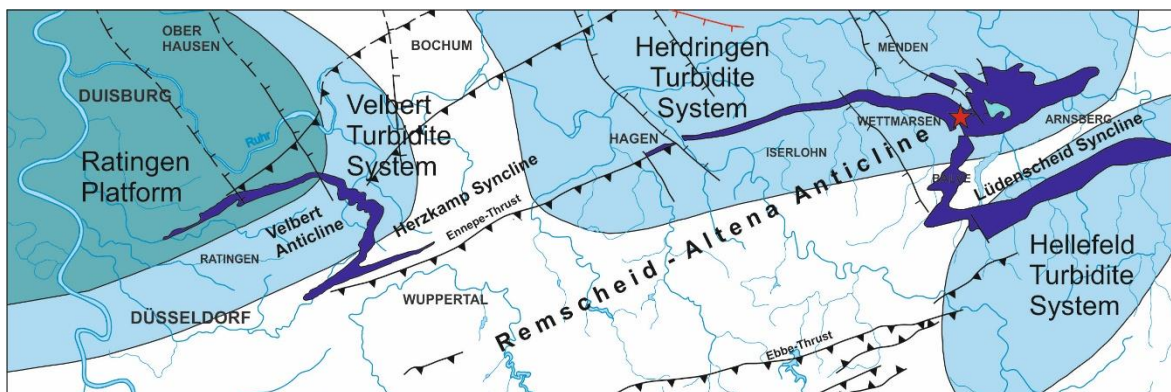
Fig. 22 Lower Carboniferous outcrop areas (dark blue) in the northern Rhenish Mountains, red asterisk marks the position of the Wettmarsen section on the northeastern flank of the Remscheid-Altena Anticline; platform (greenish) and turbidite (ligth blue) systems by KORN (2010)

The base of the Wettmarsen section is formed by cephalopod limestones (Hemberg Beds) of the Middle to Upper *velifer* Zone (SCHÄFER 1978) (= Lower and Upper *trachytera* Zone, ZIEGLER & SANDBERG 1984) followed by a depositional gap. The gap suppressed the Dasberg-Wocklum Beds, Hangenberg Black Shales and overlying Hangenberg Beds, and the lowermost part of the Kahlenberg Fm (SCHÄFER 1978, state-of-the-art nomenclature follows STD 2016). The section is continued by a few cms of shale with a layer of phosphorite nodules. They are followed by about 1 m thick lower Carboniferous sandstones, containing calcareous detritus and pebbles. A limestone pebble 30 cm below the following calciturbidite contained *Siphonodella* sp. (SCHÄFER 1978). The succeeding calciturbidite bed is composed of black, graded, detrital limestone and is partly silicified. It is approximately 30 cm thick (HERBIG 2016, 40 cm according to SCHÄFER 1978) and contains a rich conodont fauna that can be assigned to the *isosticha*-Upper *crenulata* Zone. Another sandstone bed, about 80 cm thick, similar to the first one, is situated on top of the calciturbidite bed and belongs to the Hardt Fm. After an exposure gap (approx. 50 cm), siliceous shales of the Hardt Fm form the top of the succession. STOPPEL (1977) already stressed the peculiar absence of reworked conodonts from the depositional gap on top of the middle Famennian limestones. This points to non-deposition during this interval.

7.3 Microfacies
From the calciturbidite bed of the Kahlenberg Fm two large thin sections (7.5 x 10 cm) are available. They belong to the same microfacies type which differs in certain aspects from the microfacies types studied in the examined sections Riescheid and Gladenbach.

7.3.1 Laminated radiolarian-bearing wackestone/packstone
The mainly microsparitic rarely sparitic matrix contains numerous radiolarian ghosts (Pl. 3, Fig. 3), foraminifera (Pl. 3, Fig. 11) and bivalves (Pl. 3, Fig. 7) as well as calcispheres (*Calcisphaera laevis*, *C. pachyspaerica*, Pl. 3, Fig. 15) and small lithoclasts (pseudopeloids). Besides indeterminate specimens (Pl. 3 Figs. 8, 13), parathuramminids (Pl. 3, Fig. 12) and *Brunsia* sp. (Pl. 3, Fig. 11) were identified. Palaeoberesellacean algae (Pl. 3, Fig. 5), echinoderm spines (Pl. 3, Figs. 10, 14), ostracodes (Pl. 3, Figs. 6), crinoids (Pl. 3, Fig. 9),

69

sponge spicules, coated grains (Pl. 3, Fig. 4) and (micritized) ooids (Pl. 3, Fig. 8) occur very rarely. Most pseudopeloids reach sizes of 100-200 µm, radiolarians range between 0.5 mm and 1 mm, as well as foraminifera, ostracodes and echinoderm debris, that also reach sizes of 0.5-1 mm and exceptionally 2 mm.

Lamination is caused by alternating darker and lighter laminae (Pl. 3, Figs. 1-2). The lighter laminae are rich in pseudopeloids and small bioclasts (foraminifera, bivalves, echinoderm fragments, algae), with a sparitic to microsparitic matrix, whereas the darker laminae are dominated by microsparite and radiolarian ghosts (Pl. 3, Figs. 1, 2).

Stylocumulate only occurs in the darker, radiolarian dominated laminae and is not very frequent. Bioturbation is absent.

The lighter laminae were formed by turbiditic currents originating from shallower areas of an intrabasinal swell (middle to upper slope) whereas the darker radiolarian-rich laminae contain material from deeper areas of the slope, reworked while the calciturbidite was moving down-slope.

7.4 Biostratigraphy and sequence stratigraphy

The conodont fauna retrieved from a single sample of the calciturbidite bed of the Kahlenberg Fm can be assigned to the *isosticha*-Upper *crenulata* Zone due to the common occurrence of the gnathodids *Gn. delicatus* and *Gn. typicus* M1, and the siphonodellids *Si. isosticha*, *Si. lobata*, *Si. obsoleta, Si. cooperi* (SANDBERG et al. 1978). *N. c. carina*, *N. c. communis*, *Ps. tr. pinnatus* and *Ps. tr. triangulus* are associated. Reworked genera and species from the upper Devonian (*Palmatolepis, Bispathodus*) and reworked lower Carboniferous siphonodellids (*Si. duplicata*, *Si. sulcata*) occur. The occurrence of the reworked siphonodellids, bispathodids and palmatolepids (*Pa. gracilis gracilis*) contradicts the statement of STOPPEL (1977) of missing reworked conodonts from the depositional gap on top of the middle Famennian limestones.

In Wettmarsen a SB1 at the base of the Kahlenberg Fm is recognizable by the hiatus on top of the Famennian cephalopod-limestones (Fig. 23). Referring to the description of SCHÄFER (1978) and the sequence stratigraphic interpretation of HERBIG (2016) the middle Tournaisian Kahlenberg Fm represents the undifferentiated Sequence 2 that starts with thin layers of shale and phosphate nodules followed by about 1 m of sandstone and a 0.4 m thick bed of calciturbidite. Here we differentiate the LST represented by the shale and the sandstones. An unequivocal TST is not recognized. However, comparing the already described sections (Riescheid, chapter 5.4; Gladenbach, chapter 6.4) we conclude, that the *isosticha*-Upper *crenulata* Zone coincides with the HST of Sequence 2. Therefore, also the calciturbidite of the Kahlenberg Fm in Wettmarsen is assigned to the HST of Sequence 2. The overlying sandstone at the base of the Hardt Fm constitutes the LST of Sequence 3. After an exposure gap, siliceous shales at the top of the section form the undifferentiated TST/HST of Sequence 3 (HERBIG 2016).
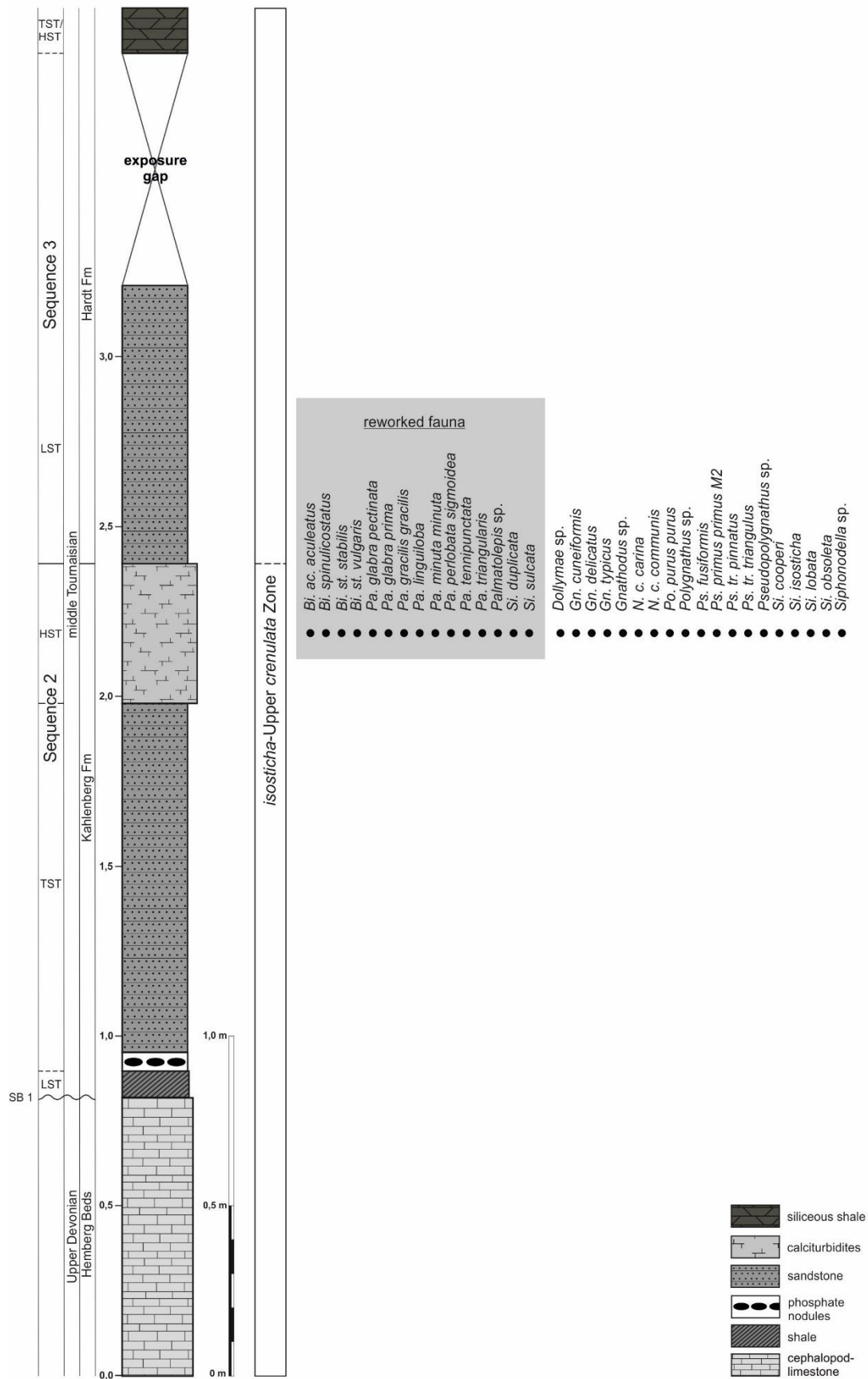
Fig. 23 Section log of the Wettmarsen section including sequence stratigraphy, conodont zonation and platform conodont species and genera, section log modified after Stoppel (1977), Schäfer (1978).

7.5 Biofacies of Wettmarsen

In the study of conodonts from the calciturbidite bed of the Kahlenberg Fm *(isosticha-* Upper *crenulata* Zone) in Wettmarsen, ramiform and platform elements were counted (Fig. 24a), but for the biofacies reconstruction only platform (Pa) elements were considered (Fig. 24b, c). Ramiform conodont elements constitute 18 % (Fig. 24a) of the studied conodont fauna and contain genera such as *Bispathodus, Branmehla* and *Mehlina* (Tab. 2).

Excluding reworked Upper Devonian taxa, the Pa elements (Tab. 2, Fig. 24b) are dominated by gnathodids and pseudopolygnathids that amount to 54% of the fauna (Fig. 24c). Twenty-four percent of the fauna (Fig. 24c) are composed of *N. c. communis*, a species that is known as a ubiquitous, facies-breaking epipelagic drifter or swimmer. Excluding *N. c. communis,* gnathodids and pseudopolygnathids reach 64% of the fauna, but are still below the threshold of 70% that is required for biofacies definintion according to SANDBERG et al. (1988). It is of interest that already KALVODA et al. (1999) noted difficulties to reach the 70% threshold in calciturbidites, as mixed sources and reworked older elements disguise the original composition of the conodont fauna.

Conodont Zone	*isosticha*-Upper *crenulata* Zone
Sample	1014/1
Bispathodus aculeatus aculeatus	2
Bispathodus spinulicostatus	1
Bispathodus stabilis stabilis	6
Bispathodus stabilis vulgaris	3
Branmehla disparilis	1
Branmehla/Mehlina sp.	44
Dollymae sp.	4
Gnathodus cuneiformis	20
Gnathodus delicatus	12
Gnathodus typicus	35
Ganthodus sp.	12
Neopolygnathus communis carina	1
Neopolygnathus communis communis	51
Ozarkodina sp.	1
Palmatolepis glabra pectinata	4
Palmatolepis glabra prima	1
Palmatolepis gracilis gracilis	1
Palmatolepis linguiloba	1
Palmatolepis minuta minuta	1
Palmatolepis perlobata sigmoidea	1
Palmatolepis tennipunctata	1
Palmatolepis triangularis	1
Palmatolepis sp.	9
Polygnathus purus purus	16
Polygnathus sp.	2
Pseudopolygnathus fusiformis	4
Pseudopolygnathus primus primus M2	17
Pseudopolygnathus triangulus pinnatus	4
Pseudopolygnathus triangulus triangulus	4
Pseudopolygnathus sp.	1
Siphonodella cooperi	1
Siphonodella duplicata	2
Siphonodella isosticha	2
Siphonodella lobata	1
Siphonodella obsoleta	2
Siphonodella sulcata	3
Siphonodella sp.	3
ramiform elements	5
Total number of conodont elements	280

Tab. 2 Distribution and numbers of conodont species and genera of Wettmarsen

The Gnathodid-Pseudopolygnathid Biofacies as described by SANDBERG & GUTSCHICK (1984), KALVODA (1991) and KALVODA et al. (1999), (see chapter 3, Figs. 7, 8, 9) indicates mostly, middle and upper slope areas. Also, siphonodellids might be admixed in these environments. Considering the carbonate microfacies, which even shows faint platform influence, such an assignment is reasonable.
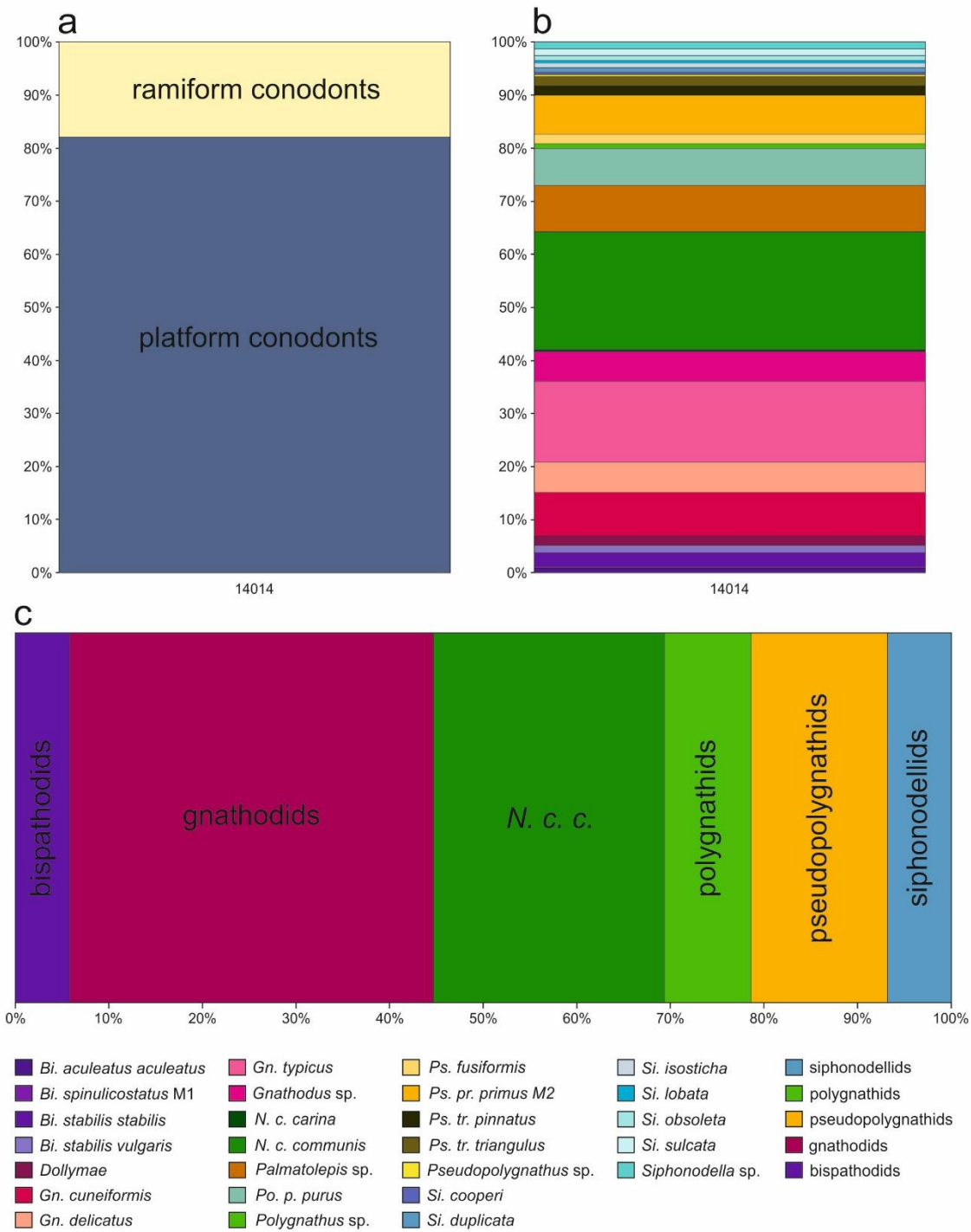
Fig. 24 Distribution of conodont species and genera **a**: distribution of platform conodonts vs. ramiform conodonts, ramiform elements include specimens of *Branmehla*, *Mehlina* and *Ozarkodina* **b**: distribution of platform species **c**: distribution of genera, reworked Devonian faunas are excluded, *N. c. c.* is pictured separately because in the biofacies models it is separated from the other polygnathids; **a** and **b** bed/sample number on x-axis; purple colours: bispathodids, pink colours: gnathodids, green colours: polygnathids and neopolygnathids, orange and red colours: palmatolepids, dark brown and yellow colours: pseudopolygnathids, blue colours: siphonodellids

The reworked Upper Devonian conodont genera *Palmatolepis* and *Bisphathodus* compose approximately 9% of the total Pa element population. As for the reworked Upper Devonian fauna of the Gladenbach section (see chapter 10.2), a Palmatolepid-Bispathodid Biofacies as introduced by Sᴀɴᴅʙᴇʀɢ (1976) and presented by Cʟᴀᴜꜱᴇɴ et al. (1989) and Kᴀʟᴠᴏᴅᴀ et al. (1999) is indicated. This is the deepest upper Devonian biofacies covering lower slope and basin environments. It is compatible with the occurring cephalopod limestones that were deposited on a deep intrabasinal swell.

7.6 Conclusions

The Upper Devonian cephalopod limestones of the Hemberg Beds (Middle to Upper *velifer* Zone, respectively Lower and Upper *trachytera* Zone) were deposited on an intrabasinal swell on top of the dead and drowned Middle Devonian Balve reef. The hiatus above, affecting Upper Famennian and lowermost Tournaisian strata, is probably related to emergence or non-deposition as reworked conodonts of the *postera* Zone are missing. According to reworked bispathodids, palmatolepids and siphonodellids in the studied calciturbidite bed, sedimentation started again earliest in the *expansa* Zone. Renewed sedimentation during the lower Tournaisian was already noted by Sᴄʜäꜰᴇʀ (1978) due to scarce *Siphonodella* sp. in a limestone pebble from the sandstone below the calciturbidite bed. The phosphorite layer close to the base of this thin siliciclastic package is interpreted to be related to reworking of a strongly condensed section, or of hardground-related phosphorite clasts.

The siliciclastics including the phosphorite layer and the overlying calciturbidite beds are attributed to the Kahlenberg Fm (Hᴇʀʙɪɢ 2016).

The calciturbidite is characterized by lighter and darker laminae that depict different source areas. They reflect a change between turbiditic currents deriving from a shallower source and quiet background sedimentation. The shallower sources of the turbidites were high rising intrabasinal swells on top of the former Devonian Balve reef complex, situated south of Wettmarsen. The gnathodid-pseudopolygnathid dominated conodont fauna of the calciturbidite indicates middle to upper shelf slope environments, rare calcareous algae, plurilocular foraminifers and ooids also indicate shallow-water platform environments. Siphonodellids were admixed during downslope movement in more basinal environments that also resulted in the formation of radiolarian-rich laminae at the tail of the turbidites.

The conodont fauna retrieved from the calciturbidite bed allowed the assignment to the *isosticha*-Upper *crenulata* Zone, although it also contained reworked elements of the Upper Devonian *marginifera, trachytera and expansa* zones (e. g. *Bi. ac. aculeatus*, *Bi. stabilis stabilis, Pa. minuta minuta, Pa. perlobata sigmoidea*) and the lower to middle Tournaisian interval (e. g. *Si. sulcata, Si. duplicata*) proving the high-energetic flow regime of the turbidites. The assignment to the *isosticha*-Upper *crenulata* Zone is also used to relate the calciturbidite bed to the HST of Sequence 2.

The following sandstones of the Hardt Fm compose the LST of Sequence 3, equivalent to the siliciclastics below the calciturbidite bed that represent the TST of Sequence 2 in the lower part of the Kahlenberg Fm. After an exposure gap, siliceous shales of the Hardt Fm form the uppermost part of the section representing the undifferentiated TST/HST of Sequence 3.

8. Dolhain

8.1 Introduction

In the recently (2010) constructed railway-cut 500 m south of the Dolhain train station, uppermost Famennian to Ivorian strata of the Vesdre-Aachen sedimentation area are exposed. The section has only been briefly described (Poty et al. 2011) and so far, no conodont studies exist.

In Dolhain, two other, long known sections exist (Dewalque 1898, Conil et al. 1961, Laloux et al. 1996b). One is situated 2.5 km north of the train station in an almost non-accessible railway cut and the other one is a steep natural slope along the Vesdre river below the rail tracks, 500 m north of the train station. Together the two sections expose a continuous succession of uppermost Famennian ("Strunian") (Dolhain Fm, not accepted and included into the Etroeungt Fm by Amler & Herbig 2006), Hastarian (Hastière Fm, Pont d'Arcole Fm, Landelies Fm), and Ivorian (lower part of Vesdre Fm) strata. Within those two sections the Dolhain Fm includes three biostromes, rich in organisms (corals: *Palaeosmilia aquisgranensis*, *Campophyllum flexuosum*, stromatopores, crinoids, tabulate corals: *Syringopora, Yavorskia*), within a shaly-sandy succession. The Hastière Fm consists of thick dark grey-bluish limestone-beds that are rich in crinoids and shaly limestones. Fine-grained, grey to black shales, platy limestones with limestone nodules and dark-grey compressed limestone beds of the Pont d'Arcole Fm contain a macrofauna including brachiopods (*Spiriferellina peracuta*). From those sections Boonen (1979) listed conodonts from the upper 7 m of the Pont d'Arcole Fm and an especially rich fauna from the uppermost 0.5 m with *Apathognathus sp., Bi. ac. ac, Bi. ac. anteposicornis, Bi. spinulicostatus, Hibbardella aff. H. macrodentata, Neoprioniodus* sp*., O. curvata, O.* sp*., Po. inornatus, Po. c. c., Ps. dentilineatus, Prioniodina* sp*., Si. obsoleta, Si. quadruplicata, Sp. scitulus, Sp. stabilis.*

The succeeding Landelies Fm is composed of crinoid-bearing limestones, still argillaceous at the base, but above characterized by thick to massive limestone beds. They become dolomitic and grade into the overlying Vesdre Fm that is composed of dolostones and dolomitized limestones with numerous chert-, calcite-, dolomite- and quartz-nodules (Laloux et al. 1996b).

The new section is well comparable. Though affected by a fault in its lower part, it is excellent for the study of the Pont d'Arcole Fm in the Condroz Sedimentation Area (CSA) and the contacts to the adjoining formations.

8.2 Geological Setting and description of the section

The Dolhain railway section (5° 56' 13,43'' E, 50° 37' 16,51'' N, Carte Geologique de Wallonie 1: 25 000, sheet 43/5-6 Limbourg-Eupen) is situated within the Verviers Syncline. It exposes a steeply northward dipping succession (Fig. 25a).

The Verviers Syncline is the eastern prolongation of the Dinant Synclinorium and extends between Liège in the W and Aachen in the E, bordered by the Stavelot Massif in the SE and by the Aguesses-Asse fault in the NW (Dejonghe 1998). The base of the Verviers Syncline is marked by a shear zone that coincides with the thrust fault known as "Faille Eifelienne", "Faille des Aguesses-Asse" (respectively Aguesses fault and Asse fault, Fig. 26) in Belgium, or Aachen Thrust Fault in Germany. It can be divided in the Herve Unit, the Vesdre Nappe (contains the Dolhain section) and the Theux Window (Fig. 26). NE-SW striking, longitudinal faults, induced by the Variscan orogeny, and NNW-SSE striking, transverse faults, connected to the Neogene tectonism along the Rhine graben, dominate the Verviers Syncline (Dejonghe 1998).

Fig. 25 Outcrop conditions of the Pont d'Arcole Fm in Dolhain, **a**: shale and limestone of the Pont d'Arcole Fm (center) embedded in the limestones of the underlying (left) Hastière Fm and overlying (right) Landelies Fm, person for scale: 171 cm; **b**: limestone beds of the underlying Hastière Fm, hammer: 28 cm; **c**: boundary between Hastière Fm (bed 6) and siliceous shales of the Pont d'Arcole Fm (bed 7 and underlying shales), hammer: 28 cm; **d**: first shaly limestone bed (bed 8) of the Pont d'Arcole Fm, hammer: 28 cm; **e**: dark grey shale package between shaly limestone beds (bed 14 and bed 16) followed by siliceous shales, hammer: 28 cm; **f**: limestone bed of the Landelies Fm, hammer: 28 cm.

The following comprehensive description of the Dolhain section relies on P*OTY* et al. (2011), who also figured a complete log.

Accordingly, the base of the section is formed by the top of the Strunian Dolhain Fm that is composed of limestones with few intercalated shale beds. The base of the lower Tournaisian Hastière Fm and the Dolhain Fm are highly tectonised. The upper undisturbed part of the Hastière Fm (Fig. 25b) is mainly composed of thick bedded, crinoidal limestones (packstones) with few corals and brachiopods. The transition to the following Pont d'Arcole Fm can be observed by the appearance of centimetric to decametric shale beds (Fig. 25c, d). Quantity and thickness of these argillaceous beds increases rapidly (Fig. 27). The Pont d'Arcole Fm itself is composed of fossiliferous limestones, shaly limestones, calcareous shales with intercalated calcareous nodules, siliceous shales and dark grey shales (Fig. 25c, d, e). In the uppermost part limestone beds occur, becoming more frequent and increasing in thickness, indicating the transition to the overlying Landelies Fm. The boundary towards the Landelies Fm is drawn above the last decimetric shale bed (P*OTY* et al. 2011). The limestones of the Landelies Fm (Fig. 25f) show a facies similar to the Hastière Fm, but form thicker beds that are richer in macrofossils. The upper part of the formation is slightly dolomitized; transition into the Vesdre Fm was not studied.
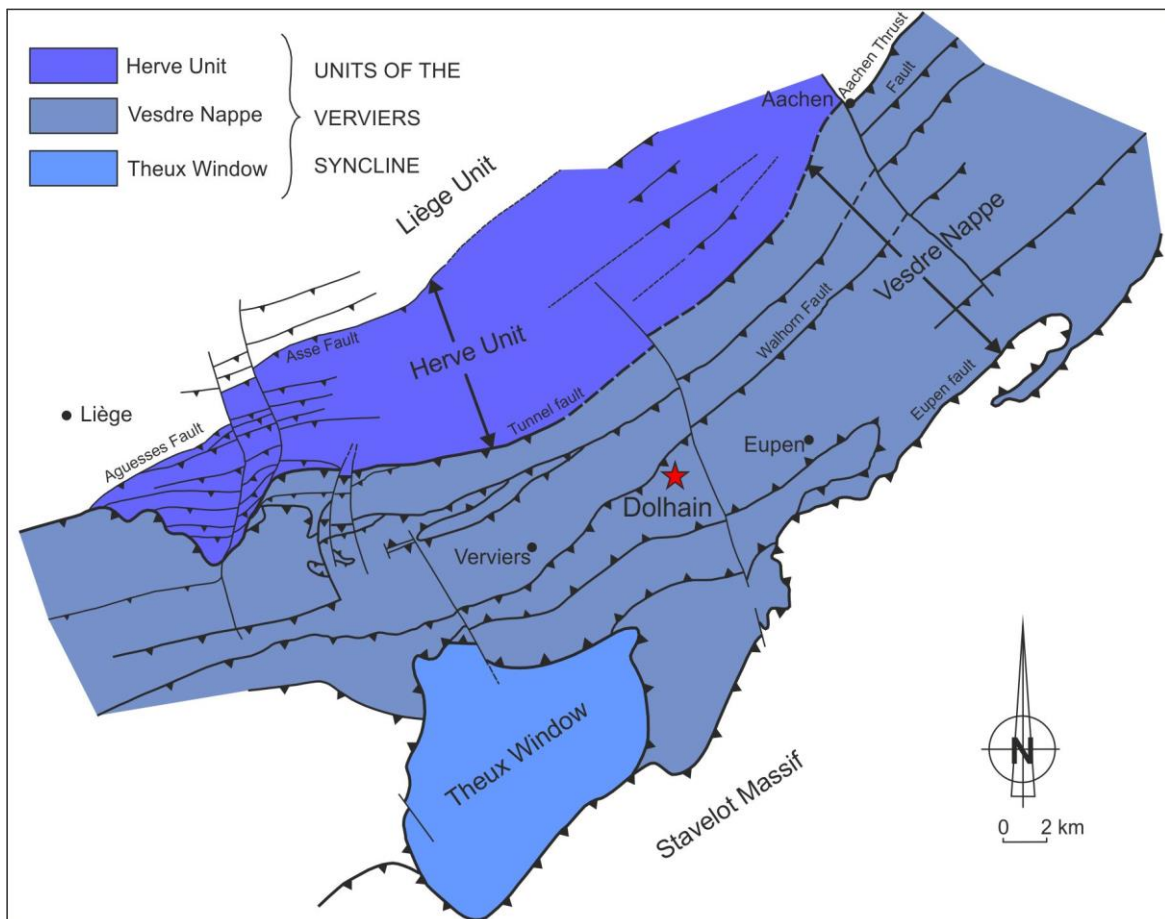
Fig. 26 Structural map of the Verviers Syncline (East Belgium, Vesdre-Aachen sedimentation area) and its three units, position of Dolhain section marked by red asterisk, modified after H*ANCE* et al. (1999).

The main focus of this work lies on the Pont d'Arcole Fm but the uppermost part of the Hastière Fm (Fig. 27) is also considered, regarding the sedimentation conditions before the accumulation of the middle Tournaisian strata.
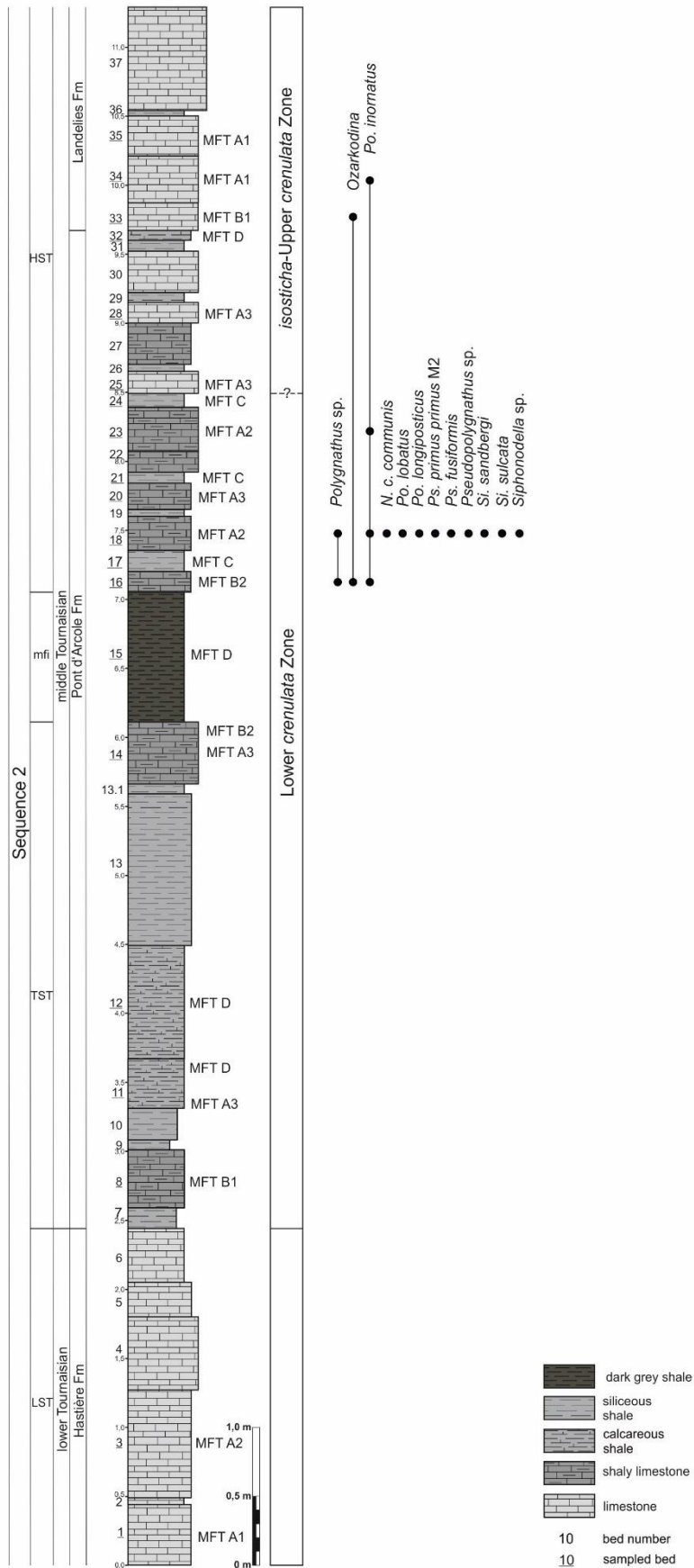
Fig. 27 Section log, microfacies types and conodonts of the Pont d'Arcole Fm, Dolhain section. The *isosticha*-Upper *crenulata* Zone is not proved. The interval might be sought in the uppermost part of the Pont d'Arcole Fm and in the lower part of the Landelies Fm.

The uppermost part of the lower Tournaisian Hastière Fm consists of non-laminated, fossil-rich limestones (Fig. 25b). The following middle Tournaisian Pont d'Arcole Fm is approximately 8 m thick and begins with 3.5 m of siliceous shale, shaly limestones (Fig. 25c, d) and calcareous shale. The shaly limestones are fine-grained, bioturbated and contain a rich fauna. The interbedded calcareous shales contain hardly any to only few fossils but are strongly bioturbated. The next unit is a 0.9 m thick succession of dark grey, strongly bioturbated, but biogen-poor shales (Fig. 25e). On top, as already seen in the lower part of the Pont d'Arcole Fm, 1.5 m of intercalated shaly limestones and siliceous shales follow. At approximately 8.5 m of the section log the first pure limestone bed of the Pont d'Arcole Fm occurs. In the following 1.1 m thick unit, siliceous shales and shaly limestones of rapidly decreasing thickness, are intercalated between in thickness increasing limestone beds. At approximately 9,6 m the first limestone bed (bed 33) of the Landelies Fm occurs on top of the last decimetric shale bed, as described by POTY et al. (2011). The limestones are dark in some cases, more or less rich in bioclasts and commonly show signs of bioturbation. Towards the top of the section the limestones of the Landelies Fm exhibit increasing thickness.

8.3 Microfacies

For the carbonate rocks of the Dolhain railway section four microfacies types are introduced. Microfacies types A and B are further subdivided based on differing matrix or dominating biogen content. The facies types are distinguished from each other based on structure and component contents.

8.3.1 MFT A: Micritic bioclast-bearing wackestone/packstone

The facies type shows various types of fine-grained matrix ranging from micrite to pelmicrite, and from poorly washed microsparite to very fine-grained microsparite. At least in part, microsparite results from recrystallized micrite. Neomorphic calcite grains occur within the matrix and within bioclasts. The fossil content is similar in all subtypes but differing in the dominating faunal groups as indicated by the subtype names. *Girvanella* sp. (Pl. 5, Fig. 4, Pl. 6, Fig. 4) occurs in the upper part of the section above bed 16 with increasing abundance upsection.

Nonbiogenic components are rare intraclasts, quartz grains, that in some cases occur along or within stylocumulate or dolomitized areas, and pyrite grains.

Bioturbation occurs throughout. It causes concentration of bioclasts (Pl. 4, Fig. 6-7, Pl. 6, Fig. 6) and formation of packstone areas or is obvious due to different matrix colours (Pl. 4, Figs. 4-5).

Dolomitization occurs from sample 18 on upwards, either along the bedding surfaces or scattered within the sample along stylolite swarms or bioclasts.

Stylocumulate, often occurring along the upper and lower margins of a sample but also within the sample, and (micro-) stylolite swarms are very common. Often, bioclasts are enriched along stylocumulate and stylolite swarms. In some cases, complete areas between stylocumulate and stylolite swarms or stylocumulate and upper bed surfaces are influenced by pressure solution. They form diagenetic packstone areas (Pl. 5, Fig. 12), dominated by echinoderm fragments within a partly recrystallized matrix. Also, detrital quartz grains are enriched along microstylolite swarms close to the bed surfaces. This effect is in some samples caused by bioturbation as well (Pl. 4, Fig. 3).

Lamination is absent in this microfacies.

Subtype A1: Peloidal wackestone/packstone (Pl. 4, Fig. 1, Pl. 5, Figs. 1-6)

The matrix is pelmicritic or sparitic (Pl. 4, Fig. 1). It contains small packed, predominating peloids, intraclasts, and unsorted small to large bioclasts (0.2-2 cm). The large bioclasts consist predominantly of brachiopod shells, and echinoderms (mostly crinoids, Pl. 5, Fig. 6). The small bioclasts consist besides the two mentioned groups of ostracodes (Pl. 5, Figs. 1, 6), thin bivalve shells, calcareous foraminifera, calcispheres (Pl. 5, Fig. 5) and sponge spicules. Rare bioclasts are echinid spines (Pl. 5, Fig. 2), trilobites (Pl. 5, Fig. 3), bryozoans and corals. In sample Do1 various not further studied foraminifera can be found, in samples Do34 and Do35 (top of the section) only the genus *Earlandia* occurs. Besides, some detrital quartz grains and dolomite are observed (hypidiomorphic dolomite grains, Pl. 5, Fig. 2).
This subtype only occurs in limestones in the upper part of the Hastière Fm and the upper part of the Pont d'Arcole Fm.

Subtype A2: Echinoderm-foraminifer wackestone/packstone (Pl. 4, Figs. 2-3, Pl. 5, Figs. 7-12)

The micritic matrix (Pl. 4, Fig. 2) contains intraclasts (in some cases pseudopeloids), and numerous bioclasts. Among the bioclasts echinoderms (crinoids, Pl. 5, Fig. 10) are very dominant and the number of calcareous foraminifera (Pl. 5, Figs. 7, 8) is very high compared to other subtypes. In samples 18, 23.1, 23.2 and 23.3 *Earlandia* sp. is dominating, in sample 18 it is the only occurring genus. Calcispheres are generally common. Moreover, ostracodes, thin-shelled bivalves, brachiopods (Pl. 5, Fig. 10), echinid spines (Pl. 5, Fig. 9) and sponge spicules occur. Gastropods (Pl. 5, Fig. 11), bryozoans, corals and trilobites occur rarely. Larger bioclasts occur among crinoids, brachiopod shells and trilobites and reach 1-4 mm, exceptionally up to 1.2 cm.
In samples 18, 23.1, 23.2 and 23.3 the micritic matrix is partly substituted by very fine calcite grains due to slight pressure solution.
The subtype occurs in limestones and shaly limestones (influence of argillaceous input visible) of the Pont d'Arcole Fm.

Subtype A3: Bioturbated, echinoderm-ostracod wackestone/packstone (Pl. 4, Figs. 4-7, Pl. 5, Figs. 13-15, Pl. 6, Figs. 1-6)

The matrix depicts a transition from pure micrite (Pl. 4, Fig. 4) to a mixture of micrite and very fine-grained microsparite (Pl. 4, Fig. 7), indicating faint recrystallisation. Besides the name giving echinoderm fragments (crinoids, Pl.5, Fig. 14, Pl. 6, Fig. 5) and ostracodes (Pl. 6, Fig. 3) the wacke- to packstones contain calcareous foraminifers, dominated by *Earlandia* (Pl. 5, Fig. 15, Pl. 6, Fig. 2), brachiopod and bivalve shells (Pl. 6, Fig. 1) and echinid spines (Pl. 6, Fig. 5). Larger bioclasts (crinoid fragments, brachiopod shells (Pl. 5, Fig. 13) and ostracodes) reach sizes of 1-2 mm, exceptionally 5-7 mm or even 2 cm (brachiopod shell, sample 14.3). Brachiopod spines, trilobites, algae, sponge spicules, calcispheres and conodonts occur rarely.
The subype occurs in calcareous shale, shaly limestones and limestones and can be compared to subtype A2, except for the high numbers of ostracodes in this facies type.

8.3.2 MFT B: Microsparitic, bioturbated, bioclast-bearing wackestone

The two suptypes of this microfacies type contain a microsparitic matrix of dark brown (B1) or brown (B2) colour and contain mainly echinoderms (mostly crinoids), brachiopods and ostracodes, accompanied by rare other bioclasts. Foraminifers and *Girvanella* sp. are

mainly absent except for sample 16.1 (Pl. 6, Fig. 12) and 33. Bioturbation is ubiquitous, causing local concentration of bioclasts (Pl. 4, Fig. 8), or different colouration of the matrix (Pl. 4, Fig. 9). Parallel alignment of bioclasts is restricted to subtype B1; quartz grains occur only in subtype B2.

Stylocumulate is less common than in facies type A but occurs regularly (e.g., in subtype B1, around a packstone area formed by pressure solution). Lamination is completely absent.

Dolomitization occurs in some samples of subtype B1 and affects the areas close to the bedding surface or in all samples of subtype B2 and is either restricted to the sample margins or reaches most parts of the sample, but complete dolomitization cannot be observed.

The facies type only occurs in shaly limestones and developed in slightly deeper areas than the subtypes A1-A2.

Subtype B1: Dark, bioturbated, bioclast-bearing wackestone (Pl. 4, Figs. 8-9, Pl. 6, Fig. 7-8)

The dark, brownish, microsparitic matrix of this facies type contains bioclasts, small intraclasts, quartz and pyrite grains. The bioclast content is similar to that of the already described microfacies types. Echinoderms (mainly crinoids, Pl. 6, Figs. 7, 8), brachiopods (Pl. 6, Fig. 7) and ostracodes reach sizes of 1-7 mm, exceptionally 1 cm. Small bioclasts have average sizes of 0.1-0.3 mm. In most cases an orientation of the larger bioclasts, parallel to the bedding plane, can be observed.

This subtype occurs in shaly limestones and limestones. The horizontally aranged larger bioclasts indicate their transport by (faint) currents. However, bioturbation demonstrates their faint intensity or waning after deposition.

Subtype B2: Bioturbated, bioclast-bearing wackestone (Pl. 4, Figs. 10-11, Pl. 6, Figs.9-12)

The microsparitic brown matrix (Pl. 4, Fig. 11) contains bioclasts mainly composed of echinoderms (mainly crinoids, Pl. 6, Fig. 11), brachiopods, and ostracodes (Pl. 6, Fig. 9). Besides, echinid spines, calcareous foraminifera and gastropods (only sample 14.4, Pl. 6, Fig. 10), rare sponge spicules and corals occur. Larger bioclasts reach sizes of mainly 0.5-5 mm, sometimes 7 mm and exceptionally 4 cm (large brachiopod shell in sample 16.1).

In contrast to subtype B1, bioclasts are not oriented parallel to the bedding plane but bioturbation (Pl. 4, Fig. 10, Pl. 6, Fig. 11) has the same effects as described there.

In this subtype signs of the influence of current flows are missing.

8.3.3 MFT C: Micritic to microsparitic, bioturbated, echinoderm wackestone (Pl. 4, Figs. 12-13, Pl. 6, Fig. 13)

The dark brown matrix is composed of a mixture of micrite and microsparite (Pl. 4, Fig. 12). It bears undefinable microbioclasts as well as definable bioclasts that are dominated by echinoderm (mainly crinoid) fragments (Pl. 4, Fig. 12, Pl. 6, Fig. 13). They are accompanied by brachiopods, bivalves, sponge spicules and ostracodes. Further biota (e.g., foraminifera, trilobites) that are present in the facies types A and B are missing. Also, bioclasts are smaller, reaching sizes of 0.5-2.5 mm. Small intraclasts are rarely seen and quartz grains occur mainly near the outer margins of the samples, i. e. in contact to adjacent shale beds.

In most cases components are aligned approximately parallel to the bedding plane, due to predominance of horizontal burrows (Pl. 4, Fig. 13). In cases, this pseudolamination is additionally enhanced by pressure solution and resulting formation of stylocumulate.

Alternatively, the ubiquitous bioturbation leads to concentration of bioclasts (Pl. 6, Fig. 13) and formation of packstone areas.

The facies type occurs only in siliceous shales and developed in a more distal (deeper) setting than the previously described MFTs.

8.3.4 MFT D: Bioturbated mudstone (Pl. 4, Figs. 14-15, Pl. 6, Figs. 14-15)

As in facies type C, the matrix is composed of a mixture of micrite and microsparite (Pl. 6, Fig. 15), containing few scattered bioclasts (crinoids and brachiopods, Pl. 6, Fig. 14, and rare sponge spicules, only sample 32). In some cases, few layers of bioclasts, approximately parallel to the bedding plane, can be seen. They are accompanied by coarser grained microsparite. Larger bioclasts reach sizes of 1-3 mm, exceptionally of 5.5-14 mm. They are oriented approximately parallel to the bedding plane. In sample 15.1 all bioclasts are recrystallized. Quartz grains are very common.

Bioturbation occurs in different intensity throughout. It is obvious by different colouration of the matrix (Pl. 4, Fig. 15, Pl. 6, Fig. 14).

Dolomitization affected most samples (Pl. 4, Fig. 14, Pl. 6, Fig. 14). Some are completely dolomitized, others are only affected near the margins or hardly at all. Stylocumulate occurs in varying frequency. In most samples, lamination is missing.

The facies type occurs in calcareous shales and dark grey shales and was accumulated in even distaler and deeper environments than MFT C.

8.4 Biostratigraphy and sequence stratigraphy

Conodont samples in the lower part of the studied succession did not yield platform elements. They could only be retrieved from beds 16, 18, 23, 33 and 34 (Tab. 3). However, only bed 18 allowed a biostratigraphic assignment to the Lower *crenulata* Zone. Sandberg et al. (1978) listed, among other species, *N. c. communis*, *Po. inornatus, Po. longiposticus, Ps. fusiformis and Ps. primus* as associated fauna of this zone. *Si. sandbergi* and *Si. sulcata* were also retrieved from bed 18 and die out in the Lower *crenulata* Zone (Sandberg et al. 1978).

Based on the changing lithology at bed 25 that indicates transition into the HST and in analogy to the Gladenbach Fm (chapter 6.4) we place the boundary between Lower *crenulata* Zone and *isosticha*-Upper *crenulata* Zone at the base of bed 25 (marked by dashed line and ?).

According to Devuyst et al. (2005), Poty et al. (2011, 2014) and Poty (2016) the LST of Sequence 2 is formed by the limestone beds of the upper member of the lower Tournaisian Hastière Fm, and the TST by the middle Tournaisian Pont d'Arcole Fm. The HST of Sequence 2 is represented in the thick and macrofossil-rich limestone beds of the Landelies Fm, followed by the FSST in the upper part of the Formation. The overlying Vesdre Fm represents the following Sequence 3.

Own observations in the Dolhain section show that the TST of Sequence 2 is represented by the shaly limestones, calcareous shales and siliceous shales in the lower part of the Pont d'Arcole Fm. The dark grey shales in the middle part of the formation (Fig. 27) indicate the highest water depth, i. e. the maximum flooding interval (mfi). Afterwards the increasing number of limestone beds in the upper part of the Pont d'Arcole Fm indicate, opposed to

present interpretation, the beginning HST already in the upper part of the Pont d'Arcole Fm. According to the gradual lithological development, the HST continues into the Landelies Fm.

8.5 Biofacies of Dolhain

Conodont recoverage from the limestones and shaly limestones of the Pont d'Arcole Fm was low (Tab. 3).

All samples in the lower part of the succession were barren or yielded only ramiform elements (Tab. 3, sample 3, Fig. 28a) without value for biostratigraphy or biofacies zonation. Bed 16 was the first sample that yielded utilizable conodont specimens (Pa elements). Only from sample 18 a significant number of specimens (71 Pa elements, Tab. 3) were recovered and could be used for biofacies analysis (Fig. 28b, c). In this sample the

Conodont Zone			Lower *crenulata* Zone				?	
Sample	1	3	8	16	18	23	33	34
Neopolygnathus communis communis					12			
Ozarkodina sp.				1			1	
Polygnathus inornatus				1	38	2		1
Polygnathus lobatus					1			
Polygnathus longiposticus					1			
Polygnathus sp.				1	1			
Pseudopolygnathus fusiformis					4			
Pseudopolygnathus primus primus M2					3			
Pseudopolygnathus sp.					1			
Siphonodella sandbergi					5			
Siphonodella sulcata					2			
Siphonodella sp.					3			
ramiform elements		1		2	20			1
Total number of conodont elements	0	1	0	5	91	2	1	2

Tab. 3 Distribution and numbers of conodont species and genera of Dolhain, "?" marks assumed, unproved *isosticha*-Upper *crenulata* Zone

conodont fauna mainly contains polygnathids (55 %) accompanied by lower numbers of pseudopolygnathids (11%) and siphonodellids (10%) (Fig. 28c). 24 % (Fig. 28c) are composed of *N. c. communis*, a ubiquitous, facies-breaking epipelagic drifter or swimmer, that is not regarded in the biofacies reconstruction. Regarding the biofacies models reviewed in chapter 3, only the Polygnathid-Siphonodellid Biofacies on deep (intrabasinal) swells and slope areas of CLAUSEN et al. (1989), erected for the *sulcata* Zone, within the Rhenish Culm Basin might be considered. However, according to KALVODA et al. (1999) siphonodellids adjoin polygnathids and pseudopolygnathids already at the shelf margin, respectively at the platform margin (cf. chapter 3, Fig. 8). According to the platform position of the Dolhain section, a deep shelf environment is considered herein. This is underlined by deposition of bed 18 immediately above the dark grey shales that represent the maximum flooding interval of Sequence 2.

Above sample 18, the quantity of condont elements decreases rapidly, only yielding one or two specimens per sample (Tab. 3). This corresponds to a rapidly falling sea level during the prograding HST.
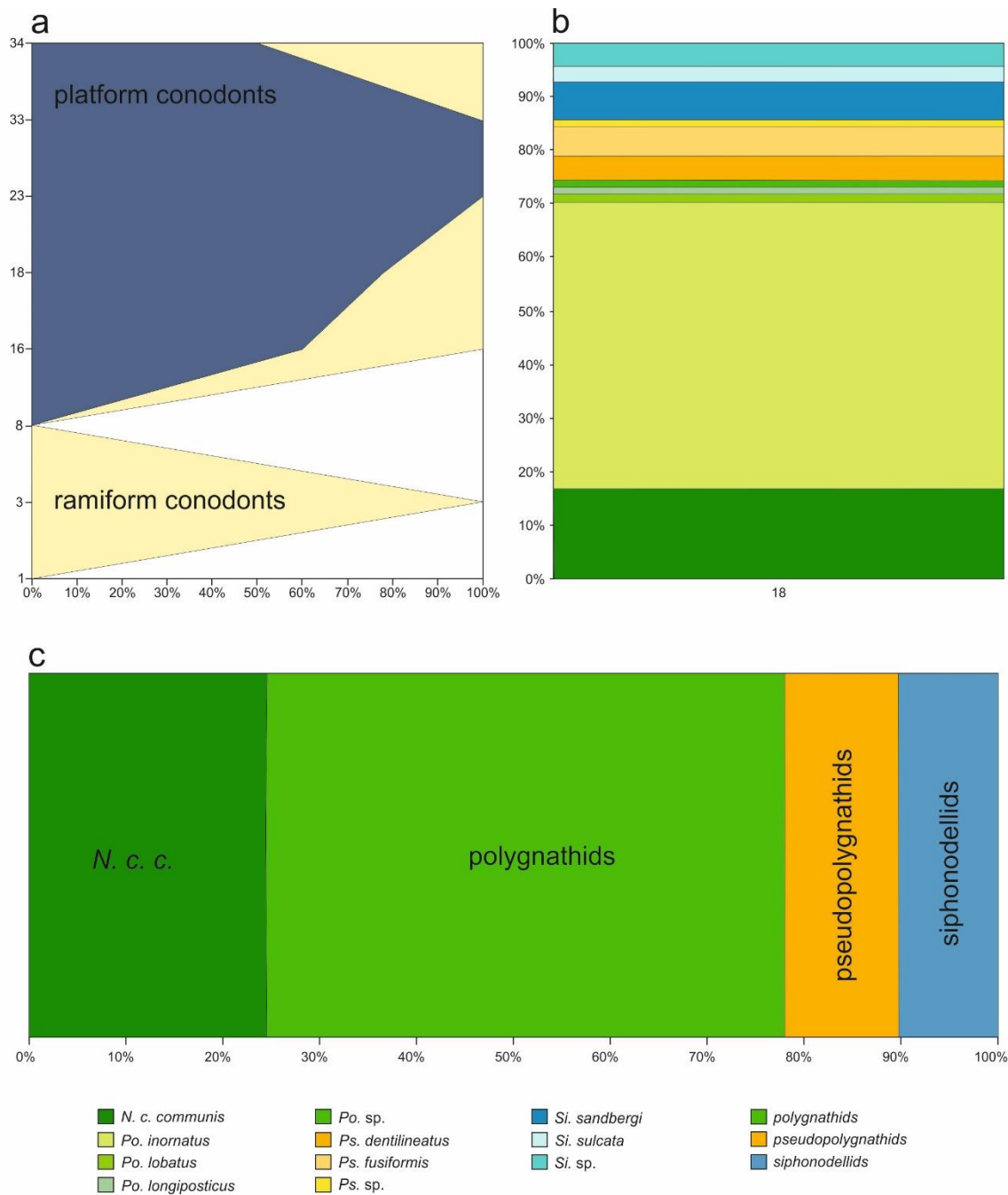
Fig. 28 Distribution of conodont species and genera, **b** and **c** show only numbers of sample 18; **a**: distribution of platform conodonts vs. ramiform conodonts, sample 1 and 8 do not contain any conodonts **b**: distribution of platform species of sample 18 **c**: distribution of genera of sample 18, *N. c. c.* is pictured separately because in the biofacies models it is separated from the other polygnathids; **a** bed/sample numbers on y-axis, **b** bed/sample number on x-axis; green colours: polygnathids and neopolygnathids, orange and yellow colours: pseudopolygnathids, blue colours: siphonodellids

8.6 Conclusions

Based on microfacies, the limestones from the uppermost Hastière Fm and the upper part of the Pont d'Arcole Fm, can be related to platform environments. According to the predominance of micrite, deposition was mostly below wave base, in cases of MFT A deposition between storm wave base and normal wave base can be assumed.

The overall present bioturbation indicates that the sediment was sufficiently oxygenated at all times to accomodate infauna.

The limestones contain numerous echinoderm (mostly crinoid) fragments, brachiopods and bivalves, ostracodes, varying numbers of low diverse calcareous foraminifera and calcispheres. Sponge spicules, trilobites, bryozoans and corals are rare. The predominance of mostly suspension or deposit feeding organisms, missing of a diversified foraminifer fauna and the extreme rarity of phototrophic organisms (corals, calcareous algae) stress deeper water platform environments. Deeper water environments are also indicated by sponge spicules. At least part of the echinoderm (mostly crinoid) ossicles might have been derived from shallower water, as construction of their stereom results in hydrodynamic behavior that favours transport over longer distances.

Bioclasts of the calcareous shales are less numerous but are the same as in the limestones. Bioturbation is also present, again indicating oxygenated sediment. The argillaceous input was induced by rising sea-level that hampered carbonate production of the shallow-water "carbonate factory".

A major difference of MFT B, compared to MFT A is the almost complete absence of calcareous foraminifera which is a further indicator of deeper water.

The calcareous shales apparently were deposited close to the lower limits of carbonate sedimentation.

The rarely occurring bioclast layers in MFT D hint to episodic sediment influx, probably triggered by storms. Bioturbation proves the presence of organisms even in the dark grey shales.

In combination with the sequence stratigraphic interpretation, a transition from shallow-water environments in the uppermost Hastière Fm (LST) to increasing water depths in the lower Pont d'Arcole Fm (TST), that culminate in the dark grey shales in the middle part of the formation (mfi), is obvious. The increasing number of limestone beds (in their lower part still have to be assigned to the Lower *crenulata* Zone) in the upper Pont d'Arcole Fm, indicates the beginning HST of Sequence 2. This is earlier than in previous sequence stratigraphic schemes that put the base of the HST at the base of the Landelies Fm.

9. Systematics

Synonymy lists are restricted to few citations. Besides the first author only descriptions used for reference were included. Further synonymies are found in the listed citations. Reworked Devonian genera and species are listed at the end of this chapter.

Single-element taxonomy is applied as the reconstruction of Tournaisian conodont apparatuses is still doubtful and not very common. All samples are stored at the University of Cologne in the Institute of Geology and Mineralogy.

The importance of the chapter is stressed, as it is the first extended taxonomic description of middle Tournaisian conodonts from Germany since the early works of BISCHOFF (1956, 1957) and VOGES (1959).

Genus *Bispathodus* MÜLLER, 1962

Type species: *Spathodus spinulicostatus* BRANSON, 1934

Original description: Representative of *Spathognathodus* with ± wide pulp cavity at or anterior to the middle of the unit and with characteristic differentiation of the denticles of the blade in transverse elements that are arranged in two ± distinctly set rows.

Remarks: MÜLLER (1962) first introduced *Bispathodus* as a subgenus. Later it was elevated by ZIEGLER et al. (1974) to genus rank.

Age and range of genus: Upper Devonian (upper part) to Early Carboniferous (Tournaisian) (ZIEGLER 1975)

Bispathodus aculeatus aculeatus (BRANSON & MEHL, 1934a)
Plate 7, Figs. 1-2

1934a *Spathodus aculeatus* n. sp. – BRANSON & MEHL: 186-187, Pl. 17, Figs. 11,14
1962 *Spathognathodus (Bispathodus) aculeatus* – MÜLLER: 114
1974 *Bispathodus aculeatus aculeatus* – ZIEGLER et al.: 101, Fig. 1, Pl. 2, Figs. 1-8
2011 *Bispathodus aculeatus aculeatus* – HARTENFELS: 216, Fig. 57, Pl. 33, Figs. 2-8

Material: 11 specimens: Gladenbach, Wettmarsen

Description: A *Bispathodus* with a straight blade. One to four nodes right of the blade positioned above the basal cavity. In one specimen also one node on the left side of the blade, as described by ZIEGLER et al. (1974). Oval basal cavity in the middle of the blade. The aboral side is smooth.

Age and range of species: Upper Devonian and lower Carboniferous (Tournaisian): from the base of the *Bi. aculeatus aculeatus* Zone into Lower *sandbergi* Zone (HARTENFELS 2011); according to BELKA (1985) the species terminates within the Lower *crenulata* Zone, in the Gladenbach and Wettmarsen sections it only occurs in the *isosticha*-Upper *crenulata* Zone.

Bispathodus spinulicostatus (BRANSON, 1934)
Morphotype 1 (typical morphotype)
Plate 7, Figs. 3-4

1934b *Spathodus sulciferus* n. sp. – Branson & Mehl: 274, Pl. 22, only Fig. 13 [non Fig. 12 = lectotype of *Spathodus sulciferus*]
1934 *Spathodus spinulicostatus* n. sp. – Branson: 305-306, Pl. 27, Fig. 19
1974 *Bispathodus spinulicostatus* – Ziegler et al.: 103, Fig. 1, Pl. 1, Figs. 6-8, Pl. 3, Figs. 20, 22
2011 *Bispathodus spinulicostatus* M1 – Hartenfels: 221, Fig. 59, Pl. 32, Fig. 4

Material: 1 specimen: Gladenbach

Description: Nearly straight blade, on the right side of the blade a row of big nodes (nodes bigger than denticles on the blade), three nodes in the middle are connected to the blade by transverse ridges. Row of nodes expands close to the posterior tip of the blade, but terminates clearly before the anterior end of the blade. On posterior end two irregular nodes are formed left of the blade, alternating with the nodes on the right side of the blade. Basal cavity asymmetrical, situated in the middle of the blade not reaching the posterior tip, approximately as long as wide. The aboral side is smooth.

Remarks: A single node, denticle, or nodose ridge on the upper surface of the basal cavity on the left side of the blade as described by Ziegler et al. (1974) was not developed on the specimen from Gladenbach.

Age and range of species: Upper Devonian to lower Carboniferous: *Bi. aculeatus aculeatus* Zone into Tournaisian (Hartenfels 2011)

Bispathodus stabilis stabilis (Branson & Mehl, 1934a)
Plate 7, Fig. 5a, b

1934 *Spathodus stabilis* n. sp. – Branson & Mehl: 188, 189, Pl. 17, Fig. 20
1974 *Bispathodus stabilis* M2 – Ziegler et al.: 98, 100, 103-104, Fig. 1, Pl. 1, fig. 10, Pl. 3, Fig. 2
2006 *Dasbergina stabilis* – Dzik: 158, 159, Figs. 116 (only B, C, ?E, F), ?138
2011 *Bispathodus stabilis stabilis* – Hartenfels: 222, Fig. 61, Plate 31, Figs. 1-4

Material: 50 specimens: Gladenbach, Wettmarsen

Description: A platform is lacking. Long, straight or slightly arched blade. The basal cavity is asymmetric oval, wider than the blade, and widest in the middle. In some specimens, the outer side of the basal cavity is wider than the inner side, and the whole basal cavity thins out toward the posterior end and continues to the posterior tip. The aboral surface is smooth without ornamentation. About twenty oral denticles of approximately the same height, size of denticles decreases slightly towards the posterior end. In some specimens, main cusp in the middle slightly bigger than the other denticles. Aboral side smooth, basal cavity large and deep, longer than wide, extending anteriorly and posteriorly into narrowing grooves. Posterior groove longer and wider than the anterior one.

Age and range of species: Upper Devonian and lower Carboniferous (Tournaisian): base of the *Bi. stabilis stabilis* Zone to the base of the Upper *duplicata* Zone (Hartenfels 2011, Kaiser 2005), Sandberg et al. (1978) report it up to the *isosticha*-Upper *crenulata* Zone, Belka (1985) and Herbig & Stoppel (2006) list it to the top of the *anchoralis* Zone

Bispathodus stabilis vulgaris Hartenfels, 2011
Plate 7, Fig. 6

1966 *Spathognathodus stabilis* – Klapper: 23, Pl. 5, only Fig. 6
1969 *Spathognathodus crassidentatus* – Rhodes et al.: 226-227, Fig. 10, Pl. 3, Figs. 1-4
1974 *Bispathodus stabilis* M1 – Ziegler et al.: 103-104, Fig. 1, only Pl. 3, Figs. 1, 3
2006 *Pandorinellina vulgaris* – Dzik: 71-72, Figs. 45 ?A, B-D, ?E, 127
2011 *Bispathodus stabilis vulgaris* – Hartenfels: 224, 225, Fig. 62, Pl. 31, Figs. 5-8

Material: 67 specimens: Gladenbach, Wettmarsen

Description: Very similar to *Bi. stabilis stabilis*. In difference to *Bi. stabilis stabilis* the basal cavity of *Bi. stabilis vulgaris* does not reach the posterior tip of the blade.

Age and range of specimen: Upper Devonian and lower Carboniferous (Tournaisian): Upper *marginifera* Zone into Upper *duplicata* Zone (Hartenfels 2011, Kaiser 2005), in Gladenbach it occurs up into the upper part of the *isosticha*-Upper *crenulata* Zone

Genus *Branmehla* Hass, 1959
Type species: *Spathodus inornatus* Branson & Mehl, 1934.

Branmehla sp.
Plate 7, Figs. 7-8

Material: 88 specimens: Gladenbach, Wettmarsen (together with specimens of *Mehlina* sp. indiff., see remarks)

Description: Specimens of the genus *Branmehla* have a straight blade with a basal cavity in the posterior part of the blade. Denticles are equally spaced, closely set, and of approximately the same height. The posterior-most denticles are slightly lower. In some specimens the anterior denticles are also slightly lower and the row of denticles looks slightly bow-shaped in lateral view. Main cusp is indistinct in most specimens.

Remarks: In this study, specimens of *Branmehla* sp. and *Mehlina* sp. were counted together because the biozonation does not rely on these two genera, but they are used for the biofacies assessment of the bispathodid group (Ziegler & Sandberg 1984).

Age and range of genus: uppermost Devonian and lower Carboniferous (lowermost Mississippian) (Hass 1959)

Genus *Dinodus* Cooper, 1939
Type species: *Dinodus leptus* Cooper, 1939

Dinodus sp.
Plate 7, Figs. 9-10

Material: 53 specimens: Gladenbach

Description: Two forms of *Dinodus* could be observed in our samples. The first form (Pl. 7, Fig. 9) is characterized by a strongly arched, straight blade. The blade is very high, with a main denticle at the highest point. Denticles are closely spaced, fused at the base and inclined towards the posterior end. The basal cavity is situated directly posterior to the mid-point of the triangular base.

The second form (Pl. 7, Fig. 10) is characterized by a straight blade that forms a 35 to 80° angle. Denticles are closely spaced and fused at the base. In some specimens a ridge, beginning at the mid-point of the base, continuing into the tip of the blade, is visible on the lateral side of the blade. In other specimens several bigger denticles, situated at the mid-point of the blade, are bent towards the posterior end, forming a whirl. The base is triangular in cross-section, thus forming a long basal groove, thinning out towards the posterior end.

Remarks: The tips of the denticles are often broken off, as well as the whirl that is described by Cooper (1939).

Age and range of genus: lower Carboniferous: lower Mississippian (Kinderhookian) of North America and Tournaisian of Germany (Klapper 1966)

Genus *Dollymae* Hass, 1959
Type species: *Dollymae sagittula* Hass, 1959

Dollymae sp.
Plate 7, Figs. 11-13

Material: 4 specimens, Wettmarsen

Description: Blade is slightly curved towards the inner side, bearing three knobbly denticles/nodes that are oriented transverse to the blade. Carina is free of denticles or nodes, not reaching posterior tip of the platform. Platform is asymmetrical in most cases, the outer side often being larger than the inner one. Platform surface is smooth. Platform is wider than long and often bears two secondary carinas, beginning at posterior tip of the main carina and curving away towards platform margin, not always reaching it. Secondary carinas are also free of denticles or nodes. One specimen lacks the secondary carinas but is ornamented with asymmetrically arranged big nodes on inner and outer platform. Pulp cavity is very large, its apex located close to anterior end of specimens.

Age and range of genus: lower Carboniferous: Groessens (1971) reported a species from the upper Tournaisian (Tn 3c), Perri & Spalletta (1998) from the *isosticha*-Upper *crenulata* Zone

Genus *Elictognathus* Cooper, 1939
Type species: *Solenognathus bialata* Branson & Mehl, 1934

Elictognathus sp.
Plate 8, Figs. 1-4

Material: 75 specimens: Gladenbach

Description: Blade looks triangular in lateral view and denticles are sawtooth-like arranged on the blade. Base is slightly curved, forming an angle of about 90 ° between blade and base. Base tapers out towards the anterior end. Posterior third of the blade is bend forming an angle of approx. 40°.

Age and range of genus: lower Carboniferous: restricted to the Tournaisian (KLAPPER 1966)

Genus *Falcodus* HUDDLE, 1934
Type species: *Falcodus angulus* HUDDLE, 1934

Falcodus sp.
Plate 8, Figs. 5-6

Material: 29 specimens: Gladenbach

Description: Blade straight, bend downwards at one or two points. Situated above the bending points is a bigger denticle. Denticles are closely spaced, fused at the base, and bend towards the posterior end. Denticles are laterally compressed. Small basal cavity is situated underneath the posterior bigger denticle.

Age and range of genus: Upper Devonian and lower Carboniferous (KLAPPER 1966)

Genus *Gnathodus* PANDER, 1856
Type species: *Gnathodus mosquensis* PANDER, 1856

Age and range of genus: lower Carboniferous and upper Carboniferous, base of *isosticha*-Upper *crenulata* Zone to near base of *Idiognathoides sinuatus* Zone (early Bashkirium) (ZIEGLER 1981)

Gnathodus cuneiformis MEHL & THOMAS, 1947
Pl. 8, Figs. 7-8, 9a, b, 10-12

1947 *Gnathodus cuneiformis* – MEHL & THOMAS: 10, Pl. 1, Fig. 2
1974 *Gnathodus cuneiformis* – PIERCE & LANGENHEIM: 159-160, Pl. 1, Fig. 15, Pl. 2, Figs. 2, 3, 7, 17 only, Pl. 3, Fig. 11
1980 *Gnathodus cuneiformis* – LANE et al.: 130, Pl. 4, Figs. 5-8, 10-11, 13, Pl. 10, Fig. 7

Material: 20 specimens, Wettmarsen

Description: The blade is nearly straight, but slightly curved towards the inner side, approximately as long as the cup or slightly longer. Denticles on free blade and carina are of same size and equally spaced.
Asymmetrical cup, longer than wide, outer side wider than the inner side. Cup is widest in anterior part and thins towards the posterior tip. Parapet, formed by various nodes, on each side of the carina. The ridge on the inner side of the cup begins a bit more anterior than the outer one. Both ridges converge towards the posterior tip. In some specimens, the ridges nearly parallel the carina, in others, the converging character is more prominent. Between the ridges and the carina, more or less prominent depressions are formed. First

node (anterior-most) of the inner ridge is often more prominent than other nodes. Sometimes a parapet is formed on the inner side of the cup.
Aboral side smooth, forming a big aboral cup.

Remarks: Specimens as pictured by Pierce & Langenheim (1974) (Pl. 1, Fig. 15), where the posterior-most nodes of the ridges and the posterior-most denticles of the carina fuse to few rows, perpendicular to the carina, do not exist in our specimens.

Age and range of species: lower Carboniferous: Perri & Spaletta (1998) and Herbig & Stoppel (2006) list it from the base of the Lower *typicus* Zone up into the *homopunctatus* Zone. Lane et al. (1980) report it from the "possibly highest part of *isosticha*-Upper *crenulata* Zone" into the *anchoralis* Zone. Mory & Crane (1982) describe the species from "low in the Lower *crenulata* Zone" into the higher parts of the *isosticha*-Upper *crenulata* Zone in eastern Australia.
In Wettmarsen the species occurs in the *isosticha*-Upper *crenulata* Zone.

Gnathodus delicatus Branson & Mehl, 1938
Pl. 9, Figs. 1a, b, 2-3

1938 *Gnathodus delicatus* – Branson & Mehl: 145, Pl. 34, Figs. 25-26
1938 *Gnathodus perplexus* – Branson & Mehl: 145, Pl. 34, Fig. 24
1959 *Gnathodus delicatus* – Voges: Pl. 33, Fig. 32 [only]
1980 *Gnathodus delicatus* – Lane et al.: 129, Pl. 3, Fig. 17; Pl. 4, Figs. 2-4

Material: 12 specimens, Wettmarsen

Description: Blade is slightly curved towards the inner side, blade as long or longer than platform. Denticles on blade are well defined and bigger than on carina, decreasing in size at the transitional area between blade and carina. Denticles on carina are slightly fused at their bases, decreasing in size towards posterior tip, reaching posterior tip of the platform. The platform is asymmetrical, the outer platform being much wider than the narrow inner platform. The platform is widest in its anterior half, thinning towards the posterior end. The inner platform is ornamented by a row of nodes, closely paralleling the carina and forming a parapet. The outer platform bears irregularly arranged nodes, forming several (2-4) curved rows.
Aboral side smooth, forming a big aboral cup.

Age and range: lower Carboniferous: base of *isosticha*-Upper *crenulata* Zone into *anchoralis* Zone (Lane et al. 1980, Ziegler 1981, Herbig & Stoppel 2006)

Gnathodus punctatus (Cooper, 1939)

1939 *Dryphenotus punctatus* – Cooper: 386, Pl. 41, Figs. 42-43, Pl. 42, Figs. 10-11
1972 *Gnathodus punctatus* – Matthews, Sadler & Selwood: 560-562, Pl. 109, Figs. 5, 13, Pl. 110, Figs. 1-4, 11-15
1973 *Gnathodus punctatus* – Butler: 498-500, Pl. 56, Figs. 1, 2

Material: 1 specimen: Gladenbach

Description: Asymmetrical, wide cup, blade longer or approximately as long as the cup. Outer side of the cup is wider than inner side, both are irregularly shaped. Outer side bears numerous nodes forming radial rows, the anterior-most paralleling the anterior margin of the cup. The inner side bears a strong parapet ornamented with a row of nodes. These nodes form a row paralleling the carina or a curved row with the convex side facing the blade. The aboral side is smooth, mirroring the form of the oral surface.

Remarks: The only existing specimen was lost during preparation for SEM photography.

Age and range of species: lower Carboniferous: base of *isosticha*-Upper *crenulata* Zone into Lower *typicus* Zone (Lane et al. 1980, Ziegler 1981)

Gnathodus typicus Cooper, 1939
Morphotype 1
Plate9, Figs. 4a, b, 5-8

1939 *Gnathodus typicus* – Cooper: 388, Pl. 42, Figs. 77, 78
1959 *Gnathodus texanus* – Voges: 284, Pl. 33, Figs. 41, 43 only
1964 *Gnathodus typicus* – Rexroad & Scott: 31-32, Pl. 2, Fig. 3
1980 *Gnathodus typicus* – Lane, Sandberg & Ziegler: 130-131, Pl. 3, Figs. 2-4,10, Pl. 10 Fig. 6

Material: 38 specimens: Gladenbach, Wettmarsen

Description: Asymmetrical, narrow cup, blade longer than the small cup. Parapet on the slender inner side of the cup. Outer side is slightly wider than inner side of the cup, reaching the posterior tip. Surface is ornamented by a few nodes or smooth. Some specimens only have nodes on the parapet, paralleling the carina. Size of denticles decreases towards the posterior end. Last denticle is on the posterior tip. Aboral side is smooth, mirroring the outlines of the oral side.

Remarks: Lane et al. (1980) distinguished two morphotypes:
Morphotype 1 (M1) has a relatively wide expanded, inflated outer cup, that extends to the posterior tip and is ornamented by random nodes. It can be distinguished from *Gn. delicatus* by the shorter parapet and the narrow inner cup and occurs from within the *isosticha*-Upper *crenulata* Zone through the *anchoralis* Zone. In the here described elements, the specimens of M1 often have a smooth outer cup, but it always reaches the posterior tip.
M2 is less inflated and the outer cup is less ornamented (Lane et al. 1980, Pl. 3, Figs. 3-4, 10, pictured specimens without ornamentation on the outer cup). It terminates anteriorly to the posterior tip. The inner cup is even narrower than in M1. Sandberg (1979) used the M2 to define the base of the *typicus* Zone. M2 also occurs up into the *anchoralis* Zone.
In the samples from Gladenbach and Wettmarsen, only M1 occurs.

Age and range of species: lower Carboniferous: from within the *isosticha*-Upper *crenulata* Zone into the *anchoralis* Zone (Lane et al. 1980, Herbig & Stoppel 2006), in Gladenbach it only occurs within the *isosticha*-Upper *crenulata* Zone

Genus *Mehlina* YOUNGQUIST, 1945
Type species: *Mehlina irregularis* YOUNGQUIST 1945 (= *Mehlina gradata* YOUNGQUIST 1945)

Mehlina sp.
Plate 14, Fig. 8

Material: 88 specimens (counted together with specimens of *Branmehla*), Gladenbach, Wettmarsen

Description: Blade straight, slightly arched, platform missing. Size of closely set denticles varies irregularly. In overall view height of denticles decreases towards the posterior end with a small increase in the anterior half of the posterior part of the blade. The elongated basal cavity is situated in the middle to posterior part of the blade.

Remarks: In this study, specimens of *Branmehla* sp. and *Mehlina* sp. were counted together because the biozonation does not rely on these two genera, but they are used for the biofacies assessment of the bispathodid group (ZIEGLER & SANDBERG, 1984).

Age and range of genus: Upper Devonian and lower Carboniferous: lower *marginifera* Zone (ZIEGLER & SANDBERG 1984) of the Fammennian, at least up to the *sandbergi* Zone (KAISER 2005) of the lower Tournaisian; in Wettmarsen the genus occurs up into the *isosticha*-Upper *crenulata* Zone, and in Gladenbach even one specimen could be retrieved from the Lower *typicus* Zone

Genus *Neopolygnathus* VORONTZOVA (in BARSKOV et al., 1991)
Type species: *Polygnathus communis* BRANSON & MEHL, 1934b

The genus *Neopolygnathus* is defined by the large, shallow depression posterior to the basal pit on the aboral side of the element.

Remarks: As stated by DZIK (1997), the generic name *Polygnathus* HINDE, 1879, serves as a taxonomic "waste basket" including hundreds of remotely related species and therefore preventing a sensible diagnosis for genus and species. The Late Devonian type species of the genus *Polygnathus*, *P. dubius* HINDE, 1879 "is an unspecialized member of an evolutionary branch with a platform of sp elements strongly ornamented with transverse ridges and the rest of the apparatus of rather generalised morphology" (DZIK 1997, p. 152). Thus, we follow VORONTZOVA in BARSKOV et al. (1991) and DZIK (1997) in separating the genus *Neopolygnathus*, a latest Devonian to early Carboniferous branch of the polygnathids, that is characterized by a well developed but morphologically simple platform.

Age and range of genus: Upper Devonian and lower Carboniferous (VORONTZOVA 1996)

Neopolygnathus communis carina HASS, 1959
Plate 10, Figs. 1-2a, b

1959 *Polygnathus communis carina* – HASS: 391, Pl. 47, Figs. 8-9
1964 *Polygnathus communis carina* – REXROAD & SCOTT: 34, Pl. 2, Figs. 24-25
1972 *Polygnathus communis carina* – MATTHEWS et al.: 563-564, Pl. 111, Figs. 6-7, 13

Material: 8 specimens: Gladenbach, Wettmarsen

Description: The appearance of this genus is similar to that of *N. c. communis.* Slightly asymmetrical, leaf-shaped platform, oral surface is smooth, except for reticulate pattern that becomes more prominent towards the platform margins. One significant difference to *N. c. communis* are two ridges in the anterior part of the platform (one on each side of the carina) that form a 30° angle with the carina (posterior part ends near the carina, anterior end points towards the anterior margin or continues into the margin of the platform). Ridges can be smooth or composed of numerous denticles. Denticles on the blade are distinct and decrease in size towards the midpoint of the platform. Denticles of carina are fused, tips slightly recognizable, size of denticles decreasing towards the posterior tip of the platform, not reaching the tip. Carina arches towards the inner side. Aboral side is smooth, has a small basal pit, followed posteriorly by a large, shallow depression. The keel is flat and faint near the basal pit but quickly becomes more prominent towards anterior and posterior end.

Remarks: Rexroad & Scott (1964) reported specimens with two or more rows of irregularly spaced nodes on the anterior part of the platform. These could not be observed in our specimens.

Age and range of species: Upper Devonian and lower Carboniferous (Tournaisian): lower part of *expansa* Zone into *anchoralis* Zone (Kaiser et al. 2009), Herbig & Stoppel (2006) list it from the base of the Lower *duplicata* Zone into the *anchoralis* Zone, in Gladenbach it occurs up into the *isosticha*-Upper *crenulata* Zone

Neopolygnathus communis communis (Branson & Mehl, 1934b)
Plate 10, Figs. 3a, b, 4a, b, 5a, b

1934b *Polygnathus communis* n. sp. – Branson & Mehl: 293, Pl. 24, Figs. 1-4
1979 *Polygnathus communis communis* – Sandberg & Ziegler: 188
1999 *Neopolygnathus communis communis* – Mawson & Talent: Pl. 7, Fig. 5 (only)
2006 *Neopolygnathus communis* – Dzik: 102, Figs. 9B, 70A-S, 130
2011 *Neopolygnathus communis* – Hartenfels: 241, Pl. 61, Figs. 1-4

Material: 395 specimens: Dolhain, Gladenbach, Wettmarsen

Description: Small platform, lanceolate in outline, free blade and platform have approximately the same length. In some specimens the blade is longer or shorter than the platform. Oral side of platform is smooth, except for reticulate pattern, platform margins are thick and upturned. Size of denticles on the blade decreases towards the midpoint of the specimen. Denticles of carina are fused together at the bottom and decrease in size towards the posterior tip of the platform. Denticles on carina are spaced widely apart, whereas distinct denticles on blade can be distinguished much better and are spaced narrower. Aboral side smooth, basal pit large compared to size of the platform, keel well recognizable. A large, shallow depression is situated posterior to the basal pit.

Remarks: In contrast to the original description by Branson & Mehl (1934b), in some of the specimens from Gladenbach the blade is shorter than the platform, and the carina bears more denticles than the blade. In specimens from Wettmarsen few or numerous nodes can be found on the upturned platform margins. In some specimens, an indentation of the upturned platform margins in the anterior half of the platform can be observed, as pictured in Gedik (1974), Pl. 4 Fig. 12a-c.

Age and range of species: Upper Devonian and lower Carboniferous: Middle *crepida* Zone (Sandberg & Ziegler 1979) into upper part of the *anchoralis* Zone (Vorontzova 1996), Herbig & Stoppel (2006) list it from the base of the *praesulcata* Zone to the top of the *anchoralis* Zone

Genus *Neoprioniodus* Rhodes & Müller, 1956

Type species: *Prioniodus conjunctus* Gunnell, 1931

Neoprioniodus sp.

Plate 10, Fig. 6

Material: 25 specimens: Gladenbach

Description: Specimens assigned to this genus have one distinctly prominent, high main denticle. A short blade with few small denticles is joined posteriorly to the main denticle, not reaching the base of the main denticle. The basal cavity varies in size. In some specimens it covers the whole base of the main denticle, in others it is situated underneath the center of the denticle.

Remarks: In contrast to the original description by Pander (1856), the specimens assembled herein do not have denticles anterior of the main denticle. The specimens of this genus were not further differentiated because it is not essential for the biozonation.

Age and range: apparently from Ordovician to Lower Triassic (Rhodes & Müller 1956)

Genus *Polygnathus* Hinde, 1879

Type species: by subsequent designation of Miller, 1889, *Polygnathus dubia* Hinde, 1879. The type of *Polygnathus dubia* designated by Roundy, 1926, as Fig. 17 on Pl. 16 of Hinde's 1879 publication.

Age and range of genus: Devonian to lower Carboniferous (Ziegler 1973)

Polygnathus inornatus Branson, 1934

Plate 10, Figs. 7a, b, 8, Pl. 11, Fig. 1

1934 *Polygnathus inornata* – Branson: 309, Pl. 25, Figs. 8, 26
1934 *Polygnathus inornata* – Branson & Mehl: 293, Pl. 24, Figs. 5-7
1975 *Polygnathus inornatus* – Ziegler: 293-297, Pl. 4, Figs. 1, 2, 4

Material: 362 specimens: Gladenbach, Dolhain

Description: Lanceolate, slightly asymmetrical platform, arched towards the inner side, about three times as long as wide. Free blade short compared to platform, transverse ridges on platform. Platform is relatively thick with reticulate pattern on the margins, platform margin upturned, especially in the anterior part of the platform. Denticles are closely arranged on the blade and stand wider apart on the carina. Size of denticles on blade decreases towards the mid-point of the platform, denticles on carina decrease in size towards posterior tip of the platform. Aboral side smooth, narrow grooves developing from the basal pit into anterior and posterior keel.

Age and range of species: lower Carboniferous: Kinderhookian in North America (ZIEGLER 1975), from the base of the *praesulcata* Zone to the top of the *anchoralis* Zone (HERBIG & STOPPEL 2006)

Polygnathus lobatus BRANSON & MEHL, 1938b
Plate 11, Fig. 2

1938b *Polygnathus lobata* – BRANSON & MEHL: 146, Pl. 334, Figs. 44-47
1939 *Polygnathus lobata* – COOPER: 401, Pl. 39, Figs. 229, 30
1969 *Polyngnathus lobatus lobatus* – RHODES, AUSTIN & DRUCE: 191-192, Pl. 9, Figs. 5a-8c

Material: 1 specimen, Dolhain

Description: The outer appearance of this species is very similar to *Po. inornatus*, but can be distinguished by a lobate process that forms in the posterior half of the outer platform.

Age and range of species: lower Carboniferous: Avonian (comparable to the Dinantian) in Scotland (RHODES et al. 1969)

Polygnathus longiposticus BRANSON & MEHL, 1934b
Plate 11, Figs. 3-4

1934 *Polygnathus longipostica* – BRANSON & MEHL: 294, Pl. 24, Figs. 8-11
1974 *Polygnathus longiposticus* – GEDIK: 19, Pl. 5, Figs. 9a, b
1975 *Polygnathus longiposticus* – ZIEGLER: 303-306, Pl. 6, Fig. 1

Material: 10 specimens: Gladenbach, Dolhain

Description: Long, slender, nearly bisymmetrical platform with transverse ridges, ornamented with reticulate pattern. Free blade short (in comparison to platform). Size of denticles on blade decreases towards the mid-point of the platform, denticles of carina low, fusing into each other, decreasing in size towards the posterior tip of the platform, last denticle sits beyond the posterior end of the platform, forming a very thin, pointed tip. Aboral side smooth, basal pit big, keel with groove near the basal pit in the anterior part, wide keel with groove in the posterior part of the platform.

Age and range of species: lower Carboniferous: Kinderhookian in North America (ZIEGLER 1975), from the *sulcata* Zone (SANDBERG et al. 1978) up into the Upper *typicus* Zone (LANE et al. 1980)

Polygnathus purus purus Voges, 1959
Plate 11, Figs. 5-6

1957 *Polygnathus communis* – Bischoff: 42, Pl. 2, Figs. 23, 25, 26 [Figs. 25, 26 = early forms, with resemblance to *Polygnathus pura subplana*]
1959 *Polygnathus pura pura* – Voges: 291-292, Pl. 34, Figs. 21-33
1974 *Polygnathus purus purus* – Gedik: 20-21, Pl. 4, Figs. 20a, b, 21a-c

Material: 17 specimens: Gladenbach, Wettmarsen

Description: Small, short, leaf-shaped platform, smooth surface except for faint reticulate pattern near the margins. Size of denticles on the blade decreases slightly towards mid-point of the platform, denticles on the carina are shallower than denticles of the blade and fuse with each other and the platform. Size and in some specimen visibility of denticles on carina decrease towards posterior tip of the platform. Aboral side smooth, small basal pit situated underneath the first denticle of the carina, prominent keel in the anterior part, faint, shallow keel in the posterior part.

Age and range of species: lower Carboniferous: from the *sulcata* Zone to the base of the Lower *crenulata* Zone (Sandberg et al. 1978), in Gladenbach the species occurs in the *isosticha*-Upper *crenulata* Zone

Genus *Pseudopolygnathus* Branson & Mehl, 1934b
Type species: *Pseudopolygnathus prima* Branson & Mehl, 1934b

Age and range of genus: Late Upper Devonian to lower Carboniferous: Upper *velifer* Zone into late Tournaisian (Ziegler 1981)

Pseudopolygnathus fusiformis Branson & Mehl, 1934b

1934 *Pseudopolygnathus fusiformis* – Branson & Mehl: 298, Pl. 23, Figs. 1-3
1959 *Pseudopolygnathus* cf. *fusiformis* – Voges: 295, Pl. 23, Figs. 42-46
1974 *Pseudopolygnathus fusiformis* – Gedik: 22, Pl. 5, Figs. 20-23

Material: 20 specimens: Gladenbach, Dolhain

Description: Slender platform, pointed towards posterior end, small nodes on platform margins. Blade high, in lateral view platform is bend downwards at anterior and posterior end. Denticles on blade and carina are well distinguishable, oval on the blade, circular on the carina. Last denticle of the carina on tip of the posterior end. Aboral side smooth, basal pit very large, in anterior part the basal pit starts before the platform. Basal pit approximately as wide as the platform, posteriorly merging into the keel with very short anterior and long posterior groove into the keel.

Age and range of species: lower Carboniferous, Kinderhookian in North America (Ziegler 1981)

Pseudopolygnathus multistriatus MEHL & THOMAS, 1947
Plate 11, Fig. 7

1947 *Pseudopolygnathus multistriata* – MEHL & THOMAS: 16, Pl. 1, Fig. 36
1957 *Pseudopolygnathus multistriata* – BISCHOFF: 51, Pl. 4, Figs. 33, 35a, b
1969 *Pseudopolygnathus multistriatus* – RHODES, AUSTIN & DRUCE: 211, 212, Pl. 5, Figs. 14-16, Pl. 6, Fig. 2

Material: 4 specimens: Gladenbach

Description: Slender, lanceolate platform, transverse ridges or elongated nodes on platform, carina straight or slightly arched. Free blade shorter than platform (approximately 1/2 to 1/3 of length of the platform). Denticles on blade and carina are closely spaced, denticles on carina fuse into each other, tips of denticles are separated. Size of denticles on the carina decreases towards the posterior tip of the platform. Aboral side smooth, large aboral pit, oval, slightly wider than platform and drawn out to the posterior, short anterior and long posterior groove in the keel.

Remarks: In contrast to the statement by BISCHOFF (1957), in our specimens the free blade is shorter than the platform and therefore fits the description by RHODES, AUSTIN & DRUCE (1969).

Age and range of species: lower Carboniferous: lower Osagean in North America (ZIEGLER 1981), from within the *isosticha*-Upper *crenulata* Zone into the *anchoralis* Zone (LANE et al. 1980), HERBIG & STOPPEL (2006) list it from within the *praesulcata* Zone to the top of the *anchoralis* Zone, in Gladenbach it occurs in the uppermost part of the Lower *crenulata* Zone

Pseudopolygnathus primus primus BRANSON & MEHL, 1934b
Morphotype 2
Plate 11, Figs. 8, 9a, b

1934 *Pseudopolygnathus irregularis* – BRANSON: 316, Pl. 26, Figs. 25-6
1934 *Pseudopolygnathus lobata* – BRANSON: 316, Pl. 26, Figs. 1-2
1934 *Pseudopolygnathus dentilineata* – BRANSON: 317, Pl. 26, Fig. 22
1957 *Pseudopolygnathus dentilineata* – BISCHOFF: 50, Pl. 4, Figs. 29-32, 34
2018 *Pseudopolygnathus primus primus* M2 – HARTENFELS & BECKER: 617-620

Material: 27 specimens: Dolhain, Gladenbach, Wettmarsen

Description: Slender, asymmetrical platform, widening towards the middle and thinning towards posterior tip and anterior end. Right platform starts to extend somewhat more anterior than the left one. Platform bears nodes or transverse ridges that form an irregular platform margin. Free blade slightly shorter than the platform, blade and carina straight. Free blade high, height of blade and carina decreases towards posterior tip, size of denticles decreases slightly towards posterior tip. Aboral side smooth, aboral pit very big in comparison to platform, aboral pit almost as wide as platform, posteriorly merging into the keel with short anterior and longer posterior groove extensions, keel high.

Remarks: In specimens from Wettmarsen the transverse ridges are not as thick as described in the literature.

Age and range of species: Late Upper Devonian to lower Carboniferous: Upper *styriacus* Zone (*Bi. stabilis stabilis* Zone, Lower *expansa* Zone) to *Si. triangulus triangulus* Zone of VOGES (*sandbergi* Zone) (ZIEGLER 1981), HARTENFELS & BECKER (2018) mention the possible oldest M2 representatives from the *Bi. aculeatus aculeatus* Zone of the Ardennes (DREESEN, DUSAR & GROESSENS 1976), HERBIG & STOPPEL (2006) list it from within the *praesulcata* Zone to the uppermost Lower *typicus* Zone
In Gladenbach it occurs from the Lower *crenulata* Zone to the *typicus* Zone, in Wettmarsen it is present within the *isosticha*-Upper *crenulata* Zone and in Dolhain within the Lower *crenulata* Zone.

Pseudopolygnathus triangulus inaequalis VOGES, 1959
Plate 11, Fig. 10a, b

1959 *Pseudopolygnathus triangula inaequalis* – VOGES: 302, Fig. 5, Pl. 34, Figs. 51-58 (57/58???)
1969 *Pseudopolygnathus triangula inaequalis* – SCHÖNLAUB: 340-341, Pl. 1, Figs. 25, 26
1974 *Pseudopolygnathus inaequalis* – GEDIK: 23: Pl. 6, Figs. 5-8, 10-11, 13
2011 *Pseudopolygnathus triangulus inaequalis*: BAHRAMI et al.: Pl. 3, Figs. 13-14

Material: 8 specimens, Wettmarsen

Description: Triangular platform, the right side of the platform begins slightly more anterior than the left one. Transverse ridges on platform, forming irregular platform margin. Blade is slightly curved towards the inner side. Denticles on blade are closer spaced and smaller than on the carina. Biggest denticle of the carina is situated in the middle of the platform. Distance between denticles on the carina increases towards posterior tip. Posterior-most denticle is situated close to the posterior tip and smaller than other denticles on the carina. Aboral side smooth, big basal cavity/pit situated near the anterior margin of the platform continuing into a keel. Keel thins towards the posterior tip. Basal cavity is characterized by a crease on the outer side.

Remarks: Following VOGES (1959) we use the triangular outline and the broader and more planar platform to differentiate this form from *Ps. primus primus*.

Age and range of species: lower Carboniferous: reported from VOGES (1959) in the Hangenbergkalk (middle Tournaisian, *sulcata* Zone to *sandbergi* Zone), BAHRAMI et al. (2011) report it from the *sandbergi* Zone, therefore our specimens are probably reworked or the species also occurs in younger strata

Pseudopolygnathus triangulus pinnatus VOGES, 1959
Plate 11, Fig. 11a, b, Plate 12, Fig. 1a, b

1959 *Pseudopolygnathus triangula pinnata* – VOGES: 302, 303, Pl. 34, Figs. 59-66, Pl. 35, Figs. 1-6
1973 *Pseudopolygnathus triangulus pinnatus* – BUTLER: 508, Pl. 58, Figs. 23-24, 27-28, 30-31, 33-34

Material: 40 specimens: Gladenbach, Wettmarsen

Description: Platform triangular, thick and asymmetrical. In the anterior part of the platform, smooth, triangular shaped grooves on each side of the blade cause wing-shaped morphology of the inner and outer platform. In some specimens one of the anterior platform edges is elongated and more prominent than the other. In lateral view the anterior part of the platform is slightly bend downwards. Platform bears transverse ridges and is ornamented with reticulate pattern. Platform margins are crenulate due to irregular transverse ridges. Outer platform is concave, inner platform more or less convex. Carina slightly arched towards the inner side. Size of oval denticles of the blade decreases towards midpoint of the platform, size of round denticles of the carina decreases towards posterior end of the platform. Aboral side is smooth, aboral pit big, keel high, short groove reaches from aboral pit into anterior keel.

Remarks: Some specimens from Wettmarsen have a very irregular platform margin outline.

Age and range of species: lower Carboniferous: from within the Upper *typicus* Zone into the *anchoralis* Zone (Lane et al. 1980), Voges (1959) also reports it from the *anchoralis* Zone, Herbig & Stoppel (2006) list it from the base of the Lower *crenulata* Zone up to the top of the *anchoralis* Zone. In Gladenbach and Wettmarsen the species occurs in the *isosticha*-Upper *crenulata* Zone.

Pseudopolygnathus triangulus triangulus Voges, 1959
Plate 12, Figs. 2a, b, 3a, b, 4

1959 *Pseudopolygnathus triangula triangula* – Voges: 304, 305, Fig. 5, Pl. 35, Figs. 7-13
1974 *Pseudopolygnathus triangulus triangulus* – Pierce & Langenheim: Pl. 4, Figs. 9, 13

Material: 63 specimens: Gladenbach, Wettmarsen

Description: Platform triangular and asymmetrical, outer side wider than inner side. Platform bend upwards towards the edges, especially in the anterior half. Just as described in the original diagnosis, at the right side the anterior part of the platform is always bigger because it emerges at a more anteriorly point out of the blade than on the other side. In lateral view, the anterior part of the platform is bend downwards. Transverse ridges and reticulate pattern on oral surface. Blade and carina nearly straight. Size of oval denticles of the blade decreases towards mid-point of the platform, size of round denticles of the carina decreases towards posterior tip of the platform, last few denticles of the carina stand wider apart. Denticles of the carina fuse increasingly with the platform towards the posterior end. Aboral side is smooth, keel is well recognizable. Big basal pit is surrounded by a rim that fuses into the keel. Short groove evolves from basal pit and continues into anterior part of the keel.

Age and range of species: lower Carboniferous: reported by Bahrami et al. (2011) from within the *sandbergi* Zone to the *isosticha*-Upper *crenulata* Zone, Herbig & Stoppel (2006) list it from the base of the Lower *duplicata* Zone up to the top of the *anchoralis* Zone

Genus *Siphonodella* Branson & Mehl, 1944

Type species: *Siphonognathus duplicata* Branson & Mehl, 1934b

Remarks: Following Kaiser et al. (2009) the subgenus *Eosiphonodella* introduced by Ji (1985) for siphonodellids with a pseudokeel is not used, awaiting further revision of the early siphonodellids.

Age and range of genus: lower Carboniferous: According to Lane et al. (1980), *Siphonodella* becomes extinct at the boundary between *isosticha*-Upper *crenulata* Zone and Lower *typicus* Zone. Therefore, the occurrence of some siphonodellid species in German successions above the *isosticha*-Upper *crenulata* Zone, in part up to the top of the uppermost *anchoralis* Zone (Voges 1959, Ziegler 1973, Herbig & Stoppel 2006), either rely on reworked elements or on outdated stratigraphic zonation. In fact, it has to be stressed that Voges (1959, 1960) did not yet recognize the *typicus* Zone and, therefore, apparently all recognized mid-Tournaisian taxa would reach up to the *anchoralis* Zone. Therefore, in the following erroneous upper ranges limits listed by Voges (1959), Ziegler (1973) and Herbig & Stoppel (2006) are not mentioned in the following descriptions.

Siphonodella cooperi Hass, 1959

Plate 12, Fig. 5

1959 *Siphonodella cooperi* – Hass: 392, Pl. 48, Figs. 35-36
1973 *Siphonodella cooperi* – Butler: 510-511, Pl. 59, Figs. 39-40
1975 *Siphonodella cooperi* – Ziegler: 345-348, Pl. 2, Figs. 4-5
2017 *Siphonodella cooperi* – Zhuravlev & Plotitsyn: 464, Pl. 2, Figs. 10-12

Material: 140 specimens: Gladenbach, Wettmarsen

Description: Compared to *Si. crenulata*, *Si. cooperi* has a slender, elongated form. Two rostral ridges; outer rostral ridge is longer than inner one, terminating posterior to the basal pit. Outer rostral ridge curves towards the platform margin, sometimes terminating before reaching the platform margin. Inner rostral ridge is straight and terminates near the basal pit. Outer platform bears transverse ridges, inner platform is nodose. In smaller (probably juvenile) specimens transverse ridges and nodes are fainter. Surface of oral side is ornamented with reticulate pattern. Carina bends towards the inner side. Denticles are biggest in the anterior part of the free blade and increase in size towards the midpoint. Denticles on carina have approximately the same size but fuse into the platform near the posterior tip. Denticles do not reach the posterior tip of the platform. Aboral side is smooth, basal pit is small, keel is well visible on anterior part of the specimen but very shallow and faint in the posterior part.

Remarks: In our specimens the outer rostral ridge never forms the outer platform margin as mentioned by Klapper (1971).

Age and range of species: lower Carboniferous: Upper *duplicata* Zone into *isosticha*-Upper *crenulata* Zone (Ziegler 1975), Lane et al. (1980) also record it from the *isosticha*-Upper *crenulata* Zone, Herbig & Stoppel (2006) list it from the base of the *sandbergi* Zone to the

top of the *istosticha*-Upper *crenulata* Zone, ZHURAVLEV & PLOTITSYN (2017) record it from the base of the Upper *duplicata* Zone to the top of the Lower *crenulata* Zone

Siphonodella crenulata (COOPER, 1939)

1939 *Siphonognathus crenulata* – COOPER: 409, Pl. 41, Figs. 1-2
1973 *Siphonodella crenulata* – ZIEGLER: 455-456, Pl. 1, Fig. 2
2017 *Siphonodella crenulata* – ZHURAVLEV & PLOTITSYN: 458-460, Pl. 3, Figs. 8-9, 11

Diagnosis (SANDBERG et al. 1978): *Siphonodella crenulata* is divided into two morphotypes. M1 is ornamented by strong transverse ridges that usually result in a crenulate platform margin, as illustrated by KLAPPER (1966, Pl. 3, Figs. 5, 6). M2 typically has a smooth outer platform, except for a reticulate micropattern, or it shows faint, narrow transverse ridges that do not affect the smooth rounded margin (illustrated by VOGES, 1959, Pl. 35, Figs. 23-30).

Age and range of species (both morphotypes): lower Carboniferous: Lower *crenulata* Zone into *anchoralis* Zone (VOGES 1959, ZIEGLER 1973), referring to HERBIG & STOPPEL (2006) Lower *crenulata* Zone to Lower *typicus* Zone in Germany, ZHURAVLEV & PLOTITSYN (2017) report it only from the Lower *crenulata* Zone

Siphonodella crenulata
Morphotype 1
Plate 12, Figs. 6a, b, 7

1966 *Siphonodella crenulata* – KLAPPER: 18, Pl. 3, Figs. 5-8
1978 *Siphonodella crenulata* M1 – SANDBERG, ZIEGLER, LEUTERITZ & BRILL: 110-111, Fig. 1

Material: 94 specimens: Gladenbach

Description: Platform asymmetrical, outer platform wider than inner platform. Outer platform with transverse ridges and crenulate outer platform margin. Inner platform with nodes. Surface ornamented with reticulate pattern. Short transverse ridges parallel to blade. Carina is arched towards the inner side. Biggest denticles are at the anterior part of the blade, denticles are more distinct on the blade than on the carina. On the carina, denticles fuse into each other and are best distinguishable on the tips. Aboral side smooth with shallow aboral ridge and aboral pit. In juvenile specimens, transverse ridges and nodes are fainter or not present on oral side of platform.

Remarks: KLAPPER (1971) mentioned that exceptionally three rostral ridges are present, in our samples only specimens with two rostral ridges occur. In Gladenbach this morphotype only occurs in the Lower *crenulata* Zone

Siphonodella crenulata
Morphotype 2
Plate 12, Figs. 8-10, Plate 13, Fig. 1

1959 *Siphonodella crenulata* – VOGES: 307-308, Pl.- 35, Figs. 23-30

1978 *Siphonodella crenulata* M2 – Sᴀɴᴅʙᴇʀɢ, Zɪᴇɢʟᴇʀ, Lᴇᴜᴛᴇʀɪᴛᴢ & Bʀɪʟʟ: 110-111, Fig. 1

Material: 546 specimens: Gladenbach

Description: Platform asymmetrical, outer platform very wide, wider than in *Si. crenulata* M1. Transverse ridges on outer platform, nodes on inner platform. Ridges and nodes less pronounced or absent in juvenile specimens but surface always ornamented by reticulate pattern. Two short, parallel rostral ridges, in juvenile specimens less pronounced. Crenulate platform margin on outer platform, pointed posterior tip. Carina bent and arched towards the inner side. Denticles of the free blade increase in size towards the midpoint. Denticles of the carina have approximately the same size but fuse more into the platform towards the posterior tip. Smooth surface on aboral side, very small aboral pit, keel well visible in the anterior half but very flat and faint in the posterior half except for the posterior tip.

Remarks: Kʟᴀᴘᴘᴇʀ (1971) mentioned that exceptionally three rostral ridges are present, in our samples only specimens with two rostral ridges occur. In Gladenbach this morphotype occurs in the Lower *crenulata* Zone up to the middle of the *isosticha*-Upper *crenulata* Zone.

Siphonodella duplicata (Bʀᴀɴsᴏɴ & Mᴇʜʟ, 1934b)
Plate 13, Figs. 3-4

1934 *Siphonognathus duplicata* – Bʀᴀɴsᴏɴ & Mᴇʜʟ: 296-297, Pl. 24, Figs. 16-17
1975 *Siphonodella duplicata* – Zɪᴇɢʟᴇʀ: 349-351, Pl. 2, Fig. 6
2017 *Siphonodella duplicata* – Zʜᴜʀᴀᴠʟᴇᴠ & Pʟᴏᴛɪᴛsʏɴ: 458, Pl. 1, Fig. 9

Mateial: 74 specimens: Gladenbach, Wettmarsen

Description: Platform asymmetrical and narrow, outline concave. Transverse ridges on inner and outer platform, oral side ornamented with reticulate pattern. Two rostral ridges on rostrum of approximately the same length. Carina is slightly arched towards the inner side. Denticles wider apart on the carina than on the blade, but well distinguishable from each other; denticles of carina do not reach the posterior tip of the platform. Aboral side is smooth, basal pit is small, keel indistinct except near the anterior end. Towards the posterior part of the platform, keel forms a narrow basal furrow.

Age and range of species: lower Carboniferous: Lower *duplicata* Zone into Lower *crenulata* Zone (Hᴇʀʙɪɢ & Sᴛᴏᴘᴘᴇʟ 2006), Zʜᴜʀᴀᴠʟᴇᴠ & Pʟᴏᴛɪᴛsʏɴ (2017) report it from within the Lower *duplicata* Zone to the top of the Lower *crenulata* Zone, in Gladenbach *Si. duplicata* occurs in the Lower *creunlata* Zone and reaches into the lower part of the *isosticha*-Upper *crenulata* Zone, possibly due to reworking

Siphonodella hassi Jɪ, 1985 (=*Siphonodella duplicata* sensu Hᴀss, 1959)
Plate 13, Figs. 6a, b, 7

1978 *Siphonodella duplicata* sensu Hᴀss – Sᴀɴᴅʙᴇʀɢ, Zɪᴇɢʟᴇʀ, Lᴇᴜᴛᴇʀɪᴛᴢ & Bʀɪʟʟ: 107-108, Fig. 1
1985 *Siphonodella (Siphonodella) hassi* – Jɪ: 59-60, 74, Fig. 14, Pl. 2, Figs. 5, 6
[non] 2016 *Siphonodella (Siphonodella) jii* – Bᴇᴄᴋᴇʀ, Kᴀɪsᴇʀ & Aʀᴇᴛᴢ: 375

Material: 14 specimens: Gladenbach

Description: Narrow asymmetrical platform, in contrast to *Si. duplicata*, *Si. hassi* bears nodes on the inner side. Outer side of platform bears transverse ridges. Oral side of the platform ornamented with reticulate pattern. The two rostral ridges are slightly convergent. Size of the denticles on the blade decreases towards the midpoint. Denticles on carina decrease in size towards the posterior tip. Denticles do not reach the posterior tip of the platform. Denticles of the carina fuse together at the bottom but are well separated at the tips, denticles of the blade are well distinguishable from each other. The aboral side is smooth. Keel widening towards the posterior end, basal pit small.

Remarks: Following PLOTITSYN & ZHURAVLEV (2016), ZHURAVLEV & PLOTITSYN (2017) and ZHURAVLEV & PLOTITSYN (2018) we use the name *Siphonodella hassi* JI provisionally. The name *Siphonodella hassi* JI, 1985 is a homonym of *Siphonodella cooperi hassi* THOMPSON & FELLOWS, 1970. The new name proposed for this taxon, *Si. jii* (by BECKER et al. 2016), unfortunately is a junior synonym of *Si. quadruplicata,* since the chosen holotype (elements figured by HASS (1959), Pl. 49, Figs. 17, 18) rather represent ontogenetic stages of *Si. quadruplicata*, possessing more than two rostral ridges (see ZHURAVLEV & PLOTITSYN 2018).

Age and range of species: lower Carboniferous: Tournaisian, Upper *duplicata* Zone through Lower *crenulata* Zone (SANDBERG et al. 1978), JI (1985) reports the species from the *hassi* Zone into the Lower *crenulata* Zone, ZHURAVLEV & PLOTITSYN (2017) report it from the base of the Upper *duplicata* Zone to the upper part of the Lower *crenulata* Zone, in Gladenbach the species appears as high as the upper part of the *isosticha*-Upper *crenulata* Zone

Siphonodella isosticha (COOPER, 1939)
Plate 13, Figs. 8-10, 11a, b, 12-13

1939 *Siphonognathus isosticha* – COOPER: 409, Pl. 41, Figs. 9-10
1973 *Siphonodella isosticha* – ZIEGLER: 459-460, Pl. 1, Fig. 3
1973 *Siphonodella isosticha* – BUTLER: 511, Pl. 59, Figs. 30-31 [only]

Material: 134 specimens: Gladenbach, Riescheid, Wettmarsen

Description: Asymmetrical narrow platform, surface smooth, except for reticulate pattern, or with nodules on inner side of platform and few nodes on the outer platform. Outer rostral ridge longer than inner one and slightly curved towards the outer margin, but not reaching the platform margin, inner rostral ridge ends near the basal cavity. Distance between denticles on free blade and carina is the same, denticles decrease in size towards the posterior end, not reaching the posterior tip of the platform. Posterior tip is rounded not pointed. Aboral side smooth, keel wide in the posterior part, basal pit small.

Age and range of species: lower Carboniferous: JI (1985) reports the species from the Lower *crenulata* Zone into the *typicus* Zone. According to HERBIG & STOPPEL (2006) it enters at the base of the *istosticha*-Upper *crenulata* Zone, normally extinction of the species is used to define the upper limit of the *isosticha*-Upper *crenulata* Zone (SANDBERG et al. 1978, LANE et al. 1980). According to SANDBERG et al. (1978) the species enters in the upper part of the Lower *crenulata* Zone, ZHURAVLEV & PLOTITSYN (2017) already record it from the base of the

Lower *crenulata* Zone. In Gladenbach it also occurs within the Lower *crenulata* Zone, but in Wettmarsen and Riescheid in the *isosticha*-Upper *crenulata* Zone.

Siphonodella lobata (BRANSON & MEHL, 1934b)
Plate 14, Fig. 1a, b

1934 *Siphonognathus lobata* – BRANSON & MEHL: 297, Pl 24, Figs. 14-15
1969 *Siphonodella lobata* – SCHÖNLAUB: 345, Pl. 2, Figs. 11-12
1973 *Siphonodella lobata* – ZIEGLER: 461-462, Pl. 1, Fig. 4
2017 *Siphonodella lobata* – ZHURAVLEV & PLOTITSYN: 460, Pl. 1, Figs. 12-14

Material: 5 specimens: Gladenbach, Wettmarsen

Description: Asymmetrical platform, outer platform is deformed by lobe in the anterior part. Transverse ridges on platform, in the area of the lobe the transverse ridges change direction to fit the orientation of the lobe. Oral side is ornamented with reticulate pattern. Two rostral ridges parallel to blade, rostral ridges are missing in some specimens. The carina curves towards the inner side. On blade and carina denticles fuse into each other, tips of denticles most distinct on the carina. Denticles continue to the posterior tip of the platform (last denticle is on posterior tip). Aboral side is smooth, basal pit is very small. The keel branches out towards the lobe where it is most distinct, on the main platform the keel is very faint.

Remarks: In our specimens the keel is not as distinct as described by BRANSON & MEHL (1934b).

Age and range of species: lower Carboniferous: upper *sandbergi* Zone into *isosticha*-Upper *crenulata* Zone (SANDBERG et al. 1978). According to HERBIG & STOPPEL (2006) it enters at the base of the *sandbergi* Zone, ZHURAVLEV & PLOTITSYN (2017) only report it from the *sandbergi* and Lower *crenulata* zones, in Gladenbach the last specimen occurs at the top of the Lower *crenulata* Zone. In Wettmarsen it occurs within the *isosticha*-Upper *crenulata* Zone.

Siphonodella obsoleta HASS, 1959
Plate 14, Fig. 3a, b

1959 *Siphonodella obsoleta* – HASS: 392, 393, Pl. 47, Figs. 1-2
1972 *Siphonodella obsoleta* – MATTHEWS et al.: 565, Pl. 111, Figs. 4-5
1973 *Siphonodella obsoleta* – ZIEGLER: 463-464, Pl 1, Fig. 7

Material: 225 specimens: Gladenbach, Wettmarsen

Description: Asymmetrical, narrow platform, inner side bears nodes, outer side ornamented with few nodes, reticulate pattern on surface. Two rostral ridges on the rostrum. The rostral ridge on the inner side is shorter and terminates anterior to the midpoint of the specimen, outer rostral ridge curves towards the platform margin and either ends there or continues as platform margin. On the blade the denticles are biggest in size and very closely spaced. Carina slightly bent towards the inner side. On the carina the denticles are smaller but biggest around the midpoint and wider spaced than on the

blade. The denticles on the carina are fused and only distinct at the tips. Denticles do not reach the posterior tip of the platform. Aboral side smooth, keel is high and slender in the anterior part. At small basal pit the keel widens and thins again towards the posterior tip.

Age and range of species: lower Carboniferous: Upper *duplicata* Zone into *isosticha*-Upper *crenulata* Zone (SANDBERG et al. 1978). According to HERBIG & STOPPEL (2006) it enters at the base of the *sandbergi* Zone. ZHURAVLEV & PLOTITSYN (2017) report it from the base of the Upper *duplicata* Zone to the top of the Lower *crenulata* Zone. In Gladenbach the species occurs in the Lower *crenulata* and *isosticha*-Upper *crenulata* zones, in Wettmarsen it is also present in the *isosticha*-Upper *crenulata* Zone.

Siphonodella quadruplicata (BRANSON & MEHL, 1934b)
1934b *Siphonognathus quadruplicata* – BRANSON & MEHL: 295, 296, Pl. 24, Figs. 18-20 [non Fig. 21= *Si. cooperi*]
1966 *Siphonodella quadruplicata* – KLAPPER: 17, 18, Pl. 2, Figs. 5-8, Pl. 3, Figs. 9-12, Pl. 4, Figs. 16, 20
2017 *Siphonodella quadruplicata* – ZHURAVLEV & PLOTITSYN: 462, Pl. 3, Figs. 1-5

Material: 3 specimens: Gladenbach

Description: Platform asymmetrical, transverse ridges on outer platform, nodules on inner platform. Four (name-giving) rostral ridges parallel to the blade, all ending approximately at the same extent on the platform. Carina is arched longitudinally towards the inner side. Denticles on blade decrease in size towards the midpoint of the platform. Denticles of the carina are fused at their bases, but the tips are clearly separated. The aboral side is smooth, basal pit very small and faint, keel is distinct in the anterior part and fainter and wider in the posterior part of the platform.

Remarks: Specimens with 3 or 5 rostral ridges as described by KLAPPER (1966, 1971) could not be observed.

Age and range of species: lower Carboniferous: *sandbergi* Zone into *isosticha*-Upper *crenulata* Zone (SANDBERG et al. 1978), HERBIG & STOPPEL (2006) list it from within the *sandbergi* Zone to the top of the *isosticha*-Upper *crenulata* Zone, higher range is erroneous (see above). ZHURAVLEV & PLOTITSYN (2017) report if from the upper part of the *sandbergi* Zone and the Lower *crenulata* Zone. In Gladenbach it occurs in the Lower *crenulata* Zone and at the base of the *isosticha*-Upper *crenulata* Zone.

Siphonodella sandbergi KLAPPER, 1966
Plate 14, Fig. 4

1966 *Siphonodella sandbergi* – KLAPPER: 19, Pl. 4, Figs. 6, 10-12, 14-15
1973 *Siphonodella sandbergi* – ZIEGLER: 467-468, Siphonodella-Pl. 1, Fig. 5

Material: 5 specimens: Dolhain

Description: Platform asymmetrical, outer side, wider than inner side. Outer platform side is smooth, inner platform bears nodes. Rostral ridges converge towards the blade. Rostral ridges on the inner side of the platform end in anterior part of the platform, rostral ridges

on outer side of the platform are longer. On the outer platform the outer rostral ridge curves towards the platform margin and ends in the middle of the platform, the inner rostral ridge is nearly straight in its posterior part and continues into the posterior half of the platform. The carina is arched toward the inner side. Denticles can only be distinguished on the blade but not on the carina. Size of denticles decreases towards the middle of the specimen. Aboral side smooth, basal pit very small, keel distinct and narrow, increasing in height towards anterior and posterior end.

Remarks: In contrast to the 5-6 rostral ridges reported by KLAPPER (1966) we can only distinguish 4-5 rostral ridges on our specimens.

Age and range of species: lower Carboniferous: from the base of the *sandbergi* Zone into the Lower *crenulata* Zone (SANDBERG et al. 1978), referring to ZIEGLER (1973) the species occurs in the *duplicata* to *sandbergi* zones (Kinderhookian) and in Europe in the *Siphonodella triangulus inaequalis* Zone (= within the lower *duplicata* Zone to the base of the *sandbergi* Zone), HERBIG & STOPPEL (2006) report it from the *sandbergi* Zone into the Lower *crenulata* Zone, in Dolhain the species occurs in the Lower *crenulata* Zone.

Siphonodella sulcata (HUDDLE, 1934)
Plate 14, Figs. 5-6

1934 *Polygnathus sulcata* – HUDDLE: 287, Pl. 8, Figs. 22-23
1975 *Siphonodella sulcata* – ZIEGLER: 357-358, Pl. 2, Figs. 2-3

Material: 8 specimens: Dolhain, Gladenbach, Wettmarsen

Description: Small, slightly asymmetrical, arched, narrow platform with pronounced transverse ridges on both platform sides, platform margin crenulate due to the transverse ridges. Denticles on the blade are well distinguishable but fuse increasingly into the platform towards the posterior tip. Denticles are more circular and broader on the carina. Aboral side is smooth, the keel is broad and encloses a large basal cavity.

Age and range of species: lower Carboniferous: base of the *sulcata* Zone into Lower *crenulata* Zone (SANDBERG et al. 1978), HERBIG & STOPPEL (2006) list it from the base of the *sulcata* Zone into the *sandbergi* Zone, in Gladenbach *Si. sulcata* occurs in the Lower *crenulata* and *isosticha*-Upper *crenulata* zones. In Wettmarsen it is present within the *isosticha*-Upper *crenulata* Zone and in Dolhain it was found in the Lower *crenulata* Zone.

9.1 Reworked Upper Devonian genera and species

Genus *Icriodus* BRANSON & MEHL, 1934
Type species: *Icriodus expansus* BRANSON & MEHL, 1938

Age and range of genus: latest Silurian through the Devonian (ZIEGLER 1975)

Icriodus alternatus alternatus Branson & Mehl, 1934a
Plate 14, Fig. 9

1934a *Icriodus alternatus* n. sp. – Branson & Mehl: 225-226, Pl. 13, Figs. 4-6
1975 *Icriodus alternatus* – Ziegler: 69-70, Pl. 3, Figs. 5, 6
1980 *Icriodus alternatus* – Dreesen & Houlleberghs: 116-117, Pl. 3, Figs. 6-8, Pl. 4; Figs. 1-4, 7
1984 *Icriodus alternatus alternatus* – Sandberg & Dreesen: 158-159, Pl. 2, Figs. 5, 11

Material: 1 specimen: Gladenbach

Description: Small drop-shaped platform, medial-row denticles round, increasing in size towards the posterior end. One row of lateral denticles on each side of the medial row, lateral-row denticles in alternating position with the medial-row denticles. Cusp situated on posterior end of platform, slightly elevated in height compared to other denticles, separated by one medial denticle from the posterior-most row of lateral denticles. The anterior end forms a small tip anterior to the anterior-most medial-row denticle. Aboral side completely composed of the basal cavity.

Remarks: In our specimen the nodes are rounder than described and pictured by Branson & Mehl (1934a) and Ziegler (1975). Instead, our specimen matches the description of the second morphotype with round medial-row denticles by Sandberg & Dreesen (1984)

Age and range of species: Upper Devonian: Upper *rhenana* Zone (Sandberg et al. 1992) into Upper *crepida* Zone (Sandberg & Dreesen 1984, Sandberg et al. 1992)

Genus *Ozarkodina* Branson & Mehl, 1933
Plate 14, Fig. 10

Type species: *Ozarkodina typica* Branson & Mehl, 1933 [= junior synonym of *Ozarkodina confluens* (Branson & Mehl, 1933)]

Material: 195 specimens: Gladenbach, Dolhain

Description: Specimens of this genus are described by defining the posterior and anterior bar, the denticles, the apical denticle and the lip of the basal cavity (see Rhodes et al. 1969 for nomenclature).
The denticles of the anterior bar are bend backwards towards the apical denticle that exceeds all other denticles in size. The denticles on the posterior bar are smaller than the ones on the anterior bar and also bend backwards. The complete bar is arched and the basal cavity is situated beneath the apical denticle.

Age and range of genus: Silurian to Devonian (Ziegler 1973)

Genus *Palmatolepis* Ulrich & Bassler, 1926
Plate 15, Figs. 1-12

Type species: *Palmatolepis perlobata* Ulrich & Bassler, 1926

The genus *Palmatolepis* was established by Ulrich & Bassler (1926). The current common diagnosis is based on Müller (1956), Ziegler (1962), Helms (1963), Glenister & Klapper (1966) and Huddle (1968) and was summarized by Ziegler (1973) (Hartenfels 2011). It is a characteristic Upper Devonian genus.

Because specimens of the genus *Palmatolepis* are reworked they are not further distinguished in the biostratigraphic and biofacies chapter. However, several species are figured in Plate 15: *Palmatolepis glabra pectinata*, *Pa. glabra prima*, *Pa. glabra* ?, *Pa. linguiloba*, *Pa. quadrantinodosalobata*, *Pa. triangularis*, *Pa.* sp.

Age and range of genus: from the base of the Upper Devonian to near the top of the Upper Devonian (Ziegler 1973)

10. Summary

The similar world-wide development of the mid-Tournaisian event, in widely scattered sedimentation realms, required globally reoccurring abiotic and biotic processes that were involved in its evolution. It was formed due to a glacio-eustatically induced sea-level rise, causing eutrophication and high primary productivity. Additionaly, it resulted in an oxygen-reduced water-body and ?sediment, though bioturbation was still active at least in places and intervals, and finally in increased accumulation of organic substance in dark shales and limestones. Different palaeoenvironmental factors such as the position on a shelf-basin transect, the influence of intrabasinal swells or platform areas and affiliated turbidity systems induced variations of sedimentation, primary productivity and faunal composition. Different approaches were used to unravel some of the processes that are involved in the evolution of the mid-Tournaisian Event.

Conodont biostratigraphy was used to confirm the age of the studied successions, and in part allowed the recognition of several conodont zones. The assignment to conodont zones also established, besides sequence stratigraphy, the stratigraphic respectively time-equivalence correlation, between the four studied sections. However, a review of numerous regionally applied conodont biozonations revealed that the correlation might be problematic, especially between platform and basin.

Sequence stratigraphy proves to be a useful tool to unravel the sedimentary history of a succession and to correlate sections with different lithologies and faunal contents. However, there exist still some correlation problems, as can be recognized when comparing the sequence stratigraphy of the Rhenish Kulm basin (HERBIG 2016) and of the southern Belgian carbonate platform of the Namur-Dinant Basin (e. g. POTY et al. 2014, POTY 2016). The comparison shows that in cases the sequence boundaries do not exactly coincide, and system tracts that might be recognizable in one area cannot be traced into the other.

Carbonate microfacies analysis reveals small scale sedimentary structures and the biotic as well as abiotic content of the rock. Therefore, the sedimentary processes and the depositional realm can be reconstructed and allow the assignment to a certain depositional realm within the basin, on the slope or on the shelf.

Conodont biofacies models employ the fact that certain conodont genera and species favour distinct environmental conditions and with independent methodology support the results of microfacies analysis.

The choice of sections depended on three premisses.
- First, the necessity to compare platform and basin.
- Second, to include a section outside of the Laurussian plate, which could be easily achieved by studying a section from the Armorica derived Hörre Nappe in the eastern Rhenish Mountains.
- Third, to study basinal sections with differentiated lithology, including carbonate rocks opposed to the almost ubiquitous, monotonous, diagenetically strongly compacted and information-poor black alum shale successions of the mid-Tournaisian. Such sections allow studies of the methodologies outlined above.

Taking all results into account the following conclusions were made:
- The Riescheid section represents the deepest accumulation realm of the studied sections. This relies on the fact that the alum shale package underlying the calciturbidites resembles the typical deep-water Kulm facies of the Herzkamp Syncline. Moreover, the hemipelagic calciturbidites contain no shallow-water components and originate from a deep intrabasinal swell, interpreted as a forebulge

(Hartenfels et al. 2016, Herbig 2016) based on an earlier assumption of Franke et al. (1975).

- The Gladenbach section reveals a peculiar situation, since it is situated within the allochthonous Hörre Nappe, derived from the Armorican Terrane Assemblage southeast of the Rhenish Mountains. The accumulated shales and calciturbidites are comparable to the other studied basinal sections from the Rhenish Mountains and prove the wide influence of the mid-Tournaisian transgression, at least on two (adjacent) lithospheric plates. The differentiated shales of the Gladenbach section are interpreted as hemipelagites with extremely fine-grained detrital influx, whereas the calciturbidites are composed of reworked deeper water platform material and hemipelagic material that is lacking any shallow-water influence in all samples except for the lower *typicus* Zone. According to conodont biofacies, lower slope areas are assumed for the main carbonate source of the turbidites.
- The Wettmarsen section bears an extraordinary rich conodont fauna in a single calciturbidite bed originating from a high rising intrabasinal swell on top of the former Devonian Balve reef complex. Source and deposition of the calciturbidite represents an intermediate position on the slope. It is the shallowest section studied in the Rhenish Kulm Basin. The gnathodid dominated conodont fauna that originates from middle to upper shelf slope areas as well as carbonate microfacies that has a faint platform connection, supports this assumption.
- The succession of the Dolhain section accumulated on deeper outer shelf areas. It represents the shallowest depositional realm of the studied sections. The mid-Tournaisian transgression becomes obvious by the accumulation of different shales and carbonates mostly deposited below storm wave base, almost devoid of phototrophic organisms.

The results clearly support a mid-Tournaisian transgression, as TST and HST of Sequence 2 are related to the Lower *crenulata* and *isosticha*-Upper *crenulata* zones. In the Rhenish Kulm Basin, the calciturbidites in Riescheid and Wettmarsen are related to highstand shedding during the *isosticha*-Upper *crenulata* Zone. In Gladenbach, thick calciturbidite packages occur already in the Lower *crenulata* Zone, but unequivocal separation between TST and HST were not possible. On the platform (Dolhain section) the base of the HST also lies within the Lower *crenulata* Zone. In summary, the presence of warm climatic conditions triggering an exaggerated transgressional phase during the middle Tournaisian is stressed. Indications of a regressive phase and lowered temperatures, due to a waxing ice-sheet are missing.

11. References

ADRICHEM BOOGAERT, H. A., VAN (1967): Devonian and Lower Carboniferous conodonts of the Cantabrian Mountains (Spain) and their stratigraphic application. Leidse Geologische Mededelingen, **39**: 129-192.

AHLBURG, J. (1918): Lieferung 208, Blatt Merenberg [Neue Nr. 5415], Gradabteilung 67, Blatt 30. - Erläuterungen zur Geologischen Karte von Preußen und benachbarten Bundesstaaten. - 128 pp., Berlin (Königlich Preußische Geologische Landesanstalt).

AMLER, M. R. W., & GEREKE, M. (eds.) (2003): Karbon-Korrelationstabelle (KKT), Carboniferous Correlation Table (CCT). – Senckenbergiana Lethaea, **83(1/2)**: 235-47.

AMLER, M. R. W. & HERBIG, H.-G. (2006): Ostrand der Kohlenkalk-Plattform und Übergang in das Kulm-Becken im westlichen Deutschland zwischen Aachen und Wuppertal. – In: Deutsche Stratigraphische Kommission (ed.): Stratigraphie von Deutschland VI. Unterkarbon (Mississippium). – Schriftenreihe der Deutschen Gesellschaft für Geowissenschaften, **41**: 441-477.

ARETZ, M, HERBIG, H. G., WANG, X. D., GRADSTEIN, F. M. AGTERBERG, F. P. & OGG, J. G. (2020): Chapter 23 - The Carboniferous Period. – In: GRADSTEIN, F. M., OGG, J. G., SCHMITZ, M. D., OGG, G. M. (eds.): Geologic Time Scale 2020, Volume 2, 811-874; Amsterdam, Oxford, Cambridge (Elsevier).

ARETZ, M., POTY, E. & HERBIG, H.-G. (with contributions of DELCULÉE, S. & HECKER, P.) (2006): From Palaeokarst to Calciturbidites – A carbonate platform-slope-transect from the Mississippian Limestone in eastern Belgium to the Kulm Basin in western Germany. – Fieldtrip, Carboniferous Conference Cologne. From Platform to Basin, September, 2006. – (to be published in Kölner Forum für Geologie und Paläontologie, **16**: 1-41).

BÁBEK, O., KALVODA, J, ARETZ, M, COSSEY, P. J., DEVUYST, X., HERBIG, H.-G. & SEVASTOPULO, G (2010): The correlation potential of magnetic susceptibility and outcrop gamma-ray logs at Tournaisian-Viséan boundary sections in Western Europe. – Geologica Belgica, **13(4)**:291-308.

BAI, D. & NING, Z. (1988): Faunal change and events across the Devonian-Carboniferous boundary at Huangmao section, Guangxi, south China. – Memoir - Canadian Society of Petroleum Geologists, **14(III)**: 147-157

BAHRAMI, A., CORRADINI, C. & YAZDI, M. (2011): Upper Devonian-Lower Carboniferous conodont biostratigraphy in the Shotori Range, Tabas area, Central-East Iran Microplate. – Bolletino della Società Paleontologica Italiana, **50(1)**: 35-53.

BARNES, C. R. & FAHRAEUS, L. E. (1975): Provinces, communities, and proposed nektobenthic habit of Ordovician conodontophorids. – Lethaia, **8**: 133-149.

BARSKOV, I. S., VORONTZOVA, T. N., KONONOVA, L. I. & KUZMIN, A. V. (1991): Opredelitely konodontov i niznego karbona. – izd-Vo MGU: 182pp., Moskow.

BECKER, R. T. (1993): Analysis of ammonoid palaeobiogeography in relation to the global Hangenberg (terminal Devonian) and Lower Alum Shale (Middle Tournaisian) events. – Annales de la Société géologique de Belgique, **115 (2)**: 459-473.

BECKER, R. T., KAISER, S. I. & ABOUSSALAM, Z. S. (2006): The Lower Alum Shale Event (Middle Tournaisiana) in Morocco – facies and faunal changes. – In: ARETZ, M. & HERBIG H.-G. (eds.): Carboniferous Conference Cologne. From Platform to Basin, Sept. 4-10 2006; program and abstracts. – Kölner Forum für Geologie und Paläontologie, **15**: 7-8.

BECKER, R. T., KAISER, S. I. & ARETZ, M. (2016): Review of chrono-, litho- and biostratigraphy across the global Hangenberg Crisis and Devonian-Carboniferous Boundary. – In: BECKER, R. T., KÖNIGSHOF, P. & BRETT, C.E. (eds.): Devonian Climate, Sea Level and Evolutionary Events. – Geological Society, London, Special Puplications, **423**: 355-386.

BECKER, R. T., KORN, D., PAPROTH, E. & STREEL, M. (1993): Beds near the Devonian-Carboniferous boundary in the Rhenish Massif, Germany. – Guidebook, International Union of Geological Sciences, Commission on Stratigraphy, Subcommission on Carboniferous Stratigraphy, 10 to 12 June, Lüttich. -86 pp.; Liege (Services associes de paleontologie de l'ULg).

BELKA, Z. (1985): Lower Carboniferous conodont biostratigraphy in the northeastern part of the Moravia-Silesia Basin. – Acta Geologica Polonica, **35(1-2)**: 33-59.

BELKA, Z. & GROESSENS, E. (1986): Conodont succession across the Tournaisian-Viséan boundary beds at Salet, Belgium. – Bulletin de la Société belge de Géologie, **95**: 257-280.

BENDER, P. (1978): Die Entwicklung der Hörre-Zone im Devon und Unterkarbon. – Zeitschrift der Deutschen Geologischen Gesellschaft, **129**: 131-140, 5 Figs., Hannover.

BENDER, P. (1989): Die Hörre und ihre Stellung im östlichen Rheinischen Schiefergebirge. – Jahresberichte und Mitteilungen des Oberrheinischen Geologischen Vereins, Neue Folge, **71**: 347-356.

BENDER, P. (2008): Lahn- und Dill-Mulde. In: Deutsche Stratigraphische Kommission (ed.), Stratigraphie von Deutschland VIII, Devon. Schriftenreihe der Deutschen Gesellschaft für Geowissenschaften, **52: 221-246**.

BENDER, P. & BRINCKMANN, J. (1969): Oberdevon und Unterkarbon südwestlich Marburg/Lahn (Lahn-Mulde und Hörre-Zone, Rheinisches Schiefergebirge). – Geologica et Palaeontologica, **3**:1-20.

BENDER, P. & HOMRIGHAUSEN, R. (1979): Die Hörre-Zone, eine Neudefinition auf lithostratigraphischer Grundlage. – Geologica et Palaeontologica, **13**: 257-260.

BENDER, P., KÖNIGSHOF, P. (1994): Regional maturation patterns of the Devonian strata in the eastern Rheinisches Schiefergebirge (Lahn–Dill area) based on conodont colour alteration (CAI). – Courier Forschungsinstitut Senckenberg **168**: 335-345.

BENDER, P. & STOPPEL, D. (2006): Der Ost- und Südostrand des Rheinischen Schiefergebirges: Lahn-Dill-Gebiet, Kellerwald, Taunus. - In: Deutsche Stratigraphische Kommission (ed.), Stratigraphie von Deutschland VI, Unterkarbon (Mississippium). – Schriftenreihe der Deutschen Gesellschaft für Geowissenschaften, **41**: 358-378.

BENDER, P., BRAUN, A. & KÖNIGSHOF, P. (1991): Radiolarien und Conodonten aus unterkarbonischen Kieselkalken und Kieselschiefern des nördlichen Rheinischen Schiefergebirges. – Geologica et Palaeontologica, **25**: 87-97.

BENDER, P., HERBIG, H.-G., GURSKY, H.-J. & AMLER, M. (1993): Beckensedimente im Oberdevon und Unterkarbon des östlichen Rheinischen Schiefergebirges - Fazies, Paläogeographie und Meeresspiegelschwankungen. – Geologica et Palaeontologica, **27**: 332-355.

BENDER, P., FRANKE, W., HINZE, L., HAHN, G., HAHN, R., HORN, M., KREBS, W., KULICK, J., MEISCHNER, D., PAPROTH, E., ROSENFELD, U. & STOPPEL, D. (1971): Devon-Karbon-Grenze, Kulm-Fazies des Dinantiums, Verzahnung Kulm-Kohlenkalk und flözleeres Namur im Harz, am Ost- und Nordrand des Rheinischen Schiefergebirges. – 7. Internationaler Kongress für Stratigraphie und Geologie des Karbons, Exkursion III. - 36+6 pp.

BERTOLA, C., BOULVAIN, F., DA SILVA, A.-C. & POTY, E. (2013): Sedimentology and magnetic susceptibility of Mississippian (Tournaisian) carbonate sections in Belgium. – Bulletin of Geosciences, **88 (1)**: 69-82.

BISCHOFF, G. (1957): Die Conodonten-Stratigraphie des rhenoherzynischen Unterkarbons mit Berücksichtigung der Wocklumeria-Stufe und der Devon/Karbon-Grenze. – Abhandlungen des Hessischen Landesamtes für Bodenforschung, **19**: 1-64.

BISCHOFF, G. & ZIEGLER, W. (1956): Das Alter der "Urfer Schichten" im Marburger Hinterland nach Conodonten. – Notizblatt des hessischen Landesamtes für Bodenforschung, **84**: 138-169.

BLESS, M.J.M., BOUCKAERT, J., BOUZET, P., CONIL, R., CORNET, P., FAIRON-DEMANET, M., GROESSENS, E., LONGERSTAEY, P.J., MEESSEN, J.P.M.TH., PAPROTH, E., PIRLET, H., STREEL, M., VAN AMEROM, H.W.J. & WOLF, M. (1976): Dinantian rocks in the subsurface north of the Brabant and Ardenno-Rhenish massifs in Belgium, the Netherlands and the Federal Republic of Germany. – Mededelingen Rijks Geologische Dienst, Nieuwe Serie, **27(3)**: 81-195.

BLUMENSTENGEL, H., BENDER, P. & HERBIG, H.-G. (1997): Ostrakoden aus der Gladenbach-Formation (Unterkarbon, Lahn-Dill-Mulde, Rheinisches Schiefergebirge). – Sonderveröffentlichungen, Geologisches Institut der Universität zu Köln, **114**: 91-121.

BOARDMAN II, D. R., THOMPSON, T. L., GODWIN, C., MAZZULLO, S. J., WILHITE, B. W. & MORRIS, B. T. (2013): High-Resolution Conodont Zonation for Kinderhookian (Middle Tournaisian) and Osagean (Upper Tournaisian-Lower Visean) Strata of the Western Edge of the Ozark Plateau, North America. – The Shale Shaker, **64(2)**: 98-151.

BOONEN, P. (1978): Une faune a conodontes du Tournaisien dans le Massif de la Vesdre. – Annales de la Société Géologique de Belgique, **101**: 127-130.

BOONEN, P. & KASIG, W. (1979): Das Dinantium zwischen Aachen und Lüttich. – Zeitschrift der Deutschen Geologischen Gesellschaft, **130**: 123-143.

BRANSON, E. B. (1934): Conodonts from the Hannibal Formation of Missouri. – University of Missouri Studies, **8**: 301-334.

BRANSON, E. B. & MEHL, M. G. (1933): Conodonts from the Bainbridge (Silurian) of Missouri. – The University of Missouri Studies, **8**: 39-52.

BRANSON, E. B. & MEHL, M. G. (1934a): Conodonts from the Grassy Creek Shale of Missouri. – The University of Missouri Studies, **8 (3)**: 171-259.

BRANSON, E. B. & MEHL, M. G. (1934b): Conodonts from the Bushberg Sandstone and equivalent formations of Missouri. – The University of Missouri Studies, **8 (4)**: 265-300.

BRANSON, E. B. & MEHL, M. G. (1938a): The conodont genus *Icriodus* and its stratigraphic distribution. – Journal of Paleontology, **12**: 156-166.

BRANSON, E. B. & MEHL, M. G. (1938b): Stratigraphy and paleontology of the lower Mississippian of Missouri; the Chouteau conodont fauna. - University of Missouri Studies, **13(4)**: 134-148.

BRANSON, E. B. & MEHL, M. G. (1941a): Conodonts from the Keokuk Formation. Journal of the Scientific Laboratories, Denison University, **35:** 179-188.

BRANSON, E. B. & MEHL, M. G. (1941b): New and little known Carboniferous conodont genera. – Journal of Paleontology, **15(2)**: 97-106.

BRANSON, E. B. & MEHL, M. G. (1944): Conodonts. – in: SHIMER, H. W. & SHROCK, R. R. (eds.): Index fossils of North America, 235-246; New York (Wiley).

BRAUCKMANN, C. (1982): Schichtfolge und Fossilführung im oberen Kulm (Unterkarbon cu III) von Riescheid in Wuppertal (Bergisches Land). – Jahresberichte der naturwissenschaftlichen Vereinigung Wuppertal, **35**: 79-88.

BRAUCKMANN, C. (1992): Trilobiten aus dem Ober-Devon und Unter-Karbon im Raum Aprath. – In: Thomas, E. (ed.): Oberdevon und Unterkarbon von Aprath im Bergischen Land (Nördliches Rheinisches Schiefergebirge). Ein Symposium zum Neubau der Bundesstraße 224, 113-167; Köln (Sven von Loga).

BRAUCKMANN, C. & MEYER, D. (1982): Exkursionen in das Niederbergische Land. Wuppertal, 8.-9. Oktober 1982. -45 pp.; Wuppertal (Subkommission für Karbonstratigraphie in der D.U.G.W).

BRINKMANN, R. (1948): Die Mitteldeutsche Schwelle. – Geologische Rundschau, **36(1)**: 56–66.

BUGGISCH, W. (2006): Is the "Liegender Alaunschiefer" really a high stand systems tract sediment? – The evolution of climate during Early Carboniferous (Mississippian). In: ARETZ, M. & HERBIG H.-G. (eds.): Carboniferous Conference Cologne. From Platform to Basin, Sept. 4-10 2006. – Kölner Forum für Geologie und Paläontologie, **15**: 15.

BUTLER, M. (1973): Lower Carboniferous conodont faunas from the eastern Mendips, England. – Palaeontology, **16(3)**: 477-517.

CHAUFF, K.M. (1981): Multielement conodont species from the Osagean (Lower Carboniferous) in Midcontinent North America and Texas. – Palaeontographica, Abteilung A: Palaeozoologie- Stratigraphie, **174/4-6**: 140-169.

CLAUSEN, C.-D., LEUTERITZ, K. & ZIEGLER, W. (1989): Ausgewählte Profile an der Devon/Karbon-Grenze im Sauerland (Rheinisches Schiefergebirge). – Fortschritte in der Geologie von Rheinland und Westfalen, **35**: 161-226.

CONIL, R., DIKENSTEIN, J. & DRICOT, E. (1961): Le biostrome strunien du massif de la Vesdre. – Bulletin de la Société Belge de Géologie, **70**: 28-34.

CONIL, R., DREESEN, R., LENTZ, M.-A., LYS, M. & PLODOWSKI, G. (1986): The Devono-Carboniferous transition in the Franco-Belgian Basin with reference to foraminifera and brachiopods. – Annales de la Société Géologique de Belgique, **109(1)**: 19-26.

CONIL, R., GROESSENS, E., LALOUX, M., POTY, E. & TOURNEUR, F. (1990): Carboniferous guide foraminifera, corals and conodonts in the Franco-Belgian and Campine Basins: their potential for widespread correlation. – Courier Forschungsinstitut Senckenberg, **130**: 15-30.

COOPER, C. L. (1939): Conodonts from a Bushberg-Hannibal horizon in Oklahoma. – Journal of Paleontology, **13**: 379-422.

DAVYDOV, V. L., KORN, D. & SCHMITZ, M. D. (2012): The Carboniferous Period (with contributions by GRADSTEIN, F.M & HAMMER, O.). – In: GRADSTEIN, F. M., OGG, J. G., SCHMITZ, M. D. & OGG, G. M. (eds.): The Geologic Time Scale 2012, 603-651; Oxford, UK (Elsevier).

DEJONGHE, L. (1998): Zinc-lead deposits of Belgium. – Ore Geology Reviews, **12**: 329-354.

DENAYER, J., PRESTIANNI, C., SAUTOIS, M., POTY, E. & MOTTEQUIN, B. (2015): The Devonian-Carboniferous Boundary and the Lower Carboniferous succession in the type area. – Strata, Communicatioins, **17**: 59-81.

DEWALQUE, G. (1898): Les schistes à *Spiriferina octoplicata*, T1b, à Dolhain. – Annales de la Société géologique de Belgique, XXV: L-LII.

DREESEN, R., SANDBERG, C. A. & ZIEGLER, W. (1986): Review of late Devonian and early Carboniferous conodont biostratigraphy and biofacies models as applied to the Ardenne shelf. – Annales de la Société géologique de Belgique, **109**: 27-42.

DROZDZEWSKI, G., KLOSTERMANN, J., RIBBERT, K.-H., WREDE, V. & ZELLER, M. (1998): Sedimentation und Tektonik im Paläozoikum und Postpaläozoikum der Niederrheinischen Bucht. – Fortschritte in der Geologie von Rheinland und Westfalen, **37**: 573-583.

DRUCE, E. C. (1969): Devonian and Carboniferous conodonts from the Bonaparte Gulf Basin, northern Australia and their use in international correlation. – Bulletin - Australia, Bureau of Mineral Resources, Geology and Geophysics, **98**: 1-242.

DRUCE. E. C. (1973): Upper Paleozoic and Triassic conodont distribution and the recognition of biofacies. – In: RHODES, F. H. T. (ed.): Conodont paleozoology. – Geological Society of America, Special Paper, **141**: 191-237.

DZIK, J. (1997): Emergence and succession of Carboniferous conodont and ammonoid communities in the Polish part of the Variscan sea. – Acta Palaeontologica Polonica, **42(1)**: 57-170.

DZIK, J. (2006): The Famennian „Golden Age" of conodonts and ammonoids in the Polish part of the Variscan sea. – Palaeontologia Polonica, **63**: 1-360.

ECKELMANN, K., NESBOR, H.-D., KÖNIGSHOF, P., LINNEMANN, U., HOFMANN, M., LANGE, J.-M. & SAGAWE, A. (2014): Plate interactions of Laurussia and Gondwana during the formation of Pangaea - Constraints from U-Pb LA-SF-ICP-MS detrital zircon ages of Devonian and Early Carboniferous siliciclastics of the Rhenohercynian zone, Central European Variscides. – Gondwana Research **25**: 1484-1500.

ENGEL, W., FRANKE, W., GROTE, C., WEBER, K., AHRENDT, H. & EDER, F. W. (1983): Nappe tectonics in the southeastern part of the Rheinisches Schiefergebirge. – In: MARTIN, H. & EDER, F. W. (eds.): Intracontinental Fold Belts, 267-287; Berlin (Springer).

ENTENMANN, W. (1990): Untersuchungen zur Geologie und Ingenieurgeologie an der Aartalsperre bei Bischoffen, Lahn-Dill-Kreis (Hessen). Teil 1: Allgemeine Geologie, Tektonik. – Geologisches Jahrbuch Hessen, **118**: 235-263.

ENTENMANN, W. (1991): Feinstratigraphie und Sedimentologie der Elnhausen-Schichten (Unterkarbon) der Hörre-Zone. – Geologica et Palaeontologica, **25**: 79-85.

ESTEBAN LOPEZ, S., BENDER, P. & HERBIG, H. -G. (2019): Middle Tournaisian (lower Mississippian) conodonts and calcareous microbiota from the Hörre Nappe, eastern Rhenish Mountains, Germany. – In: HARTENFELS, S., HERBIG, H.-G., AMLER, M.R.W. & ARETZ, M. (eds.): 19th International Congress on the Carboniferous and Permian, Cologne, July 29 – August 2, 2019. Abstracts. – Kölner Forum für Geologie und Paläontologie, **23**: 95-96.

FRANKE, W. (1995): Rhenohercynian foldbelt: autochthon and nonmetamorphic nappe units – stratigraphy. In: DALLMEYER, D., FRANKE, W., WEBER, K. (eds.): Pre-Permian Geology of Central and Eastern Europe, 33-39; Berlin (Springer).

FRANKE, W. (2000): The mid-European segment of the Variscides: tectonostratigraphic units, terrane boundaries and plate tectonic evolution. In: FRANKE, W., HAAK, V., ONCKEN, O., TANNER, D. (eds.): Orogenic Processes: Quantification and Modelling in the Variscan Belt. – Geological Society London, Special Publication, **179**: 35-61.

FRANKE, W. & ONCKEN, O. (1990): Geodynamic evolution of the northcentral Variscides – a comic strip. In: FREEMAN, R., GIESE, P., MUELLER, S. (eds.): The European Geotraverse; integrative studies, results from the fifth Earth Science Study Center, 187-194; Strasbourg, France (European Science Foundation).

FRANKE, W. & ONCKEN, O. (1995): Zur prädevonischen Geschichte des Rhenohercynischen Beckens. – Nova Acta Leopoldina, Neue Folge, **71**: 53-72.

FRANKE, W., EDER, W. & ENGEL, W. (1975): Sedimentology of a Lower Carboniferous shelfmargin (Velbert Anticline, Rheinisches Schiefergebirge, W-Germany). – Neues Jahrbuch für Geologie und Paläontologie, Abhandlungen, **150 (3)**: 314-353.

FRANKE, W., COCKS, L. R. M. & TORSVIK, T. H. (2017): The Palaeozoic Variscan Oceans Revisited. – Gondwana Research, **48**: 257-84.

FRANKE, W., BORTFELD, R.K., BRIX, M., DROZDZEWSKI, G., DÜRBAUM, H.J., GIESE, P., JANOTH, W., JÖDICKE, H., REICHERT, CH., SCHERP, A., SCHMOLL, J., THOMAS, R., THÜNKER, M., WEBER, K., WIESNER, M.G., WONG, H.K. (1990): Crustal structure of the Rhenish Massif: results of deep seismic reflection lines DEKORP 2-North and 2-North-Q. – Geologische Rundschau, **79**: 523–566.

FUCHS, A. & PAECKELMANN, W. (1928): Lieferung 263, Blatt Barmen Nr. 2721. - Erläuterungen zur geologischen Karte von Preußen und benachbarten deutschen Ländern. -99 pp.; Berlin (Preußische Geologische Landesanstalt).

GARCÍA-LÓPEZ, S. & SANZ-LÓPEZ, J. (2002): Devonian to Lower Carboniferous conodont biostratigraphy of the Bernesga Valley section (Cantabrian Zone, NW Spain). – In: GARCÍA-LÓPEZ S. & BASTIDA F. (eds.): Palaeozoic conodonts from northern Spain. – Eighth International Conodont Symposium held in Europe. Publicaciones del Instituto Geológico y Minero de España; Serie: Cuadernos del Museo Geominero, **1**: 163-205.

GEDIK, I. (1974): Conodonten aus dem Unterkarbon der Karnischen Alpen. – Abhandlungen der Geologischen Bundesanstalt, **31**: 1-29.

GEREKE, M. (2002): Conodonten-Zonen. In: AMLER, M.R.W. & GEREKE, M. (eds.): Karbon-Korrelationstabelle. Ausgabe 2002. – Senckenbergiana lethaea, **82(2)**: 695, 707–708.

GILES, P.S. (2009): Orbital forcing and Mississippian sea level change: time series analysis of marine flooding events in the Viséan Windsor Group of eastern Canada and implications for Gondwana glaciation. – Bulletin of Canadian Petroleum Geology, **57(4)**: 449-471.

GLENISTER, B. F, & KLAPPER, G. (1966): Upper Devonian conodonts from the Canning Basin, Western Australia. – Journal of Paleontology, **40(4)**: 777-842.

GROESSENS, E. (1971): Les conodontes du Tournaisien supérieur de la Belgique. Note préliminaire. – Geological Survey of Belgium Professional Paper, **4**: 1-45.

GROESSENS, E. (1974): Distribution de Conodontes dans le Dinantien de la Belgique. – In: BOUCKAERT, J. & STREEL, M. (eds.): International Symposium on Belgian Micropaleontological Limits from Emsian to Visean, Namur 1974. – Service géologique de Belgique. Publications, **17**: 1-193.

GUNNEL, F. H. (1931): Conodonts from the Fort Scott Limestone of Missouri. - Journal of Paleontology, **5(3)**: 244-252.

GURSKY, H.-J. (1997): Die Kieselgesteine des Unter-Karbons im Rhenoherzynikum. Sedimentologie, Petrographie, Geochemie und Paläozeanographie. – Geologische Abhandlungen Hessen **100**: 1-117.

GURSKY, H.-J. (2006): Paläogeographie, Paläoozeanographie und Fazies. - In: DEUTSCHE STRATIGRAPHISCHE KOMMISSION (ed.): Stratigraphie von Deutschland VI. Unterkarbon (Mississippium). – Schriftenreihe der Deutschen Geologischen Gesellschaft, **41**: 51-68.

Hance, L. & Poty, E. (2002): Sequence stratigraphy of the Belgian Lower Carboniferous - Tentative correlation with the British Isles. – In: Hills, L. V., Henderson, C. M. & Bamber, E. W. (eds.): Carboniferous and Permian of the World: XIV ICCP Proceedings. Memoir - Canadian Society of Petroleum Geologists, **19**: 41-51.

Hance, L. & Poty, E. (2006): Hastarian. In: Dejonghe, L. (ed.): Current status of chronostratigraphic units named from Belgium and adjacent areas. – Geologica Belgica, **9(1-2)**: 111-116.

Hance, L., Poty, E. & Devuyst, F.-X. (2001): Stratigraphie séquentielle du Dinantien type (Belgique) et corrélation avec le Nord de la France (Boulonnais, Avesnois). – Bulletin de la Société Géologique de France, **172(4)**: 411-426.

Hance, L., Poty, E. & Devuyst, F.-X. (2006): Tournaisian. In: Dejonghe, L. (ed.): Current status of chronostratigraphic units named from Belgium and adjacent areas. – Geologica Belgica, **9(1-2)**: 47-53.

Hance, L., Dejonghe, L., Ghysel, P., Laloux, M & Mansy, J. L. (1999): Influence of heterogeneous lithostructural layering on orogenic deformation in the Variscan Front Zone (eastern Belgium). – Tectonophysics, **309**: 191-177.

Hartenfels, S. (2011): Die globalen *Annulata*-Events und die Dasberg-Krise (Famennium, Oberdevon) in Europa und Nord-Afrika – hochauflösende Conodonten-Stratigraphie, Karbonat-Mikrofazies, Paläoökologie und Paläodiversität. – Münstersche Forschungen zur Geologie und Paläontologie, **105**: 17-527.

Hartenfels, S. (2020): Upper Devonian to Lower Carboniferous global environmental change and impact on conodonts. – Habilitation, Universität zu Köln; 91 pp., Köln (unpublished).

Hartenfels, S. & Becker, R. T. (2009): Timing of the global Dasberg Crisis - Implications for Famennian eustasy and chronostratigraphy. – In: Over, D. J. (ed.): Studies in Devonian Stratigraphy: Proceedings of the 2007 International Meeting of the Subcommission on Devonian Stratigraphy and IGCP 499. – Palaeontographica Americana, **63**: 71-97.

Hartenfels, S., & Becker, R. T. (2018): Age and correlation of the transgressive *Gonioclymenia* Limestone (Famennian, Tafilalt, eastern Anti-Atlas, Morocco). – Geological Magazine, **155(3)**: 586-629.

Hartenfels, S., Hartkopf-Fröder, C., Herbig, H.-G., Becker, R. T. & Esteban Lopez, S. (2016): Middle Famennian to Viséan stratigraphy at Riescheid (Herzkamp Syncline, Rhenish Massif). – Münstersche Forschungen zur Geologie und Paläontologie, **108**: 74-94.

Hass, W. H. (1953): Conodonts of the Barnett Formation. – Geological Survey Professional Paper, **243-F**: 69-94.

Hass, W. H. (1959): Conodonts from the Chappel Limestone of Texas. – Professional Paper, U.S. Geological Survey, **294-J**: 365-399.

Haude, R. & Thomas, E. (1989): Ein Oberdevon-/Unterkarbon-Profil im Velberter Sattel (nördliches Rheinisches Schiefergebirge) mit neuen Arten von (?) *Sostronocrinus* (Echinodermata). – Bulletin de la Sociète Belge de Géologie, **98(3-4)**: 373-383.

Helms, J. (1963): Zur "Phylogenese" und Taxonomie von *Palmatolepis* (Conodontida, Oberdevon). – Geologie, **12(4)**: 449-485.

Herbert, T. D. & Sarmiento, J. L. (1991): Ocean nutrient distribution and oxygenation: Limits on the formation of warm saline bottom water over the past 91 m. y. – Geology, **19(7)**: 702-705.

HERBIG, H.-G. (2011): Stratigraphische Sequenzen und Bioevents im Kulmbecken des Rheinischen Schiefergebirges (Mississippium, Deutschland). – Schriftenreihe der Deutschen Gesellschaft für Geowisschenschaften, **77**: 37-39.

HERBIG, H.-G. (2016): Mississippian (Early Carboniferous) sequence stratigraphy of the Rhenish Kulm Basin, Germany. – Geologica Belgica, **19(1)**: 81-110.

HERBIG, H.-G. & BENDER, P. (1992): A eustatically driven calciturbidite sequence from the Dinantian II of the Eastern Rheinisches Schiefergebirge. – Facies, **27**: 245-262.

HERBIG, H.-G. & STOPPEL, D. (2006): Conodonten. – In: DEUTSCHE STRATIGRAPHISCHE KOMMISSION (ed.), Stratigraphie von Deutschland VI. Unterkarbon (Mississippium). – Schriftenreihe der Deutschen Gesellschaft für Geowissenschaften, **41**: 202–226.

HERBIG, H.-G. & TRAGELEHN, H. (1997): Vom Eopteropoden zum Brachiopodenstachel? Eine Neubewertung des Mikroproblematikums *Magnella* nach Funden aus dem Oberfamenne des Rheinischen Schiefergebirges. – Geologische Blätter von Nordost-Bayern, **47 (1-4)**: 447-460.

HERBIG, H.-G., LOBOVA, D. & SEEKAMP, V. (2014): Sea-level history during the birth of a foreland basin: the Famennian-Visean of "Velbert 4'', westernmost Rhenish Massif, Germany. – In: ROCHA, R., PAIS, J., KULLBERG, J.C. & FINNEY, S. (eds.), STRATI 2013, First International Congress on Stratigraphy. At the cutting edge of stratigraphy, 397-402; Heidelberg, New York (Springer).

HERBIG, H.-G., TRAGELEHN, H. & AMLER, M. R. W. (2001): Höchstes Oberdevon und Mississippian im Niederbergischen Land zwischen Ratingen und Wuppertal (Velberter Sattel, Herzkamper Mulde) - Der Übergang vom Kohlenkalkschelf in das Kulmbecken. – Guidebook, Subkommission für Karbonstratigraphie in der Deutschen Stratigraphischen Kommission. - 11 pp; Köln (Geologisches Institut der Universität zu Köln).

HIGGINS, A. C. (1971): Conodont biostratigraphy of the Late Devonian-Early Carboniferous rocks of the South Central Cantabrian Cordillera. – Trabajos de Geologia - Universidad de Oviedo, **3**: 179-192.

HIGGINS, A. C. (1974): Conodont zonation of the lower Carboniferous of Spain and Portugal. Belgian Geological Survey International Symposium on Belgian Micropaleontological Limits, Namur, **4**: 1-17.

HIGGINS, A. C. (1985): The Carboniferous system. Part 2. Conodonts of the Silesian subsystem from Great Britain and Ireland. In: HIGGINS, A. C., AUSTIN, R. L. (eds.): A stratigraphical index of conodonts, 210–227; West Sussex (Ellis Horwood Ltd.).

HIGGINS, A. C. & WAGNER-GENTIS, C. H. T. (1982): Conodonts, goniatites and the biostratigraphy of the earlier Carboniferous from the Cantabrian Mountains, Spain. – Palaeontology, **25(2)**: 313- 350.

HIGGS, K. & STREEL, M. (1984): Spore stratigraphy at the Devonian-Carboniferous boundary in the northern "Rheinisches Schiefergebirge", Germany. – Courier Forschungsinstitut Senckenberg, **67**: 157-179.

HIGGS, K. & STREEL, M. (1994): Palynological age for the lower part of the Hangenberg Shales in Sauerland, Germany. – Annales de la Société Géologique de Belgique, **116(2)**: 243-247.

HINDE, G. J. (1879): On conodonts from the Chazy and Cincinnati Group of the Cambro-Silurian, and from the Hamilton and Genesee shale division of the Devonian, in Canada and the United States. – Quarterly Journal of the Geological Society of London, **35**: 351-369.

HOMRIGHAUSEN, R. (1979): Petrographische Untersuchungen an sandigen Gesteinen der Hörre-Zone (Rheinisches Schiefergebirge, Oberdevon – Unterkarbon). – Geologische Abhandlungen Hessen, **79**: 1-84.

HUDDLE, J. W. (1934): Conodonts from the New Albany Shale of Indiana. – Bulletins of American Paleontoloty, **21(72)**: 186-325 (1-136).

HUDDLE, J. W. (1968): Redescription of Upper Devonian conodont genera and species proposed by Ulrich & Bassler in 1926. – U. S. Geological Survey, Professional Paper, **578**: 1-55.

JI, Q. (1985): Study on the phylogeny, taxonomy, zonation and biofacies of *Siphonodella* (Conodonta). – Bulletin of the Institute of Geology, Chinese Academy of Geological Sciences, **11**: 52-75 (in Chinese with English abstract).

JI, Q. & ZIEGLER, W. (1992): The Lali Section: an excellent Reference Section for Upper Devonian in South China. – Courier Forschungsinstitut Senckenberg, **157**: 1-183.

JI, Q., QIN, G. R. & ZHAO, R. X. (1990): Biostratigraphy of the conodonts from the Dasaiba section in Lechang County, Northern Guangdong. – Bulletin of the Institute of Geology, Chinese Academy of Geological Sciences, **22**: 111-128 (in Chinese with English abstract).

JONES, G. LL. & SOMERVILLE, I. D. (1996): Irish Dinantian biostratigraphy: practical applications. – In: STROGEN, P., SOMERVILLE, I. D. & JONES, G. LL. (eds.): Recent Advances in Lower Carboniferous Geology. – Geological Society Special Publication, **107**: 371-385.

KAISER, S. I. (2005): Mass extinctions, climatic and oceanographic changes at the Devonian/Carboniferous boundary. – Inaugural Dissertation, Ruhr-Universität Bochum. 156 pp.; Bochum (unpublished).

KAISER, S. I. (2009): The Devonian/Carboniferous boundary stratotype section (La Serre, France) revisited. – Newsletter on Stratigraphy, **43(2)**: 195-205.

KAISER, S. I. & CORRADINI, C. (2011): The early siphonodellids (Conodonta, Late Devonian-Early Carboniferous): overview and taxonomic state. – Neues Jahrbuch für Geologie und Paläontologie, Abhandlungen, **261(1)**: 19-35.

KAISER, S. I., KUMPAN, T. & CIGLER, V. (2017): New unornamented siphonodellids (Conodonta) of the lower Tournaisian from the Rhenish Massif and Moravian Karst (Germany and Czech Republic). – Neues Jahrbuch für Geologie und Paläontologie, Abhandlungen, **286(1)**: 1-33.

KAISER, S. I., BECKER, R. T., SPALLETTA, C. & STEUBER, T. (2009): High-resolution conodont stratigraphy, biofacies, and extinctions around the Hangenberg Event in pelagic successions from Austria, Italy, and France. – In: OVER, D. J. (ed.): Studies in Devonian Stratigraphy: Proceedings of the 2007 International Meeting of the Subcommission on Devonian Stratigraphy and IGCP 499. – Palaeontographica Americana, **63**: 99-143.

KALVODA, J. (1991): The Middle-Upper Tournaisian Boundary Event. – Historical Biology, **5**: 229-37.

KALVODA, J. (1994): The conodont extinction at the Middle-Upper Tournaisian boundary. – Geolines (Praha), **1**: 12-15.

KALVODA, J. (2002): Late Devonian-Early Carboniferous foraminiferal fauna: zonations, evolutionary events, paleobiogeography and tectonic implications. – Folia, **39**: 1-213

KALVODA, J., BABEK, O. & MALOVANO, A. (1999): Sedimentary and Biofacies Records in Calciturbidites at the Devonian-Carboniferous Boundary in Moravia (Moravian-Silesian Zone, Middle Europe). – Facies, **41**: 141-158.

KALVODA, J., KUMPAN, T. & BABEK, O. (2015): Upper Famennian and Lower Tournaisian sections of the Moravian Karst (Moravo-Silesian Zone, Czech Republic): a proposed key area for correlation of the conodont and foraminiferal zonations. – Geological Journal, **50(1)**: 17-38.

KAYSER, E. (1893): Mittheilung über seine Aufnahmen im Dillenburgischen. – Jahrbuch der Königlich Preussischen Geologischen Landesanstalt der Bergakademie zu Berlin, **13**: XXXIX-XLI.

KAYSER, E. (1899): Berichte über die Exkursionen. – Berichte über die Versammlungen des Oberrheinischen Geologischen Vereins, **32**: 7-11.

KEGEL, W. (1934): Geologie der Dillmulde. – Abhandlungen der Preussischen Geologischen Landesanstalt, Neue Folge, **160**: 1-48.

KLAPPER, W. (1966): Upper Devonian and Lower Mississippian conodont zones in Montana, Wyoming, and South Dakota. – The University of Kansas, Paleontological Contributions, Papers, **3**: 1-43.

KLAPPER, W. (1971): *Patrognathus* and *Siphonodella* (Conodonta) from the Kinderhookian (Lower Mississippian) of western Kansas and southwestern Nebraska. – Kansas Geological Survey Bulletin, **202**: 1-14.

KLAPPER, G. & BARRICK, J. E. (1978): Conodont ecology: pelagic versus benthic. – Lethaia, **11**: 12-23.

KOCKEL, C. W. (1958): Schiefergebirge und Hessische Senke um Marburg/Lahn. – Sammlung Geologischer Führer, **37**: -248 pp.; Berlin (Borntraeger).

KOMBRINK, H., BESLY, B. COLLINSON, J., DEN HARTOG JAGER, D., DROZDZEWSKI, G., DUSAR, M., HOTH, P., PAGNIER, H., STEMMERIK, L., WAKSMUNDZKA, M. & WREDE, V. (2010): Carboniferous. – In: DOORNENBAL, H. & STEVENSON, A. (eds.): Petroleum Geological Atlas oft he Southern Permian Basin Area, 81-99; Houten (EAGE Publications b. v.).

KORN, D. (2003): Die Formationen der Kulm-Fazies im Rheinischen Schiefergebirge. – In: AMLER, M. R. W. & GEREKE, M. (eds.): Karbon- Korrelationstabelle (KKT). – Senckenbergiana lethaea, **83(1/2)**: 236-242.

KORN, D. (2006): Lithostratigraphische Neugliederung der Kulm-Sedimentgesteine im Rheinischen Schiefergebirge. – In: DEUTSCHE STRATIGRAPHISCHE KOMMISSION (ed.): Stratigraphie von Deutschland VI. Unterkarbon (Mississippium). – Schriftenreihe der Deutschen Gesellschaft für Geowissenschaften, **41**: 379-383.

KORN, D. (2010): Lithostratigraphy and biostratigraphy of the Kulm succession in the Rhenish Mountains. – Zeitschrift der Deutschen Gesellschaft für Geowissenschaften, **161(4)**: 431-453.

KORN, D. & WEYER, D. (2003): High resolution stratigraphy of the Devonian-Carboniferous transitional beds in the Rhenish Mountains. - Mitteilungen aus dem Museum für Naturkunde in Berlin, Geowissenschaftliche Reihe, **6**: 79-124.

KORN, D., CLAUSEN, C.D., BELKA, Z., LEUTERITZ, K., LUPPOLD, F.W., FEIST, R. & WEYER, D. (1994): Die Devon/Karbon-Grenze bei Drewer (Rheinisches Schiefergebirge). – In: KORN, D., CLAUSEN, C.D. & LUPPOLD, F.W. (eds): Die Devon/Karbon-Grenze im Rheinischen Schiefergebirge. – Geologie und Paläontologie in Westfalen, **29**: 97-147.

KOSSMAT, F. (1927): Gliederung des varistischen Gebirgsbaus. – Abhandlungen des Sächsischen Geologischen Landesamts, **1**: 1-39.

KREBS, W. (1968): Zur Frage der bretonischen Faltung im östlichen Rhenoherzynikum. – Geotektonische Forschungen, **28**: 1-71.

KÜRSCHNER, W., BECKER, R. T., BUHL, D. & VEIZER, J. (1993): Strontium isotopes in conodonts: Devonian-Carboniferous transition; the northern Rhenish Slate Mountains, Germany. – Annales de la Société géologique de Belgique, **115(2)**: 595-621.

LALOUX, M., DEJONGHE, L., GHYSEL, P. & HANCE, L. (1996a): Fléron-Verviers. – Carte Géologique de Wallonie, echelle 1: 25.000, Notice explicative, 42/7-8. -150 pp.; Namur (Ministere de la Region Wallonne).

LALOUX, M., DEJONGHE, L., GEUKENS, F., GHYSEL, P. & HANCE, L. (1996b): Limbourg-Eupen, Carte Géologique de Wallonie, échelle 1: 25 000, Notice explicative, 43/5-6. -192pp.; Namur (Ministere de la Region Wallonne).

LALOUX, M., GEUKENS, F., GHYSEL, P. & HANCE, L. (2000): Gemmenich-Botzelaar 35/5-6 - Henri Chapelle-Raeren 43/1-2 - Petergensfeld-Lammersdorf 43/3-4. – Carte Géologique de Wallonie, échelle 1: 25.000, Notice explicative. -93 pp.; Namur (Ministere de la Region Wallonne).

LANE, H. R. & ZIEGLER, W. (1978): Conodont biostratigraphy of the Riescheid exposure. – IUGS Working Group on the Devonian-Carboniferous Boundary, Field Trip, 27th Aug. - 8th Sept. 1978. - 4pp. (unpublished).

LANE, H.R. & ZIEGLER, W. (1983): Taxonomy and phylogeny of *Scaliognathus* Branson and Mehl, 1941 (Conodonta, Lower Carboniferous). – Senckenbergiana Lethaea, **64(2-4)**: 199-225.

LANE, H. R., SANDBERG, C. A. & ZIEGLER, W. (1980): Taxonomy and phylogeny of some Lower Carboniferous conodonts and preliminary standard post-Siphonella zonation. – Geologica et Palaeontologica, **14**: 117-164.

LAZAR, O. R., BOHACS, K. M., SCHIEBER, J., MACQUAKER, J. H. S. & DEMKO, T. M. (2012): Mudstone Primer: Lithofacies variations, diagnostic criteria, and sedimentologic-stratigraphic implications at lamina to bedset scales. – SEPM Concepts in Sedimentology and Paleontology, **12**: -198pp.; Tulsa, Oklahoma (SEPM Society for Sedimentary Geology).

LLOYD, C. R. (1982): The Mid-Cretaceous Earth: Paleogeography; Ocean Circulation and Temperature; Atmospheric Circulation. – The Journal of Geology, **90(4)**: 393-413.

MALEC, J. (2014): The Devonian/Carboniferous boundary in the Holy Cross Mountains (Poland). – Geological Quarterly, **58(2)**: 217-234.

MATTHEWS, S. C., SADLER, P. M. & SELWOOD, E. B. (1972): A Lower Carboniferous conodont fauna from Chillaton, Southwest Devonshire. – Palaeontology, **15(4)**: 550-568.

MAWSON, R. & TALENT, J. A. (1999): Early Carboniferous (mid-Tournaisian) conodonts from northeastern Queensland (Ruxton and Teddy Mountain formations): Age-implications and stratigraphic alignments. – Bollettino della Società Paleontologica Italiana, **37**: 407-425.

MEHL, M. G. & THOMAS, L. A. (1947): Conodonts from the Fern Glen of Missouri. – Denison University Bulletin **47**: 3-20.

MII, H.-S., GROSSMAN, E. L. & YANCEY, T. E. (1999): Carboniferous isotope stratigraphies of North America: Implications for Carboniferous paleoceanography and Mississippian glaciation. – Geological Society of America, Bulletin, **111(7)**: 960-973.

MORY, A. J. & CRANE, D. T. (1982): Early Carboniferous *Siphonodella* (Conodonta) faunas from eastern Australia. – Alcheringa, **6(4)**: 275-303.

MÜLLER, K. J. (1956): Zur Kenntnis der Conodonten-Fauna des europäischen Devons, 1: Die Gattung *Palmatolepis*. – Abhandlungen der Senckenbergischen Naturforschenden Gesellschaft, **494**: 1-70.

MÜLLER, K. J. (1962): Zur systematischen Einteilung der Conodontophorida. – Paläontologische Zeitschrift, **36(1-2)**: 109-117.

NEMYROVSKA, T. I. (1999): Bashkirian conodonts of the Donets Basin, Ukraine. – Scripta Geologica, **119**: 1–115.

NEUMANN, M., POZARYSKA, K. & VACHARD, D. (1975): Remarques sur les microfaciès du Dévonien du Lublin (Pologne). – Revue de Micropaléontologie, **18**: 38-52.

NI, SHI-ZHAO (1984): Late Palaeozoic Conodonts. – In: FENG, S., XU, S., LI, J., YANG, D., XU, G., SUN, Q., NI, S., GAO, L. & GOUFANG, Z. (eds.): Biostratigraphy of the Yangtze Gorge Area, Vol. 3, Late Palaeozoic Aera, 283-284; Beijing (Geological Publishing House) (in Chinese).

PAECKELMANN, W. (1922): Oberdevon und Untercarbon der Gegend von Barmen. – Jahrbuch der Preußischen Geologischen Landesanstalt, **41(2)** [for 1921]: 52-147.

PANDER, C. H. (1856): Monographie der fossilen Fische des Silurischen Systems der Russisch-Baltischen Gouvernements. -91pp.; St. Petersburg, Russia (Buchdruckerei der Kaiserlichen Akademie der Wissenschaften).

PAPROTH, E. & STREEL, M. (1982): Devonian-Carboniferous transitional beds of the northern "Rheinisches Schiefergebirge". – Guidebook, International Union of Geological Sciences, Commission on Stratigraphy, Working Group on the Devonian/ Carboniferous Boundary, Liège: -63 pp; Lüttich.

PAPROTH, E., DREESEN, R. & THOREZ, J. (1986): Famennian palaeogeography and event stratigraphy of northwestern Europe. – Annales de la Société Géologique de Belgique, **109**: 175-186.

PARK, S.-I. (1983): Zonenfolge, Phylogenie und Taxonomie karbonischer Conodonten zwischen Tournai und Westfal (Westeuropa). – Inaugural Dissertation, Phillips Universität Marburg, 181 pp; Marburg (Görich & Weiershäuser).

PAUL, H. (1937a): Vergleich des nordwestdeutschen Unterkarbon mit dem belgischen. – 2. Congres International de Stratigraphie et de Geologie du Carbonifère, Heerlen 1935, Compte Rendue, **2**: 74-764.

PAUL, H. (1937b): Die Transgression der Viséstufe in Nordwesteuropa.– Decheniana, **95A**: 241-247.

PAUL, H. (1937c): Neue Untersuchungen über den Kohlenkalk der Umgebung von Aachen. – Decheniana, **95 A**: 248-251.

PERRI, M. C. & SPALLETTA, C. (1998): Conodont distribution at the Tournaisian/Visean boundary in the Carnic Alps (Southern Alps, Italy). – In: SZANIAWSKI, H. (ed.): Proceedings of the Sixth European Conodont Symposium (ECOS VI). – Palaeontologia Polonica, **58**: 225-245.

PERRET, M.-F. (1977): Donées récentes de la micropaléontologie dans l'étude du Carbonifère marin des Pyrénées. – Annales Société Géologique du Nord, **97**: 77-85.

PERRET, M.-F. (1989): Recherches micropaleonotolgiques et biostratigraphiques (conodontes-foraminifères) dans le Carbonifère pyrénéen. – Inaugural Dissertation, l'Universite Paul Sabatier de Toulouse. -597pp.; Toulouse (unpublished).

PERRET, M.-F. (1993): Recherches micropaleonotolgiques et biostratigraphiques (conodontes-foraminifères) dans le Carbonifère pyrénéen. – Strata, Serie 2, **21**: 1-597.

Pierce, R. W. & Langenheim, R. L. (1974): Platform conodonts of the Monte Cristo Group, Mississippian, Arrow Canyon Range, Clark County, Nevada – Journal of Paleontology, **48(1)**: 149-169.

Plotitsyn, A. N. & Zhuravlev, A. V. (2016): Morphology of the early ontogenetic stages of advanced Siphonodellids (Conodonta, Early Carboniferous). - Vestnik of Institute of Geology of Komi Science Center of Ural Branch RAS, **8**: 21-26.

Poty, E. (1982): Paléokarsts et brèches d'effondrement dans le Frasnien moyen des environs de Visé. Leur influence dans la paléogéographie dinantien. – Annales de la Société gélogique de Belgique, **105(2)**: 315-337.

Poty, E. (1985): A rugose coral biozonation for the Dinantian of Belgium as a basis for a coral biozonation of the Dinantian of Eurasia. – Dixième Congrès International de Stratigraphie et de Géologie du Carbonifère = International Congress on Carboniferous Stratigraphy and Geology, Compte Rendue, **10(4)**: 29-31.

Poty, E. (1991): Tectonique de blocs dans le prolongement oriental du Massif du Brabant. – Annales de la Société géologique de Belgique, **114(1)**: 265-275.

Poty, E. (1997): Devonian and Carboniferous tectonics in the eastern and southeastern parts of the Brabant Massif (Belgium). – In: Camelbeeck, T., Sintubin, M. & Vandycke, S. (eds.): Belgian Symposium on structural Geology and Tectonics, Leuven 1997. – Aardkundige Mededelingen, **8**: 143-144.

Poty, E. (2016): The Dinantian (Mississippian) succession of southern Belgium and surrounding areas: stratigraphy improvement and inferred climate reconstruction. – Geologica Belgica, **19(1-2)**: 177-200.

Poty, E. & Delculée, S. (2011): Interaction between eustacy and block-faulting in the Carboniferous of the Visé-Maastricht area (Belgium, The Netherlands). – Zeitschrift der Deutschen Gesellschaft für Geowissenschaften, **162(2)**: 117-126.

Poty, E., Aretz, M. & Denayer, J. (2011): Field Trip 3: Uppermost Devonian and Lower Carboniferous of Southern Belgium. – In: 11th International Symposium on Fossil Cnidaria and Porifera, Liège 2011. - Kölner Forum für Geologie und Paläontologie, **20**: 99-150.

Poty, E., Aretz, M. & Hance, L. (2014): Belgian substages as a basis for an international chronostratigraphic division of the Tournaisian and Viséan. – Geological Magazine, **151(2)**: 229-243.

Poty, E., Devuyst, F.-X. & Hance, L. (2006): Upper Devonian and Mississippian foraminiferal and rugose coral zonations of Belgium and northern France: a tool for Eurasian correlations. – Geological Magazine, **143 (6)**: 829-857.

Poty, E., Mottequin, B. & Denayer, J. (2015): Orbitally forced sequences and climate reconstruction around the Devonian-Carboniferous boundary, and the Hangenberg Extinction Event. – In: Mottequin, B., Denayer, J., Königshof, P., Prestianni, C. & Olive, S. (eds.): IGCP 596 - SDS Symposium, climate change and biodiversity patterns in the Mid-Palaeozoic. – Strata, série 1, **16**: 121.

Poty, E., Hance, L., Lees, A. & Hennebert, M. (2001): Dinantian lithostratigraphic units (Belgium). – Geologica Belgica, **4(1-2)**: 69-94.

Ramsbottom, W. H. C. (1973): Transgressions and regressions in the Dinantian: a new synthesis of British Dinantian stratigraphy. - Proceedings of the Yorkshire Geological Society, **39(4)**: 567-607.

Rathmann, S.D. & Amler, M.R.W. (1992): Bivalven aus dem Unter-Karbon von Aprath (Wuppertal, Bergisches Land). – Geologica et Palaeontologica, **26**: 35-71.

RAVEN, J. G. M. (1983): Conodont biostratigraphy and depositional history of the Middle Devonian to Lower Carboniferous in the Cantabrian Zone (Cantabrian Mountains, Spain). – Leidse Geologische Mededelingen, **52(2)**: 265-339.

REXROAD, C. B. & SCOTT, A. J. (1964): Conodont zones in the Rockford limestone and the lower part of the New Providence Shale (Mississippian) in Indiana. – Indiana Department of Conservation, Geological Survey, Bulletin, **30**: 1-54.

RHODES, F. H. T., AUSTIN, R. L. & DRUCE, E. C. (1969): British Avonian (Carboniferous) conodont faunas and their value in local and intercontinental correlation. – Bulletin of the British Museum (Natural History) Geology, Supplement **5**: 4-313.

RHODES, F. H. T. & MÜLLER, K. J. (1956): The Conodont Genus *Prioniodus* and related forms. – Journal of Paleontology, **30(3)**: 695-699.

RICHTER, E. & AMLER, M.R.W. (1994): Bivalven und Rostroconchien aus dem Velberter Kalk von Velbert (Unter-Karbon; Bergisches Land). – Geologica et Palaeontologica, **28**: 103-139.

ROSS, C. A. & ROSS, J. R. P. (1985): Late Paleozoic depositional sequences are synchronous and worldwide. – Geology, **13**: 194-197.

ROSS, C. A. & ROSS, J. R. P. (1987): Late Paleozoic sea levels and depositional sequneces. – In: ROSS, C. A. & HAMAN, D. (eds.): Timing and depositional history of eustatic sequences: constraints on seismic stratigraphy. - Cushman Foundation for Foraminiferal Research, Special Publication, **24**: 137-149.

ROSS, C. A. & ROSS, J. R. P. (1988): Late Paleozoic transgressive-regressive deposition. - In: WILGUS, C. K., HASTINGS, B. S., KENDALL, C. G. ST. C., POSAMENTIER, H. W., ROSS, C. A. & VAN WAGONER, J. C. (eds.): Sea-level changes: An integrated approach. - Society of Economic Paleontologists and Mineralogists, Special Publication, **42**: 227-247.

ROUNDY, P. V. (1926): Part II. The Micro-fauna. – In: ROUNDY, P. V., GIRTY, G. H. & GOLDMAN, M. I. (eds.): Mississippian formations of San Saba County, Texas. – U.S. Geological Survey, Professional Paper, **146**: 5-23.

ROUNDY, P. V., GIRTY, G. H. & GOLDMAN, M. I. (1926): Mississippian formations of San Saba County, Texas. – U.S. Geological Survey, Professional Paper, **146**: 1-59.

SANDBERG, C. A. (1976): Conodont biofacies of Late Devonian *Polygnathus styriacus* Zone in western United States. – In: BARNES, C. R. (ed.): Conodont paleoecology. – Geological Association of Canada, Special Paper, **15**: 171-186.

SANDBERG, C. A. (1979): Devonian and Lower Mississippian Conodont Zonation of the Great Basin and Rocky Mountains. – Brigham Young University Geology Studies, **26(3)**: 87-105.

SANDBERG, C. A. & DREESEN, R. (1984): Late Devonian icriodontid biofacies models and alternate shallow-water conodont zonation. – In: CLARK, D. L. (ed.): Conodont biofacies and provincialism. – Geological Society of America Special Papers, **196**: 143-179.

SANDBERG, C. A. & GUTSCHICK, R. C. (1979): Guide to conodont biostratigraphy of Upper Devonian and Mississippian rocks along the Wasatch front and Cordilleran hingeline, Utah. – In: SANDBERG, C. A. & CLARK, D. L. (eds.): Conodont biostratigraphy of the Great Basin and Rocky Mountains. – Brigham Young University Geology Studies, **26(3)**: 107-134.

SANDBERG, C. A. & GUTSCHICK, R. C. (1984): Distribution, microfauna, and source-rock potential of Mississippian Delle Phosphatic Member of Woodman Formation and equivalents, Utah and adjacent States. - In: WOODWARD, J., MEISSNER, F. F. & CLAYTON,

J. L. (eds.): Hydrocarbon source rocks of the greater Rocky Mountain region, 135-178; Denver, Colorado (Rocky Mountain Association of Geologists).

SANDBERG, C. A. & POOLE, F. G. (1977): Conodont biostratigraphy and depositional complexes of Upper Devonian cratonic-platform and continental-shelf rocks in the Western United States. – In: MURPHY, M. A., BERRY, W. B. N. & SANDBERG, C. A. (eds.): Western North America; Devonian. – Campus Museum Contribution, **4**: 144-182.

SANDBERG, C. A. & ZIEGLER, W. (1979): Taxonomy and biofacies of important conodonts of Late Devonian *styriacus*-Zone, United States and Germany. – Geologica et Palaeontologica, **13**: 173-212.

SANDBERG, C. A., ZIEGLER, W., DREESEN, R. & BUTLER, J. L. (1988): Late Frasnian Mass Extinction: Conodont Event Stratigraphy, Global Changes, and Possible Causes. – Courier Forschungsinstitut Senckenberg, **102**: 263-307.

SANDBERG, C. A., ZIEGLER, W., DREESEN, R. & BUTLER, J. L. (1992): Conodont biochronology, biofacies, taxonomy, and event stratigraphy around Middle Frasnian Lion Mudmound (F2h), Frasnes, Belgium. – Courier Forschungsinstitut Senckenberg, **150**: 1-87.

SANDBERG, C. A., ZIEGLER, W., LEUTERITZ, K. & BRILL, S. M. (1978): Phylogeny, speciation, and zonation of *Siphonodella* (Conodonta, Upper Devonian and Lower Carboniferous). – Newsletter on Stratigraphy, **7**: 102-120.

SANDBERG, C. A., GUTSCHICK, R. C., JOHNSON, J. G., POOLE, F. G. & SANDO, W. J. (1983): Middle Devonian to Late Mississippian geologic history of the Overthrust Belt region, western United States. – Rocky Mountain Association of Geologists, Geologic Studies of the Cordilleran Thrust Belt, **2**: 691-719.

SANNEMANN, D. (1955): Beitrag zur Untergliederung des Oberdevons nach Conodonten. – Neues Jahrbuch für Geologie und Paläontologie, Abhandlungen, **100**: 324-31.

SCHÄFER, W. (1975): Eine oberdevonisch-unterkarbonische Schichtlücke im Bereich des Balver Riffgebietes (Rheinisches Schiefergebirge). – Neues Jahrbuch für Geologie und Paläontologie, Monatshefte, **1975(4)**: 228-241.

SCHÄFER, W. (1978): Stratigraphie, Fazies und Paläogeographie in Oberdevon und Unterkarbon im Bereich des Balver Riffgebietes (Rheinisches Schiefergebirge). – Inaugural Dissertation, Phillips-Universität Marburg. 122 pp.; Marburg (Mauersberger).

SCHINDLER, E., BROCKE, R., BECKER, R. T., BUCHHOLZ, P., JANSEN, U., LUPPOLD, F. W., NESBOR, H.-D., SALAMON, M., WELLER, H. & WEYER, D. (2017): Das Devon in der Stratigraphischen Tabelle von Deutschland 2016. – Zeitschrift der Deutschen Geologischen Gesellschft, **168(4)**: 447-63.

SCHMIDT, H. (1923): Zur Stratigraphie des Untercarbon. – Centralblatt für Mineralogie, Geologie und Paläontologie, **1923**: 741-746.

SCHMIDT, H. (1935): Die binomische Einteilung der fossilen Meeresböden. – Fortschritte in der Geologie und Paläontologie, **12 (H. 38)**: 1-154.

SCHÖNLAUB, H. P. (1969): Conodonten aus dem Oberdevon und Unterkarbon des Kronhofgrabens (Karnische Alpen, Österreich). – Jahrbuch der Geologischen Bundesanstalt, **112**: 321-354.

SCHUDACK, M. E. (1993): Karbonatzyklen in Riff- und Lagunenbereichen des devonischen Massenkalkkomplexes von Asbeck (Hönnetal, Rheinisches Schiefergebirge). – Geologie und Paläontologie in Westfalen, **26**: 77-106.

SEDDON. G. (1970): Frasnian conodonts from the Sadler Ridge-Bugle Gap area, Canning Basin, Western Australia. – Journal of the Geological Society of Australia, **16(2)**: 723-753.

SEDDON. G. & SWEET, W. C. (1971): An ecologic model for conodonts. – Journal of Paleontology, **45(5)**: 869-880.

SEDGWICK, A. & MURCHISON, R.J. (1842): On the distribution and classification of the older or Palaeozoic deposits of the north of Germany and Belgium, and their comparison with formations of the same age in the British Isles. – Transactions of the Geological Society of London **S2-6**: 221–301; London.

SEO, E.-H. & WON, M.-Z. (2009): Review of the Genus *Polyentactinia* and the Family Polyentactiniidae. – Micropaleontology, **55(1)**: 61-74.

SIEGMUND, H., TRAPPE, J., OSCHMANN, W. (2002): Sequence stratigraphic and genetic aspects of the Tournaisian "Liegender Alaunschiefer" and adjacent beds. – International Journal of Earth Sciences, **91**: 934-949.

SKOMPSKI, S., ALEKSEEV, A., MEISCHNER, D., NEMIROVSKAYA T., PERRET, M. F., VARKER, W. J. (1995): Conodont distribution across the Visean/Namurian boundary. – Courier Forschungsinstitut Senckenberg, **188**: 177-209.

SPALETTA, C., PERRI, M. C., OVER, D. J. & CORRADINI, C. (2017): Famennian (Upper Devonian) conodont zonation: revised global standard. – Bulletin of Geosciences, **92(1)**: 31-57.

STEENWINKEL, M. VAN (1990): Sequence stratigraphy from „spot" outcrops - example from a carbonate-dominated setting: Devonian-Carboniferous transition, Dinant synclinorium (Belgium). – Sedimentary Geology, **69**: 259-280.

STEENWINKEL, M. VAN (1993a): The Devonian-Carboniferous boundary in southern Belgium: biostratigraphic identification criteria of sequence boundaries. – In: POSAMENTIER, H.W., SUMMERHAYES, C.P., HAQ, B.U. & ALLEN, G.P. (eds.): Sequence stratigraphy and facies associations. – International Association of Sedimentologists, Special Publications, **18**: 237-246.

STEENWINKEL, M. VAN (1993b): The Devonian-Carboniferous boundary: Comparison between the Dinant Synclinorium and the northern border of the Rhenish Slate Mountains. – Annales de la Société Géologique Belgique [for 1992], **115(2)**: 665-681.

STD 2016 (Deutsche Stratigraphische Kommission (ed.); editing, coordination and layout: MENNING, M. & HENDRICH, A.) (2016): Stratigraphische Tabelle von Deutschland 2016. – (1) Table plain 100 x 141 cm, (2) Table folded A4; Potsdam (Deutsches GeoForschungsZentrum).

STICHLING, S., ABOUSSALAM, Z. S., BECKER, R. T., EICHHOLT, S. & HARTENFELS, S. (2015): Event-crontrolled reef drowning and extinction in the Hönne Valley (northern Rhenish Massif, Hagen-Balve reef complex). – IGCP 596 - SDS Symposium (Brussels, September 2015). – Strata, série 1, **16**: 138-139.

STOPPEL, D. (with contributions of HEUSER, H., KREBS, W., SCHÄFER, W. & UFFENORDE, H.) (1977): Exkursionen in das nordöstliche Sauerland. Warstein-Hirschberg, 19-21. Mai 1977, Subkommission für Karbonstratigraphie, -27 pp.; Hannover (unpublished).

SWENNEN, R. & VIAENE, W. (1985): The sedimentological reconstruction of the Lower Carboniferous carbonates in a near-shore environment (east Belgium): a necessity for lithostratigraphical correlations. – 10. Congres International de Stratigraphie et Géologie du Carbonifère, Madrid 1983, Compte Rendue, **3**: 231-241.

SWENNEN, R., BOONEN, P. & VIAENE, W. (1982): Stratigraphy and lithogeochemistry of the Walhorn section (Lower Visean; Vesder Basin, E.-Belgium) and its implications. – Bulletin Société Belge de Géologie, **91(4)**: 239-258.

SWEET, E. C. (1988): The Conodonta: morphology, taxonomy, paleoecology, and evolutionary history of a long-extinct animal phylum. – Oxford Monographs on Geology and Geophysics, **10**. - 212p.: Oxford (Clarendon Press).

THOMAS, E. (ed.) (1992): Oberdevon und Unterkarbon von Aprath im Bergischen Land (Nördliches Rheinisches Schiefergebirge). -468 pp.; Köln (Sven von Loga).

THOMAS, E. (1993): 150 Jahre geologische Forschung im Grenzbereich von Devon und Karbon am Südrand des Ruhrgebietes in klassischen Aufschlüssen und temporären Baustellen. – Archäologie im Ruhrgebiet, **1991**: 7-23.

THOMPSON, T.L. (1967): Conodont zonation of lower Osagean rocks (Lower Mississippian) of Southwestern Missouri. – Missouri Geological Survey and Water Resources, Report of Investigations, **39**: 7-88.

THOMPSON, T. L. & FELLOWS, L. D. (1970): Stratigraphy and conodont biostratigraphy of Kinderhookian and Osagean (lower Mississippian) rocks of south-western Missouri and adjacent areas - Report of Investigations. – Missouri, Geological Survey, **45**: 1-263.

UFFMANN, A. K., LITTKE, R., RIPPEN, D. (2012): Mineralogy and geochemistry of Mississippian and Lower Pennsylvanian Black Shales at the Northern Margin of the Variscan Mountain Belt (Germany and Belgium). – International Journal of Coal Geology, **103**: 92-108.

ULRICH, E. O. & BASSLER, R. S. (1926): A classification of the toothlike fossils, conodonts, with descriptions of American Devonian and Mississippian species. – Proceedings of the United States National Museum, **68(12)**: 1-63.

VARLAMOFF, N. (1936): Stratigraphie du Viséen du massif de la Vesdre. – Annales de la Société Géologique de Belgique, **60**: 92-105.

VOGES, A. (1959): Conodonten aus dem Unterkarbon I und II (*Gattendorfia* und *Pericyclus*-Stufe) des Sauerlandes. — Paläontologische Zeitschrift, **33**: 266-314.

VOGES, A. (1960): Die Bedeutung des Conodonten für die Stratigraphie des Unterkarbons I und II (*Gattendorfia*- und *Pericyclus*-Stufe) im Sauerland. – Fortschitte in der Geologie von Rheinland und Westfalen, **3**: 197-228.

VORONTZOVA, T. N. (1996): The genus *Neopolygnathus* (Conodonta): phylogeny and some questions of systematics. – Paleontologicheskii Zhurnal, **1996(2)**: 82-84.

WALLACE, Z. A. & ELRICK, M. (2014): Early Mississippian orbital-scale glacio-eustasy detected from high-resolution oxygen isotopes of marine apatite (conodonts). – Journal of Sedimentary Research, **84(10)**: 816-824.

WEBER, H.M. (1997): Holothurien- und Ophiocistoiden-Reste (Echinodermata) aus dem Unterkarbon des Velberter Sattels (Rheinisches Schiefergebirge). – Sonderveröffentlichungen des Geologischen Instituts der Universität zu Köln, **114**: 485-497.

WEBSTER, G. D. & GROESSENS, E. (1990): Conodont subdivision of the Lower Carboniferous. – Courier Forschungsinstitut Senckenberg, **130**: 31-40.

WELDON, S. (1996): A preliminary study of Late Devonian acritarchs from Riescheid, North Rhenish Slate Mountains, Germany. – In: FATKA, O. & SERVAIS, T. (eds.): Acritarcha in Praha 1996. Proceedings of International Meeting and Workshop. – Acta Universitatis Carolinae Geologica, **40(3-4)**: 1-699.

Wendt, J., Kaufmann, B., Belka, Z. & Korn, D. (2009): Carboniferous stratigraphy and depositional environments in the Ahnet Mouydir area (Algerian Sahara). – Facies, **55**: 443-472.

Won, M.-Z. & Seo, E.-H. (2010): Lower Carboniferous radiolarian biozones and faunas from Bergisches Land, Germany. – Journal of the Paleontological Society of Korea, **26(2)**: 193-269.

Wrede, V. (1998): Die Tektonik des präpermischen Untergrundes von Krefelder und Venloer Scholle. – Fortschritte in der Geologie von Rheinland und Westfalen, **37**: 333-380.

Wrede, V. & Hilden, H.D. (1988): Geologische Entwicklung. – In: Geologie am Niederrhein. – 4th ed., 7-14; Krefeld (Geologisches Landes-Amt Nordrhein-Westfalen).

Youngquist, W. L. (1945): Upper Devonian conodonts from the Independence Shale (?) of Iowa. – Journal of Paleontology, **19**: 355-367.

Zhuravlev, A. V. (2017a): A new species of the conodont genus *Siphonodella* Branson & Mehl (late Tournaisian). – Estonian Journal of Earth Sciences, **66(4)**: 188-192.

Zhuravlev, A. V. (2017b): Speciation and Phylogeny of the European Lineage of Shallow-Water Siphonodellids (Conodonta, Latest Famennian – middle Tournaisian). – In: Nurgaliev, D. (ed.): Kazan Golovkinsky Stratigraphic Meeting, 2017; Proceedings. Advances in Devonian, Carboniferous and Permian Research: Stratigraphy, Environments, Climate and Resources. 255–59; Bologna, Italy (Filodiritto Publisher).

Zhuravlev, A. V. (2019): A New Species of Shallow-Water Siphonodella (Conodonta) from the Tournaisian (Lower Carboniferous) of Pechora-Kozhva Uplift, Timan-Pechora Basin. (preprint*).*

Zhuravlev, A. V. & Plotitsyn, A. N. (2017): The symmetry of the rostrum as a key to taxonomy of advanced *Siphonodella* (Conodonta, Early Carboniferous). – Stratigraphy, **14(1-4)**: 457-474.

Zhuravlev, A. V. & Plotitsyn, A. N. (2018): Taxonomical reassignment of some Siphonodellids (Conodonts, Early Carboniferous) from W. Hass's collection. – Newsletter on Carboniferous Stratigraphy, **34**: 31-34.

Ziegler, W. (1962): Taxonomie und Phylogenie Oberdevonischer Conodonten und ihre stratigraphische Bedeutung. – Abhandlungen des Hessischen Landesamtes für Bodenforschung, **38**: 1-166.

Ziegler, W. (1971): A Field Trip Guidebook. Post-Symposium Excursion, Sept. 15-18, 1971, to Rhenish Slate Mountains and Hartz Mountains. - Symposium on Conodont Taxonomy Marburg/Lahn, Sept. 4 to 18, 1971. -47p.; Marburg (Philipps-Universität Marburg, Fachbereich Geowissenschaften).

Ziegler, W. (ed., 1973): Catalogue of Conodonts. – Volume I. -504 pp.; Stuttgart (Schweitzerbart'sche Verlagsbuchhandlung).

Ziegler, W. (ed., 1975): Catalogue of Conodonts. – Volume II. -404 pp.; Stuttgart (Schweitzerbart'sche Verlagsbuchhandlung).

Ziegler, W. (ed., 1981): Catalogue of Conodonts – Volume IV. -445 pp.; Stuttgart (Schweitzerbart'sche Verlagsbuchhandlung).

Ziegler, W. & Huddle, J. W. (1969): Die *Palmatolepis glabra*-Gruppe (Conodonta) nach der Revision der Typen von Ulrich & Bassler durch J. W. Huddle. – Fortschritte in der Geologie von Rheinland und Westfalen, **16**: 377-386.

ZIEGLER, W. & LANE, H. R. (1987): Cycles in conodont evolution from Devonian to mid-Carboniferous. – In: ALDRIDGE, R. J. (ed.): Paleobiology of conodonts. – British Micropalaeontological Society Series, 147-163pp.; West Sussex (Ellis Horwood).

ZIEGLER, W., & K. LEUTERITZ (1970): Conodonten. – Fortschritte in der Geologie von Rheinland und Westfalen, **17**: 679-732.

ZIEGLER, W. & SANDBERG, C. A. (1984): *Palmatolepis*-based revision of upper part of standard Late Devonian conodont zonation. – In: CLARK, D. L. (ed.): Conodont Biofacies and Provincialism. – The Geological Society of America, Special Paper, **196**: 179-194.

ZIEGLER, W. & SANDBERG, C. A. (1990): The late Devonian standard conodont zonation. – Courier Forschungsinstitut Senckenberg, **121**: 1-115.

ZIEGLER, W. & WEDDIGE, K. (1999): Zur Biologie, Taxonomie und Chronologie der Conodonten. – Paläontologische Zeitschrift, **73(1/2)**: 1-38.

ZIEGLER, W., SANDBERG, C. A. & AUSTIN, R. L. (1974): Revision of *Bispathodus* group (Conodonta) in the Upper Devonian and Lower Carboniferous. – Geologica et Palaeontologica, **8**: 97-112.

ZIMMERLE, W., GAIDA, K.-H., GEDENK, R., KOCH, R. & PAPROTH, E. (1980): Sedimentological, mineralogical, and organic-geochemical analyses of Upper Devonian and Lower Carboniferous strata of Riescheid, Federal Republic of Germany. – Mededelingen Rijks geologische Dienst, **32(5)**: 34-43.

12. Plates

Plate 1

Microfacies of Riescheid, **MFT A - Finely laminated, fine-grained packstone** (Figs. 1, 4-5, 7, 14). **MFT B - Widely spaced, ripple-laminated packstone** (Figs. 2, 8-13). **MFT C - Bioturbated packstone** (Figs. 3, 6)

1 MFT A, overview of laminated, fine-grained structure, sample Ri 92 upper part

2 MFT B, wide-spaced lamination with irregular, ripple-induced margins, sample Ri 104.2b

3 MFT C, bioturbated area, bioturbation obvious due to different sediment colours, sample Ri 107TOP.1

4 bioturbation disturbing the lamination, bioturbated area marked by black arrows, sample Ri 105b

5 ripple marks in finely-laminated packstone, sample Ri 95.2

6 dolomitized area, dolomite crystal recognizable near the right margin, numerous bright white quartz grains, sample Ri 100b

7 cross-section of an echinoderm fragment, sample Ri 92 middle part

8 cross-section of mainly recristallized radiolarian, sample Ri 96.2

9 ostracod (lower left corner) and plant fragment (upper right corner), sample Ri 104.2b

10-13 *Magnella reitlingerae* NEUMANN et al., 1975

    10 sample Ri 104.2b

    11-12 sample Ri 104.1b

    13 sample Ri 104d

14 very thin, large bivalve shell, sample Ri 92 middle part

Plate 1
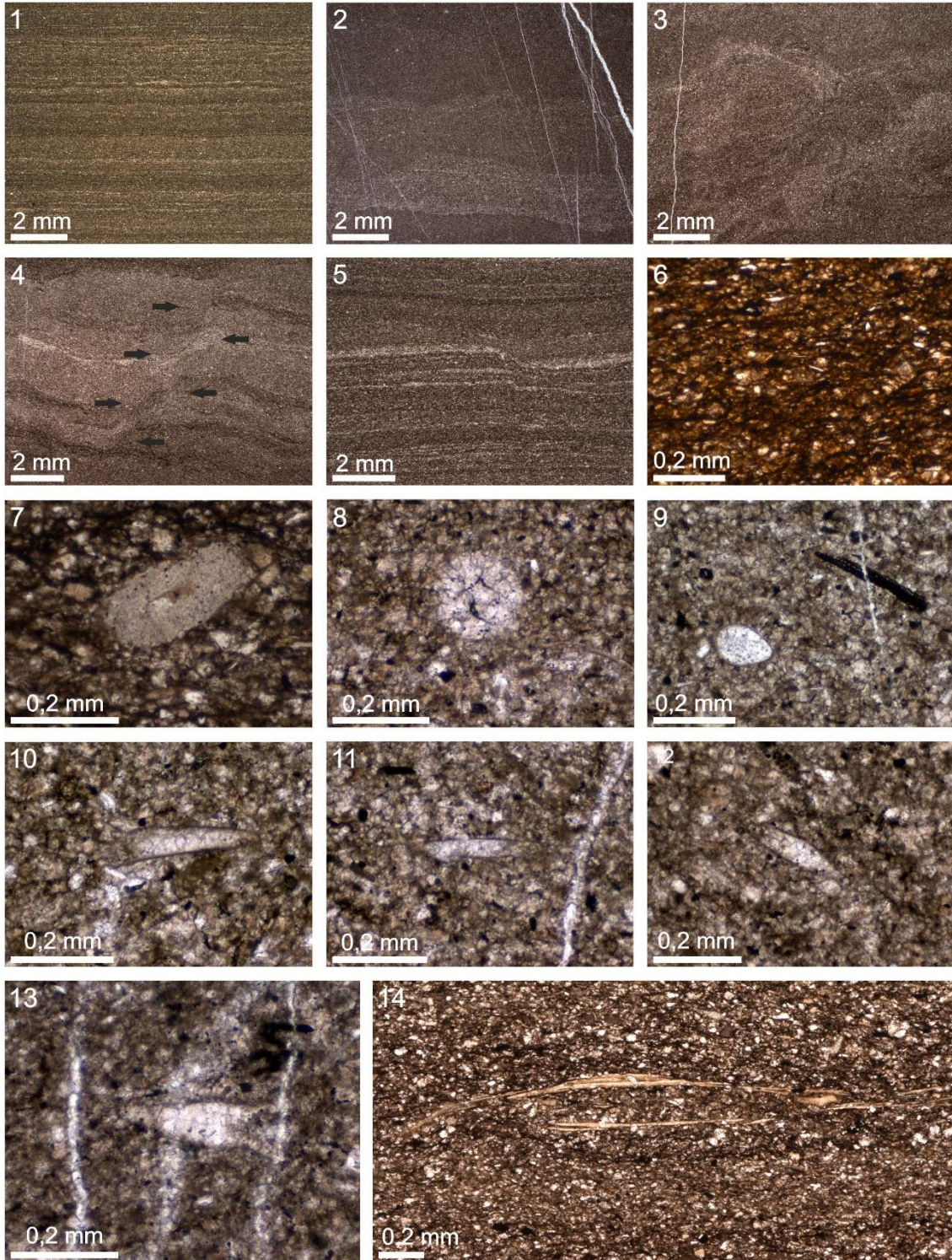
Plate 2

Microfacies of Gladenbach, **MFT A1 - Fine-grained intraclastic-bioclastic grainstone/packstone** (Figs. 1, 5-6, 8-9, 12, 17), **MFT A2 - Ooid-bearing intraclastic-bioclastic packstone** (Figs. 2, 15-16), **MFT B1 - Radiolarian-rich wackestone/packstone** (Figs. 3, 13-14, 18), **MFT B2 - Microlithoclastic-microbioclastic wackestone/packstone** (Figs. 4, 7, 10-11, 19-21)

1 MFT A1, microsparitic matrix with pseudopeloids, sample 26
2 MFT A2, coarser, sparitic matrix with micritic intraclasts, sample 31b
3 MFT B1, matrix of stylocumulate, sample 6-1
4 MFT B2, bioclast-depleted unstructured, fine grained matrix, sample 1
5 conodont, sample 22-1
6 echinoderm-fragment, sample 26
7 *Magnella reitlingerae* NEUMANN et al., 1975, sample 32
8 brachiopod spine, sample 25-2
9 ostracod, sample 9-1
10 echinoderm spine, sample 1-2
11 calcisphaera, sample 32
12 sparry calcite rim around shale-lithoclast, sample 22-1
13 microstylolite swarms, enrichment of stylolaminar structures, sample 18-1
14 detail of stylocumulate, sample 18-1
15 micritized ooids, intraclasts, detrital quartz, sample 31-2
16 detail of MFT A2, radial fibrous (recrystallized) ooid, sample 31-2
17 sponge-spicules, some with axial canal, matrix strongly affected by pressure-solution, sample 25-2
18 radiolarians, sponge spicules, sample 6-1
19 calcitized radiolarian ghosts deformed by pressure solution and concomitant formation of styloreactate, intensive pressure solution resulted in differentiation of matrix into calcitic styloreactate (dirty white) and non-calcareous stylocumulate (black), sample 8-1
20 radiolarian ghost, bioclasts, matrix rich in dolomite, sample 1
21 elongated, deformed *Planolites* burrows, sample 7-1

Plate 2
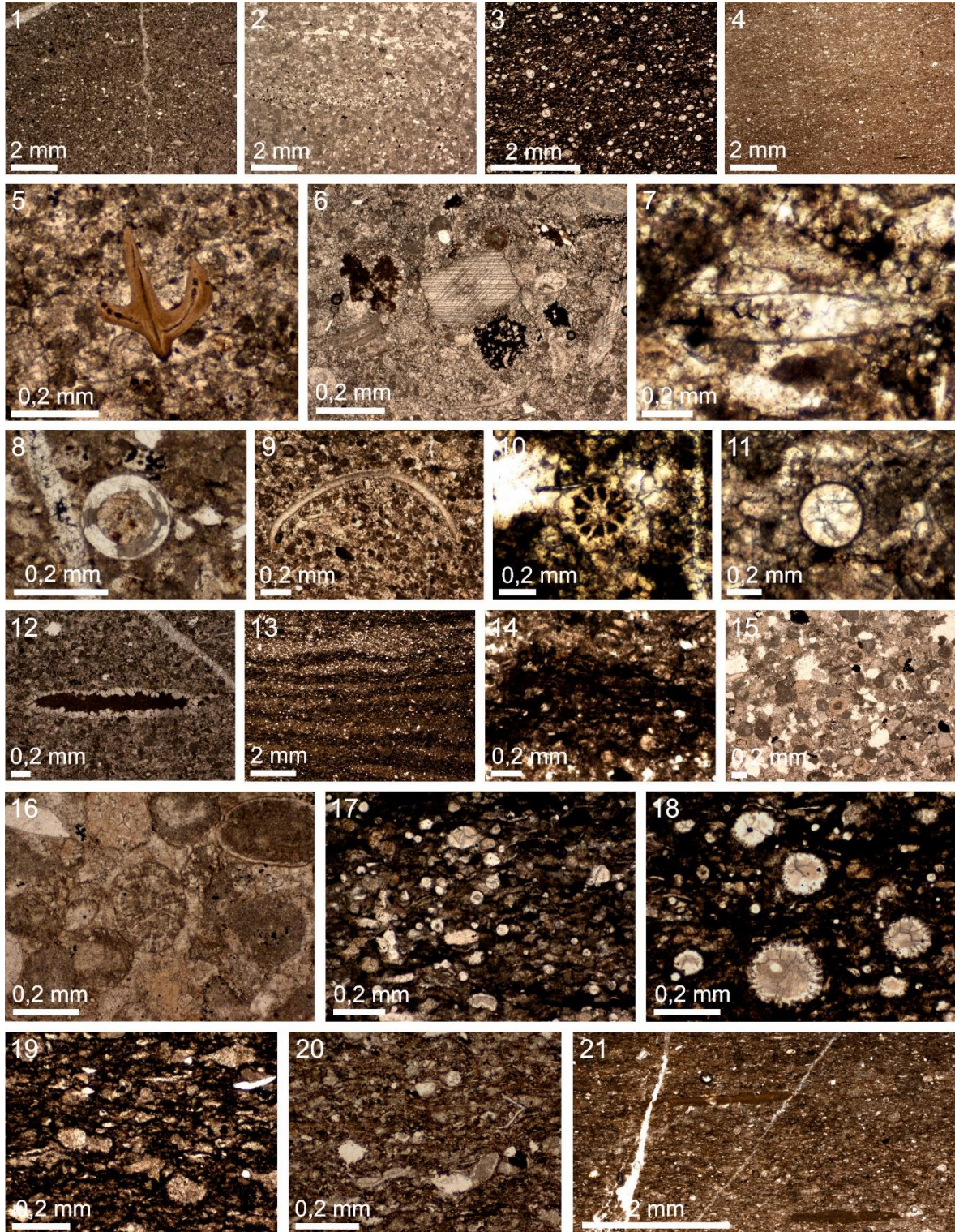
Plate 3

Microfacies of Wettmarsen, **Laminated radiolarian-bearing wackestone/ packstone**

1 overview of radiolarian-dominated darker laminae and lighter laminae dominated by pseudopeloids and small bioclasts (colours appear inverted in the picture), sample 130514_2

2 close-up of 1 with lighter bioclast-dominated layers in the center and darker radiolarian-dominated areas in upper and lower part (colours appear inverted in the picture), sample 130514_2

3 recristallized radiolarians, sample 130514_1

4 coated echinoderm grain within lighter lamina, sample 130514_2

5 Palaeoberesellacean alga, within dark lamina, sample 130514_2

6 cross-section of ostracod and echinoderm fragment, sample 130514_2

7 thin bivalve shell, sample 130514_2

8 cross-section of two fused micritized ooids and part of a calcareous foraminifera on left side, sample 130514_2

9 crinoid within radiolarian-dominated area, sample 130514_2

10 echinid spine, sample 130514_2

11 *Brunsia* sp., sample 130514_2

12 Parathuramminid foraminifer, sample 130514_1

13 indeterminate foraminifer, sample 130514_1

14 cross-section of echinoderm spine within lighter layer, sample 130514_1

15 cross-section of *Calcisphaera laevis* (upper left) and *Calcisphaera pachysphaerica* (center), sample 130514_1

Plate 3
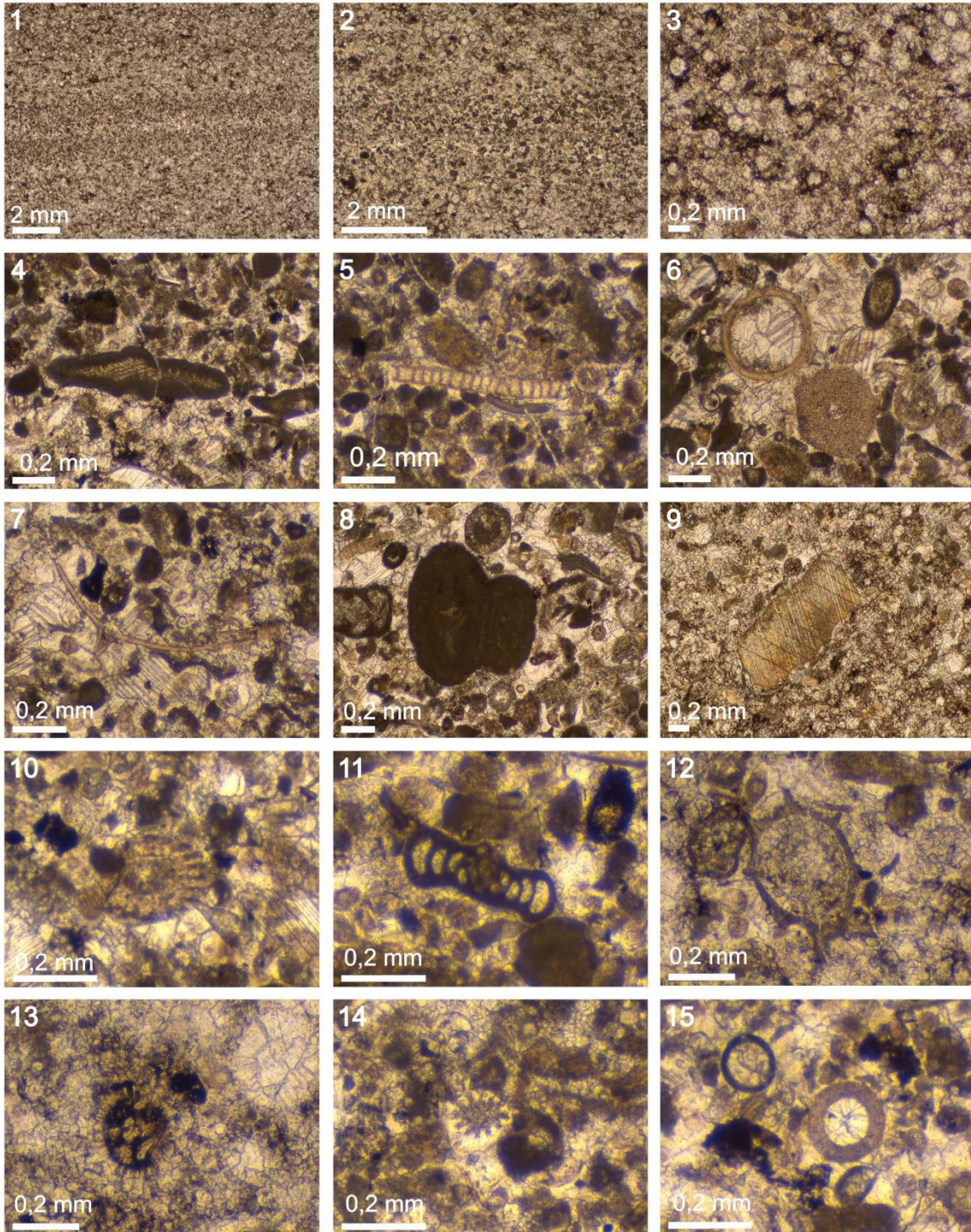
Plate 4

Microfacies of Dolhain, overview pictures of the different microfacies types, **MFT A1 - Peloidal wackestone/packstone** (Fig. 1), **MFT A2 - Echinoderm-foraminifer wackestone/packstone** (Figs. 2-3), **MFT A3 - Bioturbated, echinoderm-ostracod wackestone/packstone** (Figs. 4-7), **MFT B1 - Dark, bioturbated, bioclast-bearing wackestone/packstone** (Figs. 8-9), **MFT B2 - Bioturbated, bioclast-bearing wackestone/packstone** (Figs. 10-11), **MFT C - Micritic to microsparitic, bioturbated, echinoderm wackestone/packstone** (Figs. 12-13), **MFT D - Bioturbated mudstone** (Figs. 14-15)

1 close-up of MFT A1, showing the matrix that is mainly composed of peloids, various small bioclasts (e. g., echinoderm fragments, calcareous foraminifera) are scattered throughout the matrix, sample Do 1

2 close-up of MFT A2, dark rims were caused by bioturbation in the micritic matrix, containing few bioclasts (e. g., crinoids, calcareous foraminifera), sample Do 23.1

3 close-up of MFT A2, area with numerous bioclasts that were enriched by bioturbation, stylolite swarms give it a more structured appearance, in the upper right corner the area is influenced by dolomitization and holds a vast number of quartz grains, sample Do 23.2

4 close-up of MFT A3, micritic matrix with bioturbation (darker and lighter colours), sample Do 11.1

5 bioturbated area of MFT A3, bioclasts arranged around margins of strongly bioturbated area, sample Do 11.1

6 dolomitized area of MFT A3, burrow composed of grey, bioclast-rich material in center, sample 14.3.2

7 close-up of MFT A3, cluster mainly of ostracodes in the center, slight dolomitization at right side and center of microphotograph, sample Do 25.1

8 dark brown microsparitic matrix of MFT B1, bioclasts (mostly crinoid fragments) enriched in center of microphotograph by bioturbation, sample Do 8, middle part

9 dark brown microsparitic matrix of MFT B1, bioturbated areas are rimmed by dark margins, sample Do 8, middle part

10 detail of MFT B2, cluster of bioclasts (e. g., ostracodes, echinoderm fragments, bivalve and brachiopod shells) enriched by bioturbation, sample Do 14.4

11 close-up of brown, microsparitic matrix of MFT B2 with scatterd bioclasts, sample Do 14.4

12 dark brown micritic and microsparitic matrix of MFT C, area with numerous bioclasts (mainly echinoderm fragments), sample Do 21.1

13 overview of MFT C, sediment completely disturbed by bioturbation, areas between bioturbation marks are often affected by dolomitization and contain bioclasts, sample Do 24

14 overview of MFT D, almost all areas of the microphotograph are affected by dolomitization, layered-appearance caused by predominantly horizontal burrows and additional overprinting by slight pressure solution, sample 12.2

15 overview of MFT D, bioturbated areas are not affected by dolomitization, sample 15.1

Plate 4
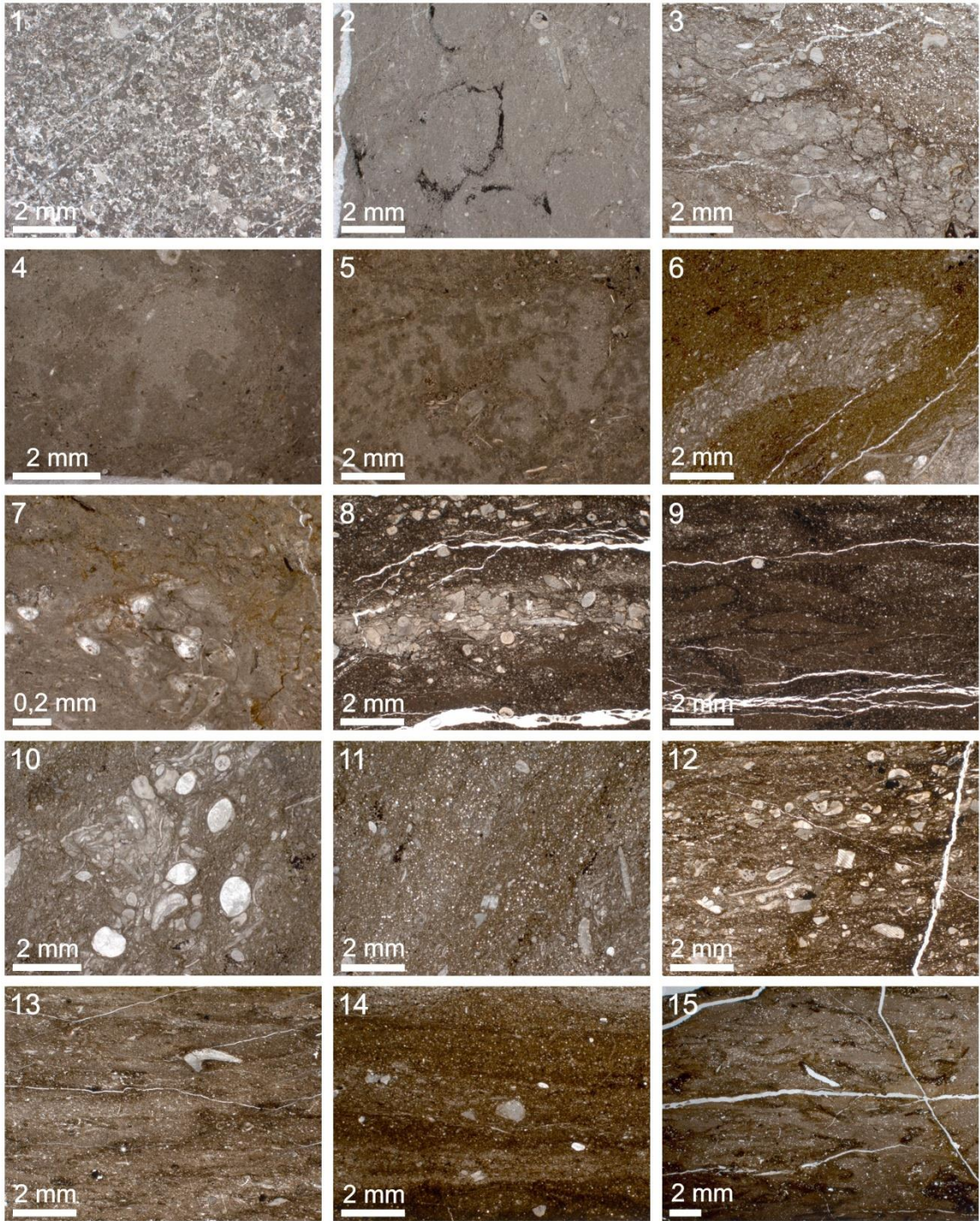
Plate 5

Microfacies of Dolhain, details of the different microfacies types, **MFT A1 - Peloidal wackestone/packstone** (Figs. 1-6), **MFT A2 - Echinoderm-foraminifer wackestone/packstone** (Figs. 7-12), **MFT A3 - Bioturbated, echinoderm-ostracod wackestone/packstone** (Figs. 13-15)

1 cross-section of ostracod in the center, sample Do 35

2 cross-section of echinoid spine in the center, surrounded mainly by crinoid fragments and sparitic calcite, sample Do 34

3 two trilobites within matrix dominated by peloids, small echinoid spine in upper left corner, sample Do 34

4 *Girvanella* sp. NICHOLSON & ETHERIDGE, 1878, sample Do 34

5 cross-section of calcisphere in the center, sample Do 34

6 cross-sections of an ostracod and crinoids, further crinoid fragments scattered in the peloid-dominated matrix, sample Do 35

7 calcareous foraminifer, sample Do 3.1

8 several calcareous foraminifers, sample Do 3.2

9 echinoid spine within micritic matrix, upper part of microphotograph shows dolomitized matrix, sample Do 3.1

10 area enriched in bioclasts, big brachiopod shell shielding mainly crinoid ossicles, sample Do 3.1

11 cross-section of big gastropod, sample Do 18

12 layer of stylocumulate in the center overlain by an area enriched in bioclasts (mainly crinoid fragments), sample Do 3.2

13 fragment of a brachiopod shell surrounded by numerous smaller bioclasts, vast areas of the matrix affected by dolomitization, sample Do 11.1

14 three connected crinoid ossicles in micritic matrix, sample Do 11.1

15 two specimens of *Earlandia* PLUMMER, 1930, sample Do 14.3

Plate 5
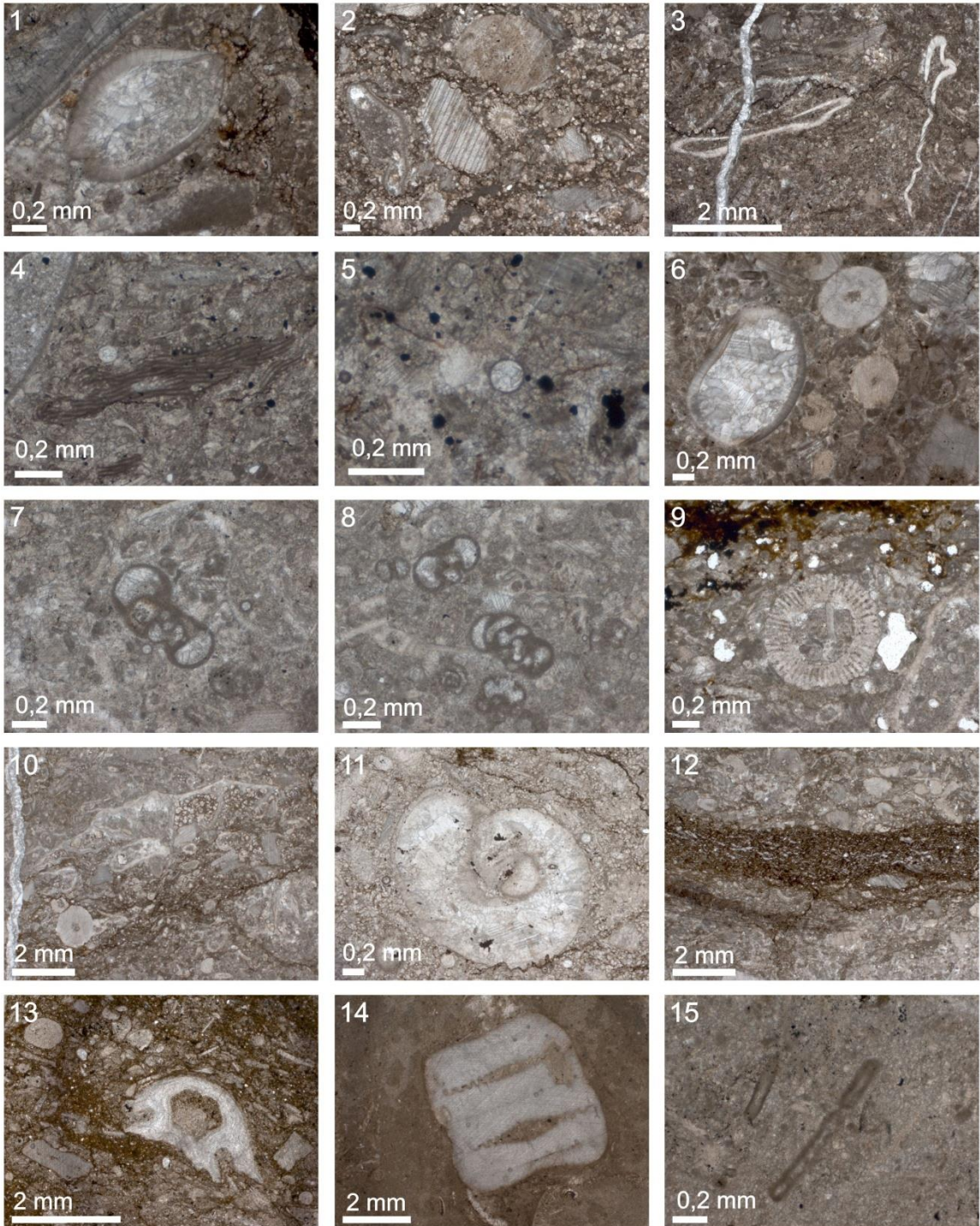
Plate 6

Microfacies of Dolhain, details of the different microfacies types, **MFT A3 - Bioturbated, echinoderm-ostracod wackestone/packstone** (Figs. 1-6), **MFT B1 - Dark, bioturbated, bioclast-bearing wackestone/packstone** (Figs. 7-8), **MFT B2 - Bioturbated, bioclast-bearing wackestone/packstone** (Figs. 9-12), **MFT C - Micritic to microsparitic, bioturbated, echinoderm wackestone/packstone** (Figs. 13), **MFT D - Bioturbated mudstone** (Figs. 14-15)

1 section of big brachiopod shell in micritic and very fine grained microsparitic matrix, sample Do 14.3

2 various specimens of *Earlandia* Plummer, 1930, cut at different angles, sample Do. 14.3.2

3 cross-section of ostracod in microsparitic matrix, most areas of the matrix affected by dolomitization, sample Do 14.3.2

4 *Girvanella* Nicholson & Etheridge, 1878, in the center of microphotograph, matrix affected by dolomitization, stylolites in upper part of microphotograph, sample Do 20

5 cross-section of crinoid ossicle and echinoid spine in the center, sample Do 20

6 bioturbated area in the lower part enriched in bioclasts, bioturbation cuts into the lighter upper micritic part, sample Do 28

7 area enriched in bioclasts (mainly brachiopod shells and crinoids) within dark brown microsparitic matrix, sample Do 8, middle part

8 large crinoid ossicles within dark brown microsparitic matrix, sample Do 8, middle part

9 thin ostracod shell in the center surrounded by microsparitic matrix, slight dolomitization on right side, sedimentary top towards the left, sample Do 14.4

10 gastropod in left upper corner, also calcareous foraminifers, bivalve and echinoderm fragments are enriched in the area, sedimentary top towards the left, sample Do 14.4

11 bioturbated area, bioclasts (mainly large echinoderm fragments) enriched by the bioturbation, sample Do 16.1

12 *Girvanella* scattered over most parts of microphotograph (marked by surrounding black line), sample Do 16.1

13 bioclasts (mainly echinoderm fragments) enriched by bioturbation within micritic and microsparitic matrix, sample Do 17

14 big brachiopod shell shielding other bioclasts underneath, matrix affected by bioturbation, most areas are dolomitized, sample Do 11.6

15 close-up of the micritic and microsparitic matrix, sample Do 32

Plate 6
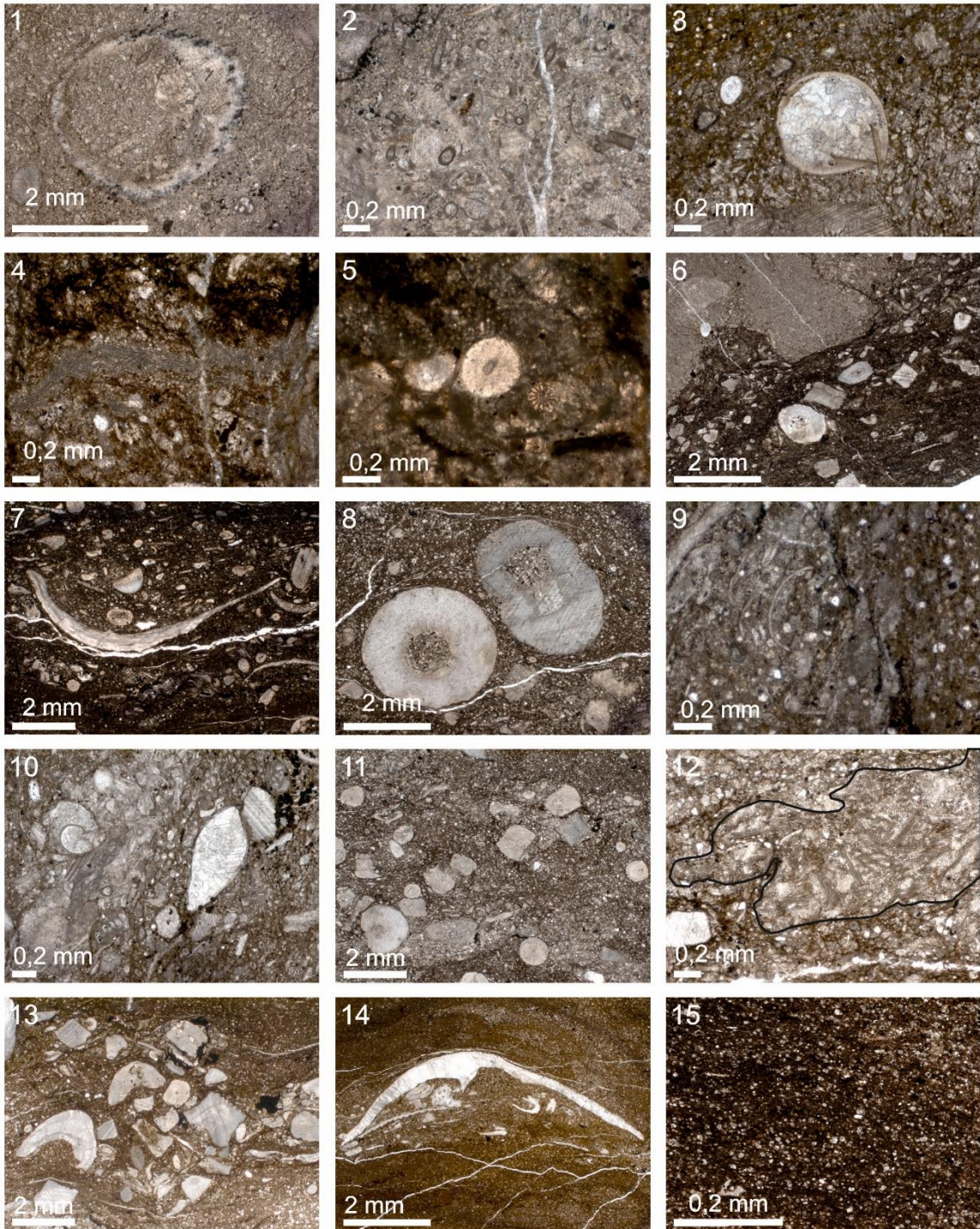
Plate 7

1-2 *Bispathodus aculeatus aculeatus* (BRANSON & MEHL, 1934a)

  1 *Bispathodus aculeatus aculeatus*, Gladenbach, Hörre Nappe, eastern Rhenish Mountains, sample 24-2, Gladenbach Fm, oral view

  2 *Bispathodus aculeatus aculeatus*, Wettmarsen, Remscheid-Altena Anticline, Rhenish Mountains, sample 14014/1, Kahlenberg Fm, oral view

3-4 *Bispathothodus spinulicostatus* M1 (BRANSON & MEHL, 1934)

  3 *Bispathothodus spinulicostatus* M1, Gladenbach, Hörre Nappe, eastern Rhenish Mountains, sample 22-1, Gladenbach Fm, oral view

  4 *Bispathodus spinulicostatus*, Dolhain, Namur-Dinant Basin, Southern Belgium, sample 18, Pont d'Arcole Fm, oral view

5 *Bispathodus stabilis stabilis* (BRANSON & MEHL, 1934a)

  Gladenbach Hörre Nappe, eastern Rhenish Mountains, sample 22, Gladenbach Fm

    a oral side

    b aboral side

6 *Bispathodus stabilis vulgaris* HARTENFELS, 2011

  Wettmarsen, Remscheid-Altena Anticline, Rhenish Mountains, sample 14014/1, Kahlenberg Fm, oral view

7-8 *Branmehla* HASS, 1959

  7 *Branmehla* sp., Gladenbach, Hörre Nappe, eastern Rhenish Mountains, sample 24-2, Gladenbach Fm, oral view

  8 *Branmehla* sp., Gladenbach, Hörre Nappe, eastern Rhenish Mountains, sample 24-2, Gladenbach Fm, oral view

9-10 *Dinodus* COOPER, 1939

  9 *Dinodus* sp., Gladenbach, Hörre Nappe, eastern Rhenish Mountains, sample 24-2, Gladenbach Fm, lateral view

  10 *Dinodus* sp., Gladenbach, Hörre Nappe, eastern Rhenish Mountains, sample 22, Gladenbach Fm, lateral view

11-13 *Dollymae* HASS, 1959

  11 *Dollymae* sp., Wettmarsen, Remscheid-Altena Anticline, Rhenish Mountains, sample 14014/1, Kahlenberg Fm, oral view

  12 *Dollymae* sp., Wettmarsen, Remscheid-Altena Anticline, Rhenish Mountains, sample 14014/1, Kahlenberg Fm, oral view

  13 *Dollymae* sp., Wettmarsen, Remscheid-Altena Anticline, Rhenish Mountains, sample 14014/1, Kahlenberg Fm, oral view

Plate 7
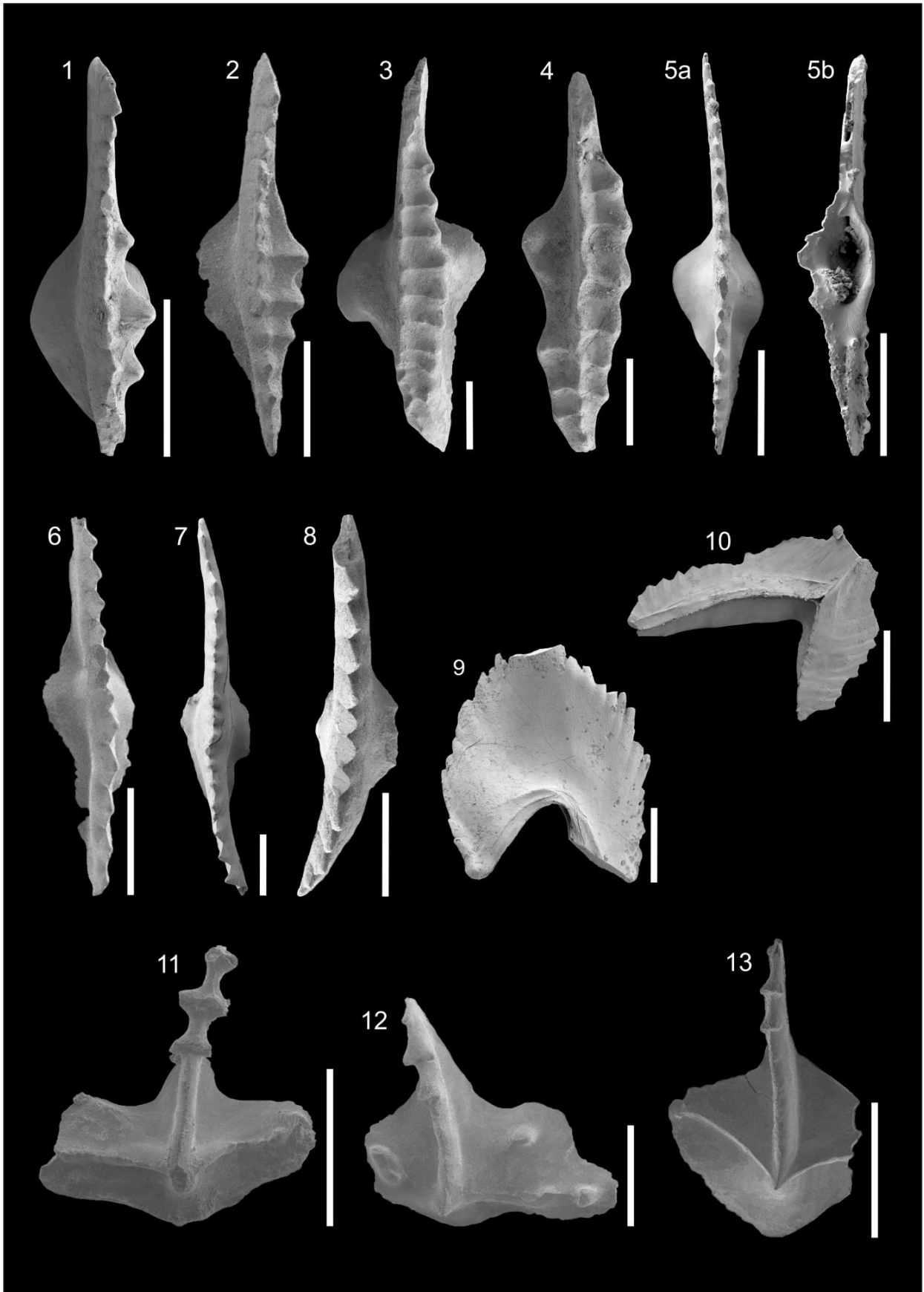
Plate 8

1-4 *Elictognathus* Cooper, 1939

   1 *Elictognathus* sp., Gladenbach, Hörre Nappe, eastern Rhenish Mountains, sample 24-2, Gladenbach Fm, lateral view

   2 *Elictognathus* sp., Gladenbach, Hörre Nappe, eastern Rhenish Mountains, sample 22, Gladenbach Fm, lateral view

   3 *Elictognathus* sp., Gladenbach, Hörre Nappe, eastern Rhenish Mountains, sample 24-2, Gladenbach Fm, oral view

   4 *Elictognathus* sp., Gladenbach, Hörre Nappe, eastern Rhenish Mountains, sample 24-2, Gladenbach Fm, aboral view

5-6 *Falcodus* Huddle, 1934

   5 *Falcodus* ? sp., Gladenbach, Hörre Nappe, eastern Rhenish Mountains, sample 22, Gladenbach Fm, lateral view

   6 *Falcodus sp.*, Gladenbach, Hörre Nappe, eastern Rhenish Mountains, sample 26, Gladenbach Fm, lateral view

7-12 *Gnathodus cuneiformis* Mehl & Thomas, 1947

   7 *Gnathodus cuneiformis*, Wettmarsen, Remscheid-Altena Anticline, Rhenish Mountains, sample 14014/1, Kahlenberg Fm

     a oral side

     b aboral side

   8 *Gnathodus cuneiformis*, Wettmarsen, Remscheid-Altena Anticline, Rhenish Mountains, sample 14014/1, Kahlenberg Fm, oral view

   9 *Gnathodus cuneiformis*, Wettmarsen, Remscheid-Altena Anticline, Rhenish Mountains, sample 14014/1, Kahlenberg Fm

     a oral side

     b aboral side

  10 *Gnathodus cuneiformis*, Wettmarsen, Remscheid-Altena Anticline, Rhenish Mountains, sample 14014/1, Kahlenberg Fm, oral view

  11 *Gnathodus cuneiformis*, Wettmarsen, Remscheid-Altena Anticline, Rhenish Mountains, sample 14014/1, Kahlenberg Fm, oral view

  12 *Gnathodus cuneiformis*, Wettmarsen, Remscheid-Altena Anticline, Rhenish Mountains, sample 14014/1, Kahlenberg Fm, oral view

Plate 8
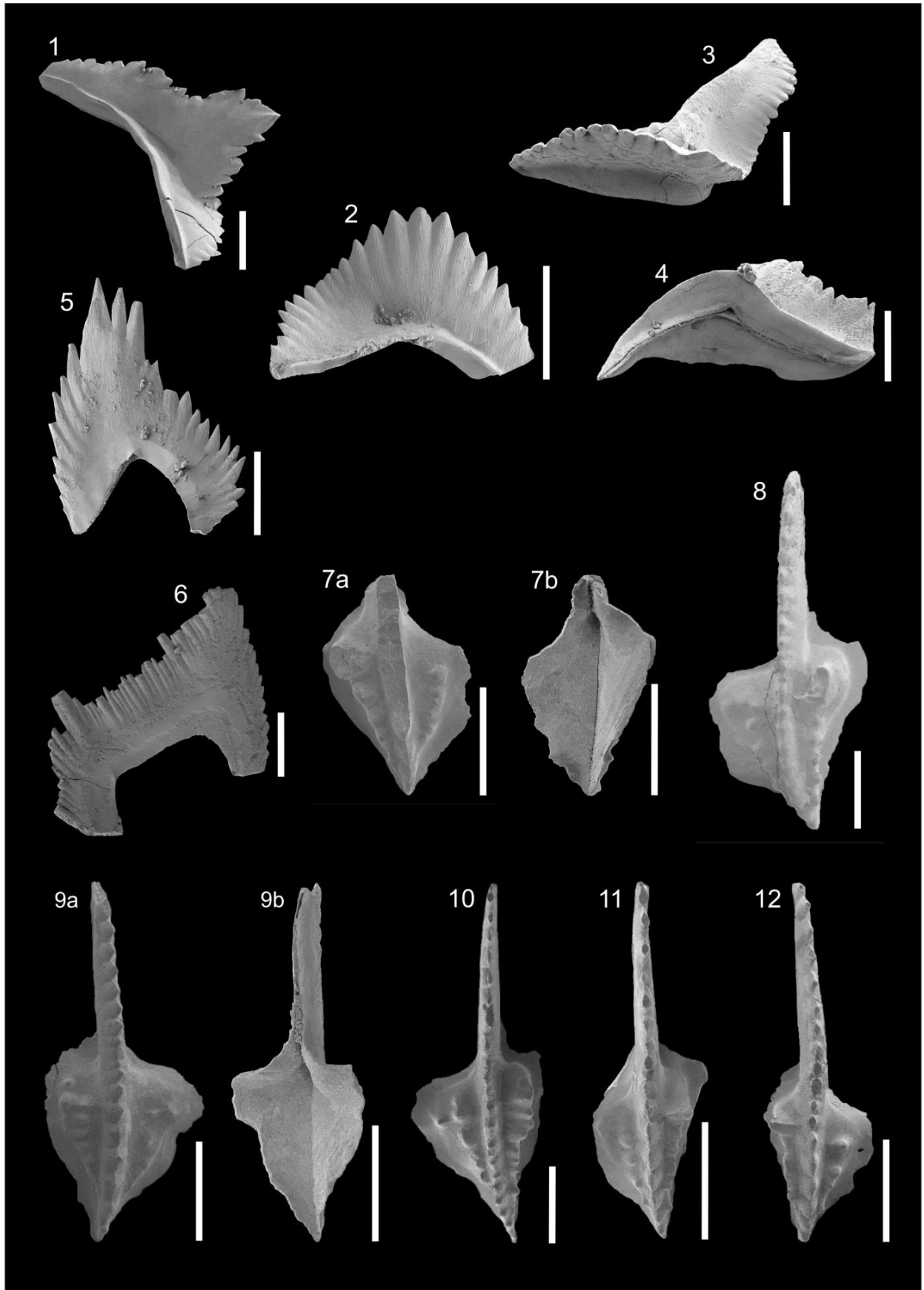
Plate 9

1-3 *Gnathodus delicatulus* Branson & Mehl, 1938

   1 *Gnathodus delicatulus*, specimen with very irregular ridge on inner platform, Wettmarsen, Remscheid-Altena Anticline, Rhenish Mountains, bed 14014/1, Kahlenberg Fm
     a oral side
     b aboral side

   2 *Gnathodus delicatulus*, Wettmarsen, Remscheid-Altena Anticline, Rhenish Mountains, sample 14014/1, Kahlenberg Fm, oral view

   3 *Gnathodus delicatulus*, Wettmarsen, Remscheid-Altena Anticline, Rhenish Mountains, bed 14014/1, Kahlenberg Fm, oral view

4-8 *Gnathodus typicus* Cooper, 1939

   4 *Gnathodus typicus*, Wettmarsen, Remscheid-Altena Anticline, Rhenish Mountains, sample 14014/1, Kahlenberg Fm
     a oral side
     b aboral side

   5 *Gnathodus typicus*, Wettmarsen, Remscheid-Altena Anticline, Rhenish Mountains, sample 14014/1, Kahlenberg Fm, oral view

   6 *Gnathodus typicus*, Wettmarsen, Remscheid-Altena Anticline, Rhenish Mountains, sample 14014/1, Kahlenberg Fm, oral view

   7 *Gnathodus typicus*, Wettmarsen, Remscheid-Altena Anticline, Rhenish Mountains, sample 14014/1, Kahlenberg Fm, oral view

   8 *Gnathodus typicus*, Gladenbach, Hörre Nappe, eastern Rhenish Mountains, sample 28, Gladenbach Fm, oral view

9-10 *Gnathodus* Pander, 1856

   9 *Gnathodus* sp., Riescheid, southern flank of the Herzkamp Syncline, western Rhenish Mountains, sample Ri 104c-e, Kahlenberg Fm
     a oral view
     b lateral view

  10 *Gnathodus* sp., Riescheid, southern flank of the Herzkamp Syncline, western Rhenish Mountains, sample Ri 104c-e, Kahlenberg Fm, oral view

Plate 9
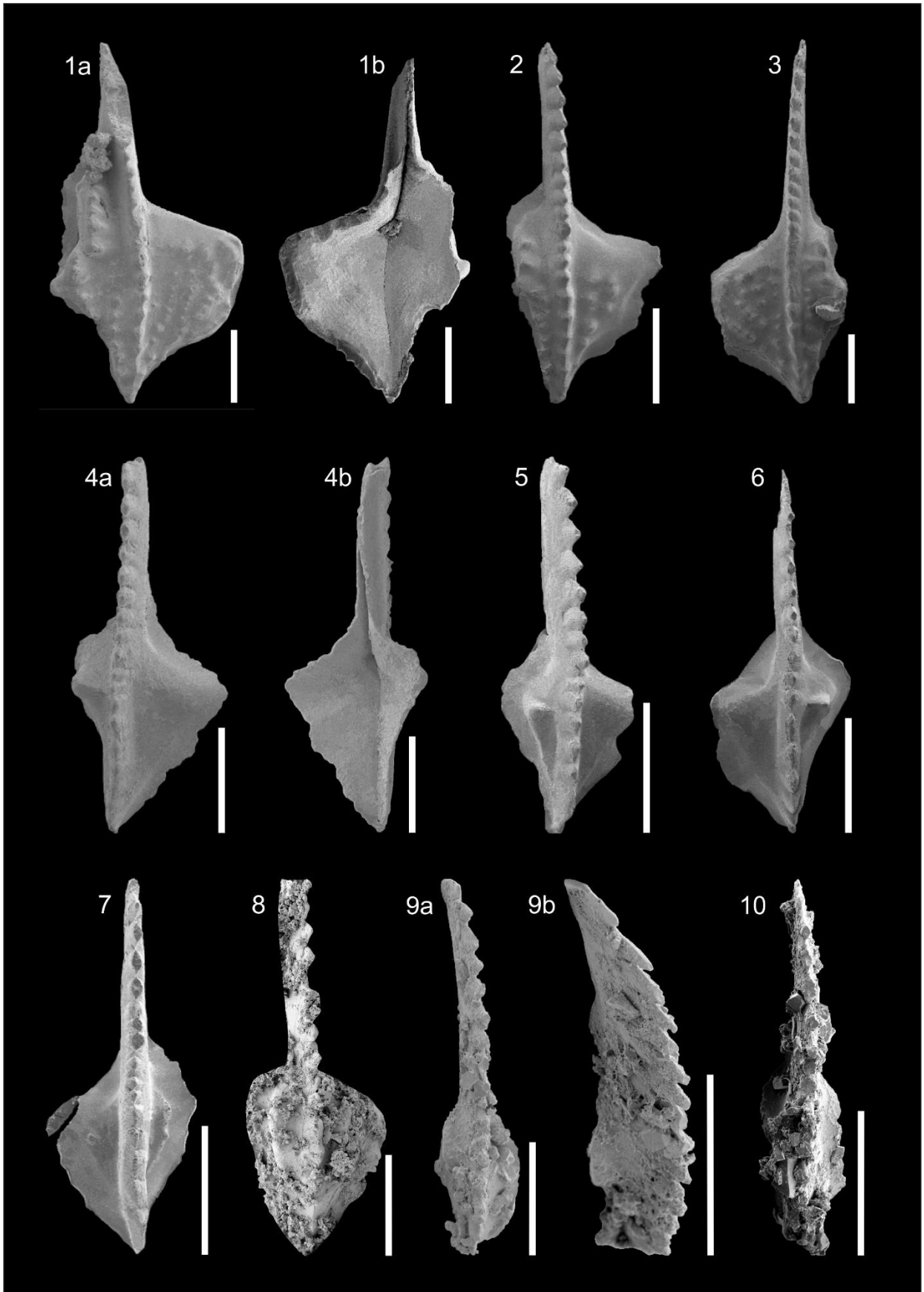
Plate 10

1-2 *Neopolygnathus communis carina* HASS, 1959

   1 *Neopolygnathus communis carina*, typical ridges are composed of 5, respectively 1 small nodes/transverse ridges, Wettmarsen, Remscheid-Altena Anticline, Rhenish Mountains, sample 14014/1, Kahlenberg Fm, oral view

   2 *Neopolygnathus communis carina*, typical ridges are composed of 5 nodes, Gladenbach, Hörre Nappe, eastern Rhenish Mountains, sample 24-2, Gladenbach Fm
      a oral view
      b aboral view

3-5 *Neopolygnathus communis communis* (BRANSON & MEHL, 1934b)

   3 *Neopolygnathus communis communis*, large, shallow depression posterior of the basal pit on aboral side is well recognizable, Gladebach, Hörre Nappe, eastern Rhenish Mountains, sample 22, Gladenbach Fm
      a oral view
      b aboral view

4 *Neopolygnathus communis communis*, numerous nodes on upturned platform margin are present, Wettmarsen, Remscheid-Altena Anticline, Rhenish Mountains, sample 14014/1, Kahlenberg Fm
      a oral view
      b aboral view

5 *Neopolygnathus communis communis*, part of blade broken off, denticles of carina less prominent than on the blade, Wettmarsen, Remscheid-Altena Anticline, Rhenish Mountains, sample 14014/1, Kahlenberg Fm
      a oral view
      b aboral view

6 *Neoprioniodus* RHODES & MÜLLER, 1956
Neoprioniodus sp., Gladenbach, Hörre Nappe, eastern Rhenish Mountains, sample 24-2, Gladenbach Fm, lateral view

7-8 *Polygnathus inornatus* BRANSON, 1934

   7 *Polygnathus inornatus*, Gladenbach, Hörre Nappe, eastern Rhenish Mountains, sample 24-2, Gladenbach Fm
      a oral view
      b aboral view

   8 *Polygnathus inornatus*, poorly preserved specimen, Dolhain, Namur-Dinant Basin, Southern Belgium, sample 18, Pont d'Arcole Fm, oral view

Plate 10
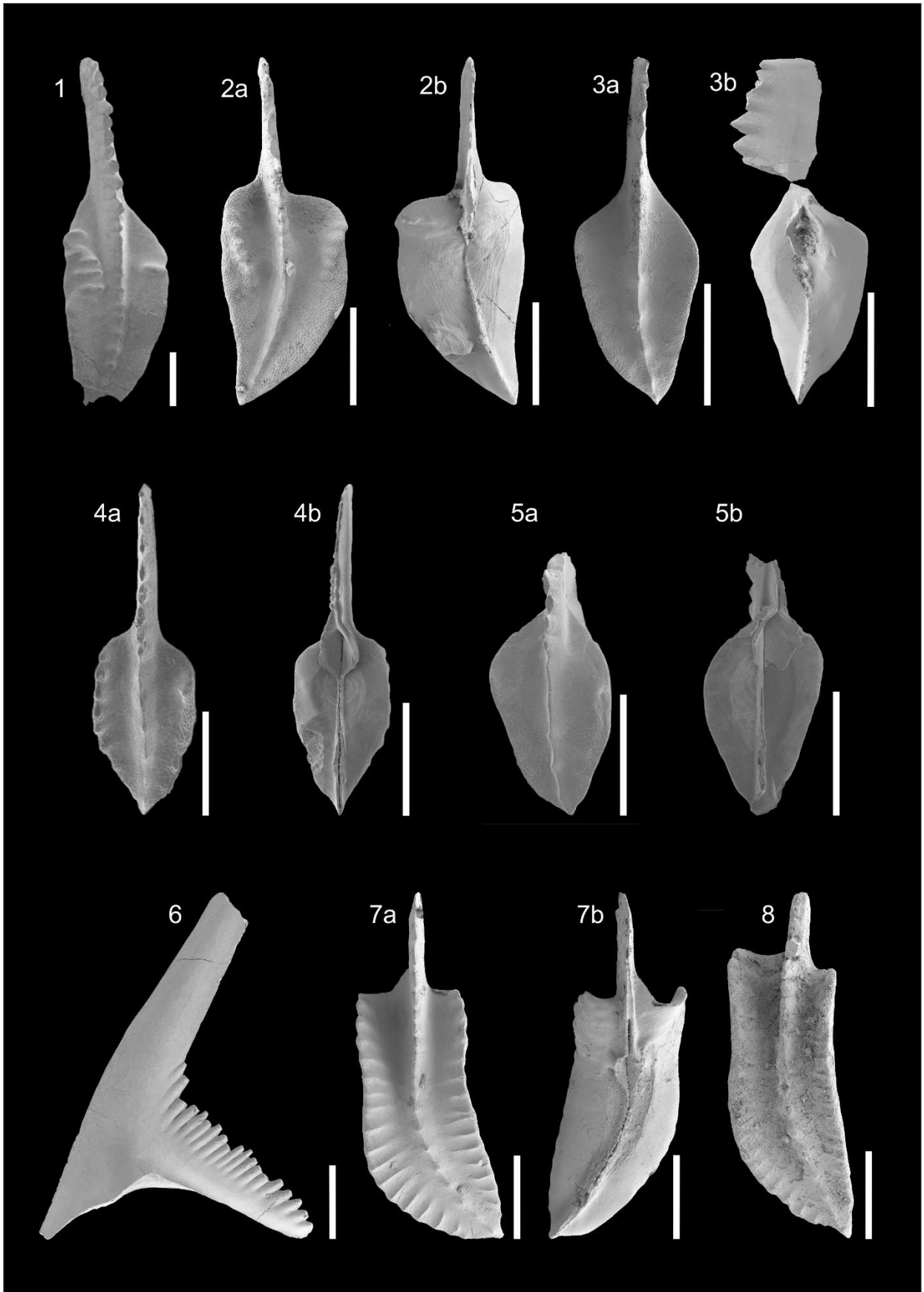
Plate 11

1 *Polygnathus inornatus*, Dolhain, Namur-Dinant Basin, Southern Belgium, sample 18, Pont d'Arcole Fm, oral view

2 *Polygnathus lobatus* BRANSON & MEHL, 1938b
free blade broken off, Dolhain, Namur-Dinant Basin, Southern Belgium, sample 18, Pont d'Arcole Fm, oral view

3-4 *Polygnathus longiposticus* BRANSON & MEHL, 1934b

   3 *Polygnathus longiposticus*, poorly preserved specimen, Gladenbach, Hörre Nappe, eastern Rhenish Mountains, sample 24-2, Gladenbach Fm, oral view

   4 *Polygnathus longiposticus*, Dolhain, Namur-Dinant Basin, Southern Belgium, sample 18, Pont d'Arcole Fm, oral view

5-6 *Polygnathus purus purus* VOGES, 1959

   5 *Polygnathus purus purus*, Gladenbach, Hörre Nappe, eastern Rhenish Mountains, sample 24-2, Gladenbach Fm, oral view

   6 *Polygnathus purus purus*, Wettmarsen, Remscheid-Altena Anticline, Rhenish Mountains, sample 14014/1, Kahlenberg Fm, oral view

7 *Pseudopolygnathus multistriatus* MEHL & THOMAS, 1947
Gladenbach, Hörre Nappe, eastern Rhenish Mountains, sample 22, Gladenbach Fm, oral view

8-9 *Pseudopolygnathus primus primus* M2 BRANSON & MEHL, 1934b

   8 *Pseudopolygnathus primus primus* M2, Wettmarsen, Remscheid-Altena Anticline, Rhenish Mountains, sample 14014/1, Kahlenberg Fm, oral view

   9 *Pseudopolygnathus primus primus* M2, Gladenbach, Hörre Nappe, eastern Rhenish Mountains, sample 22, Gladenbach Fm
     a oral view
     b aboral view

10 *Pseudopolygnathus triangulus inaequalis* VOGES, 1959
Pseudopolygnathus triangulus inaequalis, due to crippledness of anterior part of the right side of the platform, typical difference of right and left side of the anterior margin of the platform is not obvious in this specimen, characteristic crease on outer side of the basal cavity is only faintly visible, Wettmarsen, Remscheid-Altena Anticline, Rhenish Mountains, sample 14014/1, Kahlenberg Fm
     a oral view
     b aboral view

11 *Pseudopolygnathus triangulus pinnatus* VOGES, 1959
Pseudopolygnathus triangulus pinnatus, Gladenbach, Hörre Nappe, eastern Rhenish Mountains, sample 18, Gladenbach Fm
     a oral view
     b aboral view

Plate 11
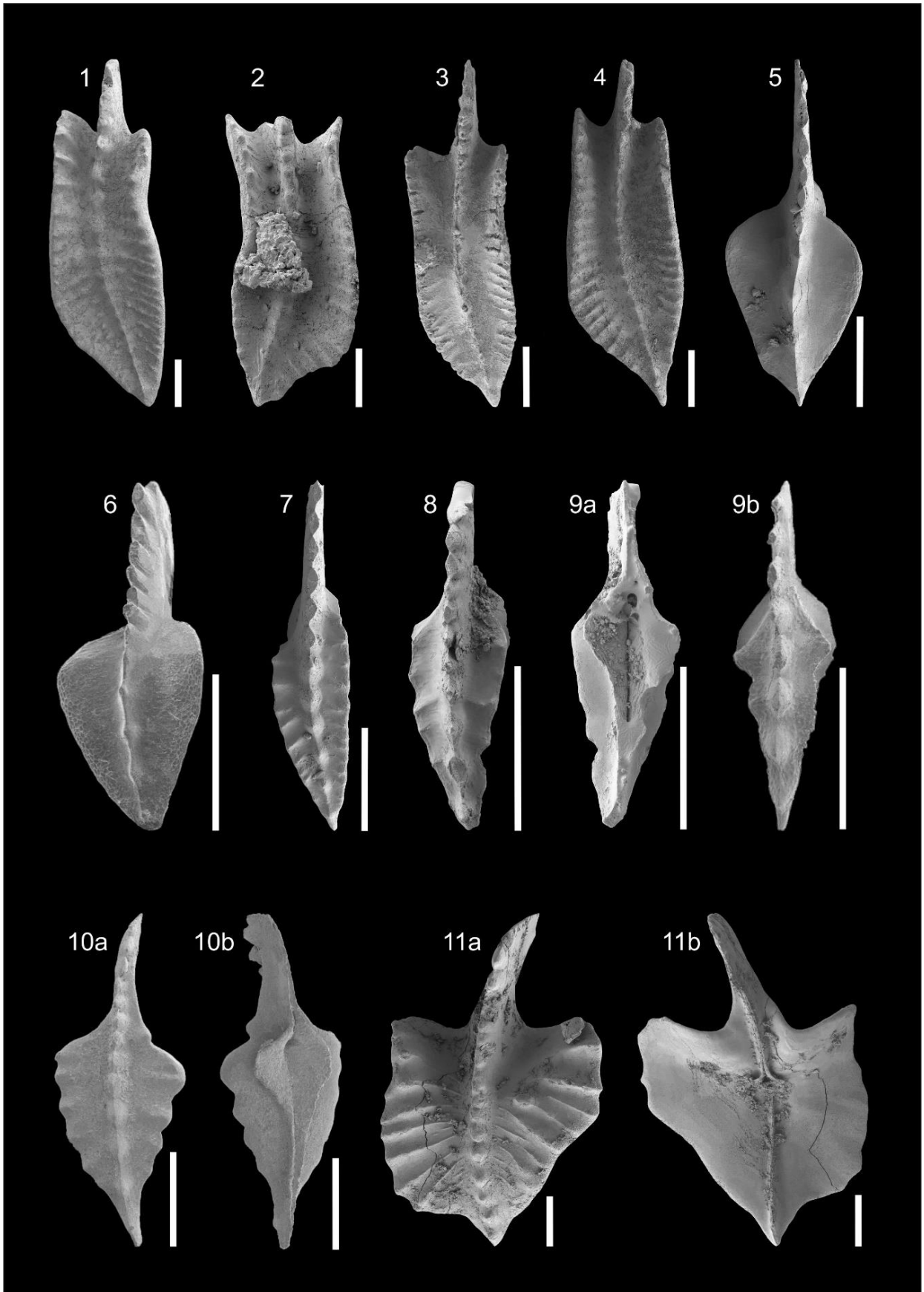
Plate 12

1 *Pseudopolygnathus triangulus pinnatus*, Wettmarsen, Remscheid-Altena Anticline, Rhenish Mountains, sample 14014/1, Kahlenberg Fm
    a oral view
    b aboral view

2-4 *Pseudopolygnathus triangulus triangulus* VOGES, 1959
  2 *Pseudopolygnathus triangulus triangulus*, Gladenbach, Hörre Nappe, eastern Rhenish Mountains, sample 24-2, Gladenbach Fm
    a oral view
    b aboral view

  3 *Pseudopolygnathus triangulus triangulus*, Wettmarsen, Remscheid-Altena Anticline, Rhenish Mountains, sample 14014/1, Kahlenberg Fm
    a oral view
    b aboral view

  4 *Pseudopolygnathus triangulus triangulus*, Wettmarsen, Remscheid-Altena Anticline, Rhenish Mountains, sample 14014/1, Kahlenberg Fm, oral view

  5 *Siphonodella cooperi* HASS, 1959
  Gladenbach, Hörre Nappe, eastern Rhenish Mountains, sample 24-2, Gladenbach Fm, oral view

6-7 *Siphonodella crenulata* M1 (COOPER, 1939)
  6 *Siphonodella crenulata* M1, Gladenbach, Hörre Nappe, eastern Rhenish Mountains, sample 18, Gladenbach Fm
    a oral view
    b aboral view

  7 *Siphonodella crenulata* M1, Gladenbach, Hörre Nappe, eastern Rhenish Mountains, sample 22-2, Gladenbach Fm, oral view

8-10 *Siphonodella crenulata* M2 (COOPER, 1939)
  8 *Siphonodella crenulata* M2, Gladenbach, Hörre Nappe, eastern Rhenish Mountains, sample 24-2, Gladenbach Fm, oral view

  9 *Siphonodella crenulata* M2, Gladenbach, Hörre Nappe, eastern Rhenish Mountains, sample 22-2, Gladenbach Fm, aboral view

  10 *Siphonodella crenulata* M2, Gladenbach, Hörre Nappe, eastern Rhenish Mountains, sample 24-2, Gladenbach Fm, oral view

Plate 12
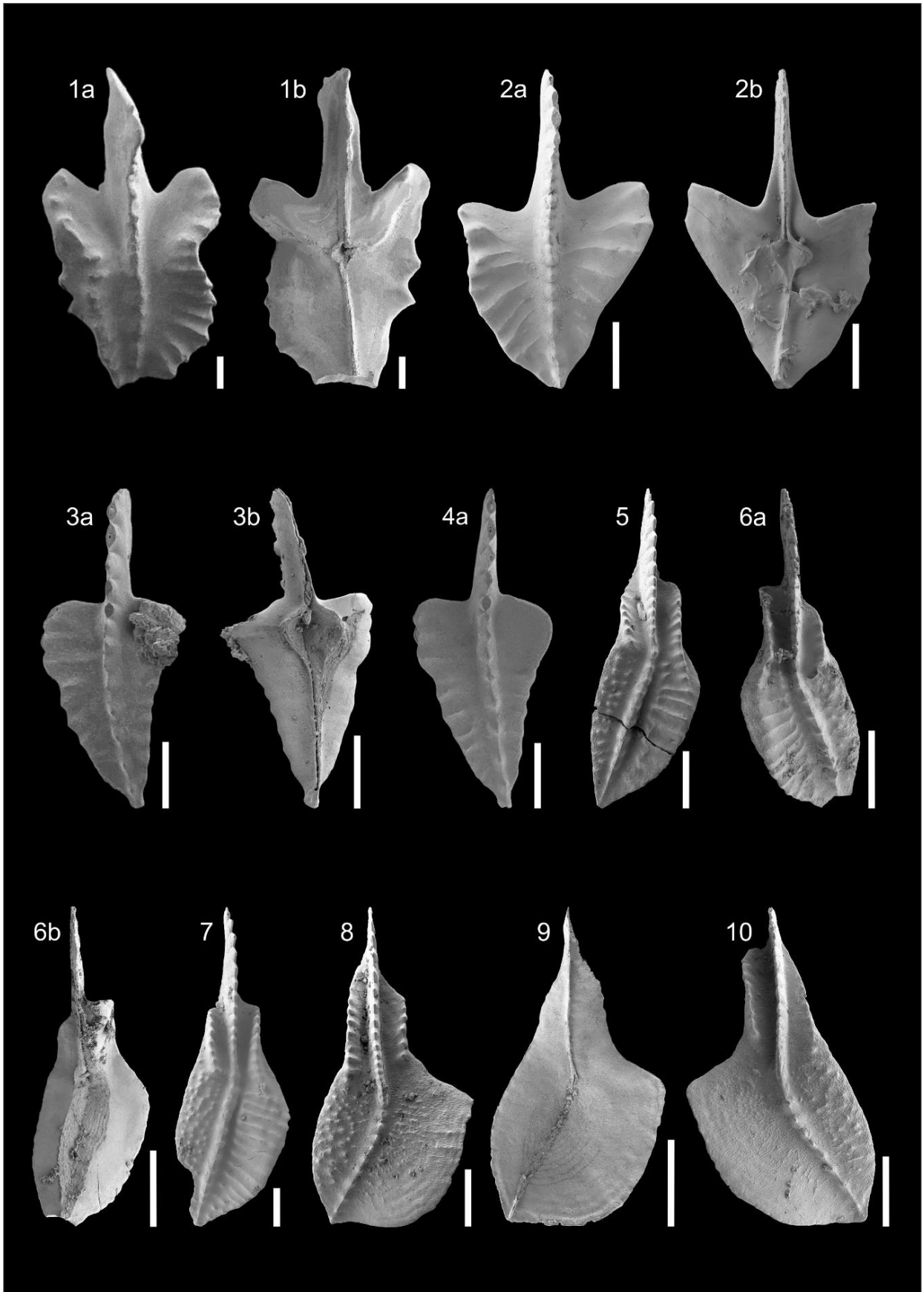
Plate 13

1 *Siphonodella crenulata* M2, Gladenbach, Hörre Nappe, eastern Rhenish Mountains, sample 24-2, Gladenbach Fm, oral view

2 *Siphonodella* cf. *crenulata*, Riescheid, southern flank of the Herzkamp Syncline, western Rhenish Mountains, sample Ri 104c-e, Kahlenberg Fm, oral view

3-4 *Siphonodella duplicata* (BRANSON & MEHL, 1934b)

    3 *Siphonodella duplicata*, Gladenbach, Hörre Nappe, eastern Rhenish Mountains, sample 22-2, Gladenbach Fm, oral view

    4 *Siphonodella duplicata*, Gladenbach, Hörre Nappe, eastern Rhenish Mountains, sample 22-1, Gladenbach Fm, oral view

5 *Siphonodella* cf. *duplicata*, the rostral ridges are more clearly developed than in other specimens of this species (compare Pl. 13, Fig. 3-4), Wettmarsen, Remscheid-Altena Anticline, Rhenish Mountains, sample 14014/1, Kahlenberg Fm

        a oral view

        b aboral view

6-7 *Siphonodella hassi* JI, 1985

    6 *Siphonodella hassi*, Gladenbach, Hörre Nappe, eastern Rhenish Mountains, sample 24-2, Gladenbach Fm

        a oral view

        b aboral view

    7 *Siphonodella hassi*, Gladenbach, Hörre Nappe, eastern Rhenish Mountains, sample 16, Gladenbach Fm, oral view

8-13 *Siphonodella isosticha* (COOPER, 1939)

    8 *Siphonodella isosticha*, Gladenbach, Hörre Nappe, eastern Rhenish Mountains, sample 22, Gladenbach Fm, oral view

    9 *Siphonodella isosticha*, Gladenbach, Hörre Nappe, eastern Rhenish Mountains, sample 22-1, Gladenbach Fm, oral view

  10 *Siphonodella isosticha*, Gladenbach, Hörre Nappe, eastern Rhenish Mountains, sample 26, Gladenbach Fm, oral view

  11 *Siphonodella isosticha*, Dolhain, Namur-Dinant Basin, Southern Belgium, sample 18, Pont d'Arcole Fm

        a oral view

        b aboral view

  12 *Siphonodella isosticha*, Riescheid, southern flank of the Herzkamp Syncline, western Rhenish Mountains, sample Ri 104c-e, Kahlenberg Fm, oral view

  13 *Siphonodella isosticha*, Riescheid, southern flank of the Herzkamp Syncline, western Rhenish Mountains, sample Ri 104c-e, Kahlenberg Fm, oral view

Plate 13
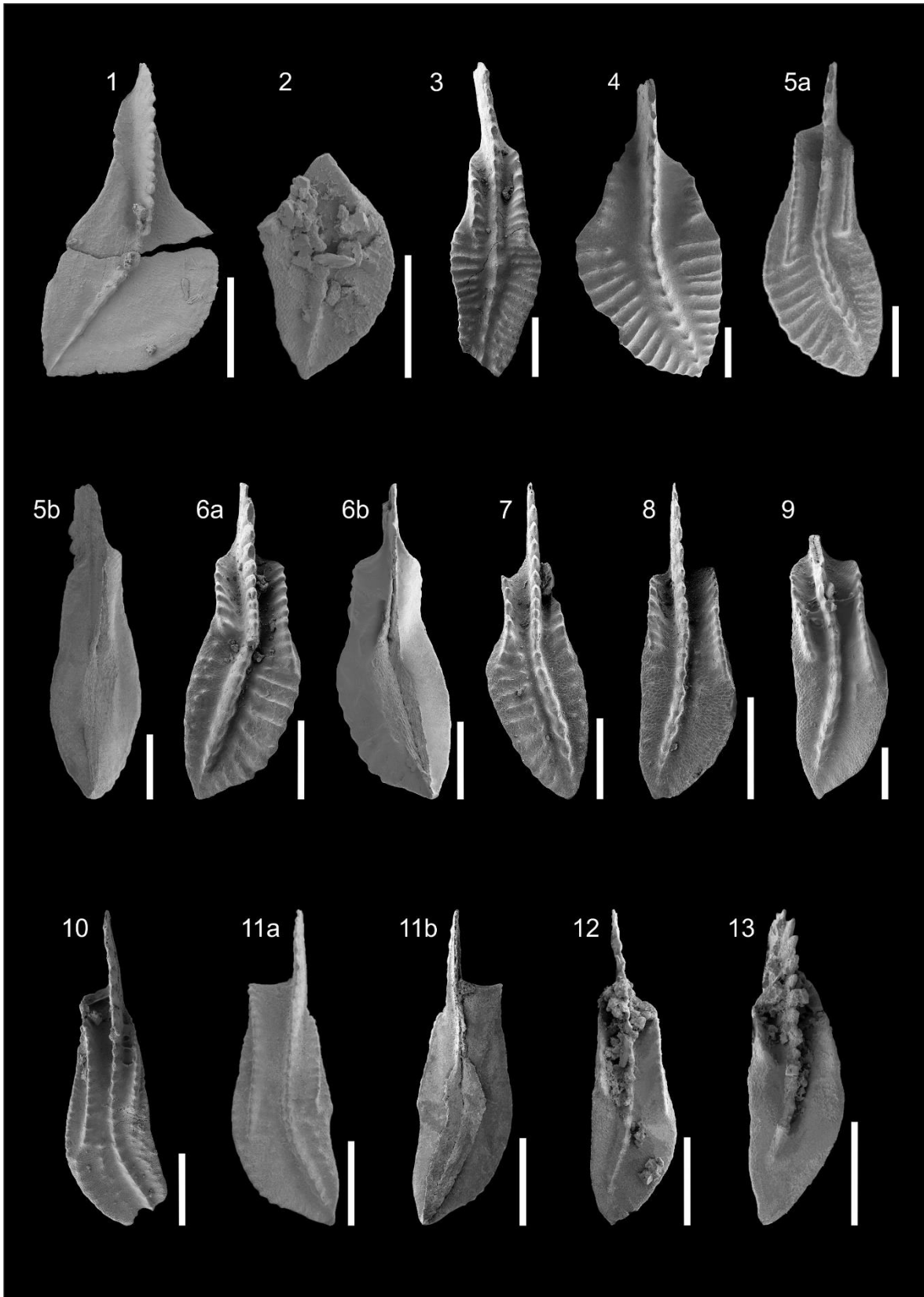
Plate 14

1 *Siphonodella lobata* (Branson & Mehl, 1934b)
Gladenbach, Hörre Nappe, eastern Rhenish Mountains, sample 22, Gladenbach Fm
  a oral view
  b aboral view
2-3 *Siphonodella obsoleta* Hass, 1959
  2 *Siphonodella obsoleta*, Gladenbach, Hörre Nappe, eastern Rhenish Mountains, sample 24-2, Gladenbach Fm
    a oral view
    b aboral view
  3 *Siphonodella obsoleta*, Wettmarsen, Remscheid-Altena Anticline, Rhenish Mountains, sample 14014/1, Kahlenberg Fm
    a oral view
    b aboral view
4 *Siphonodella sandbergi* Klapper, 1966
Dolhain, Namur-Dinant Basin, Southern Belgium, sample 18, Pont d'Arcole Fm, oral view
5-6 *Siphonodella sulcata* (Huddle, 1934)
  5 *Siphonodella sulcata*, Gladenbach, Hörre Nappe, eastern Rhenish Mountains, sample 22-2, Gladenbach Fm, oral view
  6 *Siphonodella sulcata*, Wettmarsen, Remscheid-Altena Anticline, Rhenish Mountains, sample 14014/1, Kahlenberg Fm, oral view
7 *Siphonodella* Branson & Mehl, 1944
Siphonodella sp., Riescheid, southern flank of the Herzkamp Syncline, western Rhenish Mountains, sample Ri 104c-e, Kahlenberg Fm, oral view
8 *Mehlina* Youngquist, 1945
    Wettmarsen, Remscheid-Altena Anticline, Rhenish Mountains, sample 14014/1, Kahlenberg Fm, lateral view
9 *Icriodus alternatus alternatus* Branson & Mehl, 1934a
Gladenbach, Hörre Nappe, eastern Rhenish Mountains, sample 22-1, Gladenbach Fm, oral view
10 *Ozarkodina* sp. Branson & Mehl, 1933
    Gladenbach, Hörre Nappe, eastern Rhenish Mountains, sample 19, Gladenbach Fm, lateral view

Plate 14
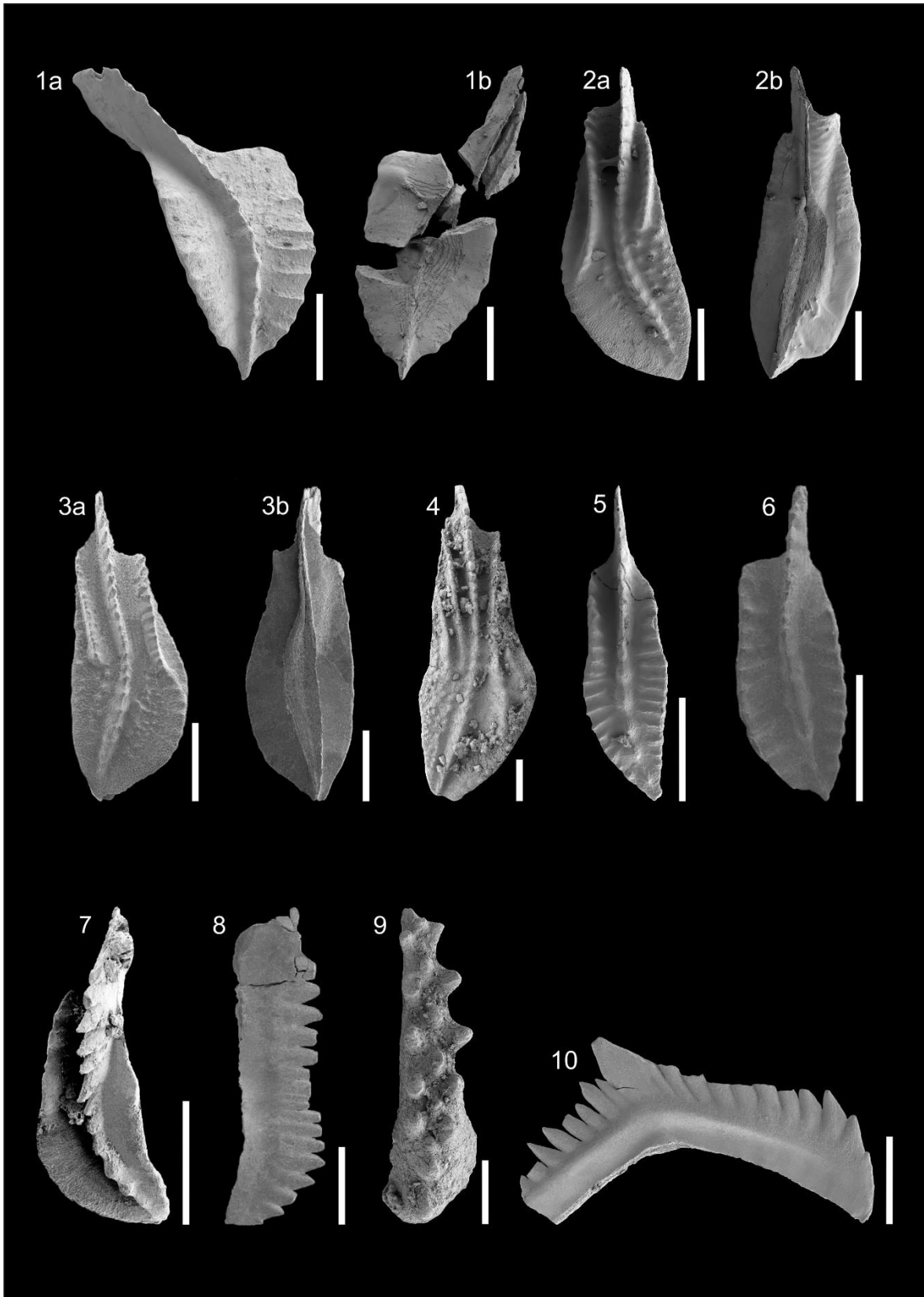
Plate 15

1-2 *Palmatolepis glabra pectinata* ZIEGLER, 1962b M1

   1 *Palmatolepis glabra pectinata*, Wettmarsen, Remscheid-Altena Anticline, Rhenish Mountains, sample 14014/1, Kahlenberg Fm, oral view

   2 *Palmatolepis glabra pectinata*, Wettmarsen, Remscheid-Altena Anticline, Rhenish Mountains, sample 14014/1, Kahlenberg Fm, oral view

3-5 *Palmatolepis glabra prima* ZIEGLER & HUDDLE, 1969 M3

   3 *Palmatolepis glabra prima*, Gladenbach, Hörre Nappe, eastern Rhenish Mountains, sample 24-1, Gladenbach Fm, oral view

4 *Palmatolepis glabra prima*, Wettmarsen, Remscheid-Altena Anticline, Rhenish Mountains, sample 14014/1, Kahlenberg Fm, oral view

5 *Palmatolepis glabra prima*, Wettmarsen, Remscheid-Altena Anticline, Rhenish Mountains, sample 14014/1, Kahlenberg Fm, oral view

6 *Palmatolepis glabra* ?
Wettmarsen, Remscheid-Altena Anticline, Rhenish Mountains, sample 14014/1, Kahlenberg Fm, oral view

7 *Palmatolepis linguiloba* (DZIK, 2006)
Wettmarsen, Remscheid-Altena Anticline, Rhenish Mountains, sample 14014/1, Kahlenberg Fm, oral view

8 *Palmatolepis quadrantinodosalobata* SANNEMANN, 1955
Gladenbach, Hörre Nappe, eastern Rhenish Mountains, sample 22-2, Gladenbach Fm, oral view

9-11 *Palmatolepis triangularis* SANNEMANN, 1955

9 *Palmatolepis triangularis*, Gladenbach, Hörre Nappe, eastern Rhenish Mountains, sample 22-2, Gladenbach Fm, oral view

10 *Palmatolepis triangularis*, Gladenbach, Hörre Nappe, eastern Rhenish Mountains, sample 4, Gladenbach Fm, oral view

11 *Palmatolepis triangularis*, Wettmarsen, Remscheid-Altena Anticline, Rhenish Mountains, sample 14014/1, Kahlenberg Fm, oral view

12 *Palmatolepis* sp.
Wettmarsen, Remscheid-Altena Anticline, Rhenish Mountains, sample 14014/1, Kahlenberg Fm, oral view

Plate 15
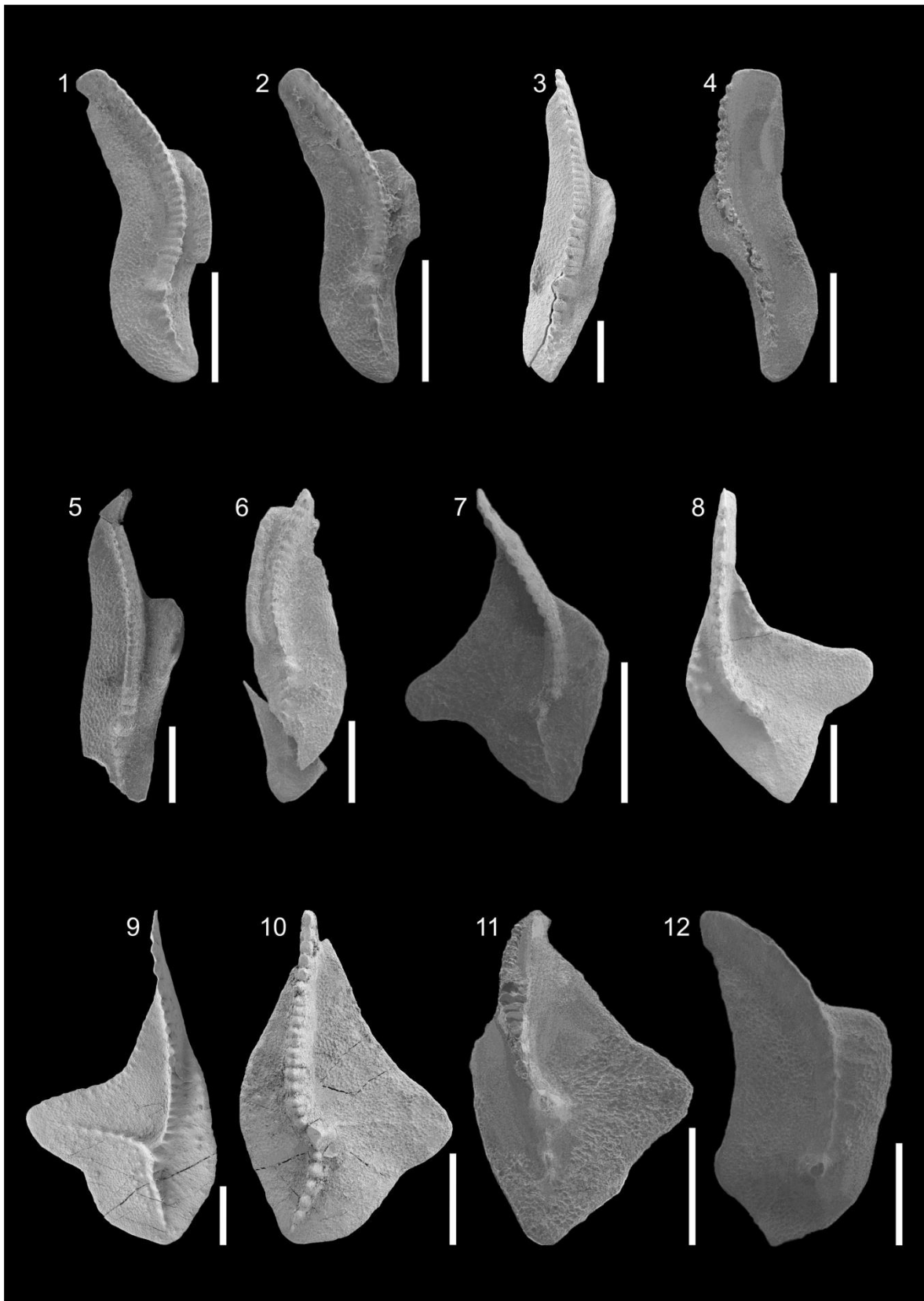
13. Erklärung

Ich versichere, dass ich die von mir vorgelegte Dissertation selbständig angefertigt, die benutzten Quellen und Hilfsmittel vollständig angegeben und die Stellen der Arbeit – einschließlich Tabellen, Karten und Abbildungen –, die anderen Werken im Wortlaut oder dem Sinn nach entnommen sind, in jedem Einzelfall als Entlehnung kenntlich gemacht habe; dass diese Dissertation noch keiner anderen Fakultät oder Universität zur Prüfung vorgelegen hat; dass sie – abgesehen von unten angegebenen Teilpublikationen – noch nicht veröffentlicht worden ist, sowie, dass ich eine solche Veröffentlichung vor Abschluss des Promotionsverfahrens nicht vornehmen werde. Die Bestimmungen der Promotionsordnung sind mir bekannt. Die von mir vorgelegte Dissertation ist von Prof. Hans-Georg Herbig betreut worden.

Folgende Teilpublikationen liegen vor:

ESTEBAN LOPEZ, S., BENDER, P. & HERBIG, H. -G. (2019): Middle Tournaisian (lower Mississippian) conodonts and calcareous microbiota from the Hörre Nappe, eastern Rhenish Mountains, Germany. – In: HARTENFELS, S., HERBIG, H.-G., AMLER, M.R.W. & ARETZ, M. (eds.): 19th International Congress on the Carboniferous and Permian, Cologne, July 29 – August 2, 2019. Abstracts. – Kölner Forum für Geologie und Paläontologie, 23: 95-96.

HARTENFELS, S., HARTKOPF-FRÖDER, C., HERBIG, H.-G., BECKER, R. T. & ESTEBAN LOPEZ, S. (2016): Middle Famennian to Viséan stratigraphy at Riescheid (Herzkamp Syncline, Rhenish Massif). – Münstersche Forschungen zur Geologie und Paläontologie, 108: 74-94.

Köln, den 23.04.2021